

**ANALYSIS OF ROBUST COMPUTATIONAL
TECHNIQUES FOR SINGULARLY PERTURBED SYSTEM
OF PARABOLIC PARTIAL DIFFERENTIAL EQUATIONS**

by

Maneesh Kumar Singh



**DEPARTMENT OF MATHEMATICS
INDIAN INSTITUTE OF TECHNOLOGY GUWAHATI
GUWAHATI-781039, INDIA**

May, 2018

**ANALYSIS OF ROBUST COMPUTATIONAL
TECHNIQUES FOR SINGULARLY PERTURBED SYSTEM
OF PARABOLIC PARTIAL DIFFERENTIAL EQUATIONS**

*A thesis submitted
in partial fulfillment of the requirements
for the degree of*

DOCTOR OF PHILOSOPHY

by

Maneesh Kumar Singh

(Roll Number: 136123007)



to the

**DEPARTMENT OF MATHEMATICS
INDIAN INSTITUTE OF TECHNOLOGY GUWAHATI**

May, 2018

DECLARATION

It is certified that the work contained in this thesis entitled “**Analysis of robust computational techniques for singularly perturbed system of parabolic partial differential equations**” has done by me, under the supervision of **Dr. Natesan Srinivasan**, Professor, Department of Mathematics, Indian Institute of Technology Guwahati for the award of the degree of Doctor of Philosophy and this work has not been submitted elsewhere for a degree.

May, 2018

Maneesh Kumar Singh

Roll No. 136123007

Department of Mathematics

Indian Institute of Technology Guwahati

CERTIFICATE

It is certified that the work contained in this thesis entitled “**Analysis of robust computational techniques for singularly perturbed system of parabolic partial differential equations**” by **Maneesh Kumar Singh**, a student of Department of Mathematics, Indian Institute of Technology Guwahati, for the award of the degree of Doctor of Philosophy has been carried out under my supervision and this work has not been submitted elsewhere for a degree.

May, 2018

Dr. Natesan Srinivasan
Professor
Department of Mathematics
Indian Institute of Technology Guwahati

In memory of my father

Shri. Mahendra Singh



Acknowledgement

First and foremost, I would like to express my sincere gratitude to my thesis supervisor Prof. Natesan Srinivasan for his guidance during my research. I am deeply indebted to him for his invaluable guidance, immense patience, utmost care and constant encouragement through out this work. I am also thankful to him for making me feel free to express my views. Without his support, this work could not have been accomplished.

Beside my supervisor, I would like to thank my doctoral committee members: Prof. D. C. Dalal, Prof. R. K. Sinha and Prof. S. N. Bora for their cooperation and useful comments during the progress of my research work.

I acknowledge my gratitude to IIT Guwahati for the financial, academic and technical support. The serene and spacious campus of the IIT Guwahati was certainly a plus point - a perfect place for walks.

I thank the following staff of Department of Mathematics: Mr. Sridhar, Mr. Saurav, Mr. Phatik for their office related support and assistance with Mr. Santanu, Mr. Pranpratim for their technical support for various issues.

I express my regards to Prof. A. K Mishra and Dr. D. R. Sahu of Department of Mathematics, Banaras Hindu University for motivating me to opt for higher studies in Mathematics. Special thanks to Prof. T. Amaranath and Dr. T. Suman Kumar of School of Mathematics and Statistics, University of Hyderabad for their constant support during my M.Sc. and encouraging me for perusing Ph.D.

I am grateful to my co-researchers for providing a stimulating and fun filled environment. My thanks go in particular to Ranjan, Ramesh, Ashish for their friendly and wonderful company in throughout my research life. I am ever indebted to my seniors Dr. Abhishek Das, Dr. Anirban Das and I admire their distinguished helping nature. I am also thankful to my friends and seniors Ankur, Swapnendu, Sougata, Balasubramani, Swarup, Madhusudan, Deb, Anand, Tamal, Devanand, Biswajit, Debasish and my junior Gautam and many others for sharing all the unforgettable moments.

Finally, I sought inspiration and I owe a great deal to my mother Smt. Saroj Devi and my father Late Shri Mahendra Singh whose selfless sacrificial life with continuous encouragement and support has empowered me to achieve the present position in my life. I would prefer to pay homage by dedicating my thesis to my late father under whose

careful protection I have been able to enjoy my life. I am also grateful to my grandfather Shri Rambali Singh for his support and inspiration during this journey. I likewise pass on my appreciation to my uncles Yogendra Nath Singh and Sanjay Singh for my first enthusiasm for mathematics. Along these lines, through this affirmation I express my heartiest respects to all my well wishers.

May, 2018

Maneesh Kumar Singh



Abstract

In this thesis, our primary interest is to provide some uniformly convergent computational techniques for solving singularly perturbed system of parabolic initial-boundary-value problems (IBVPs) of convection-diffusion and reaction-diffusion types with boundary and interior layers in one- and two-dimensions. These kinds of problems are identified by system of partial differential equations in which the highest order spatial derivatives are multiplied by small parameters ε or ε_1 and ε_2 (say) known as singular perturbation parameters. The solution of such kind of problems exhibits boundary or/and interior layers where the solution varies rapidly, while away from these layers the solution behaves smoothly. Due to appearance of the layer phenomena, it is an interesting task to develop parameter-uniform numerical methods.

The purpose of this thesis is to apply and analyze parameter-uniform fitted mesh methods (FMMs) for solving singularly perturbed system of parabolic convection-diffusion and reaction-diffusion problems in one- and two-dimensions.

We begin this thesis with an introduction followed by a section describing the objectives and the motivation for solving singularly perturbed system of parabolic PDEs. Then, we discuss preliminaries which are used throughout the thesis. Next, we move forward to the main work of the thesis. First, we analyze a uniformly convergent numerical scheme for system of 1D parabolic convection-diffusion IBVPs exhibiting overlapping boundary layers. Then, to improve the accuracy of the proposed numerical scheme, a post-processing technique is discussed. The hybrid difference numerical scheme is proposed for system of 1D parabolic PDE on the piecewise-uniform Shishkin mesh. This hybrid scheme is a proper combination of the midpoint upwind scheme and the central difference scheme. Later, we have considered uniformly convergent upwind based numerical scheme for singularly perturbed system of 1D parabolic convection-diffusion problems with overlapping interior layers. Numerical experiments are carried out to validate the theoretical findings.

Then we discuss singularly perturbed system of 2D parabolic convection-diffusion and reaction-diffusion problems. First, we analyze a fractional-step method to discretize the time-derivative of the singularly perturbed system of 2D convection-diffusion PDEs. The resulting one-dimensional equations are solved by using the classical upwind scheme. Next, we consider singularly perturbed system of two-dimensional reaction-diffusion problems with one parameter. Here, we discretize the time-derivative by the fraction-step method and spatial derivatives by the central difference scheme for the reduced stationary problem. At the end, we have considered system of 2D reaction-diffusion problem containing different diffusion parameters. The spatial derivatives are discretized by the central difference scheme on piecewise-uniform Shishkin mesh. Then, the time derivative is discretized by implicit-Euler scheme on uniform mesh in the resulting problem. Numerical results are produced to validate the theoretical error estimates.

Finally, we summarize the results obtained in this thesis. At the end of this thesis, possible future works are discussed based on the work carried out in this thesis.

Contents

Nomenclature	x
List of Figures	xii
List of Tables	xv
1 Introduction	1
1.1 Singular Perturbation Problem	1
1.2 Objective and Motivation	4
1.3 Preliminaries	7
1.4 Model Problems	10
1.4.1 Singularly perturbed system of 1D parabolic convection-diffusion problem	11
1.4.2 Singularly perturbed system of 1D semilinear parabolic problem	11
1.4.3 Singularly perturbed system of 1D parabolic convection-diffusion problem with boundary layers	12
1.4.4 Singularly perturbed system of 1D parabolic convection-diffusion problem with interior layers	12
1.4.5 Singularly perturbed system of 2D parabolic convection-diffusion problem	13
1.4.6 Singularly perturbed system of 2D parabolic reaction-diffusion problem	14
1.4.7 Singularly perturbed system of 2D parabolic reaction-diffusion problem with overlapping boundary layers	15
1.5 Outline of the Thesis	15
2 Efficient Numerical Schemes for Singularly Perturbed System of 1D Parabolic Partial Differential Equations with Boundary Layers	17
2.1 Introduction	17
2.2 Bounds of the Solution and its Derivatives	19
2.3 Analysis of the Time Semidiscretization	24
2.3.1 The time semidiscrete scheme	24
2.4 The Spatial Discretization	27

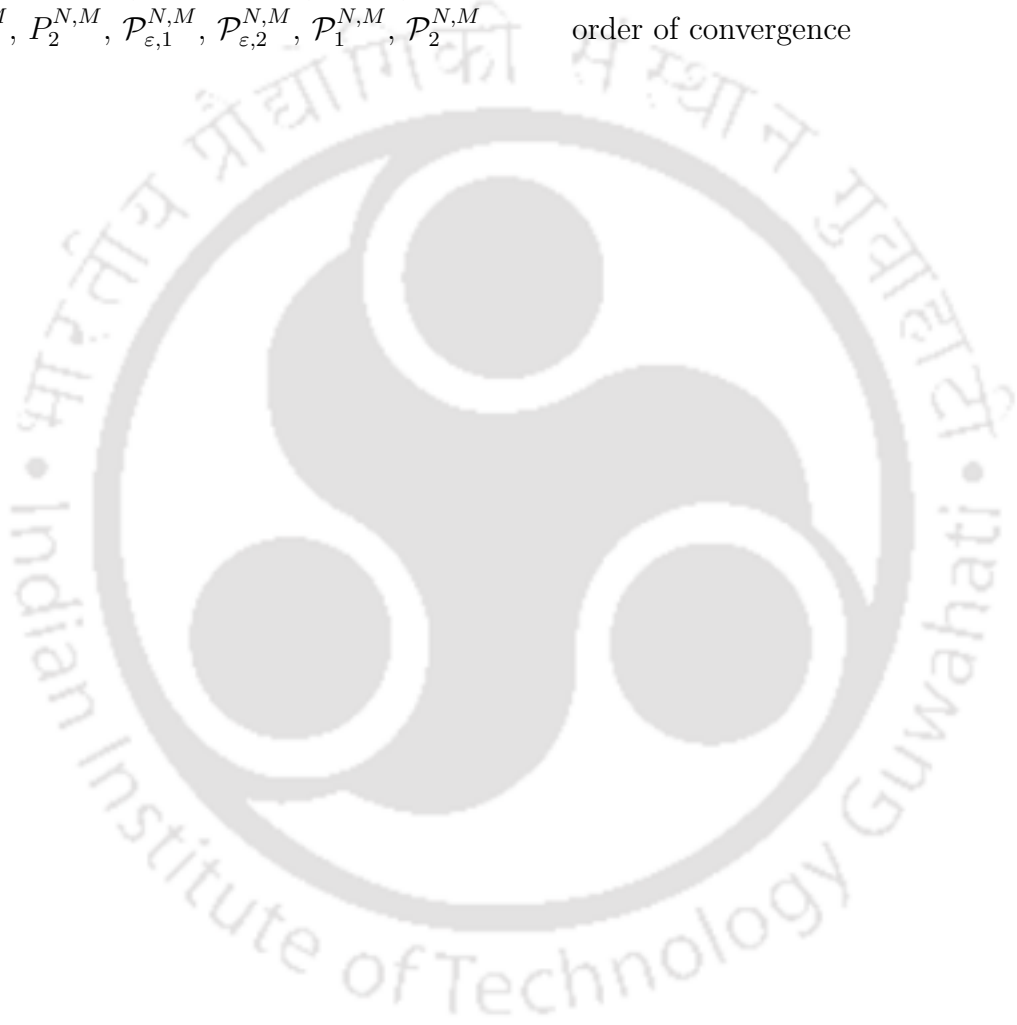
2.4.1	Discretization of the domain	27
2.4.2	The finite difference scheme	28
2.4.3	The truncation error analysis	29
2.5	The Fully Discrete Scheme	33
2.6	System of Semilinear Parabolic Problems	34
2.7	Richardson Extrapolation Technique	35
2.7.1	Extrapolation of \tilde{u}^n	35
2.7.2	Extrapolation of \tilde{U}^n	36
2.8	Numerical Results	42
2.8.1	Upwind based numerical scheme	42
2.8.2	Richardson extrapolation technique	44
2.9	Conclusions	50
3	Parameter-Uniform Hybrid Numerical Scheme for Singularly Perturbed System of 1D Parabolic Convection-Diffusion Problems	53
3.1	Introduction	53
3.2	Analytical Behavior of the Solution	54
3.3	The Time Semidiscretization	55
3.3.1	Asymptotic behavior of the solutions of semidiscrete problems	56
3.4	The Discrete Problem	59
3.4.1	The piecewise-uniform Shishkin mesh	59
3.4.2	The hybrid scheme	59
3.4.3	Error analysis	61
3.5	The Fully Discrete Scheme	71
3.6	Numerical Results	71
3.7	Conclusion	72
4	Uniformly Convergent Numerical Scheme for Singularly Perturbed System of 1D Parabolic Convection-Diffusion Problems with Interior Layers	75
4.1	Introduction	75
4.2	The Continuous Problem	77
4.2.1	Bounds on the solution and its derivatives	78
4.3	Domain Discretization	82
4.3.1	Numerical scheme	83
4.3.2	Error analysis	84
4.4	Numerical Results	88
4.5	Conclusions	89
5	A Robust Fractional-Step Method for Singularly Perturbed System of 2D Parabolic Convection-Diffusion Problems	95
5.1	Introduction	95

5.2	Continuous Problem and Solution Bounds	96
5.3	Time Semidiscretization	101
5.3.1	Asymptotic behavior of the semidiscrete solution	104
5.4	Analysis of the Spatial Discretization	106
5.4.1	The finite difference scheme	107
5.4.2	Error analysis	109
5.5	The Fully Discrete Scheme	115
5.6	Numerical Results	116
5.7	Conclusion	117
6	Uniformly Convergent Fractional-Step Method for Singularly Per-	
	turbed System of 2D Parabolic Reaction-Diffusion Problems	120
6.1	Introduction	120
6.2	The Continuous Problem	121
6.3	The Time Semidiscretization	123
6.4	The Spatial Discretization	127
6.4.1	Error analysis	129
6.5	Numerical Results	131
6.6	Conclusions	133
7	Analysis of Uniformly Convergent Numerical Scheme for Singularly	
	Perturbed System of 2D Parabolic Reaction-Diffusion Problems	138
7.1	Introduction	138
7.2	Derivative Bounds and the Solution Decomposition	139
7.3	The Spatial Semidiscretization	145
7.3.1	Discretization of the domain	146
7.3.2	The semidiscrete scheme	147
7.3.3	Truncation error	149
7.4	The Discrete Problem	151
7.4.1	The fully discrete scheme	151
7.4.2	Uniform convergence	152
7.5	Numerical Results	153
7.6	Conclusions	153
8	Summary and Future Scopes	157
8.1	Summary of the Results	157
8.2	Scope for Future Work	158
	Bibliography	161
	Publications	168

NOMENCLATURE

BVP	boundary-value problem
IVP	initial-value problem
IBVP	initial-boundary-value problem
ODE	ordinary differential equation
PDE	partial differential equation
SPP	singular perturbation problem
\mathbb{R}	set of real numbers
$\varepsilon, \varepsilon_1, \varepsilon_2$	singular perturbation parameters
$S_\varepsilon, \widehat{S}_\varepsilon$	set of perturbation parameters
$O(\cdot), o(\cdot)$	landau order symbol
N	number of mesh-intervals in the spatial direction
M	number of mesh-intervals in the time direction
T	final time
x, x_i, y, y_j	continuous and discrete spatial variables
t, t_n	continuous and discrete temporal variables
$h, h_{x,i}, h_{y,j}, H, H_x, H_y, h_x, h_y$	mesh-sizes in spatial direction
Δt	mesh-size in time direction
$\vec{C} = (C, C)^T, C$ (or subscripted)	generic positive constant independent of mesh-points, mesh-sizes and $\varepsilon, \varepsilon_1$ and ε_2
$\ \cdot\ _{\infty, D}$ or $\ \cdot\ _{\infty}$	standard supremum norm on D
$\Omega_x, \Omega_x^+, \Omega_x^-, \Omega_x^{+*}, \Omega_x^{-*}, \bar{\Omega}_x, \Omega_y, \bar{\Omega}_y, \mathcal{D}, \bar{\mathcal{D}}$	continuous spatial domains
$Q, \bar{Q}, Q^+, \bar{Q}^+, Q^-, \bar{Q}^-, Q^{+*}, \bar{Q}^{+*}$	bounded domain in $\mathbb{R} \times [0, T]$ and its closure
\mathcal{G}	$\mathcal{D} \times (0, T]$
Υ^M	discrete time interval $(0, T]$
$\bar{\Omega}_x^N, \bar{\Omega}_y^N, \bar{\mathcal{D}}_\varepsilon^N$	discrete spatial domains
$Q^{N,M}, \mathcal{G}^{N,M}$	discretization of domain Q and \mathcal{G}
$\partial\Omega_x, \partial Q, \partial\mathcal{D}, \partial\mathcal{G}$	boundary of given domains
$\mathcal{C}_\lambda^k(Q), \mathcal{C}_\lambda^k(\mathcal{G})$	function spaces
$L_{x,\bar{\varepsilon}}, \mathbb{L}_{x,\bar{\varepsilon}}, L_{\bar{\varepsilon}}, L_{\bar{\varepsilon}}^*, \mathcal{L}_{\bar{\varepsilon}}, \mathcal{L}_1, \mathcal{L}_2, \mathcal{L}_{\bar{\varepsilon}}^*$	
$\mathcal{L}_{\bar{1},\bar{\varepsilon}}, \mathcal{L}_{\bar{2},\bar{\varepsilon}}, \mathcal{L}_{11,\varepsilon}, \mathcal{L}_{12,\varepsilon}, \mathcal{L}_{21,\varepsilon}, \mathcal{L}_{22,\varepsilon}$	
$\mathcal{L}_{\bar{\varepsilon}}, \mathcal{L}_1, \mathcal{L}_2, \mathcal{L}_{\bar{1},\bar{\varepsilon}}, \mathcal{L}_{\bar{2},\bar{\varepsilon}}, \mathfrak{L}_{\bar{\varepsilon}}$	differential operators
$D_x^+, D_x^-, D_x^0, \delta_x^2, D_y^+, D_y^-, \delta_y^2, D_t^-,$	
$L_{x,\bar{\varepsilon}}^N, \tilde{L}_{x,\varepsilon_1}^N, \tilde{L}_{x,\varepsilon_2}^N, \mathbb{L}_{mu,\varepsilon_1}^N, \mathbb{L}_{mu,\varepsilon_2}^N, \mathbb{L}_{cen,\varepsilon_1}^N,$	
$\mathbb{L}_{cen,\varepsilon_2}^N, \hat{\mathbb{L}}_{\varepsilon_1}^N, \hat{\mathbb{L}}_{\varepsilon_2}^N, L_{\bar{\varepsilon}}^{N,M}, \mathcal{L}_{\bar{1},\bar{\varepsilon}}^N, \mathcal{L}_{\bar{2},\bar{\varepsilon}}^N,$	

$\mathcal{L}_{11,\varepsilon}^N, \mathcal{L}_{12,\varepsilon}^N, \mathcal{L}_{21,\varepsilon}^N, \mathcal{L}_{22,\varepsilon}^N, \widehat{\mathcal{L}}_{1,\varepsilon}^N, \widehat{\mathcal{L}}_{2,\varepsilon}^N, \widehat{\mathcal{L}}_{11,\varepsilon}^N, \widehat{\mathcal{L}}_{12,\varepsilon}^N,$ $\widehat{\mathcal{L}}_{21,\varepsilon}^N, \widehat{\mathcal{L}}_{22,\varepsilon}^N, \mathcal{L}_{1,\varepsilon}^{n+1,N}, \mathcal{L}_{2,\varepsilon}^{n+1,N}, \mathfrak{L}_{\varepsilon}^N, \mathfrak{L}_{\varepsilon}^{N,M}$	difference operators
\vec{u}_0, \vec{g}_0	initial data
\vec{g}_1, \vec{g}_2	boundary data
$d_{\varepsilon,1}^{N,M}, d_{\varepsilon,2}^{N,M}, E_{1,\varepsilon}^{N,M}, E_{2,\varepsilon}^{N,M}$	maximum pointwise error
$d_1^{N,M}, d_2^{N,M}, E_1^{N,M}, E_2^{N,M}$	maximum error
$p_{\varepsilon,1}^{N,M}, p_1^{N,M}, p_{\varepsilon,2}^{N,M}, p_2^{N,M}, P_{\varepsilon,1}^{N,M}, P_{\varepsilon,2}^{N,M},$ $P_1^{N,M}, P_2^{N,M}, \mathcal{P}_{\varepsilon,1}^{N,M}, \mathcal{P}_{\varepsilon,2}^{N,M}, \mathcal{P}_1^{N,M}, \mathcal{P}_2^{N,M}$	order of convergence



List of Figures

2.1	Numerical solution of Example 2.2.3 for $\varepsilon_1 = 2^{-8}$, $\varepsilon_2 = 2^{-4}$ and $N = 64$ at time $t = 1$	20
2.2	Example of piecewise-uniform Shishkin mesh $\overline{\Omega}_x^N$ for $N = 16$	28
2.3	Surface plot of the numerical solution U_1 of Example 2.8.1 for $\varepsilon_1 = 2^{-8}$, $\varepsilon_2 = 2^{-4}$, $N = 64$, $M = 16$	45
2.4	Surface plot of the numerical solution U_2 of Example 2.8.1 for $\varepsilon_1 = 2^{-8}$, $\varepsilon_2 = 2^{-4}$, $N = 64$, $M = 16$	45
2.5	Loglog plot for the spatial order of convergence associated with numerical solution U_1 for Example 2.8.1.	46
2.6	Loglog plot for the spatial order of convergence associated with numerical solution U_2 for Example 2.8.1.	46
2.7	Surface plot of numerical solution U_1 of Example 2.8.2 for $\varepsilon_1 = 2^{-10}$, $\varepsilon_2 = 2^{-6}$, $N = M = 32$	47
2.8	Surface plot of numerical solution U_2 of Example 2.8.2 for $\varepsilon_1 = 2^{-10}$, $\varepsilon_2 = 2^{-6}$, $N = M = 32$	47
2.9	Loglog plot for the spatial order of convergence associated with numerical solution U_1 for Example 2.8.2.	48
2.10	Loglog plot for the spatial order of convergence associated with numerical solution U_2 for Example 2.8.2.	48
2.11	Surface plot of the numerical solution U_1 of Example 2.8.3 for $\varepsilon_1 = 2^{-8}$, $\varepsilon_2 = 2^{-4}$, $N = 64$, $M = 16$	50
2.12	Surface plot of the numerical solution U_2 of Example 2.8.3 for $\varepsilon_1 = 2^{-8}$, $\varepsilon_2 = 2^{-4}$, $N = 64$, $M = 16$	51
2.13	Visualization of the order of convergence through loglog plot associated with numerical solution U_1 for Example 2.8.3.	51
2.14	Visualization of the order of convergence through loglog plot associated with numerical solution U_2 for Example 2.8.3.	52
3.1	Visualization of piecewise-uniform Shishkin mesh $\overline{\Omega}_x^N$ for $N = 16$	59

3.2	Numerical solution of Example 3.6.1 for $\varepsilon_1 = 2^{-7}, \varepsilon_2 = 2^{-5}$ and $N = 64$ at time $t = 1$	73
3.3	Visualization of the order of convergence through loglog plot for numerical solution U_1 of Example 3.6.1.	74
3.4	Visualization of the order of convergence through loglog plot for numerical solution U_2 of Example 3.6.1.	74
4.1	Numerical solutions for Example 4.2.4 for $N = 128$ at time $t = 1$	80
4.2	Piecewise-uniform Shishkin mesh $\overline{\Omega}_x^N$ for $N = 32$	83
4.3	<i>Surface plot of the numerical solution U_1 for $\varepsilon_1 = 2^{-8}, \varepsilon_2 = 2^{-6}$ and $N = 128, M = 32$ of Example 4.4.1.</i>	90
4.4	<i>Surface plot of the numerical solution U_2 for $\varepsilon_1 = 2^{-8}, \varepsilon_2 = 2^{-6}$ and $N = 128, M = 32$ of Example 4.4.1.</i>	90
4.5	<i>Surface plot of the numerical solution U_1 for $\varepsilon_1 = 2^{-8}, \varepsilon_2 = 2^{-6}$ and $N = 128, M = 32$ of Example 4.4.2.</i>	91
4.6	<i>Surface plot of the numerical solution U_2 for $\varepsilon_1 = 2^{-8}, \varepsilon_2 = 2^{-6}$ and $N = 128, M = 32$ of Example 4.4.2.</i>	91
4.7	<i>Loglog plot associated with numerical solution U_1 for Example 4.4.1.</i>	92
4.8	<i>Loglog plot associated with numerical solution U_2 for Example 4.4.1.</i>	92
4.9	<i>Loglog plot associated with numerical solution U_1 for Example 4.4.2.</i>	93
4.10	<i>Loglog plot associated with numerical solution U_2 for Example 4.4.2.</i>	93
5.1	A typical example of piecewise-uniform Shishkin mesh $\overline{\mathcal{D}}_\varepsilon^N$ for $N = 8$	107
5.2	<i>Numerical solution U_1 of Example 5.6.1 for $\varepsilon = 2^{-14}$ with $N = 32, M = 8$.</i>	117
5.3	<i>Numerical solution U_2 of Example 5.6.1 for $\varepsilon = 2^{-14}$ with $N = 32, M = 8$.</i>	118
5.4	<i>Loglog plot for the spatial order of convergence associated with numerical solution U_1 of Example 5.6.1.</i>	118
5.5	<i>Loglog plot for the spatial order of convergence associated with numerical solution U_2 of Example 5.6.1.</i>	119
6.1	A typical example of piecewise-uniform Shishkin mesh $\overline{\mathcal{D}}_\varepsilon^N$ for $N = 16$	128
6.2	<i>Surface plot of the numerical solution U_1 for $\varepsilon = 2^{-10}, N = 64, M = 4$.</i>	134
6.3	<i>Surface plot of the numerical solution U_2 for $\varepsilon = 2^{-10}, N = 64, M = 4$.</i>	134
6.4	<i>Loglog plot (for the temporal order of convergence) associated with numerical solution U_1 of Example 6.5.1.</i>	135
6.5	<i>Loglog plot (for the temporal order of convergence) associated with numerical solution U_2 of Example 6.5.1.</i>	135
6.6	<i>Visualization of the order of convergence (with respect to spatial variable) through loglog plot associated with numerical solution U_1 of Example 6.5.1.</i>	136

6.7	<i>Visualization of the order of convergence (with respect to spatial variable) through loglog plot associated with numerical solution U_2 of Example 6.5.1.</i>	136
7.1	<i>Plots of the numerical solution along the line $x = y$, for $\varepsilon_1 = 2^{-16}$, $\varepsilon_2 = 2^{-10}$ with discretization parameter $N = 64$ at time $t = 1$.</i>	143
7.2	<i>Example of Shishkin mesh \bar{D}_ε^N for $N = 16$</i>	146
7.3	<i>Loglog plot (for the temporal order of convergence) associated with numerical solution U_1 of Example 7.5.1.</i>	154
7.4	<i>Loglog plot (for the temporal order of convergence) associated with numerical solution U_2 of Example 7.5.1.</i>	155
7.5	<i>Loglog plot associated with numerical solution U_1 of Example 7.5.1.</i>	155
7.6	<i>Loglog plot associated with numerical solution U_2 of Example 7.5.1.</i>	156



List of Tables

2.1	Uniform errors and orders of convergence for Example 2.8.1.	49
2.2	Uniform errors and orders of convergence for Example 2.8.2.	49
2.3	Comparison of uniform errors and corresponding rate of convergence before extrapolation and after extrapolation for Example 2.8.3.	52
3.1	Comparison of uniform errors and corresponding rate of convergence between hybrid scheme and upwind scheme for Example 3.6.1.	73
3.2	Uniform errors and corresponding rate of convergence for Example 3.6.1 with different values of τ_0	73
3.3	Uniform errors and corresponding rate of convergence for Example 3.6.1.	74
4.1	Uniform errors and the corresponding order of convergence for Example 4.4.1.	89
4.2	Uniform errors and the corresponding order of convergence for Example 4.4.2.	94
5.1	Uniform errors and the corresponding orders of convergence for Example 5.6.1.	119
6.1	Uniform errors and the corresponding orders of convergence for Example 6.5.1.	137
6.2	Uniform errors and the corresponding orders of convergence for Example 6.5.1.	137
7.1	Uniform errors and the corresponding orders of convergence for Example 7.5.1.	154
7.2	Uniform errors and the corresponding orders of convergence for Example 7.5.1.	156

Introduction

1.1 Singular Perturbation Problem

Singular perturbation problems (SPPs) with smooth and non-smooth data are of common occurrence in several branches of engineering and applied mathematics including fluid mechanics, gas porous electrodes theory, tubular model in chemical reactor theory, neutron transport problems and heat and mass transfer processes in composite material, with sufficiently small diffusion coefficients. Typical examples include the modeling of viscous flow problems with large Reynolds numbers and convective heat transport problems with large Péclet numbers. These types of problems are identified by differential equations in which the highest order spatial derivative is multiplied by small parameters.

In particular, singularly perturbed system of differential equations arise often in several branches of engineering and applied mathematics. The well-known examples of singularly perturbed system of parabolic convection-diffusion problems are the diffusion-convection enzyme model with sufficiently small diffusion coefficients. The simplified mathematical description of enzyme-substrate convection-diffusion model is given by

$$\begin{cases} u_t - D_1 \nabla^2 u + \vec{b} \cdot \nabla u + a_1 E_o u - b_1 w = a_1 u w, \\ w_t - D_2 \nabla^2 w + \vec{b} \cdot \nabla w - a_2 E_o u + b_2 w = a_2 u w, \end{cases}$$

with suitable initial and boundary conditions. Here u , w are the concentration of substrate and enzyme-substrate complex, respectively and E_o is the total enzyme. Here, $\vec{b} = (b_1, b_2)^T$ is velocity of the convecting fluid in the reaction process and a_1, a_2 , various rates of reaction. Next, consider the double-diffusion model for saturated flow in fractured porous media with suitable initial and boundary conditions, introduced in

Barenblatt et al. [3] is as follows:

$$\begin{cases} (\beta_{c_1} + m_1\beta)p_{1t} - \frac{k_1}{\mu}\Delta p_1 + \frac{\alpha}{\mu}(p_1 - p_2) = f_1(x, y, t), \\ (\beta_{c_2} + m_2\beta)p_{2t} - \frac{k_2}{\mu}\Delta p_2 + \frac{\alpha}{\mu}(p_2 - p_1) = f_2(x, y, t), \end{cases}$$

where p_1, p_2 are the pressure of liquid in the pores of the first and second-order respectively, μ is the viscosity of liquid, β_{c_1} and β_{c_2} are positive constants, whereas k_1, k_2 are the porosity of the system of pores of first-and second-order respectively. And m_1, m_2 are the values of the first-and second-order porosity at standard pressure. For sufficiently small values of diffusion coefficients, the above models will be recognized as singularly perturbed system of parabolic problems. In these type of equations, the considerable amount of numerical difficulties arise due to the presence of boundary layers. More details on application of singularly perturbed differential equations can be found in the books by Pao [76], Morton [62] and Murray [67].

The term ‘‘boundary layer’’ was first introduced by Prandtl [77] at the Third International Congress of Mathematicians in Heidelberg in 1904. In his seven-page report on the subject of boundary layer theory, Prandtl discussed about how a quantity as small as the viscosity of common fluid such as water and air could play a crucial role in determining their flow. The boundary layer theory became the foundation stone of modern fluid dynamics. The term ‘‘singular perturbation’’ was first introduced by Friedrichs and Wasow in their paper [29], presented at New York University in 1946.

Singularly perturbed problems are identified by differential equations in which the highest order spatial derivative is multiplied by an arbitrarily small parameter ε . The perturbation is ‘singular’ in the sense that, as $\varepsilon \rightarrow 0$, the problem becomes ill-posed since the order of the differential equation is reduced, but the number of boundary conditions remain the same. In general, the solutions of SPPs possess boundary (or interior) layers which are basically thin regions in the neighborhood of the boundary (or interior) of the domain, where the gradients of the solutions steepen as the perturbation parameter ε tends to zero. Therefore, it is desirable to develop numerical methods, more precisely parameter-uniform numerical methods that solve the singularly perturbed differential equations effectively.

There are two principal approaches for solving SPPs: asymptotic analysis and numerical analysis. The asymptotic analysis tries to gain insight into the qualitative behavior of a family of problems and only semi-quantitative information about any particular member of the family, whereas the numerical analysis tries to provide quantitative information about a particular problem. Asymptotic methods treat comparatively restricted class of problems and require the problem solver to have some understanding of the

behavior of the solution. Numerical methods are intended for a broad class of problems and to minimize demands upon the problem solver. Since the mid-1960s, the theory of singular perturbation problems has grown into a substantial field of study, which has attracted several mathematicians. Numerous good textbooks have appeared in this area which either dealt with the asymptotic approach or with the numerical ones. Some of the books dealt with both of these. One may refer to the books of Miller [58], Nayfeh [72], O'Malley [73, 74], Kevorkian and Cole [41], Bush [8], Miller et al. [57], Roos et al. [82] and articles of Berger et al. [6, 7].

A common technique to study the nature of the analytical solution of SPPs as the small parameter ε goes to zero is through asymptotic expansion technique. A straightforward perturbation expansion leads to differential equations of lower order than the original governing equation by using an asymptotic series in the small parameter ε . As a result, all of the boundary or initial conditions cannot be satisfied by the perturbation expansion. To overcome from such difficulties, one has to combine the straightforward expansion known as the *outer expansion* valid away from the boundary layer, with an expansion called the *inner expansion* valid within a layer adjacent to the boundary where the boundary condition is not satisfied. The inner expansion associated within the boundary layer region is expressed in terms of a stretched variable rather than the original independent variable, which takes account of the scale of certain derivative terms. The inner and outer expansions are matched over a region located at the edge of the boundary layer using the method of *matched asymptotic expansion*. Note that one needs to know the width and the location of the boundary layer before solving the problem which can be acquired using the *principle of least degeneracy* introduced by Van Dyke [91]. For more details about the asymptotic expansion technique, one can refer to the books of Bush [8], Lagerstrom [43], O' Malley [73, 74] and the survey articles of Lagerstrom and Casten [44], Smith [85] and Miller [58].

The development of parameter-uniform numerical methods over the past few decades, can be arranged into two different categories. The first methodology involves the replacement of the standard finite difference operator by a difference operator which reflects the singularly perturbed nature of the differential operator. The modified difference operators are referred as fitted finite difference operators, which are constructed by using a proper choice of difference coefficients so that some or all of the exponential functions are in the null space of the differential operators. Such fitted finite difference operator on a standard mesh (very often a uniform mesh) are referred as *fitted operator methods* (FOMs). The FOMs were first introduced by Allen et al. [23] for solving the problem of a viscous fluid flow past a cylinder. One can find extensive amount of work on ε -uniform FOMs in Farrell [26] and in the books of Doolan et al. [25] and Miller et al.

[57]. Munyakazi [66] considered nonstandard finite difference scheme for solving system of convection-diffusion problems.

The second approach for the construction of ε -uniform method involves the use of classical finite difference schemes on spacial non-uniform meshes condensed in boundary and interior layers. Such numerical methods are referred as *fitted mesh methods* (FMMs). In FMMs, the meshes are constructed in such a way that the density of mesh points will be higher in the boundary layer regions compared to the outer regions. These methods have an extra advantages over FOMs due to their implementations with the standard operators and their extension to higher-dimensional problems. The well-known layer resolving fitted meshes are Bakhvalov meshes [2] and Shishkin meshes [83]. In both the cases one requires *a priori* information about the width and location of the boundary layer. For more details, one may refer the books by Doolan et al. [25], Farrell et al. [27], Miller et al. [57] and Roos et al. [82] and survey articles of Kadalbajoo et al. [34, 35, 36]. Marchuk [55] and Yanenko [96] considered operator splitting technique for analyzing the multi-dimensions partial differential equations.

1.2 Objective and Motivation

The main objective of this thesis is to develop and analyze parameter-uniform FMMs for solving singularly perturbed system of parabolic convection-diffusion and reaction-diffusion initial-boundary-value problems (IBVPs) in one-and two-dimensions on the piecewise-uniform Shishkin mesh. A brief survey of the literature illustrating motivation behind the present work, carried out in the thesis, is presented below:

In the recent past, construction of uniformly convergent numerical schemes for solving singularly perturbed system of ODEs have received a significant attention by several researchers. One can refer to the books of Linß [47], Shishkin, and Shishkina [84], where different types of parameter-uniform numerical schemes have been discussed. A weakly coupled system of convection-diffusion problems has been analyzed in Cen [10] and Linß [46]. Das and Natesan [20] and Liu and Chen [51] proposed an ε -uniformly convergent scheme for singularly perturbed system of ODEs, by using the mesh equidistribution technique. Bellew and O’Riordan [5] examined an upwind difference scheme to solve coupled system of convection-diffusion equations. O’Riordan and Stynes [75] analyzed an upwind difference scheme for a strongly coupled system of singularly perturbed convection-diffusion problems. Deb and Natesan [24] applied the Richardson extrapolation technique for system of convection-diffusion equation to improve the accuracy of the upwind numerical scheme. For singularly perturbed system of reaction-diffusion problems, Matthews et al. [56], Madden and Stynes [52] considered a uniformly convergent

numerical method which produces almost first-order accurate numerical approximation. To improve the accuracy (from almost first-order to almost second-order convergence) of the numerical approximation of both the previous articles, Linß and Madden [48, 49] followed a special approach for the error estimate of the proposed numerical method. Das and Natesan [22] used the mesh equidistribution technique to obtain optimal error estimate for singularly perturbed system of reaction-diffusion BVPs. For weakly coupled system of ODEs with discontinuous source term, Tamilselvan et al. [89, 90] analyzed parameter-uniform numerical method. A detailed survey on singularly perturbed system of differential equation is presented in Linß and Stynes [50].

For the past few years, a great amount of work have been done by many researchers for singularly perturbed stationary and non-stationary problems. Cai and Liu [9] and Stynes [86] developed uniformly convergent numerical methods on the piecewise-uniform Shishkin mesh for the convection-diffusion problems. Gowrisankar and Natesan [30, 31] proposed parameter-uniform computational techniques to solve singularly perturbed delay parabolic partial differential equations. Majumdar and Natesan [54], considered second-order uniformly convergent Richardson extrapolation method for singularly perturbed degenerate parabolic problems. Mohapatra and Natesan [59, 60, 61] used the adaptive mesh generation method to solve singularly perturbed boundary-value problems (BVPs). Also, one can look at the articles [4, 68, 69, 70, 71, 92, 93], in which Natesan and his collaborators have proposed initial-value techniques and parallel boundary-value techniques for singularly perturbed BVPs. Xenophontos and Oberbroeckling [95] discussed p/hp finite element approximation for systems of reaction-diffusion equations. Later, Xenophontos et al. [94] analyzed finite element approximation of convection-diffusion problems by using an exponentially graded mesh. Ramos [79, 80] developed exponentially-fitted methods for singularly perturbed differential equations and differential-difference equations.

Here, we cite some articles, which are dealt with the hybrid numerical scheme. The hybrid numerical scheme is a proper combination of the midpoint upwind scheme (for the outer region) and the central difference scheme (for the inner region). The midpoint upwind scheme was first introduced by Abrahamsson et al. [1]. Then, Stynes and Roos [87] combined this scheme with the central difference scheme to solve 1D singularly perturbed two-point BVPs. For stationary singularly perturbed system, Priyadharshini et al. [78] proposed the hybrid scheme. In [21], Das and Natesan analyzed a uniformly convergent hybrid scheme for singularly perturbed system of reaction-diffusion Robin type boundary-value problems. Cen et al. [11] considered the hybrid difference method for a system of singularly perturbed initial value problems on Shishkin mesh. For singularly perturbed parabolic PDEs, Mukherjee and Natesan proposed the hybrid scheme in [63].

Also Mukherjee and Natesan [65] considered the hybrid numerical scheme to improve the accuracy of the numerical approximate solution of parabolic IBVPs with interior layers. Clavero et al. [12] analyzed the hybrid numerical method for time-dependent convection-diffusion problems by simplifying the truncation error analysis. Later on Das and Natesan [17] extended the idea of hybrid scheme to solve singularly perturbed delay parabolic PDEs.

In recent years, various ε -uniform numerical schemes are proposed in the literature for singularly perturbed 2D parabolic initial-boundary-value problems. For instance, Clavero et al. [16] proposed a numerical scheme, which consists of an alternating direction scheme for the temporal discretization and central finite difference method for the spatial discretization. Clavero and Jorge [13] considered a monotone finite difference schemes to approximate 2D singularly perturbed parabolic problems of convection-reaction-diffusion type with implicit-Euler method as time integrators. Das and Natesan [19] analyzed a parameter-uniform numerical method for solving singularly perturbed 2D delay parabolic convection-diffusion problems on Shishkin mesh. Das and Natesan [18] proposed a higher-order fractional-step method for singularly perturbed 2D parabolic convection-diffusion problems. Majumdar and Natesan [53] analyzed an ADI numerical scheme for singularly perturbed 2D degenerate parabolic problems on Shishkin mesh.

However, the theory and numerical solution of singularly perturbed system of parabolic PDEs are still at the primary stage. Rao and Srivastava [81] analyzed a numerical scheme which is a combination of HODIE scheme and the central difference scheme in space with backward-Euler method in time direction to solve time-dependent singularly perturbed system of convection-diffusion problems with a single parameter. The proposed numerical scheme is of almost second-order accurate in space and first-order accurate in time. Gracia and Lisbona [32] applied a classical finite difference scheme on the Shishkin mesh to obtain the uniformly convergent numerical solution of singularly perturbed system of parabolic problems of reaction-diffusion type. They proved that the numerical scheme is uniformly convergent, having first-order convergence in time and almost second-order convergence in space. In [33], Gracia et al. applied the central difference scheme to solve singularly perturbed coupled system of parabolic reaction-diffusion equations. The proposed numerical scheme is of almost first-order accurate in space and first-order accurate in time. Franklin et al. [28] studied a central difference scheme for singularly perturbed system of parabolic reaction-diffusion problems. It is shown that the numerical approximations obtained with this method are first-order convergent in time and almost second-order convergent in the spatial variable.

Finally, we turn our attention to develop parameter-uniform numerical methods for singularly perturbed system of convection-diffusion and reaction-diffusion problems in

two-dimension. In [39], Kellogg et al. considered a class of singularly perturbed system of 2D elliptic reaction-diffusion problems with a single parameter. In [38], Kellogg et al. studied the same problem with different hypothesis on the reaction coefficients. Because of the hypothesis, later the model problem did not satisfy the maximum principle. For both the problems in [39, 38], they applied the standard central finite difference scheme on the Shishkin mesh and Shishkin-type mesh, respectively. The proposed schemes are ε -uniformly convergent of almost second-order for Shishkin mesh while second-order uniform convergence for the Bakhvalov mesh.

From the literature, one can observe that no work has been carried out till now to solve singularly perturbed system of parabolic PDEs of convection-diffusion type with different parameters in one-dimension. Some work has been carried out with single parameter case only. And for the system of reaction-diffusion problems, the previous research work has been limited to one-dimension only. By considering all these facts, we propose some numerical schemes for solving singularly perturbed system of parabolic convection-diffusion and reaction-diffusion problems in one- and two-dimensions.

1.3 Preliminaries

In this section, we introduce some essential definitions, notations and convention which will be used throughout the thesis.

We denote $C^k(\mathcal{Q})$ as the space of all functions whose derivatives up to order $k \geq 0$ are continuous on \mathcal{Q} , where \mathcal{Q} is a bounded domain in $\mathbb{R}^n \times [0, T]$.

Next, we introduce the Hölder continuous function. The set of all Hölder continuous functions in \mathcal{Q} , forms a normed linear vector space $C_\lambda^0(\mathcal{Q})$ with the norm

$$\|u\|_{\lambda, \mathcal{Q}} \equiv \|u\|_{\mathcal{Q}} + \sup_{(\mathbf{x}_1, t_1), (\mathbf{x}_2, t_2) \in \mathcal{Q}} \left\{ \frac{|u(\mathbf{x}_1, t_1) - u(\mathbf{x}_2, t_2)|}{(|\mathbf{x}_1 - \mathbf{x}_2|^2 + |t_1 - t_2|)^{\lambda/2}} \right\},$$

where $\|u\|_{\mathcal{Q}} = \sup_{(\mathbf{x}, t) \in \mathcal{Q}} |u(\mathbf{x}, t)|$.

For each integer $k \geq 1$ and all non-negative integers k_x, k_t , the subspaces $C_\lambda^k(\mathcal{Q})$ of $C_\lambda^0(\mathcal{Q})$, which contain functions having Hölder continuous derivatives defined as follows:

$$C_\lambda^k(\mathcal{Q}) = \left\{ u : \frac{\partial^{k_x+k_t} u}{\partial \mathbf{x}^{k_x} \partial t^{k_t}} \in C_\lambda^0(\mathcal{Q}), \text{ such that } 0 \leq k_x + 2k_t \leq k \right\}.$$

The norm on $C_\lambda^k(\mathcal{Q})$ is taken to be

$$\|u\|_{k, \lambda, \mathcal{Q}} = \max_{0 \leq k_x + 2k_t \leq k} \left\| \frac{\partial^{k_x+k_t} u}{\partial \mathbf{x}^{k_x} \partial t^{k_t}} \right\|_{\lambda, \mathcal{Q}}.$$

For vector-valued function $\vec{u} = (u_1, u_2) \in (C_\lambda^k(\mathcal{Q}))^2$, the norm of \vec{u} is defined by $\|\vec{u}\|_{k, \lambda, \mathcal{Q}} = \max\{\|u_1\|_{k, \lambda, \mathcal{Q}}, \|u_2\|_{k, \lambda, \mathcal{Q}}\}$.

In the analysis, we use the standard supremum norm $\|\cdot\|_{\infty, \mathcal{Q}}$, which is defined by

$$\|g(\mathbf{x}, t)\|_{\infty, \mathcal{Q}} = \max_{(\mathbf{x}, t) \in \mathcal{Q}} |g(\mathbf{x}, t)|,$$

for a scalar function $g(\mathbf{x}, t)$. It is a convention that when the domain is obvious, or of no particular significance, \mathcal{Q} is omitted. For vector-valued function $\vec{g}(\mathbf{x}, t) := (g_1(\mathbf{x}, t), g_2(\mathbf{x}, t))^T$, set $|\vec{g}(\mathbf{x}, t)| = (|g_1(\mathbf{x}, t)|, |g_2(\mathbf{x}, t)|)^T$, and we define the standard supremum norm by

$$\|\vec{g}\|_{\infty, \mathcal{Q}} = \max \{ \|g_1(\mathbf{x}, t)\|_{\infty, \mathcal{Q}}, \|g_2(\mathbf{x}, t)\|_{\infty, \mathcal{Q}} \}.$$

Throughout this thesis $\vec{C} = (C, C)^T$, C denotes a generic positive constant, which is independent of ε , ε_1 , ε_2 and of mesh parameters, not necessarily taking the same values at different occurrences.

Now, we define the standard finite difference operators which are useful for describing the difference schemes in the subsequent chapters. For that, we consider the arbitrary meshes in the spatial directions as $\bar{\Omega}_x^N = \{0 = x_0 < x_1 < \dots < x_N = 1\}$, $\bar{\Omega}_y^N = \{0 = y_0 < y_1 < \dots < y_N = 1\}$ and in the temporal direction as $\Upsilon^M = \{0 = t_0 < t_1 < \dots < t_n = T\}$.

For a given mesh function $v(x_i, t_n) = v_i^n$, define the forward, backward and central difference operators D_x^+ , D_x^- and D_x^0 in space by

$$D_x^+ v_i^n = \frac{v_{i+1}^n - v_i^n}{x_{i+1} - x_i}, \quad D_x^- v_i^n = \frac{v_i^n - v_{i-1}^n}{x_i - x_{i-1}} \quad \text{and} \quad D_x^0 v_i^n = \frac{v_{i+1}^n - v_{i-1}^n}{x_{i+1} - x_{i-1}},$$

respectively, and we define the second-order central difference operator δ_x^2 by

$$\delta_x^2 v_i^n = \frac{2(D_x^+ v_i^n - D_x^- v_i^n)}{x_{i+1} - x_{i-1}},$$

and define the backward difference operator D_t^- in time by

$$D_t^- v_i^n = \frac{v_i^n - v_i^{n-1}}{t_n - t_{n-1}}.$$

In an analogous way, for a given mesh function $v(x_i, y, t_n) = v_{x_i, y}^n$, $y \in \Omega_y^N$, we define the forward difference operator D_x^+ , the backward difference operator D_x^- (for first-order spatial derivative) and the central difference operator δ_x^2 (for second-order spatial derivative) in spatial x -direction by

$$D_x^+ v_{x_i, y}^n = \frac{v_{x_{i+1}, y}^n - v_{x_i, y}^n}{x_{i+1} - x_i}, \quad D_x^- v_{x_i, y}^n = \frac{v_{x_i, y}^n - v_{x_{i-1}, y}^n}{x_i - x_{i-1}} \quad \text{and} \quad \delta_x^2 v_{x_i, y}^n = \frac{2(D_x^+ v_{x_i, y}^n - D_x^- v_{x_i, y}^n)}{x_{i+1} - x_{i-1}},$$

respectively.

Similarly, we define all the difference operators in the y -direction. The backward difference operator D_t^- is defined by

$$D_t^- v_{x_i, y_j}^n = \frac{v_{x_i, y_j}^n - v_{x_i, y_j}^{n-1}}{t_n - t_{n-1}}$$

to approximate the first-order time derivative.

To measure the performance and the robustness of a numerical method, let us introduce the concept of uniform accuracy.

Definition 1.3.1. (\mathcal{E} -Uniform numerical method) Let \vec{u}_ε be the solution of a singularly perturbed system of parabolic problem, and let \vec{U}_ε be a numerical approximation of \vec{u}_ε obtained by a numerical method on the discrete space $\overline{Q}^{N, \Delta t}$ with the discretization parameters N and Δt . The numerical method is said to be **uniformly convergent** or **robust** with respect to perturbation parameters $\varepsilon_1, \varepsilon_2$ in the norm $\|\cdot\|_\infty$, if there exist a positive integer N_0 and positive number 'C', p and q such that for all $N \geq N_0$ and $M \geq M_0$, where $M = T/\Delta t$, we have

$$\sup_{0 < \varepsilon_1, \varepsilon_2 \ll 1} \|\vec{U}_\varepsilon - \vec{u}_\varepsilon\|_\infty \leq C (N^{-p} + \Delta t^q),$$

where N_0, M_0, C, p and q are independent of $\varepsilon_1, \varepsilon_2$.

Here p and q are \mathcal{E} -uniform order of convergence with respect to the spatial and temporal variables, respectively, and C is called the \mathcal{E} -uniform error constant.

We will use frequently the maximum norm in our analysis. This is due to the measurement of the errors from the small part of the domain where boundary layer occurs. Other norms, specially the root mean square norm fails to capture the local behavior of the error inside the boundary layer regions. for further discussion on the choice of the norms, one can refer book of Miller et al. [57].

The next definition is of **Landau's order symbols** O (big-oh) and o (little-oh), which are used throughout the thesis. Let $f(\varepsilon)$ and $g(\varepsilon)$ be two real valued functions, where $0 < \varepsilon \leq \varepsilon_0 \ll 1$.

Definition 1.3.2. The expression $f(\varepsilon) = O(g(\varepsilon))$ as $\varepsilon \rightarrow 0$, defines that there exist some positive constants C and ε_0 satisfying $\varepsilon \in (0, \varepsilon_0]$ such that

$$|f(\varepsilon)| \leq C |g(\varepsilon)|, \quad \varepsilon \rightarrow 0.$$

Definition 1.3.3. The expression $f(\varepsilon) = o(g(\varepsilon))$ as $\varepsilon \rightarrow 0$, defines that

$$\lim_{\varepsilon \rightarrow 0} \frac{f(\varepsilon)}{g(\varepsilon)} = 0.$$

Definition 1.3.4. A matrix $\mathbf{A} = (a_{lm}) \in \mathbb{R}^{n,n}$ is an L_0 -matrix if $a_{ll} > 0$ and $a_{lm} \leq 0$, for all $l \neq m$, $1 \leq l, m \leq k$.

Definition 1.3.5. A matrix $\mathbf{A} = (a_{lm}) \in \mathbb{R}^{n,n}$ is an M -matrix if \mathbf{A} is nonsingular, $\mathbf{A}^{-1} \geq 0$ and $a_{lm} \leq 0$, for all $l \neq m$, $1 \leq l, m \leq k$.

Finally, for the sake of simplicity, we define some functions which will be used frequently while estimating the derivative bounds of the solution and their components:

- $B_{\varepsilon_1}^0(x) = \exp(-\alpha x/\varepsilon_1)$, $B_{\varepsilon_2}^0(x) = \exp(-\alpha x/\varepsilon_2)$,
- $B_{\varepsilon}^1(x) = \exp(-\alpha(1-x)/\varepsilon)$, $B_{\varepsilon}^1(y) = \exp(-\alpha(1-y)/\varepsilon)$,
- $B_{\varepsilon_1}^1(x) = \exp(-\alpha(1-x)/\varepsilon_1)$, $B_{\varepsilon_2}^1(x) = \exp(-\alpha(1-x)/\varepsilon_2)$,
- $B_{\varepsilon_1}^-(x) = \exp(-\alpha(\xi-x)/\varepsilon_1)$, $B_{\varepsilon_2}^-(x) = \exp(-\alpha(\xi-x)/\varepsilon_2)$,
- $B_{\varepsilon_1}^+(x) = \exp(-\alpha(x-\xi)/\varepsilon_1)$, $B_{\varepsilon_2}^+(x) = \exp(-\alpha(x-\xi)/\varepsilon_2)$,
- $\mathcal{B}_{\varepsilon}(x) = \exp(-\beta x/\varepsilon) + \exp(-\beta(1-x)/\varepsilon)$,
- $\mathcal{B}_{\varepsilon}(y) = \exp(-\beta y/\varepsilon) + \exp(-\beta(1-y)/\varepsilon)$
- $\mathcal{B}_{\varepsilon_1}(x) = \exp(-\beta x/\varepsilon_1) + \exp(-\beta(1-x)/\varepsilon_1)$,
- $\mathcal{B}_{\varepsilon_1}(y) = \exp(-\beta y/\varepsilon_1) + \exp(-\beta(1-y)/\varepsilon_1)$,
- $\mathcal{B}_{\varepsilon_2}(x) = \exp(-\beta x/\varepsilon_2) + \exp(-\beta(1-x)/\varepsilon_2)$,
- $\mathcal{B}_{\varepsilon_2}(y) = \exp(-\beta y/\varepsilon_2) + \exp(-\beta(1-y)/\varepsilon_2)$,

where α and β will be fixed later in following chapters and ξ is the point of discontinuity of the convection coefficients and the source term in model problem (1.4.4) and problem discussed in Chapter 4.

1.4 Model Problems

In this section, the model problems considered in this thesis are described briefly. For clarity of the presentation, we elaborately provide these model problems with suitable information on the given data at the beginning of the subsequent chapters.

The following types of model problems are considered and their concise descriptions are given below:

1.4.1 Singularly perturbed system of 1D parabolic convection-diffusion problem

Consider the following singularly perturbed system of parabolic convection-diffusion IBVP in the domain $Q := \Omega_x \times (0, T]$, $\Omega_x = (0, 1)$:

$$\begin{cases} \frac{\partial \vec{u}}{\partial t} + L_{x,\varepsilon} \vec{u} = \vec{f}, & (x, t) \in Q, \\ \vec{u}(x, 0) = \vec{u}_0(x), & x \in \bar{\Omega}_x, \\ \vec{u}(0, t) = \vec{0}, \quad \vec{u}(1, t) = \vec{0}, & t \in (0, T], \end{cases} \quad (1.4.1)$$

where the spatial differential operator $L_{x,\varepsilon}$ is given by

$$L_{x,\varepsilon} \equiv -\mathcal{E} \frac{\partial^2}{\partial x^2} - A(x) \frac{\partial}{\partial x} + B(x),$$

and the coefficient matrices are $\mathcal{E} = \text{diag}(\varepsilon_1, \varepsilon_2)$, $A(x) = \text{diag}(a_1(x), a_2(x))$ and $B(x) = \{b_{lm}(x)\}_{l,m=1}^2$.

Without loss of generality, we assume that $\varepsilon_1, \varepsilon_2$ satisfy $0 < \varepsilon_1 \leq \varepsilon_2 \ll 1$, and the coefficients of the convection matrix A satisfies the following positivity conditions:

$$a_1(x) \geq \alpha > 0, \quad a_2(x) \geq \alpha > 0.$$

In addition, we assume that B is an L_0 -matrix with

$$\min_{x \in \bar{\Omega}_x} \{b_{11}(x) + b_{12}(x), b_{21}(x) + b_{22}(x)\} \geq \beta > 0.$$

Under sufficient smoothness and compatibility conditions imposed on the data of the model problem (1.4.1), the exact solution \vec{u} has overlapping boundary layers at $x = 0$.

1.4.2 Singularly perturbed system of 1D semilinear parabolic problem

Consider the following singularly perturbed system of semilinear parabolic convection-diffusion IBVP:

$$\begin{cases} \frac{\partial \vec{u}}{\partial t} - \mathcal{E} \frac{\partial^2 \vec{u}}{\partial x^2} - A(x) \frac{\partial \vec{u}}{\partial x} + \vec{f}(x, t, \vec{u}) = \vec{0}, & (x, t) \in Q, \\ \vec{u}(x, 0) = \vec{u}_0(x), & x \in \bar{\Omega}_x, \\ \vec{u}(0, t) = \vec{0}, \quad \vec{u}(1, t) = \vec{0}, & t \in (0, T], \end{cases} \quad (1.4.2)$$

where $\vec{f}(x, t, \vec{u}) = (f_1(x, t, u_1, u_2), f_2(x, t, u_1, u_2))^T$. The coefficient matrices \mathcal{E} and A are defined as in the previous subsection. We also assume that f_1 and f_2 are sufficiently smooth functions satisfying certain regularity conditions.

1.4.3 Singularly perturbed system of 1D parabolic convection-diffusion problem with boundary layers

Consider the following class of singularly perturbed system of parabolic convection-diffusion IBVP:

$$\begin{cases} \frac{\partial \vec{u}}{\partial t} + \mathbb{L}_{x,\varepsilon} \vec{u} = \vec{f}, & (x, t) \in Q, \\ \vec{u}(x, 0) = \vec{u}_0(x), & x \in \bar{\Omega}_x, \\ \vec{u}(0, t) = \vec{0}, \quad \vec{u}(1, t) = \vec{0}, & t \in (0, T], \end{cases} \quad (1.4.3)$$

where the spatial differential operator $\mathbb{L}_{x,\varepsilon}$ is given by

$$\mathbb{L}_{x,\varepsilon} \equiv -\mathcal{E} \frac{\partial^2}{\partial x^2} + A(x) \frac{\partial}{\partial x} + B(x).$$

The coefficient matrices are given as $\mathcal{E} = \text{diag}(\varepsilon_1, \varepsilon_2)$, $0 < \varepsilon_1 \leq \varepsilon_2 \ll 1$, $A(x) = \text{diag}(a_1(x), a_2(x))$ and $B(x) = \{b_{lm}(x)\}_{l,m=1}^2$. The coefficient matrices A and B satisfy positivity condition from previous subsection. Under sufficient smoothness and compatibility conditions imposed on the data of the IBVP (1.4.3), the exact solution \vec{u} exhibits overlapping boundary layers at $x = 1$.

1.4.4 Singularly perturbed system of 1D parabolic convection-diffusion problem with interior layers

Denote the domain for describing the model problem by

$$Q^- = \Omega_x^- \times (0, T], \quad Q^+ = \Omega_x^+ \times (0, T], \quad Q = \Omega_x \times (0, T], \quad \Omega_x^- = (0, \xi), \quad \Omega_x^+ = (\xi, 1), \quad \Omega_x = (0, 1).$$

Consider the following class of singular perturbed system of parabolic convection-diffusion problems in the domain $Q^- \cup Q^+$:

$$\begin{cases} L_\varepsilon \vec{u} \equiv \frac{\partial \vec{u}}{\partial t} - \mathcal{E} \frac{\partial^2 \vec{u}}{\partial x^2} + A(x) \frac{\partial \vec{u}}{\partial x} + B(x) \vec{u} = \vec{f}, & (x, t) \in Q^- \cup Q^+, \\ \vec{u}(x, 0) = \vec{g}_0(x) \quad \forall x \in \bar{\Omega}_x, \\ \vec{u}(0, t) = \vec{g}_1(t), \quad \vec{u}(1, t) = \vec{g}_2(t) \quad \forall t \in [0, T], \end{cases} \quad (1.4.4)$$

where coefficients $\mathcal{E} = \text{diag}(\varepsilon_1, \varepsilon_2)$ and $B = \{b_{lm}\}_{l,m=1}^2$ with the convection coefficient $A = \text{diag}(a_1, a_2)$, where a_1 and a_2 are defined as

$$a_1(x) = \begin{cases} a_1^-(x), & x \in \Omega_x^- \\ a_1^+(x), & x \in \Omega_x^+, \end{cases} \quad a_2(x) = \begin{cases} a_2^-(x), & x \in \Omega_x^- \\ a_2^+(x), & x \in \Omega_x^+. \end{cases}$$

We assume that the convection coefficients and source terms satisfy

$$\begin{cases} |[a_1]| \leq C, |[a_2]| \leq C, |[f_1]| \leq C, \text{ and } |[f_2]| \leq C, \text{ at } x = \xi \\ \alpha_1^* \geq a_1^-(x), a_2^-(x) \geq \alpha_1 > 0, x < \xi \text{ and } -\alpha_2^* \leq a_1^+(x), a_2^+(x) \leq -\alpha_2 < 0, x > \xi, \end{cases}$$

and we assume that $B = \{b_{lm}\}_{l,m=1}^2$ is an L_0 -matrix with

$$\min_{x \in \overline{\Omega}_x} \{b_{11}(x) + b_{12}(x), b_{21}(x) + b_{22}(x)\} \geq \beta > 0.$$

It will be assumed that the convection coefficient A is sufficiently smooth on $\Omega_x^- \cup \Omega_x^+$, whereas the source term $\vec{f}(x, t)$ is sufficiently smooth on $Q^- \cup Q^+$ and the reaction coefficient B is a sufficiently smooth function on \overline{Q} .

The solution $\vec{u} = (u_1, u_2)^T$ satisfies the following interface conditions

$$[u_l] = 0, \quad \left[\frac{\partial u_l}{\partial x} \right] = 0, \quad \text{at } x = \xi, \quad l = 1, 2.$$

We define the jump of the solution components u_l , denoted by $[u_l]$, across the point of discontinuity $x = \xi$ by

$$[u_l](\xi, t) = u_l(\xi^+, t) - u_l(\xi^-, t), \quad \text{where } u_l(\xi^\pm, t) = \lim_{x \rightarrow \xi^\pm 0} u_l(x, t).$$

Due to the presence of discontinuity in the convection coefficient $A(x)$ and the source term $\vec{f}(x, t)$, the exact solution $\vec{u}(x, t)$ of the problem (1.4.4) possesses overlapping interior layers in the neighborhood of the point $x = \xi$. In fact, the nature of the interior layer depends on the sign of the convection coefficient $A(x)$ on either side of the line of discontinuity.

1.4.5 Singularly perturbed system of 2D parabolic convection-diffusion problem

Consider the following singularly perturbed system of 2D parabolic convection-diffusion IBVP in the domain $\mathcal{G} := \mathcal{D} \times (0, T]$, $\mathcal{D} = \Omega_x \times \Omega_y = (0, 1) \times (0, 1)$:

$$\begin{cases} \frac{\partial \vec{u}}{\partial t}(x, y, t) + \mathcal{L}_\varepsilon \vec{u}(x, y, t) = \vec{f}(x, y, t), & (x, y, t) \in \mathcal{G}, \\ \vec{u}(x, y, 0) = \vec{u}_0(x, y), & (x, y) \in \overline{\mathcal{D}}, \\ \vec{u}(0, y, t) = \vec{u}(1, y, t) = \vec{0}, & (y, t) \in [0, 1] \times [0, T], \\ \vec{u}(x, 0, t) = \vec{u}(x, 1, t) = \vec{0}, & (x, t) \in [0, 1] \times [0, T], \end{cases} \quad (1.4.5)$$

where the spatial differential operator \mathcal{L}_ε is given by

$$\mathcal{L}_\varepsilon \equiv -\mathcal{E} \left(\frac{\partial^2}{\partial x^2} + \frac{\partial^2}{\partial y^2} \right) + A_1(x, y) \frac{\partial}{\partial x} + A_2(x, y) \frac{\partial}{\partial y} + B(x, y).$$

The coefficient matrices of the model problem (1.4.5) are given as $\mathcal{E} = \text{diag}(\varepsilon, \varepsilon)$, $A_1 = \text{diag}(a_{11}, a_{12})$, $A_2 = \text{diag}(a_{21}, a_{22})$ and $B = \{b_{lm}(x)\}_{l,m=1}^2$. We assume that the diffusion

coefficient $0 < \varepsilon \ll 1$. Assume that the matrices A_1 , A_2 and B are sufficiently smooth and satisfy the following conditions:

$$\left\{ \begin{array}{l} a_{11}(x, y), a_{12}(x, y) > \alpha_1 > 0, \quad a_{21}(x, y), a_{22}(x, y) > \alpha_2 > 0, \\ b_{ll}(x, y) > \gamma_\beta > 0, \quad b_{lm}(x, y) \leq 0, \text{ for } l \neq m, \\ \min_{(x,y) \in \overline{\mathcal{D}}} \{b_{11}(x, y) + b_{12}(x, y), b_{21}(x, y) + b_{22}(x, y)\} \geq \beta > 0, \\ \gamma_1 = \max_{\overline{\mathcal{D}}} \{|b_{12}(x, y)|/b_{11}(x, y)\}, \quad \gamma_2 = \max_{\overline{\mathcal{D}}} \{|b_{21}(x, y)|/b_{22}(x, y)\}. \end{array} \right.$$

Under sufficient smoothness and compatibility conditions imposed on the data of the IBVP (1.4.5), the exact solution \vec{u} exhibits boundary layers along the sides $x = 1$ and $y = 1$, and a corner layer at $(x, y) = (1, 1)$.

1.4.6 Singularly perturbed system of 2D parabolic reaction-diffusion problem

Consider the following singularly perturbed system of 2D parabolic reaction-diffusion IBVP:

$$\left\{ \begin{array}{l} \frac{\partial \vec{u}}{\partial t}(x, y, t) + \mathcal{L}_\varepsilon \vec{u}(x, y, t) = \vec{f}(x, y, t), \quad (x, y, t) \in \mathcal{G}, \\ \vec{u}(x, y, 0) = \vec{u}_0(x, y), \quad (x, y) \in \overline{\mathcal{D}}, \\ \vec{u}(0, y, t) = \vec{u}(1, y, t) = \vec{0}, \quad (y, t) \in [0, 1] \times [0, T], \\ \vec{u}(x, 0, t) = \vec{u}(x, 1, t) = \vec{0}, \quad (x, t) \in [0, 1] \times [0, T], \end{array} \right. \quad (1.4.6)$$

where the spatial differential operator \mathcal{L}_ε is given by

$$\mathcal{L}_\varepsilon \equiv -\varepsilon^2 \Delta + B(x, y, t).$$

The diffusion and reaction coefficients of the model problem (1.4.6) are given by $\mathcal{E} = \text{diag}(\varepsilon, \varepsilon)$, $0 < \varepsilon \ll 1$ and $B = \{b_{lm}(x)\}_{l,m=1}^2$, respectively. The coefficients of reaction matrix $B(x, y, t)$ satisfies the following conditions:

$$\left\{ \begin{array}{l} b_{ll}(x, y, t) > \gamma_\beta > 0, \quad b_{lm}(x, y, t) \leq 0, \text{ for } l \neq m, \\ \min_{(x,y,t) \in \overline{\mathcal{G}}} \{b_{11}(x, y, t) + b_{12}(x, y, t), b_{21}(x, y, t) + b_{22}(x, y, t)\} \geq \beta^2 > 0. \end{array} \right.$$

Also we assume that $\gamma_1 = \max_{\overline{\mathcal{G}}} \{|b_{12}|/b_{11}\}$, $\gamma_2 = \max_{\overline{\mathcal{G}}} \{|b_{21}|/b_{22}\}$, $0 \leq \gamma := \max\{\gamma_1, \gamma_2\} < 1$. We consider the certain smoothness assumptions for the source term and the initial condition such that the exact solution \vec{u} of model problem (1.4.6) exhibits boundary layers along the sides $x = 0, 1$ and $y = 0, 1$ with corner layers at all corners of the spatial domain.

1.4.7 Singularly perturbed system of 2D parabolic reaction-diffusion problem with overlapping boundary layers

Consider the following singularly perturbed system of 2D parabolic reaction-diffusion IBVP:

$$\begin{cases} \frac{\partial \vec{u}}{\partial t}(x, y, t) + \mathfrak{L}_\varepsilon \vec{u}(x, y, t) = \vec{f}(x, y, t), & (x, y, t) \in \mathcal{G}, \\ \vec{u}(x, y, 0) = \vec{u}_0(x, y), & (x, y) \in \bar{\mathcal{D}}, \\ \vec{u}(0, y, t) = \vec{u}(1, y, t) = \vec{0}, & (y, t) \in [0, 1] \times [0, T], \\ \vec{u}(x, 0, t) = \vec{u}(x, 1, t) = \vec{0}, & (x, t) \in [0, 1] \times [0, T], \end{cases} \quad (1.4.7)$$

where the spatial differential operator \mathfrak{L}_ε is given by

$$\mathfrak{L}_\varepsilon \equiv -\mathcal{E}^2 \Delta + B(x, y, t).$$

The diffusion and reaction coefficients of the model problem (1.4.7) are given by $\mathcal{E} = \text{diag}(\varepsilon_1, \varepsilon_2)$, $0 < \varepsilon_1 \leq \varepsilon_2 \ll 1$ and $B = \{b_{lm}(x)\}_{l,m=1}^2$, respectively. Under sufficient smoothness and compatibility conditions imposed on the source term and the initial data, the model problem (1.4.7) admits a unique solution, which exhibits overlapping boundary layers along the sides $x = 0, 1$ and $y = 0, 1$ with corner layers at all corners of the spatial domain.

1.5 Outline of the Thesis

This thesis consists of eight chapters. **Chapter 1** presents the general introduction along with the historical background of the related work done in field of SPPs. It also provides the motivation and objective for solving singularly perturbed system of parabolic PDEs in one and two-dimensions. The rest of this thesis includes seven chapters and is organized as follows:

Chapter 2 is devoted to the study of a parameter-uniform numerical method for one-dimensional singularly perturbed system of convection-diffusion problem of type (1.4.1). We use the implicit-Euler scheme to discretize the time derivative and the upwind scheme to discretize the spatial derivatives on the piecewise-uniform Shishkin mesh. The method converges uniformly with first-order (up to a logarithmic factor) in space and first-order in time. A post-processing technique is discussed, which improves the accuracy of the proposed numerical scheme on the piecewise-uniform Shishkin mesh. Numerical results are presented to verify the theoretical error estimates. It is shown that above computational technique can be extended for a singularity perturbed system of semilinear parabolic PDE of the form (1.4.2).

In **Chapter 3**, a parameter-uniform hybrid numerical is constructed for solving singularly perturbed system of parabolic IBVP (1.4.3). First, the time derivative is discretized by implicit-Euler scheme on uniform mesh. Then, the spatial derivatives are approximated by the hybrid numerical scheme on piecewise-uniform Shishkin mesh in the resulting time semidiscrete problem. The numerical method converges uniformly almost second-order in space and first-order in time irrespective of the singular perturbation parameters. Numerical experiments are carried out to validate the theoretical findings.

Chapter 4 deals with singularly perturbed system of parabolic PDE of the form (1.4.4) with discontinuous convection coefficient and source term. We discretize the temporal domain with uniform mesh and the spatial domains with a special piecewise-uniform Shishkin mesh. To discretize the model problem, we use the implicit-Euler scheme and the classical upwind scheme for the temporal and spatial derivatives, respectively. This numerical method converges uniformly first-order in time and first-order up-to logarithmic in space. Numerical results are given to validate the theoretical error estimates.

In **Chapter 5**, we analyze a singularly perturbed system of 2D parabolic convection-diffusion problem of the form (1.4.5) with the fractional-step method on the uniform mesh in the temporal direction and the piecewise-uniform Shishkin mesh in the spatial directions. It is shown that the error estimate obtained for the proposed numerical scheme is almost first-order accurate in space and first-order in time. Numerical results are produced to validate the theoretical error estimates.

Chapter 6 is concerned with construction of ε -uniformly convergent fraction-step method for solving singularly perturbed system of 2D parabolic reaction-diffusion IBVP of the form (1.4.6). The theoretical and numerical results explain that the error converges at the rate of first-order in temporal variable and almost second-order in spatial variables. To support the analysis, numerical experiments are carried out.

Chapter 7 presents the analysis for singularly perturbed system of 2D parabolic PDE of the form (1.4.7). We construct an efficient numerical scheme by using a special rectangular mesh involving piecewise-uniform Shishkin mesh in the spatial directions. It is shown both theoretically and numerically that that the proposed numerical scheme is almost second-order accurate in space and first-order in time.

In **Chapter 8**, we address the brief summary of the results highlighting the contribution made by this thesis. It also provides various ideas for the scope of future investigations of the present work.

Extensive numerical experiments are conducted to support the theoretical findings. The corresponding numerical results are presented at the end of each chapter of the thesis in the form of figures and tables to validate the analytical results.

Efficient Numerical Schemes for Singularly Perturbed System of 1D Parabolic Partial Differential Equations with Boundary Layers

In this chapter, we obtain the numerical solution of singularly perturbed system of 1D parabolic convection-diffusion problems exhibiting overlapping boundary layers. The proposed numerical scheme consists of the implicit-Euler method for the time derivative and an upwind finite difference scheme for the spatial derivatives. We analyze the scheme on a piecewise-uniform Shishkin mesh for the spatial discretization to establish the uniform convergence with respect to the perturbation parameters. For the proposed scheme, the stability analysis is discussed and parameter-uniform error estimate is derived. To enhance the order of convergence, from almost first-order to almost second-order, we use the Richardson extrapolation technique. In support of the theoretical results, numerical experiments are performed by employing the proposed techniques.

2.1 Introduction

Consider the following singularly perturbed system of 1D parabolic convection-diffusion IBVP in the domain $Q := \Omega_x \times (0, T]$, $\Omega_x = (0, 1)$:

$$\begin{cases} \frac{\partial \vec{u}}{\partial t} + L_{x,\varepsilon} \vec{u} = \vec{f}, & (x, t) \in Q, \\ \vec{u}(x, 0) = \vec{u}_0(x), & x \in \bar{\Omega}_x, \\ \vec{u}(0, t) = \vec{0}, \quad \vec{u}(1, t) = \vec{0}, & t \in [0, T], \end{cases} \quad (2.1.1)$$

where the spatial differential operator $L_{x,\varepsilon}$ is given by

$$L_{x,\varepsilon} \equiv -\mathcal{E} \frac{\partial^2}{\partial x^2} - A(x) \frac{\partial}{\partial x} + B(x),$$

with $\mathcal{E} = \text{diag}(\varepsilon_1, \varepsilon_2)$, $A(x) = \text{diag}(a_1(x), a_2(x))$, $B(x) = \{b_{lm}(x)\}_{l,m=1}^2$.

We assume that $\varepsilon_1, \varepsilon_2$ satisfy $0 < \varepsilon_1 \leq \varepsilon_2 \ll 1$, and the coefficients of convection matrix A satisfy the following positivity conditions:

$$a_1(x) \geq \alpha > 0, \quad a_2(x) \geq \alpha > 0. \quad (2.1.2)$$

In addition, assume that B is an L_0 -matrix with

$$\min_{x \in \overline{\Omega}_x} \{b_{11}(x) + b_{12}(x), b_{21}(x) + b_{22}(x)\} \geq \beta > 0. \quad (2.1.3)$$

We assume that the data of the model problem (2.1.1) are sufficiently smooth functions and also satisfy sufficient compatibility conditions so that it admits a unique solution $\vec{u}(x, t) \in (\mathcal{C}_\lambda^4(Q))^2$. For instance, typical smoothness assumptions for the source term and the initial condition are given by

$$\vec{f} \in (\mathcal{C}_\lambda^2(\overline{Q}))^2 \quad \text{and} \quad \vec{u}_0 \in (\mathcal{C}_0^4(\overline{\Omega}_x))^2. \quad (2.1.4)$$

Also the compatibility conditions for the data of problem (2.1.1) are as follows

$$\begin{cases} \vec{u}_0(x) = \vec{0}, & x \in \{0, 1\}, \\ \vec{f}(x, 0) - L_{x,\varepsilon} \vec{u}_0(x) = \vec{0}, & x \in \{0, 1\}, \\ \vec{f}_t(x, 0) + (L_{x,\varepsilon})^2 \vec{u}_0(x) - L_{x,\varepsilon} \vec{f}(x, 0) = \vec{0}, & x \in \{0, 1\}. \end{cases} \quad (2.1.5)$$

which are the extensions of compatibility conditions used for the scalar case in [42].

In this chapter, we consider singularly perturbed system of 1D parabolic convection-diffusion IBVP with different diffusion coefficients $\varepsilon_1, \varepsilon_2$, associated with each equation. The overlapping boundary layers occur in the left side of the spatial domain, *i.e.*, along $x = 0$, therefore the non-uniform mesh will be employed for the spatial variable and uniform mesh for the temporal direction. The proposed numerical scheme is the combination of time semidiscretization process which consists of the implicit-Euler scheme and spatial discretization by using the upwind difference scheme. Error estimates of order $O(N^{-1} \ln N + \Delta t)$ are obtained for the numerical solution, where N is the discretization parameter in spatial domain and Δt is the time step. Later, we use the Richardson extrapolation technique, to improve the accuracy of the approximate numerical solution.

This chapter is structured as follows: In Section 2.2, we establish some analytical properties of the continuous problem. Section 2.3 deals with the time semidiscretization process. Further, we discuss the derivative bounds of the exact solution of the time semidiscrete scheme. Section 2.4 describes the construction of the piecewise-uniform Shishkin mesh and the upwind difference scheme for the spatial discretization. In Section 2.5, we discuss the fully discrete scheme and derive the global error estimate. In

Section 2.6, we study the numerical solution of a singularly perturbed system of semilinear parabolic convection-diffusion IBVP. To enhance the accuracy of numerical solution, Richardson extrapolation technique is studied in Section 2.7. Section 2.8 contains numerical experiments for test examples that confirm the theoretical findings.

2.2 Bounds of the Solution and its Derivatives

In this section, we study the analytical properties of the exact solution of the continuous problem (2.1.1), like maximum principle and bounds of the solution derivatives.

Lemma 2.2.1. (Maximum Principle). *Let $(\frac{\partial}{\partial t} + L_{x,\varepsilon})$ be the differential operator given in (2.1.1) and we assume that the matrices A and B satisfy conditions (2.1.2) and (2.1.3), respectively. Then for $\vec{z} \geq \vec{0}$ on ∂Q and $(\frac{\partial}{\partial t} + L_{x,\varepsilon}) \vec{z} \geq \vec{0}$ in Q , we have $\vec{z} \geq \vec{0}$, for all $(x, t) \in \bar{Q}$.*

Proof. We prove this lemma by contradiction. Assume that there exists a point $(x_0, t_0) \in Q$ such that

$$\min\{z_1(x_0, t_0), z_2(x_0, t_0)\} = \min\left\{\min_{(x,t) \in \bar{Q}} z_1(x, t), \min_{(x,t) \in \bar{Q}} z_2(x, t)\right\} < 0.$$

Without loss of generality we assume that $z_1(x_0, t_0) \leq z_2(x_0, t_0)$. Then the first component of $(\frac{\partial}{\partial t} + L_{x,\varepsilon}) \vec{z}$ satisfies

$$\frac{\partial z_1}{\partial t} + L_{x,\varepsilon_1} \vec{z}(x_0, t_0) \leq b_{11}(x_0)z_1(x_0, t_0) + b_{12}(x_0)z_2(x_0, t_0) < 0,$$

which contradicts the hypothesis of this lemma, therefore $\vec{z} \geq \vec{0}$, for all $(x, t) \in \bar{Q}$. ■

The following lemma will help us to find the bound for the exact solution \vec{u} .

Lemma 2.2.2. *The solution \vec{u} of the problem (2.1.1) satisfies the following estimate*

$$|\vec{u}(x, t) - \vec{u}(x, 0)| \leq \vec{C}t, \quad (x, t) \in \bar{Q},$$

where C is independent of $\varepsilon_1, \varepsilon_2$.

Proof. We shall establish the estimate only for the first component u_1 , one can prove the result for u_2 in the same way. Set $\vec{\phi}(x, t) = \vec{u}(x, t) - \vec{u}_0(x)$, where $\vec{u}(x, 0) = \vec{u}_0(x)$. Then $\vec{\phi}$ satisfies the following problem:

$$\begin{cases} \frac{\partial \phi_1}{\partial t} + L_{x,\varepsilon_1} \vec{\phi}(x, t) = f_1(x, t) - L_{x,\varepsilon_1} \vec{u}_0(x), \\ \phi_1(x, 0) = 0 \quad \text{for } 0 < x < 1, \\ \phi_1(0, t) = 0 \quad \text{and} \quad \phi_1(1, t) = 0 \quad \text{for } 0 \leq t \leq T. \end{cases}$$

Set $\vec{\psi}(x, t) = \vec{C}t$, for sufficiently large positive constant $\vec{C} = (C, C)^T$, therefore it is easy to see that

$$\begin{cases} \frac{\partial \psi_1}{\partial t} + L_{x, \varepsilon_1} \vec{\psi}(x, t) = C + C(b_{11} + b_{12})t, \\ \psi_1(x, 0) = 0 \quad \text{for } 0 < x < 1, \\ \psi_1(0, t) = \psi_1(1, t) = Ct \quad \text{for } 0 \leq t \leq T. \end{cases}$$

By using the maximum principle given in Lemma 2.2.1, we can obtain that

$$|\phi_1(x, t)| = |u_1(x, t) - u_1(x, 0)| \leq Ct.$$

Similarly, we can get $|\phi_2(x, t)| = |u_2(x, t) - u_2(x, 0)| \leq Ct$. This completes the proof. ■

Before getting into the detailed analysis of derivative bounds for the solution $\vec{u}(x, t)$ of (2.1.1), we discuss the qualitative behavior graphically.

Example 2.2.3. Consider problem (2.1.1) where values of A, B are given as

$$A = \begin{pmatrix} 1 & 0 \\ 0 & 1 \end{pmatrix}, \quad B = \begin{pmatrix} 2+x & -1 \\ -1 & 2+2x \end{pmatrix}$$

and the source term $\vec{f} = (1, 1)^T$ with zero initial and boundary condition.

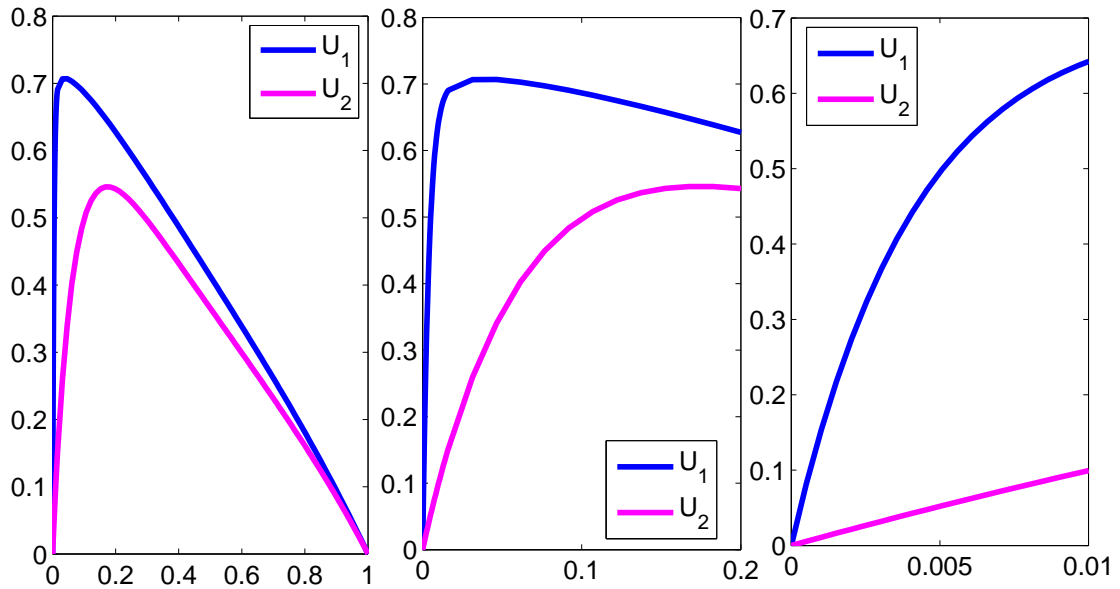


Figure 2.1: Numerical solution of Example 2.2.3 for $\varepsilon_1 = 2^{-8}$, $\varepsilon_2 = 2^{-4}$ and $N = 64$ at time $t = 1$.

From Fig. 2.1, one can visualize the overlapping boundary layers along the side $x = 0$. While both components have boundary layers of width $O(\varepsilon_2 \ln \varepsilon_2)$, only $u_1(x, t)$

has an additional sublayer of width $O(\varepsilon_1 \ln \varepsilon_1)$ and this phenomena is demonstrated in Fig. 2.1. In particular, one can observe the differences in the behavior of the two curves in the rightmost diagram.

Theorem 2.2.4. *For all non-negative integers k, k_0 , satisfying $0 \leq k + k_0 \leq 2$, the derivatives of the exact solution $\vec{u} = (u_1, u_2)^T$ of the IBVP (2.1.1) satisfy the following estimates:*

$$\left| \frac{\partial^{k+k_0} u_l}{\partial x^k \partial t^{k_0}} \right| \leq \begin{cases} C, & \text{for } k = 0, \\ C(1 + \varepsilon_l^{-1} B_{\varepsilon_l}^0(x)), & \text{for } k = 1, \\ C(1 + \varepsilon_l^{-1} (\varepsilon_1^{-1} B_{\varepsilon_1}^0(x) + \varepsilon_2^{-2} B_{\varepsilon_2}^0(x))), & \text{for } k = 2, \end{cases}$$

for all $(x, t) \in \bar{Q}$ and $l = 1, 2$.

Proof. To prove the bounds of the derivative of the exact solution \vec{u} of (2.1.1), we will consider various cases.

Case 1. Here we consider the case for $k = 0$ and $k_0 = 0$. The required bound follows directly from Lemma 2.2.2.

Case 2. Let us take $k = 0$ and $k_0 = 1$. Since $\vec{u}(0, t) = \vec{u}(1, t) = \vec{0}$ for $t \in [0, 1]$, which implies that $\vec{u}_t = \vec{0}$. Also, by using the regularity condition (2.1.4), we get $|\vec{u}_t(x, 0)| \leq \vec{C}$ for all $x \in [0, 1]$. Differentiating (2.1.1) with respect to t , we have

$$\left(\frac{\partial}{\partial t} + L_{x, \varepsilon} \right) \vec{u}_t(x, t) = \vec{u}_{tt} - \mathcal{E} \vec{u}_{txx} - A \vec{u}_{tx} + B \vec{u}_t = \vec{f}_t. \quad (2.2.1)$$

Since \vec{f} is a sufficiently smooth function, therefore by using the maximum principle on \bar{Q} , we can conclude that $|\vec{u}_t| \leq \vec{C}$.

Case 3. Now we consider the case, where $k = 1$ and $k_0 = 0$. We have

$$\frac{\partial u_1}{\partial t} - \varepsilon_1 \frac{\partial^2 u_1}{\partial x^2} - a_1 \frac{\partial u_1}{\partial x} + b_{11} u_1 + b_{12} u_2 = f_1, \quad \text{on } \bar{Q}.$$

The above equation can be rewritten as

$$\varepsilon_1 \frac{\partial^2 u_1}{\partial x^2} = \frac{\partial u_1}{\partial t} - a_1 \frac{\partial u_1}{\partial x} + b_{11} u_1 + b_{12} u_2 - f_1. \quad (2.2.2)$$

For a fixed $t \in [0, T]$, there exists $\theta \in (0, 1)$ such that

$$\frac{\partial u_1}{\partial x}(\theta, t) = \frac{u_1(\varepsilon_1, t) - u_1(0, t)}{\varepsilon_1},$$

which implies that $\varepsilon_1 |(\partial u_1 / \partial x)(\theta, t)| \leq 2 \|u_1\|_\infty$. For a fixed $t \in [0, T]$, by integrating (2.2.2) with respect to x and after integration by parts, we have

$$\begin{aligned} \varepsilon_1 \left| \frac{\partial u_1}{\partial x}(\theta, t) - \frac{\partial u_1}{\partial x}(0, t) \right| &= \int_0^\theta \frac{\partial u_1}{\partial t}(s, t) ds - [a_1(s) u_1(s, t)]_0^\theta + \int_0^\theta \frac{\partial a_1}{\partial s}(s) u_1(s, t) ds \\ &\quad + \int_0^\theta (b_{11}(s) u_1(s, t) + b_{12}(s) u_2(s, t)) ds - \int_0^\theta f_1(s, t) ds. \end{aligned}$$

Therefore, we obtain that

$$\varepsilon_1 \left| \frac{\partial u_1}{\partial x}(0, t) \right| \leq \|f_1\|_\infty + \left\| \frac{\partial u_1}{\partial t} \right\|_\infty + C(\|u_1\|_\infty + \|u_2\|_\infty).$$

By using the bound of $|\vec{u}|$ and $|\vec{u}_t|$, one can get

$$\left| \frac{\partial u_1}{\partial x}(0, t) \right| \leq C\varepsilon_1^{-1}.$$

Next, the equation (2.2.2) can be expressed as

$$\varepsilon_1 \frac{\partial^2 u_1}{\partial x^2} + a_1 \frac{\partial u_1}{\partial x} = \frac{\partial u_1}{\partial t} + b_{11}u_1 + b_{12}u_2 - f_1 \equiv \Lambda_1(x, t). \quad (2.2.3)$$

By integrating (2.2.3) with respect to x , we have

$$\frac{\partial u_1}{\partial x}(x, t) = \frac{\partial u_1}{\partial x}(0, t) \exp\left(\frac{-(\eta_1(x) - \eta_1(0))}{\varepsilon_2}\right) - \varepsilon_1^{-1} \int_0^x \Lambda_1(s, t) \exp\left(\frac{-(\eta_2(s) - \eta_1(0))}{\varepsilon_1}\right) ds,$$

where $\eta_1(x)$ is an indefinite integral of $a_1(x)$. By using the bounds of $\frac{\partial u_1}{\partial x}(0, t)$ and $\Lambda_1(x, t)$, we can obtain that

$$\left| \frac{\partial u_1}{\partial x} \right| \leq C(1 + \varepsilon_1^{-1} B_{\varepsilon_1}^0(x)).$$

In a similar way, we can deduce that

$$\left| \frac{\partial u_2}{\partial x} \right| \leq C(1 + \varepsilon_2^{-1} B_{\varepsilon_2}^0(x)).$$

Case 4. Let $k = 0$ and $k_0 = 2$. Since $\vec{u}(0, t) = \vec{u}(1, t) = \vec{0}$ for $t \in [0, 1]$, therefore $\vec{u}_t = \vec{u}_{tt} = \vec{0}$. Again, using the regularity condition and estimate given in **Case 2**, we have $|\vec{u}_{tt}(x, 0)| \leq \vec{C}$, for all $x \in [0, 1]$. Next differentiating (2.2.1) with respect to t , we obtain

$$\left(\frac{\partial}{\partial t} + L_{x, \vec{\varepsilon}} \right) \vec{u}_{tt} = \vec{u}_{ttt} - \mathcal{E} \vec{u}_{ttxx} - A \vec{u}_{ttx} + B \vec{u}_{tt} = \vec{f}_{tt}.$$

Since \vec{f}_{tt} is a bounded function, by using the maximum principle given in Lemma 2.2.1, we get $|\vec{u}_{tt}| \leq \vec{C}$ on \bar{Q} .

Case 5. Here we consider the case $k = 1$ and $k_0 = 1$. First we shall discuss bounds for the derivative of component u_1 . For a fixed $t \in [0, T]$, there exist $\theta \in (0, 1)$ such that

$$\frac{\partial^2 u_1}{\partial x \partial t}(\theta, t) = \frac{1}{\varepsilon_1} \left(\frac{\partial u_1}{\partial t}(\varepsilon_1, t) - \frac{\partial u_1}{\partial t}(0, t) \right),$$

which implies that $\varepsilon_1 |(\partial^2 u_1 / \partial x \partial t)(\theta, t)| \leq 2 \|\partial u_1 / \partial t\|_\infty$. Differentiating (2.2.2) with respect to t and rearranging the terms, we have

$$\varepsilon_1 \frac{\partial^3 u_1}{\partial x^2 \partial t} = \frac{\partial^2 u_1}{\partial t^2} - a_1 \frac{\partial^2 u_1}{\partial x \partial t} + b_{11} \frac{\partial u_1}{\partial t} + b_{12} \frac{\partial u_2}{\partial t} - \frac{\partial f_1}{\partial t}. \quad (2.2.4)$$

By integrating (2.2.4) with respect to x and following the approach of **Case 3**, we obtain

$$\varepsilon_1 \left| \frac{\partial^2 u_1}{\partial x \partial t}(0, t) \right| \leq \left\| \frac{\partial f_1}{\partial t} \right\|_{\infty} + \left\| \frac{\partial^2 u_1}{\partial t^2} \right\|_{\infty} + C \left(\left\| \frac{\partial u_1}{\partial t} \right\|_{\infty} + \left\| \frac{\partial u_2}{\partial t} \right\|_{\infty} \right).$$

Using the bound of $|\vec{u}_t|$ and $|\vec{u}_{tt}|$, we get

$$\left| \frac{\partial^2 u_1}{\partial x \partial t}(0, t) \right| \leq C \varepsilon_1^{-1}.$$

Now (2.2.4) can be expressed as

$$\varepsilon_1 \frac{\partial^3 u_1}{\partial x^2 \partial t} + a_1 \frac{\partial^2 u_1}{\partial x \partial t} = \Lambda_2(x, t), \quad \text{where } \Lambda_2(x, t) = \frac{\partial^2 u_1}{\partial t^2} - \frac{\partial f_1}{\partial t} + b_{11} \frac{\partial u_1}{\partial t} + b_{12} \frac{\partial u_2}{\partial t}.$$

By following the argument of **Case 3**, we can obtain that

$$\left| \frac{\partial^2 u_1}{\partial x \partial t} \right| \leq C (1 + \varepsilon_1^{-1} B_{\varepsilon_1}^0(x)).$$

In a similar manner one can find the required bound for component u_2 .

Case 6. Next consider the case, where $k = 2$ and $k_0 = 0$. We shall provide the estimate for component u_1 first. Consider the first component of (2.1.1) in the following form

$$\varepsilon_1 \frac{\partial^2 u_1}{\partial x^2} = \frac{\partial u_1}{\partial t} - a_1 \frac{\partial u_1}{\partial x} + b_{11} u_1 + b_{12} u_2 - f_1. \quad (2.2.5)$$

By following the approach discussed in **Case 3**, one has

$$\left| \frac{\partial u_1}{\partial x}(0, t) \right| \leq C \varepsilon_1^{-1}.$$

From (2.2.5) and previous estimate, it is easy to obtain that

$$\left| \frac{\partial^2 u_1}{\partial x^2}(0, t) \right| \leq C \varepsilon_1^{-2}.$$

Differentiating (2.2.5) with respect to x , we have

$$\varepsilon_1 \frac{\partial^3 u_1}{\partial x^3} + a_1 \frac{\partial^2 u_1}{\partial x^2} = \Lambda_3(x, t), \quad \text{on } \bar{Q}, \quad (2.2.6)$$

where $\Lambda_3(x, t) = -\frac{\partial f_1}{\partial x} - \frac{\partial a_1}{\partial x} \frac{\partial u_1}{\partial x} + \frac{\partial (b_{11} u_1 + b_{12} u_2)}{\partial x} + \frac{\partial^2 u_1}{\partial x \partial t}$. By using **Case 3** and **Case 5**, one can get

$$|\Lambda_3(x, t)| \leq C (1 + \varepsilon_1^{-1} B_{\varepsilon_1}^0(x) + \varepsilon_2^{-1} B_{\varepsilon_2}^0(x)).$$

Then applying the argument of **Case 3** and the bound of $\Lambda_3(x, t)$, we can deduce that

$$\left| \frac{\partial^2 u_1}{\partial x^2} \right| \leq C (1 + \varepsilon_1^{-1} (\varepsilon_1^{-1} B_{\varepsilon_2}^0(x) + \varepsilon_2^{-1} B_{\varepsilon_2}^0(x))).$$

Analogously, one can derive estimate for u_2 . This completes the proof. \blacksquare

2.3 Analysis of the Time Semidiscretization

Here, we study the time semidiscretization process which is essential for the convergence analysis of the fully discrete scheme. Further, we will derive the asymptotic behavior of the exact solution of the semidiscrete problems.

2.3.1 The time semidiscrete scheme

We discretize problem (2.1.1) with the implicit-Euler method for the time derivative on uniform mesh $\bar{\Upsilon}^M = \{t_n = n\Delta t, n = 0, 1, \dots, M\}$. The semidiscrete scheme can be expressed as

$$\begin{cases} \bar{u}^0(x) = \bar{u}(x, 0), & x \in \bar{\Omega}_x, \\ (I + \Delta t L_{x,\bar{\varepsilon}})\bar{u}^{n+1}(x) = \bar{u}^n(x) + \Delta t \bar{f}(x, t_{n+1}), \\ \bar{u}^{n+1}(0) = \bar{0}, \quad \bar{u}^{n+1}(1) = \bar{0}, \end{cases} \quad (2.3.1)$$

where $\bar{u}^n(x)$ is the time semidiscrete approximation of $\bar{u}(x, t)$ at time level $t_n = n\Delta t$.

Lemma 2.3.1. *Let $\bar{z}^{n+1} \geq \bar{0}$ on $\partial\Omega_x$ and $(I + \Delta t L_{x,\bar{\varepsilon}}^{n+1})\bar{z}^{n+1} \geq \bar{0}$, for $x \in \Omega_x$, then $\bar{z}^{n+1} \geq \bar{0}$ for all $x \in \bar{\Omega}_x$.*

Proof. As in the continuous case, suppose that this lemma is not true. Assume that there exists a point $x_0 \in \Omega_x$ such that

$$\min\{z_1^{n+1}(x_0), z_2^{n+1}(x_0)\} = \min\left\{\min_{x \in \bar{\Omega}_x} z_1^{n+1}, \min_{x \in \bar{\Omega}_x} z_2^{n+1}\right\} < 0.$$

Without loss of generality we assume that $z_1^{n+1}(x_0) \leq z_2^{n+1}(x_0)$. Then the first component of operator $(I + \Delta t L_{x,\bar{\varepsilon}}^{n+1})\bar{z}^{n+1}$ satisfies

$$(I + \Delta t L_{x,\bar{\varepsilon}_1}^{n+1})\bar{z}^{n+1}(x_0) \leq (1 + \Delta t b_{11}^1)z_1^{n+1}(x_0) + \Delta t b_{12}^1 z_2^{n+1}(x_0) < 0,$$

which is a contradiction. Hence we get the desired result. \blacksquare

Convergence analysis

First, we discuss the stability and the consistency of the scheme (2.3.1). Later we derive the convergence analysis in the classical way. We define the operator $(I + \Delta t L_{x,\bar{\varepsilon}})^{-1}$, as follows: $\bar{z}^{n+1} = (I + \Delta t L_{x,\bar{\varepsilon}})^{-1}\bar{u}^{n+1}$ is the solution of the following problem

$$\begin{cases} (I + \Delta t L_{x,\bar{\varepsilon}})\bar{z}^{n+1}(x) = \bar{u}^{n+1}(x), & x \in \Omega_x, \\ \bar{z}^{n+1}(0) = \bar{z}^{n+1}(1) = 0. \end{cases}$$

Next, consider $\vec{z} = (\tilde{z}, \tilde{z})^T$ with $\tilde{z} = \frac{\|\vec{u}^{n+1}\|_\infty}{(1 + \beta\Delta t)}$. Therefore, we have

$$(I + \Delta t L_{x,\varepsilon_1})\vec{z} = (1 + (b_{11} + b_{12})\Delta t) \frac{\|\vec{u}^{n+1}\|_\infty}{(1 + \beta\Delta t)} \geq \|\vec{u}^{n+1}\|_\infty = \|(I + \Delta t L_{x,\varepsilon})\vec{z}^{n+1}\|_\infty.$$

Since the operator $(I + \Delta t L_{x,\varepsilon})$ satisfies the maximum principle (Lemma 2.3.1), we have

$$\|\vec{z}^{n+1}\|_\infty \leq \frac{\|\vec{u}^{n+1}\|_\infty}{(1 + \beta\Delta t)}.$$

Therefore, we obtain that

$$\|(I + \Delta t L_{x,\varepsilon_1})^{-1}\|_\infty \leq \frac{1}{1 + \beta\Delta t}, \quad \|(I + \Delta t L_{x,\varepsilon_2})^{-1}\|_\infty \leq \frac{1}{1 + \beta\Delta t}. \quad (2.3.2)$$

Next, we define the local truncation error \vec{e}_{n+1} for the semidiscrete scheme (2.3.1) as follows

$$\vec{e}_{n+1} = \vec{u}(x, t_{n+1}) - \vec{u}^{n+1}(x),$$

where $\vec{u}^{n+1}(x)$ is the solution obtained after one step of the semidiscrete scheme by taking the exact value $\vec{u}(t_n)$, instead of $\vec{u}^n(x)$ as the starting data. Concretely, we have

$$\begin{cases} (I + \Delta t L_{x,\varepsilon})\vec{u}^{n+1}(x) = \vec{u}(x, t_n) + \Delta t \vec{f}(x, t_{n+1}), & x \in \Omega_x, \\ \vec{u}^{n+1}(0) = \vec{u}^{n+1}(1) = 0. \end{cases} \quad (2.3.3)$$

Lemma 2.3.2. *The local truncation error \vec{e}_{n+1} satisfies*

$$\|\vec{e}_{n+1}\|_\infty \leq C(\Delta t^2). \quad (2.3.4)$$

Proof. The exact solution $\vec{u}(x, t_n)$ of (2.1.1) satisfies

$$\vec{u}(x, t_n) = (I + \Delta t L_{x,\varepsilon})\vec{u}(x, t_{n+1}) - \Delta t \vec{f}(x, t_{n+1}) + O(\Delta t^2).$$

Thus, the local truncation error \vec{e}_{n+1} satisfies

$$\begin{cases} (I + \Delta t L_{x,\varepsilon})\vec{e}_{n+1} = O(\Delta t^2), \\ \vec{e}_{n+1}(0) = \vec{e}_{n+1}(1) = 0. \end{cases}$$

By using the maximum principle (Lemma 2.3.1), we can obtain the desired result. \blacksquare

Lemma 2.3.3. *The global error $\vec{e}_n := \vec{u}(x, t_n) - \vec{u}^n$ satisfies*

$$\sup_{n \leq T/\Delta t} \|\vec{e}_n\|_\infty \leq C\Delta t. \quad (2.3.5)$$

Proof. By combining the operator bounds given in (2.3.2) and Lemma 2.3.2, one can get the following uniform convergence result. \blacksquare

The time semidiscretization process is uniformly convergent of first-order in time.

As a technical requirement, we assume that

$$|L_{x,\varepsilon}\vec{u}(x, t_n)| \leq \vec{C}. \quad (2.3.6)$$

One can obtain this estimate by using the maximum principle with suitable smoothness and compatibility conditions on \vec{f} and initial data \vec{u}_0 .

Lemma 2.3.4. *The exact solution of (2.3.3) satisfies the following estimate :*

$$\left| \frac{d^k \tilde{u}_1^{n+1}}{dx^k} \right| \leq \begin{cases} C, & \text{for } k = 0, \\ C(1 + \varepsilon_1^{-1} B_{\varepsilon_1}^0(x)), & \text{for } k = 1, \end{cases}$$

and

$$\left| \frac{d^k \tilde{u}_2^{n+1}}{dx^k} \right| \leq \begin{cases} C, & \text{for } k = 0, \\ C(1 + \varepsilon_2^{-1} B_{\varepsilon_2}^0(x)), & \text{for } k = 1. \end{cases}$$

Proof. Let $\vec{\varrho} = (\tilde{u}^{n+1} - \vec{u}(x, t_n))/\Delta t$ be the solution of the following problem

$$\begin{cases} (I + \Delta t L_{x,\varepsilon})\vec{\varrho}(x) = -L_{x,\varepsilon}\vec{u}(x, t_n) + \vec{f}(x, t_{n+1}), \\ \vec{\varrho}(0) = \vec{0}, \quad \vec{\varrho}(1) = \vec{0}. \end{cases} \quad (2.3.7)$$

Using the stability condition (2.3.2) and assumption (2.3.6), we can obtain $|\vec{\varrho}| \leq \vec{C}$ on $\bar{\Omega}_x$. Also, $\tilde{u}^{n+1}(x)$ is the solution of

$$\begin{cases} L_{x,\varepsilon}\tilde{u}^{n+1}(x) = -\vec{\varrho} + \vec{f}(x, t_{n+1}), \\ \tilde{u}^{n+1}(0) = \vec{0}, \quad \tilde{u}^{n+1}(1) = \vec{0}. \end{cases} \quad (2.3.8)$$

By using the maximum principle and bound of $\vec{\varrho}$, one can get $|\tilde{u}^{n+1}| \leq C$, for all $x \in \bar{\Omega}_x$. The first component of (2.3.8) can be written as

$$\begin{cases} -\varepsilon_1 \frac{d^2 \tilde{u}_1^{n+1}}{dx^2} - a_1 \frac{d\tilde{u}_1^{n+1}}{dx} + b_{11}\tilde{u}_1^{n+1} + b_{12}\tilde{u}_2^{n+1} = -\varrho_1 + f_1, \\ \tilde{u}_1^{n+1}(0) = \tilde{u}_1^{n+1}(1) = 0. \end{cases} \quad (2.3.9)$$

By following the technique of Theorem 2.2.4, we can show that

$$\left| \frac{d\tilde{u}_1^{n+1}}{dx}(x) \right| \leq C(1 + \varepsilon_1^{-1} B_{\varepsilon_1}^0(x)).$$

By using the previous methodology, we show that

$$\left| \frac{d\tilde{u}_2^{n+1}}{dx}(x) \right| \leq C (1 + \varepsilon_2^{-1} B_{\varepsilon_2}^0(x)).$$

This completes the proof. \blacksquare

Here, we decompose the solution \tilde{u}^{n+1} of (2.3.3) as $\tilde{u}^{n+1} = \tilde{v}^{n+1} + \tilde{w}^{n+1}$, where \tilde{v}^{n+1} is the smooth component and \tilde{w}^{n+1} is the layer component. By following the methodology from [10, Lemma 3] and [10, Lemma 4], one can easily obtain the following bounds:

$$\left\| \frac{d^k \tilde{v}^{n+1}}{dx^k} \right\|_{\infty} \leq C, \quad \text{for } 0 \leq k \leq 4, \quad (2.3.10)$$

and

$$\left| \frac{d^k \tilde{w}_1^{n+1}}{dx^k} \right| \leq \begin{cases} C, & \text{for } k = 0, \\ C (\varepsilon_1^{-k} B_{\varepsilon_1}^0(x) + \varepsilon_2^{-k} B_{\varepsilon_2}^0(x)), & \text{for } k = 1, 2, 3, 4, \end{cases} \quad (2.3.11)$$

$$\left| \frac{d^k \tilde{w}_2^{n+1}}{dx^k} \right| \leq \begin{cases} C, & \text{for } k = 0, \\ C \varepsilon_2^{-k} B_{\varepsilon_2}^0(x), & \text{for } k = 1, 2, \\ C \varepsilon_2^{2-k} (\varepsilon_1^{-2} B_{\varepsilon_1}^0(x) + \varepsilon_2^{-2} B_{\varepsilon_2}^0(x)), & \text{for } k = 3, 4, \end{cases} \quad (2.3.12)$$

for all $x \in \bar{\Omega}_x$.

2.4 The Spatial Discretization

In this section, we construct the piecewise-uniform Shishkin mesh for the spatial discretization and also describe the finite difference scheme used to approximate the semidiscrete problem (2.3.3). And later, we carry out the error analysis for the spatial discretization process which combines with results from previous section to produce the error estimate of the fully discrete scheme given in the next section.

2.4.1 Discretization of the domain

Consider the domain $\bar{\Omega}_x = [0, 1]$ and let $N \geq 8$ be an even positive integer. Here, we construct a piecewise-uniform mesh $\bar{\Omega}_x^N$ as follows:

Shishkin mesh for convection-diffusion BVP with a single parameter divides the interval $[0, 1]$ into two subintervals, on each of which the mesh is uniform. When $0 \leq \varepsilon_1 \leq \varepsilon_2 \ll 1$, the solution of the system of parabolic IBVP (2.1.1) has overlapping boundary layers of width $O(\varepsilon_1 \ln \varepsilon_1)$ and $O(\varepsilon_2 \ln \varepsilon_2)$ at $x = 0$. This necessitates the construction of a mesh that is uniform on each of the following three subintervals. In

the main subinterval, where the solution is smooth, the mesh is coarse, and on the other two subintervals, it is very fine. We define the transition parameters τ_{ε_1} and τ_{ε_2} as

$$\tau_{\varepsilon_2} = \min \left\{ \frac{1}{2}, \frac{2\varepsilon_2}{\alpha} \ln N \right\} \quad \text{and} \quad \tau_{\varepsilon_1} = \min \left\{ \frac{1}{4}, \frac{\tau_{\varepsilon_2}}{2}, \frac{2\varepsilon_1}{\alpha} \ln N \right\}.$$

A piecewise-uniform Shishkin mesh $\bar{\Omega}_x^N$ is constructed by dividing the spatial domain $[0, 1]$ into three subintervals such as $[0, \tau_{\varepsilon_1}]$, $[\tau_{\varepsilon_1}, \tau_{\varepsilon_2}]$, and $[\tau_{\varepsilon_2}, 1]$. Then divide $[\tau_{\varepsilon_2}, 1]$ into $N/2$ mesh-intervals, and divide each of the other two subintervals $[0, \tau_{\varepsilon_1}]$, $[\tau_{\varepsilon_1}, \tau_{\varepsilon_2}]$ into $N/4$ mesh-intervals. Figure 2.2 shows a typical discretized domain with the Shishkin mesh.

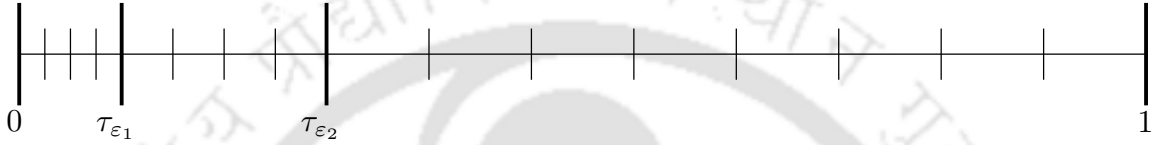


Figure 2.2: Example of piecewise-uniform Shishkin mesh $\bar{\Omega}_x^N$ for $N = 16$.

When $\tau_{\varepsilon_1} = \tau_{\varepsilon_2}/2$, then $\varepsilon_2 = O(\varepsilon_1)$, in this case, the error estimate can be easily obtained. Henceforth, we consider only the case $\tau_{\varepsilon_1} < \tau_{\varepsilon_2}/2$.

2.4.2 The finite difference scheme

For simplicity, we denote a function $v_{k,i} = v_k(x_i)$, $k = 1, 2$, and mesh function V by $V_{k,i}^{n+1} = V_k^{n+1}(x_i)$, $k = 1, 2$.

We propose the finite difference scheme for the spatial discretization of the semidiscrete scheme (2.3.3) as follows:

$$\begin{cases} \tilde{U}_i^0 = \bar{u}(x_i, 0), \\ (I + \Delta t L_{x,\bar{\varepsilon}}^N) \tilde{U}_i^{n+1} = \bar{u}(x_i, t_n) + \Delta t \bar{f}_i^{n+1} \quad \text{in } \Omega_x^N, \\ \tilde{U}_0^{n+1} = \tilde{U}_N^{n+1} = 0, \end{cases} \quad (2.4.1)$$

where the spatial difference operator $(I + \Delta t L_{x,\bar{\varepsilon}}^N)$ is given by

$$\begin{cases} (I + \Delta t L_{x,\varepsilon_1}^N) \tilde{U}_i^{n+1} := \tilde{L}_{x,\varepsilon_1}^N \tilde{U}_{1,i}^{n+1} + \Delta t b_{12,i} \tilde{U}_{2,i}^{n+1}, \\ (I + \Delta t L_{x,\varepsilon_2}^N) \tilde{U}_i^{n+1} := \tilde{L}_{x,\varepsilon_2}^N \tilde{U}_{2,i}^{n+1} + \Delta t b_{21,i} \tilde{U}_{1,i}^{n+1}, \end{cases}$$

with

$$\begin{cases} \tilde{L}_{x,\varepsilon_1}^N \tilde{U}_{1,i}^{n+1} := -\Delta t \varepsilon_1 D_x^+ D_x^- \tilde{U}_{1,i}^{n+1} - \Delta t a_{1,i} D_x^+ \tilde{U}_{1,i}^{n+1} + (1 + \Delta t b_{11,i}) \tilde{U}_{1,i}^{n+1}, \\ \tilde{L}_{x,\varepsilon_2}^N \tilde{U}_{2,i}^{n+1} := -\Delta t \varepsilon_2 D_x^+ D_x^- \tilde{U}_{2,i}^{n+1} - \Delta t a_{2,i} D_x^+ \tilde{U}_{2,i}^{n+1} + (1 + \Delta t b_{22,i}) \tilde{U}_{2,i}^{n+1}. \end{cases}$$

Next, we define a matrix $\widehat{B} = \{\widehat{B}_{lm}\}_{l,m=1}^2$ as

$$\widehat{B}_{ll} = 1, \quad \widehat{B}_{lm} = - \left\| \frac{\Delta t b_{lm,i}}{(1 + \Delta t b_{ll,i})} \right\|_{\infty}, \quad \text{for } l \neq m.$$

Assume that the matrix \widehat{B} is inverse monotone, *i.e.*, $\widehat{B}^{-1} \geq 0$.

Lemma 2.4.1. (Discrete Maximum Principle) *Assume that the mesh function $\{\vec{Z}(x_i)\}_{i=0}^N$ satisfies $\vec{Z}(0) \geq \vec{0}$, $\vec{Z}(1) \geq \vec{0}$. Then $(I + \Delta t L_{x,\varepsilon}^N)\vec{Z} \geq \vec{0}$ in Ω_x^N implies that $\vec{Z} \geq \vec{0}$ at each point of $\overline{\Omega}_x^N$.*

Proof. We prove this lemma by contradiction. Assume that there exists an $x_{i^*} \in \Omega_x^N$ such that

$$\min \{Z_1(x_{i^*}), Z_2(x_{i^*})\} = \min \left\{ \min_{x_i \in \overline{\Omega}_x^N} Z_1, \min_{x_i \in \overline{\Omega}_x^N} Z_2 \right\} < 0,$$

without loss of generality we assume that $Z_1(x_{i^*}) \leq Z_2(x_{i^*})$. From the hypothesis, it is clear that $x_{i^*} \neq 0, 1$. Therefore, it follows that

$$\begin{aligned} (I + \Delta t L_{x,\varepsilon_1}^N)\vec{Z}(x_{i^*}) &= -\Delta t \varepsilon_1 D_x^+ D_x^- Z_1(x_{i^*}) - \Delta t a_1(x_{i^*}) D_x^+ Z_1(x_{i^*}) \\ &\quad + (1 + \Delta t b_{11}(x_{i^*}))Z_1(x_{i^*}) + \Delta t b_{12}(x_{i^*})Z_2(x_{i^*}) < 0, \end{aligned}$$

which contradicts the hypothesis. Hence, we have $\vec{Z} \geq \vec{0}$, for all $x_i \in \overline{\Omega}_x^N$. \blacksquare

Similar to the stability estimate given in (2.3.2) of the time semidiscrete operator, one can easily obtain the following stability result:

$$\|(I + \Delta t L_{x,\varepsilon_1}^N)^{-1}\|_{\infty} \leq \frac{1}{1 + \beta \Delta t}, \quad \|(I + \Delta t L_{x,\varepsilon_2}^N)^{-1}\|_{\infty} \leq \frac{1}{1 + \beta \Delta t}. \quad (2.4.2)$$

Hence, the discrete scheme (2.4.1) is uniformly stable.

2.4.3 The truncation error analysis

The local truncation error, for the numerical scheme (2.4.1), $\vec{E}_i = \vec{U}_i^{n+1} - \vec{u}^{n+1}(x_i)$ is decomposed as

$$\vec{E} = \vec{E}^1 + \vec{E}^2$$

where $\vec{E}^1 = (E_1^1, E_2^1)^T$ is the solution of

$$\begin{cases} \tilde{L}_{x,\varepsilon_l}^N E_{l,i}^1 = (I + \Delta t L_{x,\varepsilon_l}^N)(\vec{U}_i^{n+1} - \vec{u}^{n+1}(x_i)), & \text{in } \Omega_x^N, \\ E_{l,0}^1 = E_{l,N}^1 = 0, \quad l = 1, 2, \end{cases} \quad (2.4.3)$$

and $\vec{E}^2 = (E_1^2, E_2^2)^T$ satisfies

$$\begin{cases} \tilde{L}_{x,\varepsilon_l}^N E_{l,i}^2 = -\Delta t b_{lm,i} E_{m,i}, & l \neq m, \quad \text{in } \Omega_x^N, \\ E_{l,0}^2 = E_{l,N}^2 = 0, & l = 1, 2. \end{cases} \quad (2.4.4)$$

For $l = 1, 2$, by employing (2.4.3) and (2.4.4) with [46, Lemma 2], we obtain

$$\begin{aligned} \|E_l\|_\infty &\leq \|E_l^1\|_\infty + \|E_l^2\|_\infty \\ &\leq \|E_l^1\|_\infty + \left\| \frac{\Delta t b_{lm,i}}{(1 + \Delta t b_{ll,i})} \right\|_\infty \|E_m\|_\infty, \quad l \neq m. \end{aligned}$$

From the definition of matrix \hat{B} , one can show that

$$\|E_l\|_\infty + \hat{B}_{lm} \|E_m\|_\infty \leq \|E_l^1\|_\infty, \quad l \neq m.$$

Hence, we can obtain that

$$\|\vec{E}\|_\infty = \left\| \vec{U}_i^{n+1} - \vec{u}^{n+1} \right\|_\infty \leq C \|\vec{E}^1\|_\infty. \quad (2.4.5)$$

Therefore, for obtaining the estimate for the spatial discretization error $\|\vec{E}\|_\infty$, one need to calculate the bound of the error component \vec{E}^1 .

We introduce the continuous and discrete operators associated with the first component (given in [47, Chapter 4]), as follows:

$$\mathcal{P}_1 \vec{v} := \Delta t \varepsilon_1 \frac{dv_1}{dx} + \Delta t a_1 v_1 + \int_x^1 \Delta t \frac{da_1}{ds} v_1(s) ds + \int_x^1 ((1 + \Delta t b_{11}) v_1 + \Delta t b_{12} v_2)(s) ds$$

and

$$\begin{aligned} \mathcal{P}_1^N \vec{v} := & \Delta t \varepsilon_1 D_x^- v_1 + \Delta t a_1 v_1 + \sum_{j=i}^{N-1} \Delta t h_{j+1} (D_x^+ a_{1,j}) v_{1,j+1} \\ & + \sum_{j=i}^{N-1} h_{j+1} ((1 + \Delta t b_{11,j}) v_{1,j} + \Delta t b_{12,j} v_{2,j}) \end{aligned}$$

with the source functions

$$\mathcal{F}_1 := \int_x^1 (u_1(s, t_n) + \Delta t f_1^{n+1}(s)) ds, \quad \mathcal{F}_1^N := \sum_{j=i}^{N-1} h_{j+1} (u_1(x_j, t_n) + \Delta t f_{1,j}^{n+1}).$$

In a similar manner, we define the continuous and discrete operators \mathcal{P}_2 and \mathcal{P}_2^N with source functions \mathcal{F}_2 and \mathcal{F}_2^N .

From the definition of the continuous and the discrete operators with source functions, for $l = 1, 2$, one can easily show that

$$\frac{d}{dx} \left(\mathcal{P}_l \vec{u}^{n+1} - \mathcal{F}_l \right) = 0, \quad \text{and} \quad D_x^+ \left(\mathcal{P}_l^N \vec{U}^{n+1} - \mathcal{F}_l^N \right) = 0,$$

which implies that

$$\mathcal{P}_l \tilde{u}^{n+1} - \mathcal{F}_l \equiv \gamma, \text{ on } \Omega_x, \quad \mathcal{P}_l^N \tilde{U}_i^{n+1} - \mathcal{F}_{l,i}^N \equiv \delta, \text{ on } \Omega_x^N, \quad (2.4.6)$$

where γ, δ are positive constants.

Applying the stability inequality from [47, Theorem 4.3] to (2.4.3), one can get

$$\|E_l^1\|_\infty \leq C \min_{\lambda \in \mathbb{R}} \left\| \mathcal{P}_l^N (\tilde{u}^{n+1} - \tilde{U}_i^{n+1}) + \lambda \right\|_\infty.$$

By taking $\lambda = \delta - \gamma$, we obtain

$$\|E_l^1\|_\infty \leq C \left\| \mathcal{P}_l^N \tilde{u}^{n+1} - \mathcal{P}_l \tilde{u}^{n+1} - \mathcal{F}_l^N + \mathcal{F}_l \right\|_\infty. \quad (2.4.7)$$

Firstly, we discuss the bound for $(\mathcal{P}_1^N \tilde{u}^{n+1} - \mathcal{P}_1 \tilde{u}^{n+1} - \mathcal{F}_1^N + \mathcal{F}_1)$. In a similar manner, one can obtain results associated with the second component \tilde{U}_2 .

From the definition of the continuous and the discrete operators, we have

$$\begin{aligned} & (\mathcal{P}_1^N \tilde{u}_i^{n+1} - \mathcal{P}_1 \tilde{u}_i^{n+1} - \mathcal{F}_{1,i}^N + \mathcal{F}_{1,i}) \\ &= \Delta t \varepsilon_1 \left(D_x^- \tilde{u}_{1,i}^{n+1} - \frac{d\tilde{u}_{1,i}^{n+1}}{dx} \right) + \sum_{j=i}^{N-1} \Delta t h_{j+1} (D_x^+ a_{1,j}) \tilde{u}_{1,j+1}^{n+1} - \int_{x_i}^{x_N} \Delta t \frac{da_1}{ds} \tilde{u}_1^{n+1}(s) ds \\ &+ \sum_{j=i}^{N-1} h_{j+1} \left((1 + \Delta t b_{11,j}) \tilde{u}_{1,j}^{n+1} + \Delta t b_{12,j} \tilde{u}_{2,j}^{n+1} - (u_1(x_j, t_n) + \Delta t f_{1,j}^{n+1}) \right) \\ &- \int_{x_i}^{x_N} \left((1 + \Delta t b_{11}) \tilde{u}_1^{n+1} + \Delta t b_{12} \tilde{u}_2^{n+1} - (u_1(s, t_n) + \Delta t f_1^{n+1}) \right) (s) ds. \end{aligned} \quad (2.4.8)$$

Next, we will use the Taylor's expansions with integral form of the remainder technique separately for each component as follows:

$$\begin{aligned} & h_{j+1} \left((1 + \Delta t b_{11,j}) \tilde{u}_{1,j}^{n+1} + \Delta t b_{12,j} \tilde{u}_{2,j}^{n+1} - (u_1(x_j, t_n) + \Delta t f_{1,j}^{n+1}) \right) \\ &- \int_{x_j}^{x_{j+1}} \left((1 + \Delta t b_{11}) \tilde{u}_1^{n+1} + \Delta t b_{12} \tilde{u}_2^{n+1} - (u_1(s, t_n) + \Delta t f_1^{n+1}) \right) (x) dx \\ &= \int_{x_j}^{x_{j+1}} \int_x^{x_j} \frac{d}{ds} \left((1 + \Delta t b_{11}) \tilde{u}_1^{n+1} + \Delta t b_{12} \tilde{u}_2^{n+1} - (u_1(s, t_n) + \Delta t f_1^{n+1}) \right) (s) ds dx \end{aligned}$$

and

$$\begin{aligned} & \Delta t h_{j+1} (D_x^+ a_{1,j}) \tilde{u}_{1,j+1}^{n+1} - \int_{x_j}^{x_{j+1}} \Delta t \frac{da_1}{dx} \tilde{u}_1^{n+1}(x) dx \\ &= \Delta t \int_{x_j}^{x_{j+1}} \frac{da_1(x)}{dx} \int_x^{x_{j+1}} \frac{d\tilde{u}_1^{n+1}(s)}{ds} ds dx \end{aligned}$$

also by using (2.3.3), we can have

$$\begin{aligned} \Delta t \varepsilon_1 \left(D_x^- \tilde{u}_{1,i}^{n+1} - \frac{d\tilde{u}_{1,i}^{n+1}}{dx} \right) &= \frac{1}{h_j} \int_{x_{j-1}}^{x_j} \int_x^{x_j} -\Delta t \varepsilon_1 \frac{d^2 \tilde{u}_{1,i}^{n+1}(s)}{ds^2} ds dx \\ &= \frac{1}{h_j} \int_{x_{j-1}}^{x_j} \int_x^{x_j} \left(\Delta t \frac{da_1}{ds} \frac{d\tilde{u}_1^{n+1}}{ds} - ((1 + \Delta t b_{11}) \tilde{u}_1^{n+1} \right. \\ &\quad \left. + \Delta t b_{12} \tilde{u}_2^{n+1}) + (u_1(s, t_n) + \Delta t f_1^{n+1}) \right) (s) ds dx. \end{aligned}$$

Combining these representations with (2.4.8), for $l = 1, 2$, we can have

$$\left\| \mathcal{P}_l^N \tilde{u}^{n+1} - \mathcal{P}_l \tilde{u}^{n+1} - \mathcal{F}_l^N + \mathcal{F}_l \right\|_\infty \leq C \max_{j=1, \dots, N} \Delta t \int_{x_{j-1}}^{x_j} \left(1 + \left| \frac{d\tilde{u}_1^{n+1}}{ds} \right| + \left| \frac{d\tilde{u}_2^{n+1}}{ds} \right| \right) ds.$$

Therefore, from (2.4.7), we obtain

$$\|\vec{E}^1\|_\infty \leq C \max_{j=1, \dots, N} \Delta t \int_{x_{j-1}}^{x_j} \left(1 + \left| \frac{d\tilde{u}_1^{n+1}}{ds} \right| + \left| \frac{d\tilde{u}_2^{n+1}}{ds} \right| \right) ds. \quad (2.4.9)$$

Lemma 2.4.2. Let \tilde{u}^{n+1} be the solution of (2.3.3) and \tilde{U}_i^{n+1} be the solution of (2.4.1). If the coefficients of the matrices A, B satisfy conditions (2.1.2) and (2.1.3), then

$$\left\| \tilde{U}_i^{n+1} - \tilde{u}^{n+1} \right\|_\infty \leq C \Delta t N^{-1} \ln N, \quad (2.4.10)$$

where C is independent of $N, \Delta t$ and $\varepsilon_1, \varepsilon_2$.

Proof. By using (2.4.9) in to (2.4.5), we obtain

$$\left\| \tilde{U}_i^{n+1} - \tilde{u}^{n+1} \right\|_\infty \leq C \max_{j=1, \dots, N} \Delta t \int_{x_{j-1}}^{x_j} \left(1 + \left| \frac{d\tilde{u}_1^{n+1}}{ds} \right| + \left| \frac{d\tilde{u}_2^{n+1}}{ds} \right| \right) ds.$$

Employing the derivative bounds of \tilde{u}_l^{n+1} , $l = 1, 2$, from Lemma 2.3.4, we get

$$\left\| \tilde{U}_i^{n+1} - \tilde{u}^{n+1} \right\|_\infty \leq C \max_{j=1, \dots, N} \Delta t \int_{x_{j-1}}^{x_j} (1 + \varepsilon_1^{-1} B_{\varepsilon_2}^0(s) + \varepsilon_2^{-1} B_{\varepsilon_2}^0(s)) ds.$$

After simplifying above equation, the error estimate can be obtained as

$$\left\| \tilde{U}_i^{n+1} - \tilde{u}^{n+1} \right\|_\infty \leq C \Delta t N^{-1} \ln N.$$

This completes the proof. ■

2.5 The Fully Discrete Scheme

Combining the time semidiscrete scheme (2.3.3) and the spatial discretization scheme (2.4.1), the fully discrete scheme is obtained on the mesh $\bar{Q}^{N,M} = \bar{\Omega}_x^N \times \bar{\Upsilon}^M$ as

$$\begin{cases} \vec{U}_i^0 = \vec{u}_0(x_i), & i = 0, \dots, N, \\ (I + \Delta t L_{x,\bar{\varepsilon}}^N) \vec{U}_i^{n+1} = \vec{U}_i^n + \Delta t \vec{f}_i^{n+1} & \text{for } 1 \leq i \leq N-1, \\ \vec{U}_0^{n+1} = \vec{U}_N^{n+1} = \vec{0}, & \text{for } n = 0, \dots, M-1, \end{cases} \quad (2.5.1)$$

where \vec{U}_i^n is the fully discrete approximation to the exact solution $\vec{u}(x, t)$ of (2.1.1) at the mesh point $(x_i, t_n) \in \bar{Q}^{N,M}$.

Theorem 2.5.1. *Let \vec{U}_i^n be the discrete solution of the fully discrete scheme (2.5.1). The error estimate related to the fully discrete scheme (2.5.1) at time level t_n satisfies*

$$\left\| \vec{u} - \vec{U}_i^n \right\|_{\infty} \leq C(\Delta t + N^{-1} \ln N). \quad (2.5.2)$$

Proof. The global error at time level t_n be denoted by $\vec{\mathfrak{E}}_i^n = (\vec{u}(x_i, t_n) - \vec{U}_i^n)$. Then, the global error $\vec{\mathfrak{E}}_i^n$ can be expressed as

$$\left\| \vec{\mathfrak{E}}_i^n \right\|_{\infty} \leq \left\| \vec{u} - \vec{u}^n(x_i) \right\|_{\infty} + \left\| \vec{u}^n - \vec{U}_i^n \right\|_{\infty} + \left\| \vec{U}_i^n - \vec{U}_i^n \right\|_{\infty}. \quad (2.5.3)$$

By substituting the results (2.3.5) and (2.4.10) in (2.5.3), we obtain

$$\left\| \vec{\mathfrak{E}}_i^n \right\|_{\infty} \leq C\Delta t(\Delta t + N^{-1} \ln N) + \left\| \vec{U}_i^n - \vec{U}_i^n \right\|_{\infty}, \quad \text{for } 1 < i \leq N-1. \quad (2.5.4)$$

From (2.4.1) and (2.5.1), we have

$$(I + \Delta t L_{x,\bar{\varepsilon}}^N) \left(\vec{U}_i^n - \vec{U}_i^n \right) = \left(\vec{u}(x_i, t_{n-1}) - \vec{U}_i^{n-1} \right).$$

Applying the stability result (2.4.2), one can obtain

$$\left\| \vec{U}_i^n - \vec{U}_i^n \right\|_{\infty} \leq \left\| \vec{u}(x_i, t_{n-1}) - \vec{U}_i^{n-1} \right\|_{\infty}. \quad (2.5.5)$$

Then, from (2.5.4) and (2.5.5), a recurrence relation for the global errors follows

$$\left\| \vec{\mathfrak{E}}_i^n \right\|_{\infty} \leq C\Delta t(\Delta t + N^{-1} \ln N) + \left\| \vec{\mathfrak{E}}_i^{n-1} \right\|_{\infty}, \quad \text{for } 1 < i \leq N-1. \quad (2.5.6)$$

Hence, we obtain the desired result (2.5.2) from estimate (2.5.6). \blacksquare

2.6 System of Semilinear Parabolic Problems

Here, we apply the difference scheme proposed in the previous section to solve the following system of semilinear parabolic convection-diffusion IBVP:

$$\begin{cases} \frac{\partial \vec{u}}{\partial t} - \mathcal{E} \frac{\partial^2 \vec{u}}{\partial x^2} - A(x) \frac{\partial \vec{u}}{\partial x} + \vec{f}(x, t, \vec{u}) = \vec{0}, & (x, t) \in Q, \\ \vec{u}(x, 0) = \vec{u}_0(x), & x \in \bar{\Omega}_x, \\ \vec{u}(0, t) = \vec{0}, \quad \vec{u}(1, t) = \vec{0}, & t \in (0, T], \end{cases} \quad (2.6.1)$$

where $\vec{f}(x, t, \vec{u}) = (f_1(x, t, u_1, u_2), f_2(x, t, u_1, u_2))^T$. We assume that f_1 and f_2 are sufficiently smooth functions. Furthermore, we assume

$$\frac{\partial f_1}{\partial u_1} \geq \gamma_\beta > 0, \quad \frac{\partial f_2}{\partial u_2} \geq \gamma_\beta > 0, \quad \frac{\partial f_1}{\partial u_2} < 0, \quad \frac{\partial f_2}{\partial u_1} < 0, \quad \text{in } \bar{\Omega}_x \times [0, T] \times \mathbb{R}^2, \quad (2.6.2)$$

$$\min \left\{ \frac{\partial f_1}{\partial u_1} + \frac{\partial f_1}{\partial u_2}, \frac{\partial f_2}{\partial u_1} + \frac{\partial f_2}{\partial u_2} \right\} \geq \tilde{\beta} > 0, \quad \text{in } \bar{\Omega}_x \times [0, T] \times \mathbb{R}^2. \quad (2.6.3)$$

These conditions (2.6.2) and (2.6.3) with the implicit function theorem ensure that there exists a unique solution $\vec{u}(x, t) \in (C_0^2(\bar{Q}))^2$ of problem (2.6.1), also the solution $\vec{u}(x, t)$ has overlapping boundary layers along $x = 0$.

Firstly, we will employ the Newton's quasi-linearization technique to linearize the semilinear problem (2.6.1) and obtained a sequence of linear problems. Whose solutions $\vec{u}^p(x, t)$ with a proper initial guess $\vec{u}^0(x, t)$ converge to the exact solution \vec{u} . And, $\vec{u}^{p+1}(x, t)$ is solution of the following linear parabolic IBVP:

$$\begin{cases} \frac{\partial \vec{u}^{p+1}}{\partial t} - \mathcal{E} \frac{\partial^2 \vec{u}^{p+1}}{\partial x^2} - A(x) \frac{\partial \vec{u}^{p+1}}{\partial x} + \mathcal{J} \vec{u}^{p+1} = \mathcal{F}(x, t, u_1^p, u_2^p), & (x, t) \in Q, \\ \vec{u}(x, 0) = \vec{u}_0(x), & x \in \bar{\Omega}_x, \\ \vec{u}(0, t) = \vec{0}, \quad \vec{u}(1, t) = \vec{0}, & t \in (0, T], \end{cases} \quad (2.6.4)$$

where the reaction coefficient \mathcal{J} (the Jacobian matrix) is given by

$$\mathcal{J}(x, t) = \begin{pmatrix} \frac{\partial f_1(x, t, u_1^p, u_2^p)}{\partial u_1} & \frac{\partial f_1(x, t, u_1^p, u_2^p)}{\partial u_2} \\ \frac{\partial f_2(x, t, u_1^p, u_2^p)}{\partial u_1} & \frac{\partial f_2(x, t, u_1^p, u_2^p)}{\partial u_2} \end{pmatrix}$$

and the source term $\mathcal{F}(x, t, u_1^p, u_2^p) = \mathcal{J}(x, t) \vec{u}^p - \vec{f}(x, t, u_1^p, u_2^p)$. By using conditions given in (2.6.2)-(2.6.3), we can conclude that $\mathcal{J}(x, t)$ is an L_0 -matrix.

For $p \in \mathbb{N}$, consider the following stopping criteria

$$|\vec{u}^{p+1}(x_i, t_n) - \vec{u}^p(x_i, t_n)| \leq Tol, \quad \text{for } (x_i, t_n) \in Q^{N,M}, \quad p \geq 0.$$

Here, Tol denotes the user chosen tolerance bound. Numerical results of system of semilinear IBVP of the form (2.6.1) and (2.6.4) are presented in last section.

2.7 Richardson Extrapolation Technique

In this section, first we introduces the extrapolation of the time semidiscrete solution \vec{u}^n . Later, we describe the Richardson extrapolation technique in the spatial direction, which is used to increase the accuracy of the computed solutions of the upwind based numerical scheme obtained in Section 2.5.

2.7.1 Extrapolation of \vec{u}^n

For the improvement of the semidiscrete solution \vec{u}^n , one need to solve the semidiscrete problem (2.3.3) on the fine mesh Υ^{2M} , with $2M$ number of mesh intervals in the temporal direction. From such construction, it is clear that $\Upsilon^M \subset \Upsilon^{2M}$. In fact, Υ^{2M} is obtained from Υ^M by bisecting each mesh-interval. Therefore, $\tilde{t}_n - \tilde{t}_{n-1} = \Delta t/2$, for $\tilde{t}_n \in \Upsilon^{2M}$. Let \vec{z}^n be the solution of the semidiscrete problem (2.3.3) on the mesh Υ^{2M} . We have

$$\vec{u}^n - \vec{u}(t_n) = \Delta t + o(\Delta t), \quad t_n \in \Upsilon^M. \quad (2.7.1)$$

In a similar way, one can obtain that

$$\vec{z}(\tilde{t}_n) - \vec{u}(\tilde{t}_n) = \Delta t/2 + o(\Delta t), \quad \tilde{t}_n \in \Upsilon^{2M}. \quad (2.7.2)$$

Then, from (2.7.1) and (2.7.2), we get

$$\vec{u}(t_n) - (2\vec{z}(\tilde{t}_n) - \vec{u}(t_n)) = o(\Delta t), \quad t_n \in \Upsilon^M.$$

Therefore, we will use the following extrapolation formula

$$\vec{u}_{\text{extpt}}(t_n) = 2\vec{z}(\tilde{t}_n) - \vec{u}(t_n), \quad t_n \in \Upsilon^M, \quad (2.7.3)$$

to acquire a better semidiscrete solution of the model problem (2.1.1).

Note that, we decompose $\vec{z}(\tilde{t}_n)$ as $\vec{z}(\tilde{t}_n) = \vec{\chi}_{\tilde{v}}(\tilde{t}_n) + \vec{\chi}_{\tilde{w}}(\tilde{t}_n)$, $\tilde{t}_n \in \Upsilon^{2M}$.

Lemma 2.7.1. *Let \vec{u} be the solution of the continuous problem (2.1.1) and \vec{u}_{extpt} be the solution obtained via the Richardson extrapolation technique (2.7.3), by solving the semidiscrete scheme (2.3.3). Then, we have*

$$(\vec{u} - \vec{u}_{\text{extpt}})(x, t_n) = O(\Delta t^3).$$

Proof. By following the methodology from [18], one can obtain the desired result. ■

2.7.2 Extrapolation of \tilde{U}^n

In this subsection, we describe the Richardson extrapolation technique in the spatial direction, which is used to increase the accuracy of the computed solutions of the numerical scheme (2.5.1). To apply this technique, we will solve the discrete problem (2.4.1) on the fine mesh $\bar{\Omega}_x^{2N}$ with $2N$ mesh-intervals in the spatial direction, where $\bar{\Omega}_x^{2N}$ is the piecewise-uniform Shishkin meshes having the same transition points τ_{ε_1} and τ_{ε_2} , as used in $\bar{\Omega}_x^N$. The discrete domain $\bar{\Omega}_x^{2N}$ can be obtained through bisecting each mesh-interval of $\bar{\Omega}_x^N$. Hence the corresponding mesh-sizes in $\bar{\Omega}_x^{2N}$ can be given by

$$\tilde{x}_i - \tilde{x}_{i-1} = \begin{cases} H_1/2, & \text{for } \tilde{x}_i \in \bar{\Omega}_x^{2N} \cap [0, \tau_{\varepsilon_1}], \\ H_2/2, & \text{for } \tilde{x}_i \in \bar{\Omega}_x^{2N} \cap [\tau_{\varepsilon_1}, \tau_{\varepsilon_2}], \\ H_3/2, & \text{for } \tilde{x}_i \in \bar{\Omega}_x^{2N} \cap [\tau_{\varepsilon_2}, 1]. \end{cases}$$

Let \tilde{U}_i^n be the solution of discrete problem (2.4.1) on the mesh $\bar{\Omega}_x^N$. From Lemma 2.4.2, it follows that

$$\begin{aligned} (\tilde{U}^n - \tilde{u}^n)(x_i) &= \vec{C} (N^{-1} \ln N) + o(N^{-1} \ln N) \\ &= \vec{C}_1 (N^{-1} (\alpha \tau_{\varepsilon_2} / 2\varepsilon_2)) + o(N^{-1} \ln N), \quad x_i \in \bar{\Omega}_x^N, \end{aligned} \quad (2.7.4)$$

where \vec{C}_1 is some fixed positive constant. Similarly, if $\tilde{U}^n(\tilde{x}_i)$ is the solution of the discrete problem (2.4.1) on the mesh $\bar{\Omega}_x^{2N}$, then we have

$$(\tilde{U}^n - \tilde{u}^n)(\tilde{x}_i) = \vec{C}_1 ((2N)^{-1} (\alpha \tau_{\varepsilon_2} / 2\varepsilon_2)) + o(N^{-1} \ln N), \quad x_i \in \bar{\Omega}_x^{2N}. \quad (2.7.5)$$

Now, from (2.7.4) and (2.7.5), eliminating $O(N^{-1})$, we get

$$\left(\tilde{u}^n - \left(2\tilde{U}^n - \tilde{U}^n \right) \right) (x_i) = o(N^{-1} \ln N), \quad x_i \in \bar{\Omega}_x^N.$$

Therefore, we shall use the following extrapolation formula

$$\tilde{U}_{extp}^n(x_i) = (2\tilde{U}^n - \tilde{U}^n)(x_i), \quad x_i \in \bar{\Omega}_x^N, \quad (2.7.6)$$

which will yield an approximation to \tilde{u}^n more accurate than both \tilde{U}^n and \tilde{U}^n .

To obtain the estimate of the nodal error, we decompose the solution \tilde{U}^n as $\tilde{U}^n = \tilde{V}^n + \tilde{W}^n$, where the smooth component \tilde{V}^n is the solution of following discrete problem:

$$\begin{cases} (I + \Delta t L_{x,\varepsilon}^N) \tilde{V}^{n+1}(x_i) = \vec{v}(x_i, t_n) + \Delta t \vec{f}(x_i, t_{n+1}), & i = 1, \dots, N-1, \\ \tilde{V}^{n+1}(0) = \vec{v}^{n+1}(0), \quad \tilde{V}^{n+1}(1) = \vec{v}^{n+1}(1), \end{cases}$$

and the layer component $\tilde{W}^{\rightarrow n}$ satisfies

$$\begin{cases} (I + \Delta t L_{x,\varepsilon}^N) \tilde{W}^{\rightarrow n+1}(x_i) = \tilde{w}(x_i, t_n), & i = 1, \dots, N-1, \\ \tilde{W}^{\rightarrow n+1}(0) = \tilde{w}^{\rightarrow n+1}(0), & \tilde{W}^{\rightarrow n+1}(1) = \tilde{w}^{\rightarrow n+1}(1). \end{cases}$$

Similarly, we can write the decomposition of $\tilde{U}^{\rightarrow n+1}(\tilde{x}_i)$ on the fine mesh of the temporal direction, as

$$\tilde{U}^{\rightarrow n+1}(\tilde{x}_i) = \tilde{\mathcal{V}}^{\rightarrow n+1}(\tilde{x}_i) + \tilde{\mathcal{W}}^{\rightarrow n+1}(\tilde{x}_i).$$

Therefore, the error can be expressed in the following form

$$\left(\tilde{U}^{\rightarrow n+1} - \tilde{u}^{\rightarrow n+1} \right)(x_i) = \left(\tilde{V}^{\rightarrow n+1} - \tilde{v}^{\rightarrow n+1} \right)(x_i) + \left(\tilde{W}^{\rightarrow n+1} - \tilde{w}^{\rightarrow n+1} \right)(x_i),$$

and

$$\left(\tilde{U}^{\rightarrow n+1} - \tilde{u}^{\rightarrow n+1} \right)(\tilde{x}_i) = \left(\tilde{\mathcal{V}}^{\rightarrow n+1} - \tilde{v}^{\rightarrow n+1} \right)(\tilde{x}_i) + \left(\tilde{\mathcal{W}}^{\rightarrow n+1} - \tilde{w}^{\rightarrow n+1} \right)(\tilde{x}_i).$$

Error estimate for the extrapolated smooth component

Lemma 2.7.2. *Assume that $0 < \varepsilon_1 \leq \varepsilon_2 \leq N^{-1}$. Then, for $1 \leq i \leq N-1$, the local truncation error associated with the smooth component satisfies*

$$\begin{aligned} (I + \Delta t L_{x,\varepsilon_1}^N) (\tilde{V}^{\rightarrow n+1} - \tilde{v}^{\rightarrow n+1})(x_i) &= \Delta t \frac{h_i}{2} a_1(x_i) \frac{\partial^2 \tilde{v}_1^{\rightarrow n+1}}{\partial x^2}(x_i) + O(H_3^2), \\ (I + \Delta t L_{x,\varepsilon_2}^N) (\tilde{V}^{\rightarrow n+1} - \tilde{v}^{\rightarrow n+1})(x_i) &= \Delta t \frac{h_i}{2} a_2(x_i) \frac{\partial^2 \tilde{v}_2^{\rightarrow n+1}}{\partial x^2}(x_i) + O(H_3^2). \end{aligned}$$

Proof. By using the Taylor's expansions and the derivative bounds of $\tilde{v}^{\rightarrow n+1}$ given in (2.3.10), we obtain

$$\begin{aligned} (I + \Delta t L_{x,\varepsilon_1}^N) (\tilde{V}^{\rightarrow n+1} - \tilde{v}^{\rightarrow n+1})(x_i) &= \frac{\varepsilon_1 \Delta t}{3(h_i + h_{i+1})} \left[h_{i+1}^2 \frac{\partial^3 \tilde{v}_1}{\partial x^3}(\xi_1, t_{n+1}) - h_i^2 \frac{\partial^3 \tilde{v}_1}{\partial x^3}(\xi_2, t_{n+1}) \right] \\ &\quad + \Delta t \frac{h_i}{2} a_1(x_i) \frac{\partial^2 \tilde{v}_1}{\partial x^2}(x_i, t_{n+1}) - \Delta t \frac{h_i^2}{6} a_1(x_i) \frac{\partial^3 \tilde{v}_1}{\partial x^3}(\xi_3, t_{n+1}), \end{aligned}$$

for some $\xi_1, \xi_3 \in (x_i, x_{i+1})$, $\xi_2 \in (x_{i-1}, x_i)$. An analogous argument establishes the desired estimate for $(I + \Delta t L_{x,\varepsilon_2}^N) (\tilde{V}^{\rightarrow n+1} - \tilde{v}^{\rightarrow n+1})$. This completes the proof. \blacksquare

By adopting the approach provided in Keller [37], the function $\tilde{\tilde{E}}(x)$ is defined as the solutions of the following problems:

$$\begin{cases} (I + \Delta t L_{x,\varepsilon}) \tilde{\tilde{E}}(x) = \Delta t \frac{h_i}{2} A(x) \frac{\partial^2 \tilde{\tilde{v}}}{\partial x^2}(x, t_{n+1}), \\ \tilde{\tilde{E}}(0) = \tilde{\tilde{E}}(1) = \vec{0}. \end{cases} \quad (2.7.7)$$

Similar to the decomposition of \tilde{u}^{n+1} , we decompose $\tilde{E}(x)$ as $\tilde{E}(x) = \tilde{E}_v(x) + \tilde{E}_w(x)$, where the smooth component $\tilde{E}_v(x)$ and the layer component $\tilde{E}_w(x)$ satisfy

$$\begin{cases} (I + \Delta t L_{x,\tilde{\varepsilon}}) \tilde{E}_v(x) = \Delta t \frac{h_i}{2} A(x) \frac{\partial^2 \tilde{v}}{\partial x^2}(x, t_{n+1}), \\ (I + \Delta t L_{x,\tilde{\varepsilon}}) \tilde{E}_w(x) = \vec{0}, \\ \tilde{E}_v(1) = \tilde{E}_w(1) = \vec{0}, \\ \tilde{E}_w(0) = -\tilde{E}_v(0). \end{cases} \quad (2.7.8)$$

Lemma 2.7.3. *For all non-negative integer k , satisfying $0 \leq k \leq 3$, the smooth components \tilde{E}_v , defined in (2.7.8) satisfy the following bounds*

$$\left\| \frac{\partial^k \tilde{E}_v}{\partial x^k} \right\|_{\infty} \leq C, \quad k = 1, 2, \quad \left\| \frac{\partial^3 \tilde{E}_v}{\partial x^3} \right\|_{\infty} \leq C(1 + \varepsilon_1^{-1} + \varepsilon_2^{-1}).$$

Proof. By using the methodology of Mukharjee and Natesan [64] and applying the bounds of the derivatives of \tilde{v}^{n+1} given in (2.3.10), one can get the required bounds. ■

Lemma 2.7.4. *Assume that $0 < \varepsilon_1 \leq \varepsilon_2 \leq N^{-1}$. Then, for $1 \leq i \leq N - 1$, we have*

$$(\tilde{V}^{n+1} - \tilde{v}^{n+1})(x_i) = h_i \tilde{E}_v(x_i) + O(H_3^2).$$

Proof. Consider $1 \leq i \leq N - 1$. By employing Lemma 2.7.2 and (2.7.8), we have

$$(I + \Delta t L_{x,\tilde{\varepsilon}}^N)(\tilde{V}^{n+1} - \tilde{v}^{n+1})(x_i) = h_i (I + \Delta t L_{x,\tilde{\varepsilon}}^N) \tilde{E}_v(x_i) + O(H_3^2)$$

By using the Taylor's expansion and Lemma 2.7.3, it is easy to get

$$\left| h_i ((I + \Delta t L_{x,\tilde{\varepsilon}}^N) - (I + \Delta t L_{x,\tilde{\varepsilon}})) \tilde{E}_v(x_i) \right| \leq \vec{C} H_3^2. \quad (2.7.9)$$

Therefore, (2.7.9) implies that

$$(I + \Delta t L_{x,\tilde{\varepsilon}}^N) \left[(\tilde{V}^{n+1} - \tilde{v}^{n+1})(x_i) - h_i \tilde{E}_v(x_i) \right] \leq \vec{C} H_3^2.$$

By using the discrete maximum principle (Lemma 2.4.1), we get the desired result. ■

Similarly, in the finer mesh of the temporal direction, we get that

$$(\tilde{V}^{n+1} - \tilde{\chi}_v^{n+1})(x_i) = h_i \tilde{E}_v(x_i) + O(H_3^2).$$

Therefore, we have

$$\left| \left(\tilde{V}_{extpt} - \tilde{v}_{extpt} \right) (x_i, t_n) \right| \leq \vec{C} N^{-2}, \quad \text{for } 1 \leq i \leq N - 1.$$

where \tilde{v}_{extpt} and \tilde{V}_{extpt} are the time extrapolated solutions of \tilde{v} and \tilde{V} , respectively.

Lemma 2.7.5. *Assume that $0 < \varepsilon_1 \leq \varepsilon_2 \leq N^{-1}$. Then, the error after extrapolation associated with the smooth component satisfies*

$$\left| \left(\vec{V}_{extp} - \vec{v}_{extp^t} \right) (x_i, t_n) \right| \leq \vec{C}N^{-2}, \quad \text{for } 1 \leq i \leq N-1.$$

Proof. Based on the construction of the meshes in $\overline{Q}^{2N,2M}$ and $\overline{Q}^{N,M}$, we have

$$\left(\vec{V}_{extp^t} - \vec{v}_{extp^t} \right) (x_i, t_n) = \begin{cases} \frac{H_1}{2} \vec{E}_v(x_i, t_n) + O(N^{-2}), & \text{for } 1 \leq i \leq \frac{N}{4}, \\ \frac{H_2}{2} \vec{E}_v(x_i, t_n) + O(N^{-2}), & \text{for } \frac{N}{4} + 1 \leq i \leq \frac{N}{2}, \\ \frac{H_3}{2} \vec{E}_v(x_i, t_n) + O(N^{-2}), & \text{for } \frac{N}{2} + 1 \leq i \leq N-1, \end{cases}$$

where \vec{V}_{extp} is the time extrapolated solution in $\overline{Q}^{2N,M}$.

Therefore, we have

$$\begin{aligned} \left(\vec{V}_{extp} - \vec{v}_{extp^t} \right) (x_i, t_n) &= \left(\left(2\vec{V}_{extp^t} - \vec{V}_{extp^t} \right) - \vec{v}_{extp^t} \right) (x_i, t_n) \\ &= \left(2 \left(\vec{V}_{extp^t} - \vec{v}_{extp^t} \right) - \left(\vec{V}_{extp^t} - \vec{v}_{extp^t} \right) \right) (x_i, t_n) = O(N^{-2}), \end{aligned}$$

which is the required result. \blacksquare

Error estimate for the extrapolated layer component

Lemma 2.7.6. *Assume that $0 < \varepsilon_1 \leq \varepsilon_2 \leq N^{-1}$. The error after extrapolation associated to the layer component satisfies*

$$\left| \left(\vec{W}_{extp} - \vec{w}_{extp^t} \right) (x_i, t_n) \right| \leq \vec{C}N^{-2}, \quad \text{for } N/2 \leq i \leq N-1.$$

Proof. By combining the methodology from [18, Lemma 5.5] with extrapolation formulas (2.7.3) and (2.7.6) associated with the layer component, one can obtain the required estimate. \blacksquare

For the sake of simplicity, define the functions $\vec{\rho} = (\rho_1, \rho_2)^T$, as

$$\rho_1(x, t_{n+1}) = \frac{2\varepsilon_1}{\alpha} a_1(x) \frac{\partial^2 \tilde{w}_1}{\partial x^2}(x, t_{n+1}) \quad \text{and} \quad \rho_2(x, t_{n+1}) = \frac{2\varepsilon_2}{\alpha} a_2(x) \frac{\partial^2 \tilde{w}_2}{\partial x^2}(x, t_{n+1}).$$

Next, we analyze the effect of the extrapolation for $x_i \in [0, \tau_{\varepsilon_2})$.

Lemma 2.7.7. *For $1 \leq i \leq N/2 - 1$, the extrapolation error associated with the layer component satisfies*

$$\begin{aligned} (I + \Delta t L_{x, \varepsilon_1}^N)(\vec{W} - \vec{w})(x_i, t_{n+1}) &= (N^{-1} \ln N) \rho_l(x_i, t_{n+1}) + O(N^{-2} \ln^2 N (\varepsilon_1^{-1} B_{\varepsilon_1}^0(x_{i-1}) \\ &\quad + \varepsilon_2^{-1} B_{\varepsilon_2}^0(x_{i-1}))), \quad l = 1, 2. \end{aligned}$$

Proof. First, consider $x_i \in (0, \tau_{\varepsilon_1})$. By using Taylor's expansion with derivative bounds (2.3.11) and (2.3.12), for $\xi_1, \xi_3 \in (x_i, x_{i+1})$ and $\xi_2 \in (x_{i-1}, x_i)$, we have

$$\begin{aligned} \left| (I + \Delta t L_{x, \varepsilon_1}^N)(\vec{W} - \vec{w})(x_i, t_{n+1}) \right| &= \frac{\varepsilon_1 \Delta t H_1^2}{4!} \left[\frac{\partial^4 \tilde{w}_1}{\partial x^4}(\xi_1, t_{n+1}) + \frac{\partial^4 \tilde{w}_1}{\partial x^4}(\xi_2, t_{n+1}) \right] \\ &\quad + \Delta t a_1(x_i) \left[\frac{H_1}{2} \frac{\partial^2 \tilde{w}_1}{\partial x^2}(x_i, t_{n+1}) - \frac{H_1^2}{3!} \frac{\partial^3 \tilde{w}_1}{\partial x^3}(\xi_3, t_{n+1}) \right] \\ &\leq C \Delta t (N^{-1} \ln N) \rho_1(x_i, t_{n+1}) \\ &\quad + O(N^{-2} \ln^2 N (\varepsilon_1^{-1} B_{\varepsilon_1}^0(x_{i-1}) + \varepsilon_2^{-1} B_{\varepsilon_2}^0(x_{i-1}))). \end{aligned}$$

Similar estimate will hold for $(I + \Delta t L_{x, \varepsilon_2}^N)(\vec{W} - \vec{w})$. Next we shall consider the truncation error at $x_i = \tau_{\varepsilon_1}$, where $h_i \neq h_{i+1}$. It can be easily verified that

$$\varepsilon_1^{-k} B_{\varepsilon_1}^0(\tau) \leq C \varepsilon_2^{-k} B_{\varepsilon_2}^0(\tau), \quad \text{for } \tau > \frac{2\varepsilon_1}{\alpha}, \quad k = 1, 2, 3, 4. \quad (2.7.10)$$

By using Taylor's expansion with derivative bounds (2.3.11) and (2.3.12) with inequality (2.7.10), one can deduce that

$$\begin{aligned} \left| (I + \Delta t L_{x, \varepsilon_1}^N)(\vec{W} - \vec{w})(x_i, t_{n+1}) \right| &\leq C \Delta t (N^{-1} \ln N) \rho_l(x, t_{n+1}) \\ &\quad + O(\varepsilon_2^{-1} B_{\varepsilon_2}^0(x_{i-1}) N^{-2} \ln^2 N), \quad \text{for } l = 1, 2. \end{aligned}$$

In a similar manner, one can obtain above estimates for $x_i \in (\tau_{\varepsilon_1}, \tau_{\varepsilon_2})$. This completes the proof. \blacksquare

Next, we consider the BVP

$$\begin{cases} (I + \Delta t L_{x, \varepsilon}^N) \vec{F}(x) = \vec{\rho}(x, t_{n+1}), & \text{in } (0, \tau_{\varepsilon_2}), \\ \vec{F}(0) = \vec{F}(1) = \vec{0}. \end{cases} \quad (2.7.11)$$

Now, we discuss the derivative bounds of \vec{F} in the following lemma.

Lemma 2.7.8. *For all non-negative integers k satisfying $0 \leq k \leq 3$, the derivatives of the $\vec{F} = (\tilde{F}_1, \tilde{F}_2)^T$ satisfy estimates*

$$\begin{aligned} \left| \frac{\partial^k \tilde{F}_1}{\partial x^k}(x) \right| &\leq C \begin{cases} B_{\varepsilon_2}^0(x), & \text{for } k = 0, \\ (\varepsilon_1^{-k} B_{\varepsilon_1}^0(x) + \varepsilon_2^{-k} B_{\varepsilon_2}^0(x)), & \text{for } k = 1, 2, 3 \end{cases} \\ \left| \frac{\partial^k \tilde{F}_2}{\partial x^k}(x) \right| &\leq C \begin{cases} \varepsilon_2^{-k} B_{\varepsilon_2}^0(x), & \text{for } k = 0, 1, 2, \\ \varepsilon_2^{-1} (\varepsilon_1^{-2} B_{\varepsilon_1}^0(x) + \varepsilon_2^{-2} B_{\varepsilon_2}^0(x)), & \text{for } k = 3. \end{cases} \end{aligned}$$

Proof. By following the technique from Theorem 2.2.4, one can obtain the desired derivative bounds. ■

Lemma 2.7.9. For $1 \leq i \leq N/2 - 1$, we have

$$(\vec{W} - \vec{w})(x_i, t_{n+1}) = (N^{-1} \ln N) \vec{F}(x_i) + O(N^{-2} \ln^3 N). \quad (2.7.12)$$

Proof. First, we consider the case for $1 \leq i \leq N/4 - 1$. By using Lemmas 2.7.7 and 2.7.8 with (2.7.11), for $1 \leq i \leq N/2 - 1$, we deduce that

$$\begin{aligned} \left| (I + \Delta t L_{x, \varepsilon}^N) \left[(\vec{W} - \vec{w}) - (N^{-1} \ln N) \vec{F}(x_i) \right] (x_i, t_{n+1}) \right| \\ \leq \vec{C} N^{-2} \ln^2 N (\varepsilon_1^{-1} B_{\varepsilon_1}(x_{i-1}) + \varepsilon_2^{-1} B_{\varepsilon_2}(x_{i-1})). \end{aligned} \quad (2.7.13)$$

Now consider the discrete barrier function $\vec{\mathfrak{B}}_w(x_i) = (\mathfrak{B}_w(x_i), \mathfrak{B}_w(x_i))^T$, where

$$\mathfrak{B}_w(x_i) = C \begin{cases} N^{-2}(1 - x_i) + N^{-2} \ln^2 N (\varepsilon_1^{-1} + \varepsilon_2^{-1}) (\tau_{\varepsilon_1} - x_i), & i \leq N/4 - 1 \\ N^{-2}(1 - x_i) + N^{-2} \ln^2 N \varepsilon_2^{-1} (\tau_{\varepsilon_2} - x_i), & N/4 \leq i \leq N/2 - 1. \end{cases}$$

For $1 \leq i \leq N/2 - 1$, it is easy to show from (2.7.13) that

$$(I + \Delta t L_{x, \varepsilon}^N) \vec{\mathfrak{B}}_w(x_i) \geq \left| (I + \Delta t L_{x, \varepsilon}^N) \left[(\vec{W} - \vec{w}) - (N^{-1} \ln N) \vec{F} \right] (x_i, t_{n+1}) \right|.$$

By using discrete maximum principle (Lemma 2.4.1), we can obtain (2.7.12). ■

In a similar way, in the finer mesh of temporal direction, we get that

$$(\vec{W} - \vec{\chi}_w)(x_i, t_{n+1}) = (N^{-1} \ln N) \vec{F}(x_i, t_{n+1}) + O(N^{-2} \ln^3 N). \quad (2.7.14)$$

Lemma 2.7.10. The error after extrapolation associated with the layer component \vec{W}_{extp} satisfies following estimate

$$\left| \left(\vec{W}_{extp} - \vec{w}_{extp}^t \right) (x_i, t_n) \right| \leq \vec{C} N^{-2} \ln^3 N, \quad \text{for } 1 \leq i \leq N/2 - 1.$$

Proof. By following the technique from Lemma 2.7.5 with estimates (2.7.12) and (2.7.14), we can obtain the desired result. ■

Now, by combining the results of Lemmas 2.7.5, 2.7.6 and 2.7.10, we can deduce that

$$\left| \left(\vec{U}_{extp} - \vec{u}_{extp}^t \right) (x_i, t_n) \right| \leq \vec{C} N^{-2} \ln^3 N, \quad \text{for } 1 \leq i \leq N - 1. \quad (2.7.15)$$

Theorem 2.7.11. (Error after extrapolation) Assume that $0 < \varepsilon_1 \leq \varepsilon_2 \leq N^{-1}$. Let \vec{u} be the solution of the continuous problem (2.1.1) and \vec{U}_{extp} be the solution obtained via the Richardson extrapolation technique by solving the discrete problem (2.5.1) on the two nested meshes $\overline{Q}^{N,M}$ and $\overline{Q}^{2N,2M}$. Then, for $0 < \nu < 1$, we have the following error bound associated with \vec{U}_{extp} :

$$\left\| (\vec{u} - \vec{U}_{extp})(x_i, t_n) \right\|_{\infty} \leq C (N^{-2+\nu} \ln^3 N + \Delta t^2), \text{ for } 1 \leq i \leq N-1. \quad (2.7.16)$$

Proof. By using Lemma 2.7.1 and estimate (2.7.15), we have

$$\begin{aligned} \left\| \vec{u}(x_i, t_n) - \vec{U}_{extp}(x_i, t_n) \right\|_{\infty} &= \left\| \left(\vec{u} - \vec{u}_{extp^t} + \vec{u}_{extp^t} - \vec{U}_{extp} + \vec{U}_{extp} - \vec{U}_{extp} \right) (x_i, t_n) \right\|_{\infty} \\ &\leq \left\| (\vec{u} - \vec{u}_{extp^t})(x_i, t_n) \right\|_{\infty} + \left\| \left(\vec{u}_{extp^t} - \vec{U}_{extp} \right) (x_i, t_n) \right\|_{\infty} \\ &\quad + \left\| \left(\vec{U}_{extp} - \vec{U}_{extp} \right) (x_i, t_n) \right\|_{\infty} \\ &\leq C (\Delta t^3 + N^{-2} \ln^3 N) + \left\| \left(\vec{U}_{extp} - \vec{U}_{extp} \right) (x_i, t_n) \right\|_{\infty} \end{aligned}$$

Note that, if we take $N^{-\nu} \leq C\Delta t$ with $0 < \nu < 1$, one can deduce that

$$\left\| \vec{u}(x_i, t_n) - \vec{U}_{extp}(x_i, t_n) \right\|_{\infty} \leq C (\Delta t^3 + N^{-2+\nu} \ln^3 N) + \left\| \left(\vec{U}_{extp} - \vec{U}_{extp} \right) (x_i, t_n) \right\|_{\infty}.$$

By following the methodology from Theorem 2.5.1, we can get the desired result. \blacksquare

2.8 Numerical Results

In this section, we present numerical results for some test problems on the piecewise-uniform rectangular mesh $\overline{Q}^{N,M}$ to validate the theoretical results derived in the previous section. We have considered system of linear convection-diffusion problem and semilinear convection-diffusion problem. For all examples, we perform the numerical experiments by choosing the constant $\alpha = 0.5$.

2.8.1 Upwind based numerical scheme

Example 2.8.1. Consider the following system of parabolic IBVP on $Q = (0, 1) \times (0, 1]$:

$$\begin{cases} \frac{\partial u_1}{\partial t} - \varepsilon_1 \frac{\partial^2 u_1}{\partial x^2} - \frac{\partial u_1}{\partial x} + (1+x)u_1 - u_2 = (x^2 - x)(t^2 + 1) \exp(-t), \\ \frac{\partial u_2}{\partial t} - \varepsilon_2 \frac{\partial^2 u_2}{\partial x^2} - \frac{\partial u_2}{\partial x} + (1+2x)u_2 - u_1 = (x-1)(t^2 - 4t) \exp(-4t), \\ u_1(x, 0) = 0, \quad u_2(x, 0) = 0, \\ u_1(0, t) = u_1(1, t) = 0, \quad u_2(0, t) = u_2(1, t) = 0, \quad t \in [0, 1]. \end{cases}$$

As the exact solution of the Example 2.8.1 is not known, we use the double-mesh principle to obtain the accuracy of the numerical approximation of the proposed scheme, which is described as follows:

Let \vec{U}_i^n be the numerical approximation of $\vec{u}(x, t)$ on mesh $\bar{Q}^{N,M}$ with N mesh-intervals in the spatial direction and M mesh-intervals in the time direction and \vec{U}_{2i}^{2n} be the numerical solution obtained on the fine mesh $\bar{Q}^{2N,2M}$, which contains the mesh points of the original mesh and their midpoints.

For $l = 1, 2$, we calculate the maximum pointwise errors and uniform errors by

$$d_{\varepsilon,l}^{N,M} = \max_{0 \leq n \leq M} \max_{0 \leq i \leq N} |U_{l,i}^n - U_{l,2i}^{2n}|, \quad d_l^{N,M} = \max_{S_\varepsilon} d_{\varepsilon,l}^{N,M}.$$

In addition, we determine the corresponding order of convergence and the uniform order of convergence by

$$p_{\varepsilon,l}^{N,M} = \log_2 \left(\frac{d_{\varepsilon,l}^{N,M}}{d_{\varepsilon,l}^{2N,2M}} \right), \quad p_l^{N,M} = \log_2 \left(\frac{d_l^{N,M}}{d_l^{2N,2M}} \right).$$

The spatial discretization parameter takes the values $N = 32, 64, 128, 256, 512$ and time discretization parameter $\Delta t = 1/M$, $M = N/4$. Here the singular perturbation parameters take values from the set $S_\varepsilon = \{(\varepsilon_1, \varepsilon_2) | \varepsilon_2 = 2^{-2}, \dots, 2^{-18}, \varepsilon_1 = 2^{-4}\varepsilon_2\}$, which is a sufficiently small choice to bring out the singularly perturbed nature of the problem.

We have plotted the surface plots of the numerical solution for $N = 64, M = 16$ with $\varepsilon_1 = 2^{-8}, \varepsilon_2 = 2^{-4}$ in Fig. 2.3 and Fig. 2.4, which confirm the boundary layer phenomena of solutions of Example 2.8.1.

In Table 2.1, uniform errors and the corresponding orders of convergence for Example 2.8.1 are presented for various values of $\varepsilon_1, \varepsilon_2$ and N . We have plotted the maximum pointwise errors in loglog plot in Fig. 2.5 and Fig. 2.6, which confirm the order of convergence.

Example 2.8.2. Consider the following system of semilinear parabolic IBVP on $Q = (0, 1) \times (0, 1]$:

$$\begin{cases} \frac{\partial u_1}{\partial t} - \varepsilon_1 \frac{\partial^2 u_1}{\partial x^2} - \frac{\partial u_1}{\partial x} + \exp(u_1 - u_2) = 0, \\ \frac{\partial u_2}{\partial t} - \varepsilon_2 \frac{\partial^2 u_2}{\partial x^2} - \frac{\partial u_2}{\partial x} + \exp(u_2 - u_1) = 0, \\ u_1(x, 0) = \frac{1 - \exp(-x/\varepsilon_1)}{1 - \exp(-1/\varepsilon_1)} - x, \quad u_2(x, 0) = \frac{1 - \exp(-x/\varepsilon_2)}{1 - \exp(-1/\varepsilon_2)} - x, \\ u_1(0, t) = u_1(1, t) = 0, \quad u_2(0, t) = u_2(1, t) = 0, \quad t \in [0, 1]. \end{cases}$$

By applying the Newton's linearization process (2.6.3) to Example 2.8.2, we obtain the following singular perturbation system of linear parabolic IBVP:

$$\left\{ \begin{array}{l} \frac{\partial u_1^{p+1}}{\partial t} - \varepsilon_1 \frac{\partial^2 u_1^{p+1}}{\partial x^2} - \frac{\partial u_1^{p+1}}{\partial x} + \exp(u_1^p - u_2^p)u_1^{p+1} - \exp(u_1^p - u_2^p)u_2^{p+1} \\ \quad = (\exp(u_1^p - u_2^p) - 1)u_1^p - \exp(u_1^p - u_2^p)u_2^p, \\ \frac{\partial u_2^{p+1}}{\partial t} - \varepsilon_2 \frac{\partial^2 u_2^{p+1}}{\partial x^2} - \frac{\partial u_2^{p+1}}{\partial x} - \exp(u_2^p - u_1^p)u_1^{p+1} + \exp(u_2^p - u_1^p)u_2^{p+1} \\ \quad = -\exp(u_2^p - u_1^p)u_1^p + (\exp(u_2^p - u_1^p) - 1)u_2^p, \\ u_1^{p+1}(x, 0) = u_1(x, 0), \quad u_2^{p+1}(x, 0) = u_2(x, 0), \\ u_1^{p+1}(0, t) = u_1^{p+1}(1, t) = 0, \quad u_2^{p+1}(0, t) = u_2^{p+1}(1, t) = 0, \quad t \in [0, 1]. \end{array} \right.$$

Hence for a fixed p , we solve the above linearized problem by using the computational method discussed in Section 2.6. As a convergence criterion for the Newton's linearization process, we use

$$\max \left\{ \left| U_{1,i}^{n^{(p)}} - U_{1,i}^{n^{(p-1)}} \right|, \left| U_{2,i}^{n^{(p)}} - U_{2,i}^{n^{(p-1)}} \right| \right\} \leq 10^{-7},$$

where, we choose $U_{1,i}^{n^{(0)}} = U_{2,i}^{n^{(0)}} = 0$ as an initial guess. Once we get the prescribed tolerance bound we terminate the iteration and take that as the solution to the problem.

Since, the exact solution of Example 2.8.2 is also not known, to obtain the accuracy of the numerical solution and also to demonstrate the \mathcal{E} -uniform convergence of the proposed scheme, we will follow the double-mesh principle as described previously.

Fig. 2.7 and Fig. 2.8 show the numerical solution of Example 2.8.2, where boundary layers can be observed. From Table 2.2, we see the monotonically decreasing behavior of ε -uniform errors obtained for $N = 32, 64, 128, 256, 512$ and $M = N$ with the singular perturbation parameters $\widehat{S}_\varepsilon = \{(\varepsilon_1, \varepsilon_2) | (2^{-18}, 2^{-8}), (2^{-20}, 2^{-10})\}$. One can also observe the uniform error behavior via loglog plots given in Fig. 2.9 and Fig. 2.10.

2.8.2 Richardson extrapolation technique

Example 2.8.3. Consider the following system of parabolic IBVP on $Q = (0, 1) \times (0, 1]$:

$$\left\{ \begin{array}{l} \frac{\partial u_1}{\partial t} - \varepsilon_1 \frac{\partial^2 u_1}{\partial x^2} - \frac{\partial u_1}{\partial x} + (1+x)u_1 - u_2 = (x^2 - x + 1) \exp(-t), \\ \frac{\partial u_2}{\partial t} - \varepsilon_2 \frac{\partial^2 u_2}{\partial x^2} - \frac{\partial u_2}{\partial x} + (1+2x)u_2 - u_1 = \exp(-4t), \\ u_1(x, 0) = \frac{1 - \exp(-x/\varepsilon_1)}{1 - \exp(-1/\varepsilon_1)} - x, \quad u_2(x, 0) = \frac{1 - \exp(-x/\varepsilon_2)}{1 - \exp(-1/\varepsilon_2)} - x, \\ u_1(0, t) = u_1(1, t) = 0, \quad u_2(0, t) = u_2(1, t) = 0, \quad t \in [0, 1]. \end{array} \right.$$

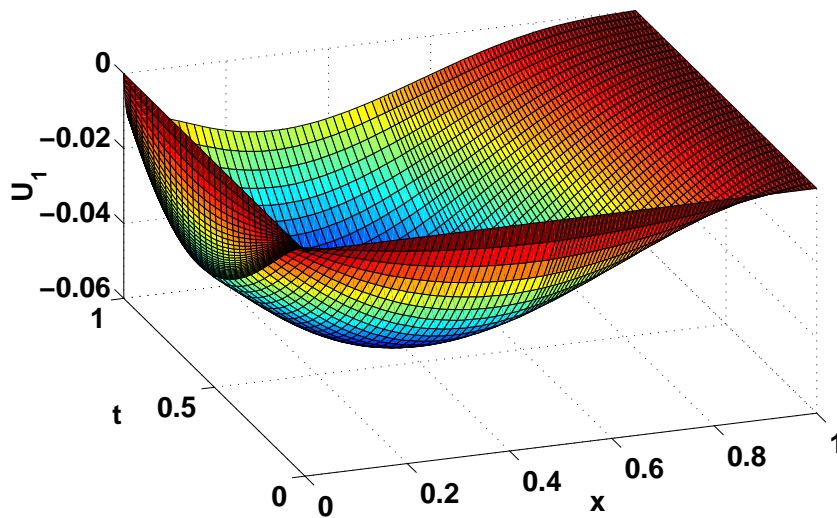


Figure 2.3: Surface plot of the numerical solution U_1 of Example 2.8.1 for $\varepsilon_1 = 2^{-8}$, $\varepsilon_2 = 2^{-4}$, $N = 64$, $M = 16$.

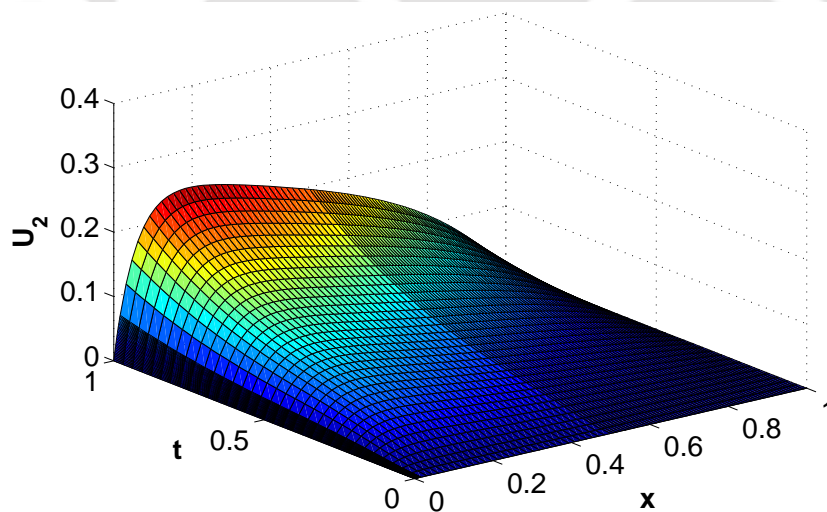


Figure 2.4: Surface plot of the numerical solution U_2 of Example 2.8.1 for $\varepsilon_1 = 2^{-8}$, $\varepsilon_2 = 2^{-4}$, $N = 64$, $M = 16$.

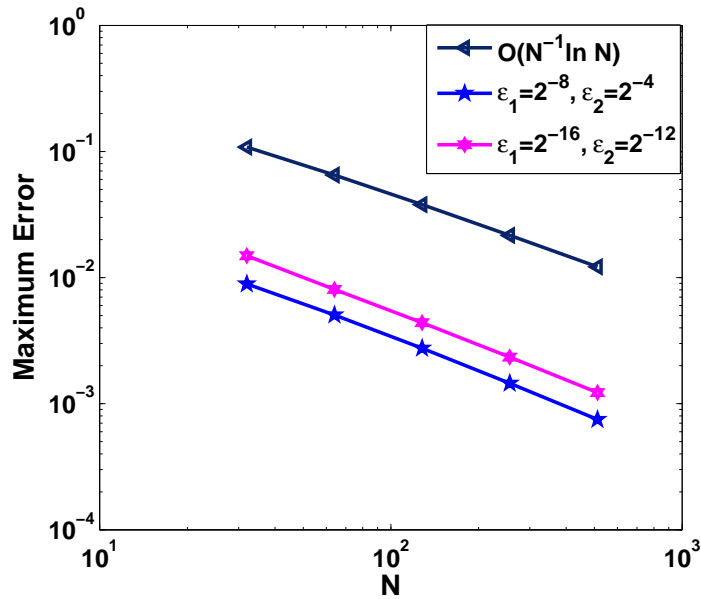


Figure 2.5: *Loglog plot for the spatial order of convergence associated with numerical solution U_1 for Example 2.8.1.*

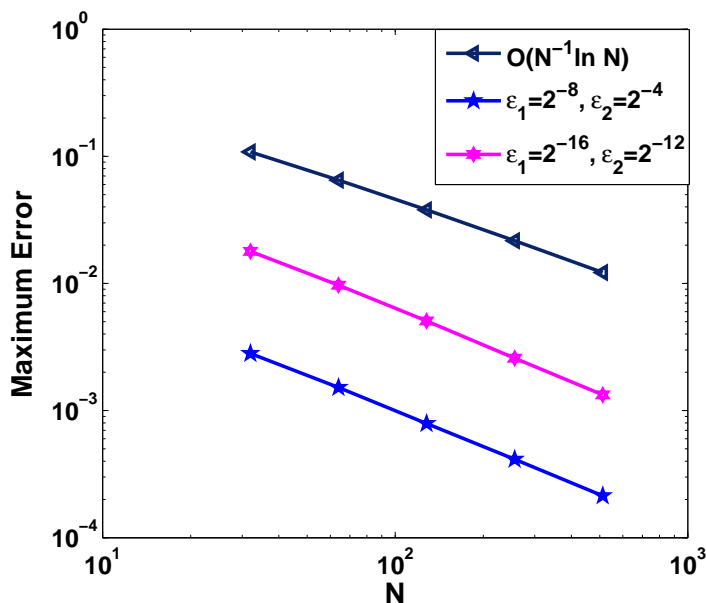


Figure 2.6: *Loglog plot for the spatial order of convergence associated with numerical solution U_2 for Example 2.8.1.*

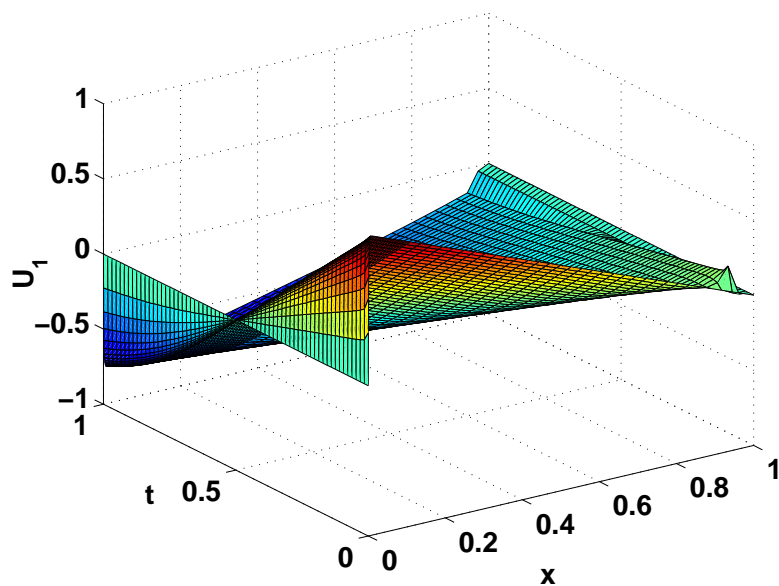


Figure 2.7: Surface plot of numerical solution U_1 of Example 2.8.2 for $\varepsilon_1 = 2^{-10}$, $\varepsilon_2 = 2^{-6}$, $N = M = 32$.

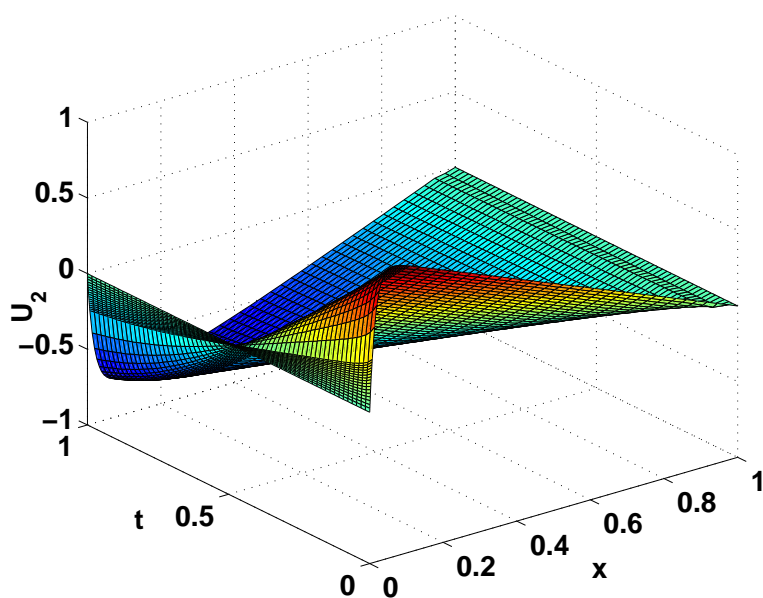


Figure 2.8: Surface plot of numerical solution U_2 of Example 2.8.2 for $\varepsilon_1 = 2^{-10}$, $\varepsilon_2 = 2^{-6}$, $N = M = 32$.

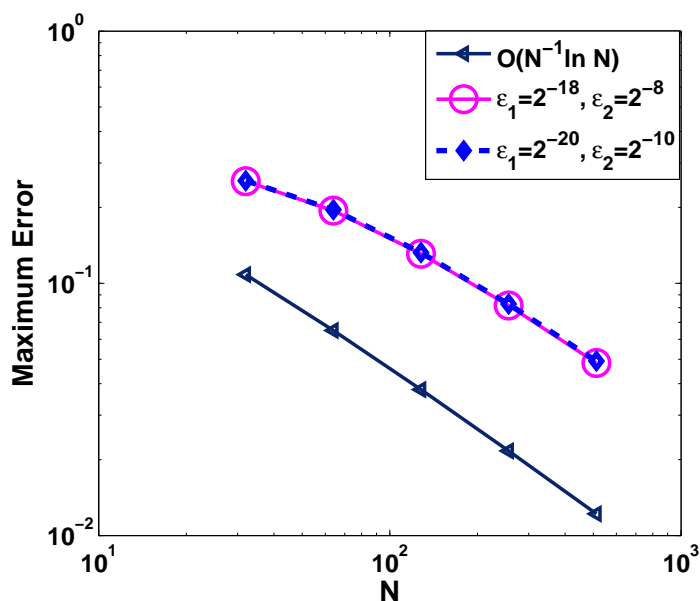


Figure 2.9: *Loglog plot for the spatial order of convergence associated with numerical solution U_1 for Example 2.8.2.*

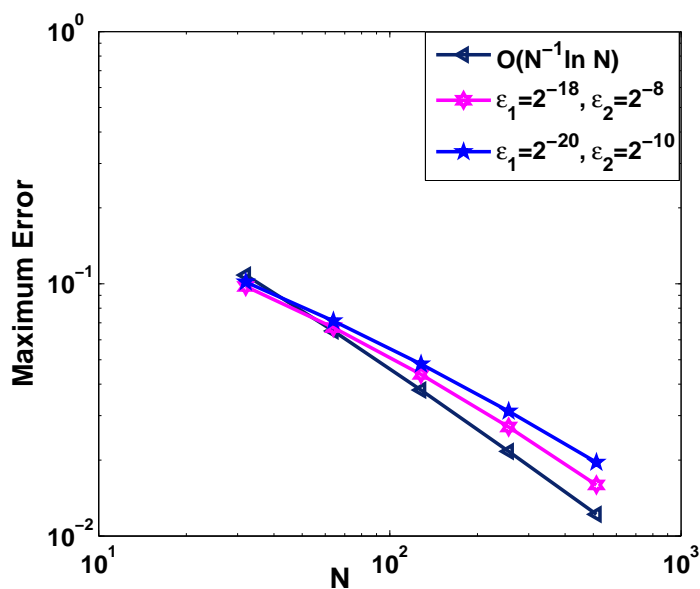


Figure 2.10: *Loglog plot for the spatial order of convergence associated with numerical solution U_2 for Example 2.8.2.*

Table 2.1: Uniform errors and orders of convergence for Example 2.8.1.

$(\varepsilon_1, \varepsilon_2) \in S_\varepsilon$	Number of mesh-intervals N				
	32	64	128	256	512
$d_1^{N,M}$	1.5232e-02	8.2587e-03	4.5142e-03	2.4143e-03	1.2674e-03
$p_1^{N,M}$	0.8830	0.8714	0.9028	0.9297	
$d_2^{N,M}$	1.8285e-02	9.9229e-03	5.2100e-03	2.6692e-03	1.3590e-03
$p_2^{N,M}$	0.8818	0.9294	0.9648	0.9738	

Table 2.2: Uniform errors and orders of convergence for Example 2.8.2.

$(\varepsilon_1, \varepsilon_2) \in \widehat{S}_\varepsilon$	Number of mesh-intervals N				
	32	64	128	256	512
$d_1^{N,M}$	2.5401e-01	1.9414e-01	1.3103e-01	8.1675e-02	4.8349e-02
$p_1^{N,M}$	0.5077	0.5631	0.6819	0.7564	
$d_2^{N,M}$	1.0165e-01	7.1302e-02	4.8036e-02	3.1249e-02	1.9604e-02
$p_2^{N,M}$	0.6967	0.7447	0.7769	0.8079	

For $l = 1, 2$, we calculate the maximum pointwise error and uniform error after extrapolation by

$$d_{\varepsilon, l \text{ extp}}^{N,M} = \max_{0 \leq n \leq M} \max_{0 \leq i \leq N} |U_{l, i \text{ extp}}^n - U_{l, 2i \text{ extp}}^{2n}|, \quad d_{l \text{ extp}}^{N,M} = \max_{\widehat{S}_\varepsilon} d_{\varepsilon, l \text{ extp}}^{N,M},$$

where $U_{l, i \text{ extp}}^n$ and $U_{l, 2i \text{ extp}}^{2n}$ are the numerical solution obtained after extrapolation on $\overline{Q}^{N,M}$ and $\overline{Q}^{2N, 2M}$, respectively. We determine the corresponding order of convergence for each $\varepsilon_1, \varepsilon_2$ by

$$p_{\varepsilon, l \text{ extp}}^{N,M} = \log_2 \left(\frac{d_{\varepsilon, l \text{ extp}}^{N,M}}{d_{\varepsilon, l \text{ extp}}^{2N, 2M}} \right), \quad p_{l \text{ extp}}^{N,M} = \log_2 \left(\frac{d_{l \text{ extp}}^{N,M}}{d_{l \text{ extp}}^{2N, 2M}} \right).$$

For this example, the singular perturbation parameters take values from $\widetilde{S}_\varepsilon = \{(\varepsilon_1, \varepsilon_2) | (2^{-10}, 2^{-0}), (2^{-20}, 2^{-10}), (2^{-30}, 2^{-20}), (2^{-40}, 2^{-30})\}$. We perform the numerical experiments by choosing the time step $\Delta t = 2/N$. From Fig. 2.11 and Fig. 2.12, one

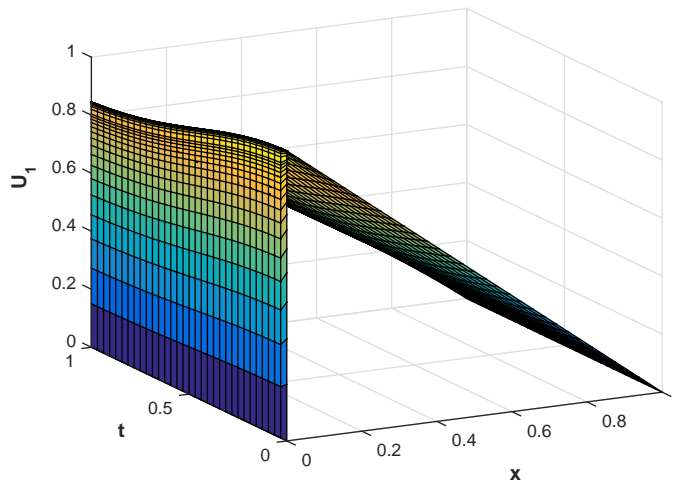


Figure 2.11: Surface plot of the numerical solution U_1 of Example 2.8.3 for $\varepsilon_1 = 2^{-8}$, $\varepsilon_2 = 2^{-4}$, $N = 64$, $M = 16$.

can observe the boundary layer behavior of numerical solution of Example 2.8.3. The calculated maximum pointwise errors and the corresponding order of convergence before and after extrapolation are presented in Table 2.3, which confirm that the upwind finite difference scheme (2.5.1) and the extrapolated technique are \mathcal{E} -uniform convergent. Moreover, one can observe that results presented in Table 2.3, reflects the fact that the extrapolation technique produces almost second-order convergence up to logarithmic factor. One can also observe the uniform error behavior via loglog plots given in Fig. 2.13 and Fig. 2.14 for Example 2.8.3.

2.9 Conclusions

In this chapter, we have presented a uniformly convergent numerical method for a class of singularly perturbed system of linear and semilinear parabolic convection-diffusion problems. A uniform mesh in the temporal direction and a piecewise-uniform Shishkin mesh for the spatial direction to discretize the domain have been used. The proposed numerical scheme is of first-order in time and first-order accurate up to logarithmic factor in space. Next, by fixing the transition parameters in the Shishkin mesh, we have computed the solution on the fine mesh with $2N \times 2M$ number of mesh-intervals. Finally, combining the computed solutions obtained on the coarse and the fine meshes, the Richardson extrapolation technique is implemented and we have shown that the extrapolation technique improves the almost first-order convergence of the simple upwinding into almost second-order convergence. Some numerical experiments have been established to validate the theoretical results.

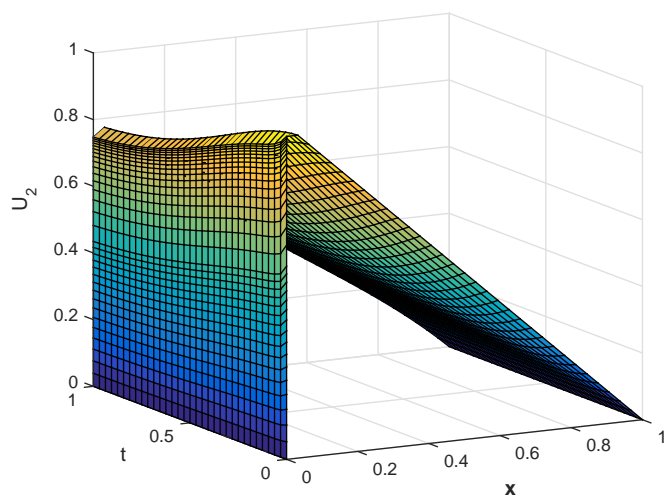


Figure 2.12: Surface plot of the numerical solution U_2 of Example 2.8.3 for $\varepsilon_1 = 2^{-8}$, $\varepsilon_2 = 2^{-4}$, $N = 64$, $M = 16$.

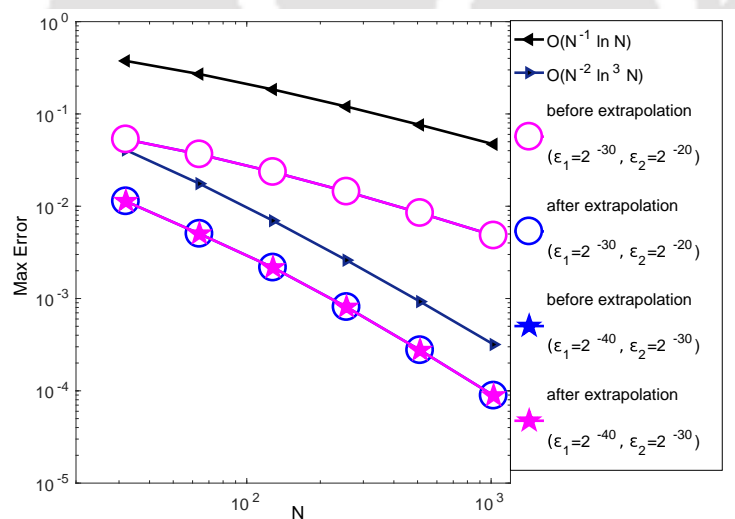
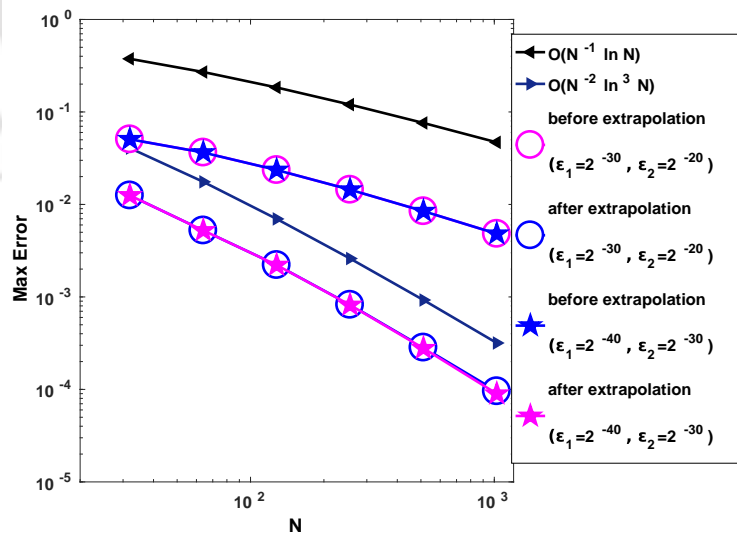


Figure 2.13: Visualization of the order of convergence through loglog plot associated with numerical solution U_1 for Example 2.8.3.

Table 2.3: Comparison of uniform errors and corresponding rate of convergence before extrapolation and after extrapolation for Example 2.8.3.

\tilde{S}_ϵ	Extrapolation	Number of mesh-intervals N				
		32	64	128	256	512
$d_1^{N,M}$ $p_1^{N,M}$	Before	5.3054e-02	3.6533e-02	2.3523e-02	1.4413e-02	8.4534e-03
		0.5382	0.6351	0.7066	0.7698	
$d_1^{N,M}$ $p_1^{N,M}$	After	1.1319e-02	5.0315e-03	2.1665e-03	8.0933e-04	2.7569e-04
		1.1697	1.2156	1.4205	1.5536	
$d_2^{N,M}$ $p_2^{N,M}$	Before	5.3054e-02	3.6533e-02	2.3523e-02	1.4413e-02	8.4534e-03
		0.4757	0.6275	0.7070	0.7717	
$d_2^{N,M}$ $p_2^{N,M}$	After	1.2521e-02	5.2347e-03	2.2110e-03	8.1858e-04	2.7839e-04
		1.2582	1.2433	1.4334	1.5560	

Figure 2.14: Visualization of the order of convergence through loglog plot associated with numerical solution U_2 for Example 2.8.3.

Parameter-Uniform Hybrid Numerical Scheme for Singularly Perturbed System of 1D Parabolic Convection-Diffusion Problems

This chapter is devoted to the study of hybrid numerical scheme for singularly perturbed system of 1D parabolic convection-diffusion problems exhibiting overlapping boundary layers. To solve these problems, we discretize the time derivative by the implicit-Euler method and the spatial derivatives by a hybrid finite difference scheme on the layer adapted piecewise-uniform Shishkin mesh. It is proved that the proposed numerical method converges uniformly in the discrete supremum norm with first-order accuracy in time and almost second-order accuracy in space. Numerical results are presented in supporting the theory.

3.1 Introduction

Here, we consider the following class of singularly perturbed system of 1D parabolic convection-diffusion IBVP on the domain $Q := \Omega_x \times (0, T]$, $\Omega_x = (0, 1)$:

$$\begin{cases} \frac{\partial \vec{u}}{\partial t} + \mathbb{L}_{x,\varepsilon} \vec{u} = \vec{f}, & (x, t) \in Q, \\ \vec{u}(x, 0) = \vec{u}_0(x), & x \in \bar{\Omega}_x, \\ \vec{u}(0, t) = \vec{0}, \quad \vec{u}(1, t) = \vec{0}, & t \in [0, T], \end{cases} \quad (3.1.1)$$

where the spatial differential operator $\mathbb{L}_{x,\varepsilon}$ is given by

$$\mathbb{L}_{x,\varepsilon} \equiv -\mathcal{E} \frac{\partial^2}{\partial x^2} + A(x) \frac{\partial}{\partial x} + B(x).$$

The coefficient matrices are given as $\mathcal{E} = \text{diag}(\varepsilon_1, \varepsilon_2)$, $0 < \varepsilon_1 \leq \varepsilon_2 \ll 1$ and $A(x) = \text{diag}(a_1(x), a_2(x))$, $B(x) = \{b_{lm}(x)\}_{l,m=1}^2$. The convection coefficients satisfy $a_1(x) \geq$

$\alpha > 0$, $a_2(x) \geq \alpha > 0$. In addition, we assume that B is an L_0 -matrix and satisfy

$$\min_{x \in \Omega_x} \{b_{11}(x) + b_{12}(x), b_{21}(x) + b_{22}(x)\} \geq \beta > 0. \quad (3.1.2)$$

The source term and the initial condition satisfy the following smoothness conditions

$$\vec{f} \in (\mathcal{C}_\lambda^2(\bar{Q}))^2, \quad \vec{u}_0 \in (\mathcal{C}_0^4(\bar{\Omega}_x))^2$$

and the compatibility conditions

$$\begin{cases} \vec{u}_0(x) = \vec{0}, & x \in \{0, 1\}, \\ \vec{f}(x, 0) - \mathbb{L}_{x,\varepsilon} \vec{u}_0(x) = \vec{0}, & x \in \{0, 1\}, \\ \vec{f}_t(x, 0) + (\mathbb{L}_{x,\varepsilon})^2 \vec{u}_0(x) - \mathbb{L}_{x,\varepsilon} \vec{f}(x, 0) = \vec{0}, & x \in \{0, 1\}. \end{cases} \quad (3.1.3)$$

Under these sufficient smoothness with compatibility conditions imposed on source term, initial and boundary data, the model problem (3.1.1) admits a unique solution.

This main aim of this chapter is to analyze the hybrid finite difference scheme for singularly perturbed system of parabolic convection-diffusion problems. In this method the time derivative is approximated by the implicit-Euler scheme on uniform mesh and the spatial derivatives are approximated by the hybrid numerical scheme on the piecewise-uniform Shishkin mesh. The hybrid difference scheme uses the classical central difference method whenever the local mesh size allows us to do this without losing stability but employs the midpoint upwind difference method away from the boundary layers. Then we show that the proposed scheme is first-order in time and almost second-order convergent in space.

We organize the rest of this chapter as follows: The analytical behavior of the exact solution is discussed in Section 3.2. Section 3.3 describes the uniform convergence of the semidiscrete scheme and later we discuss the asymptotic behavior of the solutions of the semidiscrete problems. In Section 3.4, we study the piecewise-uniform Shishkin mesh and provide the detailed construction of the newly proposed hybrid finite difference scheme. Section 3.5 contains the main theoretical result. In Section 3.6, we present the numerical experiments to validate the theoretical results. Finally in Section 3.7, we summarize the main conclusions of this chapter.

3.2 Analytical Behavior of the Solution

The differential operator defined in (3.1.1) satisfies the following maximum principle.

Lemma 3.2.1. (Maximum Principle) *Let $(\frac{\partial}{\partial t} + \mathbb{L}_{x,\varepsilon})$ be the differential operator given in (3.1.1). Then for $\vec{Y} \geq \vec{0}$ on ∂Q and $(\frac{\partial}{\partial t} + \mathbb{L}_{x,\varepsilon}) \vec{Y} \geq \vec{0}$ in Q , we have $\vec{Y} \geq \vec{0}$, for all $(x, t) \in \bar{Q}$.*

Proof. By following the approach discussed in Lemma 2.2.1, one can prove the maximum principle. ■

Next, we present the derivative bounds with respect to spatial and temporal variable, of the exact solution of the model problem (3.1.1).

Theorem 3.2.2. *For all non-negative integers k and k_0 satisfying $0 \leq k + k_0 \leq 2$ and $l = 1, 2$, the derivatives of the exact solution \vec{u} of the IBVP (3.1.1) satisfies*

$$\left| \frac{\partial^{k+k_0} u_l}{\partial x^k \partial t^{k_0}} \right| \leq \begin{cases} C, & \text{for } k = 0, \\ C (1 + \varepsilon_l^{-1} B_{\varepsilon_l}^1(x)), & \text{for } k = 1, \\ C (1 + \varepsilon_l^{-1} (\varepsilon_1^{-1} B_{\varepsilon_1}^1(x) + \varepsilon_2^{-1} B_{\varepsilon_2}^1(x))), & \text{for } k = 2. \end{cases}$$

Proof. By following the technique of Theorem 2.2.4, we can get the desired result. ■

3.3 The Time Semidiscretization

First, we discretize the time domain $\bar{\Upsilon}^M$ by uniform mesh with mesh-size Δt , such that $\Upsilon^M = \{t_n = n\Delta t, n = 0, \dots, M, \Delta t = T/M\}$, where M is the number of mesh-points in the time direction.

Now, we introduce a time semidiscretization process by means of the following implicit-Euler scheme:

$$\begin{cases} \vec{u}^0(x) = \vec{u}(x, 0), & x \in \bar{\Omega}_x, \\ (I + \Delta t \mathbb{L}_{x, \varepsilon}) \vec{u}^{n+1}(x) = \vec{u}^n(x) + \Delta t \vec{f}(x, t_{n+1}), \\ \vec{u}^{n+1}(0) = \vec{u}^{n+1}(1) = 0. \end{cases} \quad (3.3.1)$$

By using Lemma 2.3.1, one can easily obtain the maximum principle for the differential operator $(I + \Delta t \mathbb{L}_{x, \varepsilon})$. Also, we get

$$\|(I + \Delta t \mathbb{L}_{x, \varepsilon_1})^{-1}\|_{\infty} \leq \frac{1}{1 + \beta \Delta t}, \quad \|(I + \Delta t \mathbb{L}_{x, \varepsilon_2})^{-1}\|_{\infty} \leq \frac{1}{1 + \beta \Delta t}. \quad (3.3.2)$$

Next, define the local truncation error \vec{e}_{n+1} for the time semidiscrete scheme (3.3.1) by

$$\vec{e}_{n+1} = \vec{u}(x, t_{n+1}) - \vec{u}^{n+1}(x),$$

where $\vec{u}^{n+1}(x)$ is solution of following system:

$$\begin{cases} (1 + \Delta t \mathbb{L}_{x, \varepsilon}) \vec{u}^{n+1} = \vec{u}(x, t_n) + \Delta t \vec{f}(x, t_{n+1}), \\ \vec{u}^{n+1}(0) = \vec{u}^{n+1}(1) = 0. \end{cases} \quad (3.3.3)$$

By using Lemma 2.3.2, one can obtain that

$$\|\vec{e}_{n+1}\|_{\infty} \leq \vec{C}(\Delta t^2).$$

Thus, the global error corresponding to the scheme (3.3.1) satisfies

$$\sup_{n \leq T/\Delta t} \|\vec{u}(x, t_n) - \vec{u}^n\|_\infty \leq \vec{C} \Delta t. \quad (3.3.4)$$

Hence, we conclude that the time semidiscretization process is uniformly convergent of first-order in time.

Note: As a technical requirement, we assume that

$$|\mathbb{L}_{x,\varepsilon} \vec{u}(x, t_n)| \leq \vec{C}, \quad |\mathbb{L}_{x,\varepsilon}^2 \vec{u}(x, t_n)| \leq \vec{C}. \quad (3.3.5)$$

3.3.1 Asymptotic behavior of the solutions of semidiscrete problems

To prove the uniform convergence of the semidiscrete problem (3.3.3), we need a more precise decomposition of the exact solution \vec{u}^{n+1} of the time semidiscrete problem (3.3.3).

Lemma 3.3.1. *The exact solution of (3.3.3) is decomposed in the following way*

$$\vec{u}^{n+1}(x) = \vec{\eta} \vec{w}^{n+1}(x) + \vec{z}^{n+1}(x), \quad (3.3.6)$$

where the components $\vec{w}^{n+1}(x)$ and $\vec{z}^{n+1}(x)$ satisfy

$$\left\{ \begin{array}{l} \vec{w}_l^{n+1}(x) = \exp(-a_l(1)(1-x)/\varepsilon_l), \quad \eta_l = \frac{\varepsilon_l}{a_l(1)} \frac{d\vec{u}_l^{n+1}}{dx}(1), \quad l = 1, 2, \\ \left| \frac{d^k \vec{z}_l^{n+1}(x)}{dx^k} \right| \leq C (1 + \varepsilon_l^{-k+1} B_{\varepsilon_l}^1(x)), \quad k = 1, 2, \\ \left| \frac{d^k \vec{z}_l^{n+1}(x)}{dx^k} \right| \leq C (1 + \varepsilon_l^{2-k} (\varepsilon_1^{-1} B_{\varepsilon_1}^1(x) + \varepsilon_2^{-1} B_{\varepsilon_2}^1(x))), \quad k = 3, 4. \end{array} \right. \quad (3.3.7)$$

Proof. To establish the derivative bounds of $\vec{z}^{n+1}(x)$, first we need to acquire the derivative bounds for $\vec{u}^{n+1}(x)$. Assume that $\vec{\varrho} = (\vec{u}^{n+1} - \vec{u}(x, t_n))/\Delta t$, then $\vec{\varrho}$ is the solution of the following problem

$$\left\{ \begin{array}{l} (I + \Delta t \mathbb{L}_{x,\varepsilon}) \vec{\varrho} = -\mathbb{L}_{x,\varepsilon} \vec{u}(x, t_{n+1}) + \vec{f}(x, t_{n+1}) \\ \vec{\varrho}(0) = \vec{0}, \quad \vec{\varrho}(1) = \vec{0}. \end{array} \right. \quad (3.3.8)$$

From (3.3.8), one can express \vec{u} as the solution of the BVP:

$$\left\{ \begin{array}{l} \mathbb{L}_{x,\varepsilon} \vec{u}^{n+1}(x) = -\vec{\varrho} + \vec{f}(x, t_{n+1}) \\ \vec{u}^{n+1}(0) = \vec{0}, \quad \vec{u}^{n+1}(1) = \vec{0}. \end{array} \right. \quad (3.3.9)$$

By following the argument from Theorem 2.2.4, we can obtain that

$$\left| \frac{d\vec{u}_1^{n+1}}{dx}(0) \right| \leq C, \quad \left| \frac{d\vec{u}_1^{n+1}}{dx}(1) \right| \leq C \varepsilon_1^{-1}, \quad \left| \frac{d\vec{u}_1^{n+1}}{dx}(x) \right| \leq C (1 + \varepsilon_1^{-1} B_{\varepsilon_1}^1), \quad \forall x \in \bar{\Omega}_x.$$

In a similar manner, one can show

$$\left| \frac{d\tilde{u}_2^{n+1}}{dx}(0) \right| \leq C, \quad \left| \frac{d\tilde{u}_2^{n+1}}{dx}(1) \right| \leq C\varepsilon_2^{-1}, \quad \left| \frac{d\tilde{u}_2^{n+1}}{dx}(x) \right| \leq C(1 + \varepsilon_2^{-1}B_{\varepsilon_2}^1), \quad \forall x \in \bar{\Omega}_x.$$

Differentiating first component of (3.3.9) with respect to x and rearranging, we get

$$-\varepsilon_1 \frac{d^3\tilde{u}_1^{n+1}}{dx^3} + a_1 \frac{d^2\tilde{u}_1^{n+1}}{dx^2} = -\frac{d\rho_1}{dx} + \frac{df_1}{dx} - \frac{da_1}{dx} \frac{d\tilde{u}_1^{n+1}}{dx} - \frac{d(b_{11}\tilde{u}_1^{n+1} + b_{12}\tilde{u}_2^{n+1})}{dx}. \quad (3.3.10)$$

To acquire the bound for $d^2\tilde{u}_1^{n+1}/dx^2$, one needs to obtain the estimate for $d\rho_1/dx$. Assume that $\vec{\Phi} = \mathbb{L}_{x,\varepsilon}\vec{\rho}$, which satisfies

$$\begin{cases} (1 + \Delta t \mathbb{L}_{x,\varepsilon})\vec{\Phi} = -\mathbb{L}_{x,\varepsilon}^2\vec{u} + \mathbb{L}_{x,\varepsilon}\vec{f}(x, t_{n+1}), \\ \vec{\Phi}(0) = \frac{1}{\Delta t}(\vec{f}(0, t_{n+1}) - \mathbb{L}_{x,\varepsilon}\vec{u}(0, t_{n+1})), \\ \vec{\Phi}(1) = \frac{1}{\Delta t}(\vec{f}(1, t_{n+1}) - \mathbb{L}_{x,\varepsilon}\vec{u}(1, t_{n+1})). \end{cases}$$

By using the compatibility condition for \vec{f} given in (2.1.5) with $|\mathbb{L}_{x,\varepsilon}^2\vec{u}| \leq \vec{C}$ and $\mathbb{L}_{x,\varepsilon}\vec{u}(0, t_{n+1}) = \vec{f}(0, t_{n+1})$, $\mathbb{L}_{x,\varepsilon}\vec{u}(1, t_{n+1}) = \vec{f}(1, t_{n+1})$, we get $|\vec{\Phi}| \leq \vec{C}$, $x \in \bar{\Omega}_x$.

The component ρ_1 is the solution of the BVP:

$$\begin{cases} -\varepsilon_1 \frac{d^2\rho_1}{dx^2} + a_1 \frac{d\rho_1}{dx} + b_{11}\rho_1 = \Phi_1 - b_{12}\rho_2, \\ \rho_1(0) = \rho_1(1) = 0. \end{cases} \quad (3.3.11)$$

By following the technique of Theorem 2.2.4, we obtain that

$$\left| \frac{d\rho_1}{dx} \right| \leq C(1 + \varepsilon_1^{-1}B_{\varepsilon_1}^1(x)), \quad \forall x \in \bar{\Omega}_x.$$

Using the above bound and methodology of Lemma 2.3.4 in (3.3.10), we get

$$\left| \frac{d^2\tilde{u}_1^{n+1}}{dx^2} \right| \leq C(1 + \varepsilon_1^{-2}B_{\varepsilon_1}^1(x)).$$

In a similar way, one can obtain the corresponding bounds for the higher derivatives of component \tilde{u}_1^{n+1} . Analogously, we can get the desired derivative bounds for \tilde{u}_2^{n+1} .

By using decomposition (3.3.6), it holds that

$$|\tilde{z}_l^{n+1}(0)| \leq C, \quad |\tilde{z}_l^{n+1}(1)| \leq C, \quad \left| \frac{d\tilde{z}_l^{n+1}}{dx}(0) \right| \leq C, \quad \frac{d\tilde{z}_l^{n+1}}{dx}(1) = 0, \quad l = 1, 2. \quad (3.3.12)$$

Next, we consider

$$\begin{aligned} \mathbb{L}_{x,\varepsilon_1}\tilde{z}^{n+1} &= -\rho_1 + f_1 - b_{11}(\tilde{u}_1^{n+1} - \tilde{z}_1^{n+1}) - b_{12}(\tilde{u}_2^{n+1} - \tilde{z}_2^{n+1}) \\ &\quad + \eta_2(a_1(1) - a_1(x)) \frac{d\tilde{w}_1^{n+1}}{dx} \equiv \phi_1(x). \end{aligned} \quad (3.3.13)$$

By using the argument from [15] and bounds (3.3.12), we obtain that

$$\left| \frac{d^k \tilde{z}_1^{n+1}}{dx^k} \right| \leq C (1 + \varepsilon_1^{-k+1} B_{\varepsilon_1}^1(x)), \quad k = 1.$$

An analogous result holds for component \tilde{z}_2^{n+1} .

Differentiating (3.3.13) with respect to x and rearranging, we obtain

$$\mathbb{L}_{x,\varepsilon_1} \frac{d \tilde{z}^{n+1}}{dx} = \frac{d\phi_1}{dx} - \frac{da_1}{dx} \frac{d(\tilde{u}_1^{n+1} - \eta_1 \tilde{w}_1^{n+1})}{dx} - \frac{db_{11}}{dx} \tilde{z}_1^{n+1} - \frac{db_{12}}{dx} \tilde{z}_2^{n+1} \equiv \phi_2(x). \quad (3.3.14)$$

By employing the previous bounds, one can easily deduce that

$$|\phi_2(x)| \leq C (1 + \varepsilon_1^{-1} B_{\varepsilon_1}^1(x)).$$

Since $d\tilde{z}^{n+1}/dx$ is bounded at the boundary points, then it follows that

$$\left| \frac{d^k \tilde{z}_1^{n+1}}{dx^k} \right| \leq C (1 + \varepsilon_1^{-k+1} B_{\varepsilon_1}^1(x)), \quad \text{for } k = 2. \quad (3.3.15)$$

In a similar way, one can obtain derivative bounds for component \tilde{z}_2^{n+1} .

Again differentiating (3.3.14) with respect to x , we obtain

$$\mathbb{L}_{x,\varepsilon_1} \frac{d^2 \tilde{z}^{n+1}}{dx^2} = \frac{d\phi_2}{dx} - \frac{da_1}{dx} \frac{d^2(\tilde{u}_1^{n+1} - \eta_1 \tilde{w}_1^{n+1})}{dx^2} - \frac{db_{11}}{dx} \frac{d\tilde{z}_1^{n+1}}{dx} - \frac{db_{12}}{dx} \frac{d\tilde{z}_2^{n+1}}{dx} \equiv \phi_3(x). \quad (3.3.16)$$

And, the associated boundary conditions satisfy the following estimates

$$\left| \frac{d^2 \tilde{z}_1^{n+1}}{dx^2}(0) \right| \leq C, \quad \left| \frac{d^2 \tilde{z}_1^{n+1}}{dx^2}(1) \right| \leq C \varepsilon_1^{-1}.$$

By employing the required derivative bounds of components \tilde{z}_l^{n+1} , $l = 1, 2$, we get

$$|\phi_3(x)| \leq C (1 + \varepsilon_1^{-1} B_{\varepsilon_1}^1(x) + \varepsilon_2^{-1} B_{\varepsilon_2}^1(x)).$$

By using technique of Lemma 2.3.4 in (3.3.16), we get

$$\left| \frac{d^3 \tilde{z}_1^{n+1}}{dx^3} \right| \leq C (1 + \varepsilon_1^{-1} (\varepsilon_1^{-1} B_{\varepsilon_1}^1(x) + \varepsilon_2^{-1} B_{\varepsilon_2}^1(x)))$$

In a similar manner, one can deduce that

$$\left| \frac{d^3 \tilde{z}_2^{n+1}}{dx^3} \right| \leq C (1 + \varepsilon_2^{-1} (\varepsilon_1^{-1} B_{\varepsilon_1}^1(x) + \varepsilon_2^{-1} B_{\varepsilon_2}^1(x)))$$

By using the previous technique, we can obtain the derivative bounds for $k = 4$. ■

3.4 The Discrete Problem

In this section, we describe the piecewise-uniform Shishkin mesh for the spatial discretization of the domain and study error analysis for the proposed numerical scheme used to discretize the problem (3.3.3) for the spatial variable.

3.4.1 The piecewise-uniform Shishkin mesh

The piecewise-uniform Shishkin mesh is constructed by dividing the domain $\bar{\Omega}_x^N$ into three subdomains such as $[0, 1 - \tau_{\varepsilon_2}]$, $[1 - \tau_{\varepsilon_2}, 1 - \tau_{\varepsilon_1}]$ and $[1 - \tau_{\varepsilon_1}, 1]$. Then divide $[0, 1 - \tau_{\varepsilon_2}]$ into $N/2$ mesh-intervals, and divide $[1 - \tau_{\varepsilon_2}, 1 - \tau_{\varepsilon_1}]$ and $[1 - \tau_{\varepsilon_1}, 1]$ into $N/4$ mesh-intervals. Then, the discretized spatial domain $\bar{\Omega}_x^N$ look like

$$\bar{\Omega}_x^N = \{0 = x_0, x_1, \dots, x_{N/2} = 1 - \tau_{\varepsilon_2}, \dots, x_{3N/4} = 1 - \tau_{\varepsilon_1}, \dots, x_N = 1\},$$

where

$$\tau_{\varepsilon_2} = \min \left\{ \frac{1}{2}, \tau_0 \varepsilon_2 \ln N \right\} \quad \text{and} \quad \tau_{\varepsilon_1} = \min \left\{ \frac{1}{4}, \frac{\tau_{\varepsilon_2}}{2}, \tau_0 \varepsilon_1 \ln N \right\},$$

τ_0 is a constant will be chosen later. Fig. 3.1 displays a typical piecewise-uniform Shishkin mesh.

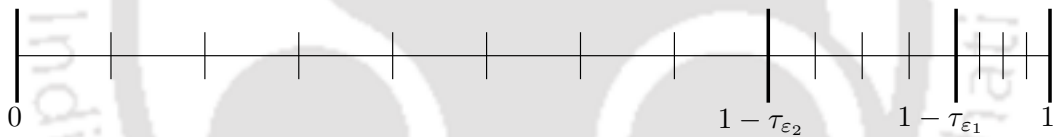


Figure 3.1: Visualization of piecewise-uniform Shishkin mesh $\bar{\Omega}_x^N$ for $N = 16$.

Therefore, the step sizes of the mesh $\bar{\Omega}_x^N$ are given by

$$h_i = \begin{cases} H_1 = \frac{2(1-\tau_{\varepsilon_2})}{N}, & i = 1, \dots, N/2, \\ H_2 = \frac{4(\tau_{\varepsilon_2}-\tau_{\varepsilon_1})}{N}, & i = N/2 + 1, \dots, 3N/4, \\ H_3 = \frac{4\tau_{\varepsilon_1}}{N}, & i = 3N/4 + 1, \dots, N. \end{cases} \quad (3.4.1)$$

It is clear from (3.4.1) that $N^{-1} \leq H_1 \leq 2N^{-1}$, $H_2 = 4\tau_0(\varepsilon_2 - \varepsilon_1)N^{-1} \ln N$, and $H_3 = 4\tau_0\varepsilon_1 N^{-1} \ln N$. Let us denote $\tilde{h}_i = h_i + h_{i+1}$ for $i = 1, \dots, N-1$ and $\rho_i^{\varepsilon_l} = h_i/\varepsilon_l$, $l = 1, 2$, for $i = 1, \dots, N$. When $v(x_i) = v_i$, we define $v_{i-1/2} = (v_i + v_{i-1})/2$.

3.4.2 The hybrid scheme

For spatial discretization of (3.3.3), we use the hybrid scheme which is a proper combination of the midpoint upwind scheme and central difference scheme. More precisely, for spatial derivatives, we apply the midpoint upwind scheme in the outer regions $[0, 1 - \tau_{\varepsilon_2}]$

where the coefficients are given by

$$\begin{cases} r_{1,i}^- = \Delta t r_{mu,1,i}^- + \frac{1}{2}, & r_{1,i}^c = \Delta t r_{mu,1,i}^c + \frac{1}{2}, & r_{1,i}^+ = \Delta t r_{mu,1,i}^+, \\ q_{1,i}^- = \Delta t q_{mu,1,i}^-, & q_{1,i}^c = \Delta t q_{mu,1,i}^c, & q_{1,i}^+ = 0, \text{ for } 1 \leq i \leq N/2, \\ r_{1,i}^- = \Delta t r_{cen,1,i}^-, & r_{1,i}^c = \Delta t r_{cen,1,i}^c + 1, & r_{1,i}^+ = \Delta t r_{cen,1,i}^+, \\ q_{1,i}^- = 0, & q_{1,i}^c = \Delta t q_{cen,1,i}^c, & q_{1,i}^+ = 0, \text{ for } N/2 < i \leq N-1, \end{cases}$$

and

$$\begin{cases} r_{2,i}^- = \Delta t r_{mu,2,i}^- + \frac{1}{2}, & r_{2,i}^c = \Delta t r_{mu,2,i}^c + \frac{1}{2}, & r_{2,i}^+ = \Delta t r_{mu,2,i}^+, \\ q_{2,i}^- = \Delta t q_{mu,2,i}^-, & q_{2,i}^c = \Delta t q_{mu,2,i}^c, & q_{2,i}^+ = 0, \text{ for } 1 \leq i \leq N/2, \\ r_{2,i}^- = \Delta t r_{cen,2,i}^-, & r_{2,i}^c = \Delta t r_{cen,2,i}^c + 1, & r_{2,i}^+ = \Delta t r_{cen,2,i}^+, \\ q_{2,i}^- = 0, & q_{2,i}^c = \Delta t q_{cen,2,i}^c, & q_{2,i}^+ = 0, \text{ for } N/2 < i \leq N-1, \end{cases}$$

here, the above coefficients are described, for $l = 1, 2$, as follows

$$\begin{cases} r_{mu,l,i}^- = \frac{-2\varepsilon_l}{\widetilde{h}_i h_i} - \frac{a_{l,i-1/2}}{h_i} + \frac{b_{ll,i-1/2}}{2}, \\ r_{mu,l,i}^c = \frac{2\varepsilon_l}{h_{i+1} h_i} + \frac{a_{l,i-1/2}}{h_i} + \frac{b_{ll,i-1/2}}{2}, \\ r_{mu,l,i}^+ = \frac{-2\varepsilon_l}{\widetilde{h}_i h_i}, \\ q_{mu,1,i}^- = \frac{b_{12,i-1/2}}{2}, & q_{mu,2,i}^- = \frac{b_{21,i-1/2}}{2}, \\ q_{mu,1,i}^c = \frac{b_{12,i-1/2}}{2}, & q_{mu,2,i}^c = \frac{b_{21,i-1/2}}{2}, \\ q_{mu,l,i}^+ = 0, \end{cases} \quad \text{and} \quad \begin{cases} r_{cen,l,i}^- = \frac{-2\varepsilon_l}{\widetilde{h}_i h_i} - \frac{a_{l,i}}{\widetilde{h}_i}, \\ r_{cen,l,i}^c = \frac{2\varepsilon_l}{h_{i+1} h_i} + \frac{b_{ll,i}}{2}, \\ r_{cen,l,i}^+ = \frac{-2\varepsilon_l}{\widetilde{h}_i h_{i+1}} + \frac{a_{l,i}}{\widetilde{h}_i}, \\ q_{cen,l,i}^- = 0, \\ q_{cen,1,i}^c = b_{12,i}, & q_{cen,2,i}^c = b_{21,i}, \\ q_{cen,l,i}^+ = 0. \end{cases}$$

3.4.3 Error analysis

We will study about the stability of the proposed hybrid numerical scheme (3.4.2) here. Later, we discuss the convergence analysis of the spatial discretization process.

Assumption 1. Suppose that $N \geq N_0$, where

$$\frac{N_0}{\ln N_0} \geq \max \{ \tau_0 \|a_1\|_\infty, \tau_0 \|a_2\|_\infty \}, \quad (3.4.5)$$

$$(\|b_{11}\|_\infty + \Delta t^{-1}) \leq \alpha N_0, \quad (\|b_{22}\|_\infty + \Delta t^{-1}) \leq \alpha N_0. \quad (3.4.6)$$

The difference operator satisfies the following discrete maximum principle.

Lemma 3.4.1. (Discrete maximum principle) Let $\widehat{\mathbb{L}}_\varepsilon^N$ be the difference operator given in (3.4.4), and we assume that the coefficients of matrices $A(x_i)$, $B(x_i)$, satisfy

conditions (3.4.5) and (3.4.6) respectively. Assume that a mesh function $\{\tilde{Z}^{\varepsilon, n+1}(x_i)\}_{i=0}^N$ satisfies $\tilde{Z}^{\varepsilon, n+1}(0) \geq \vec{0}$ and $\tilde{Z}^{\varepsilon, n+1}(1) \geq \vec{0}$. Then $\widehat{\mathbb{L}}_{\varepsilon}^N \tilde{Z}^{\varepsilon, n+1}(x_i) \geq \vec{0}$ in Ω_x^N implies that $\tilde{Z}^{\varepsilon, n+1}(x_i) \geq \vec{0}$ at each point of $\overline{\Omega}_x^N$.

Proof. We will prove this lemma by contradiction. Assume that there exist $x_{i^*} \in \Omega_x^N$ such that

$$\min \left\{ \tilde{Z}_1^{\varepsilon, n+1}(x_{i^*}), \tilde{Z}_2^{\varepsilon, n+1}(x_{i^*}) \right\} = \min \left\{ \min_{x_i \in \Omega_x^N} \tilde{Z}_1^{\varepsilon, n+1}(x_i), \min_{x_i \in \Omega_x^N} \tilde{Z}_2^{\varepsilon, n+1}(x_i) \right\} < 0,$$

without loss of generality we assume that $\tilde{Z}_2^{\varepsilon, n+1}(x_{i^*}) \leq \tilde{Z}_1^{\varepsilon, n+1}(x_{i^*})$. Consider the second component of $\widehat{\mathbb{L}}_{\varepsilon}^N \tilde{Z}^{\varepsilon, n+1}(x_{i^*})$ as

$$\begin{aligned} \widehat{\mathbb{L}}_{\varepsilon_2}^N \tilde{Z}^{\varepsilon, n+1}(x_{i^*}) &\equiv r_{2,i}^- \tilde{Z}_2^{\varepsilon, n+1}(x_{i^*-1}) + r_{2,i}^c \tilde{Z}_2^{\varepsilon, n+1}(x_{i^*}) + r_{2,i}^+ \tilde{Z}_2^{\varepsilon, n+1}(x_{i^*+1}) \\ &\quad + q_{2,i}^- \tilde{Z}_1^{\varepsilon, n+1}(x_{i^*-1}) + q_{2,i}^c \tilde{Z}_1^{\varepsilon, n+1}(x_{i^*}) + q_{2,i}^+ \tilde{Z}_1^{\varepsilon, n+1}(x_{i^*+1}). \end{aligned} \quad (3.4.7)$$

Firstly, we take the case for $1 \leq i \leq N/2$. To deduce $\widehat{\mathbb{L}}_{\varepsilon_2}^N \tilde{Z}^{\varepsilon, n+1}(x_{i^*}) < \vec{0}$, it is enough to show that $r_{2,i}^- < 0$. By using (3.4.6), we get

$$\begin{aligned} r_{2,i}^- &= \Delta t \left(\frac{-2\varepsilon_2}{\widetilde{h}_i h_i} - \frac{a_{2,i-1/2}}{h_i} + \frac{b_{22,i-1/2}}{2} \right) + \frac{1}{2} \\ &= \Delta t \left(\frac{-2\varepsilon_2}{2H_1^2} - \frac{a_{2,i-1/2}}{H_1} \right) + \frac{\Delta t}{2} (b_{22,i-1/2} + \Delta t^{-1}) \\ &\leq \Delta t \left(\frac{-2\varepsilon_2}{2H_1^2} - \frac{a_{2,i-1/2}}{H_1} \right) + \frac{\Delta t}{2} (\|b_{22}\|_{\infty} + \Delta t^{-1}) \\ &\leq -C_1 \varepsilon_2 \Delta t N^2 - C_2 \frac{\Delta t}{2} (a_{2,i-1/2} N - \alpha N) < 0. \end{aligned}$$

Next, we assume that $N/2 + 1 \leq i \leq N$. To show $\widehat{\mathbb{L}}_{\varepsilon_2}^N \tilde{Z}^{\varepsilon, n+1}(x_{i^*}) < \vec{0}$, it is enough to obtain that $r_{2,i}^+ < 0$. Using assumption (3.4.5), we have

$$r_{2,i}^+ = \Delta t \left(\frac{-2\varepsilon_2}{\widetilde{h}_i h_{i+1}} + \frac{a_{2,i}}{\widetilde{h}_i} \right) \leq -\frac{\Delta t}{\widetilde{h}_i} \left(\frac{2\varepsilon_2}{h_{i+1}} - \|a_2\|_{\infty} \right) < 0,$$

which contradicts the hypothesis of the lemma. Hence, we get the desired result. \blacksquare

Truncation error

Now, for the numerical scheme (3.4.4), we define the local truncation error as

$$\zeta_{i,\tilde{u}}^1 = \widehat{\mathbb{L}}_{\varepsilon_1}^N [\tilde{u}_i^{\varepsilon, n+1} - \tilde{U}_i^{\varepsilon, n+1}] = \Delta t \zeta_{i,\tilde{u}}^{1,x}, \quad \zeta_{i,\tilde{u}}^2 = \widehat{\mathbb{L}}_{\varepsilon_2}^N [\tilde{u}_i^{\varepsilon, n+1} - \tilde{U}_i^{\varepsilon, n+1}] = \Delta t \zeta_{i,\tilde{u}}^{2,x}$$

where

$$\zeta_{i,\tilde{u}}^1 = \begin{cases} r_{1,i}^- \tilde{u}_{1,i-1}^{n+1} + r_{1,i}^c \tilde{u}_{1,i}^{n+1} + r_{1,i}^+ \tilde{u}_{1,i+1}^{n+1} + q_{1,i}^- \tilde{u}_{2,i-1}^{n+1} + q_{1,i}^c \tilde{u}_{2,i}^{n+1} + q_{1,i}^+ \tilde{u}_{2,i+1}^{n+1} \\ - \frac{1}{2} \left(\tilde{u}_{1,i-1}^{n+1} + \Delta t (\mathbb{L}_{x,\varepsilon_1} \tilde{u}^{n+1})(x_{i-1}) \right) - \frac{1}{2} \left(\tilde{u}_{1,i}^{n+1} + \Delta t (\mathbb{L}_{x,\varepsilon_1} \tilde{u}^{n+1})(x_i) \right), \\ \text{for } 1 \leq i \leq N/2, \\ r_{1,i}^- \tilde{u}_{1,i-1}^{n+1} + r_{1,i}^c \tilde{u}_{1,i}^{n+1} + r_{1,i}^+ \tilde{u}_{1,i+1}^{n+1} + q_{1,i}^- \tilde{u}_{2,i-1}^{n+1} + q_{1,i}^c \tilde{u}_{2,i}^{n+1} + q_{1,i}^+ \tilde{u}_{2,i+1}^{n+1} \\ - \left(\tilde{u}_{1,i}^{n+1} + \Delta t (\mathbb{L}_{x,\varepsilon_1} \tilde{u}^{n+1})(x_i) \right), \quad \text{for } N/2 < i \leq N-1, \end{cases}$$

$$\zeta_{i,\tilde{u}}^2 = \begin{cases} r_{2,i}^- \tilde{u}_{2,i-1}^{n+1} + r_{2,i}^c \tilde{u}_{2,i}^{n+1} + r_{2,i}^+ \tilde{u}_{2,i+1}^{n+1} + q_{2,i}^- \tilde{u}_{1,i-1}^{n+1} + q_{2,i}^c \tilde{u}_{1,i}^{n+1} + q_{2,i}^+ \tilde{u}_{1,i+1}^{n+1} \\ - \frac{1}{2} \left(\tilde{u}_{2,i-1}^{n+1} + \Delta t (\mathbb{L}_{x,\varepsilon_2} \tilde{u}^{n+1})(x_{i-1}) \right) - \frac{1}{2} \left(\tilde{u}_{2,i}^{n+1} + \Delta t (\mathbb{L}_{x,\varepsilon_2} \tilde{u}^{n+1})(x_i) \right), \\ \text{for } 1 \leq i \leq N/2, \\ r_{2,i}^- \tilde{u}_{2,i-1}^{n+1} + r_{2,i}^c \tilde{u}_{2,i}^{n+1} + r_{2,i}^+ \tilde{u}_{2,i+1}^{n+1} + q_{2,i}^- \tilde{u}_{1,i-1}^{n+1} + q_{2,i}^c \tilde{u}_{1,i}^{n+1} + q_{2,i}^+ \tilde{u}_{1,i+1}^{n+1} \\ - \left(\tilde{u}_{2,i}^{n+1} + \Delta t (\mathbb{L}_{x,\varepsilon_2} \tilde{u}^{n+1})(x_i) \right), \quad \text{for } N/2 < i \leq N-1, \end{cases}$$

therefore, one can deduce the following relation:

$$\zeta_{i,\tilde{u}}^{1,x} = \begin{cases} \mathbb{L}_{mu,\varepsilon_1}^N \tilde{u}_i - (\mathbb{L}_{x,\varepsilon_1} \tilde{u})_{i-1/2}, \quad \text{for } 1 \leq i \leq N/2, \\ \mathbb{L}_{cen,\varepsilon_1}^N \tilde{u}_i - (\mathbb{L}_{x,\varepsilon_1} \tilde{u})(x_i), \quad \text{for } N/2 < i \leq N-1, \end{cases} \quad (3.4.8)$$

$$\zeta_{i,\tilde{u}}^{2,x} = \begin{cases} \mathbb{L}_{mu,\varepsilon_2}^N \tilde{u}_i - (\mathbb{L}_{x,\varepsilon_2} \tilde{u})_{i-1/2}, \quad \text{for } 1 \leq i \leq N/2, \\ \mathbb{L}_{cen,\varepsilon_2}^N \tilde{u}_i - (\mathbb{L}_{x,\varepsilon_2} \tilde{u})(x_i), \quad \text{for } N/2 < i \leq N-1. \end{cases} \quad (3.4.9)$$

Thus, $\zeta_{i,\tilde{u}}^{1,x}$, $\zeta_{i,\tilde{u}}^{2,x}$ are the truncation error components corresponding to the hybrid scheme used for stationary singularly perturbed system of convection-diffusion problem.

Lemma 3.4.2. *Let $\vec{g} = (g_1, g_2)^T$ be a smooth function defined on $[0, 1]$ Then, for $1 \leq i \leq N/2$, the following estimates for the truncation error hold true*

$$\begin{aligned} \left| \mathbb{L}_{mu,\varepsilon_1}^N (\vec{g}_i) - (\mathbb{L}_{x,\varepsilon_1} \vec{g})_{i-1/2} \right| &\leq C\varepsilon_1 \int_{x_{i-1}}^{x_{i+1}} |g_1^{(3)}(s)| ds \\ &\quad + Ch_i \int_{x_{i-1}}^{x_i} \left(|g_1^{(3)}(s)| + |g_1^{(2)}(s)| + |g_1^{(1)}(s)| \right) ds, \\ \left| \mathbb{L}_{mu,\varepsilon_2}^N (\vec{g}_i) - (\mathbb{L}_{x,\varepsilon_2} \vec{g})_{i-1/2} \right| &\leq C\varepsilon_2 \int_{x_{i-1}}^{x_{i+1}} |g_2^{(3)}(s)| ds \\ &\quad + Ch_i \int_{x_{i-1}}^{x_i} \left(|g_2^{(3)}(s)| + |g_2^{(2)}(s)| + |g_2^{(1)}(s)| \right) ds, \end{aligned} \quad (3.4.10)$$

and, for $N/2 < i \leq N/2$,

$$\begin{aligned} |\mathbb{L}_{cen,\varepsilon_1}^N(\vec{g}_i) - (\mathbb{L}_{x,\varepsilon_1}\vec{g})(x_i)| &\leq Ch_i \int_{x_{i-1}}^{x_{i+1}} \left(\varepsilon_1 |g_1^{(4)}(s)| + |g_1^{(3)}(s)| \right) ds, \\ |\mathbb{L}_{cen,\varepsilon_2}^N(\vec{g}_i) - (\mathbb{L}_{x,\varepsilon_2}\vec{g})(x_i)| &\leq Ch_i \int_{x_{i-1}}^{x_{i+1}} \left(\varepsilon_2 |g_2^{(4)}(s)| + |g_2^{(3)}(s)| \right) ds. \end{aligned} \quad (3.4.11)$$

Proof. By following the technique from proof of [40, Lemma 3.3], one can obtain the required estimates. \blacksquare

To obtain appropriate estimates for the local truncation errors $\tau_{i,\tilde{z}^{n+1}}^1, \zeta_{i,\tilde{z}^{n+1}}^2$, firstly we derive estimates of the truncation errors $\zeta_{i,\tilde{z}^{n+1}}^{1,x}, \zeta_{i,\tilde{z}^{n+1}}^{2,x}$ in the following lemma.

Lemma 3.4.3. *The truncation error given in (3.4.8) and (3.4.9) satisfy the following estimates:*

$$\zeta_{i,\tilde{z}^{n+1}}^{1,x} \leq \begin{cases} C \left[(\varepsilon_1 + h_i)h_i + \frac{B_{\varepsilon_1}^1(x_i)}{\max\{\varepsilon_1, h_i\}} + \frac{B_{\varepsilon_2}^1(x_i)}{\max\{\varepsilon_2, h_i\}} \right], & \text{for } 1 < i < \frac{N}{2}, \\ C [(\varepsilon_1 + h_i)h_i + \varepsilon_1^{-1}B_{\varepsilon_1}^1(x_i) + \varepsilon_2^{-1}B_{\varepsilon_2}^1(x_i)], & \text{for } i = \frac{N}{2}, \\ C [H_2^2 + H_2^2 (\varepsilon_1^{-3}B_{\varepsilon_1}^1(x_i) + \varepsilon_2^{-3}B_{\varepsilon_2}^1(x_i))], & \text{for } \frac{N}{2} < i \leq \frac{3N}{4}, \\ C [H_3^2 + H_3^2 (\varepsilon_1^{-3}B_{\varepsilon_1}^1(x_i) + \varepsilon_2^{-3}B_{\varepsilon_2}^1(x_i))], & \text{for } \frac{3N}{4} < i \leq N-1, \end{cases}$$

$$\zeta_{i,\tilde{z}^{n+1}}^{2,x} \leq \begin{cases} C \left[(\varepsilon_2 + h_i)h_i + \frac{B_{\varepsilon_1}^1(x_i)}{\max\{\varepsilon_1, h_i\}} + \frac{B_{\varepsilon_2}^1(x_i)}{\max\{\varepsilon_2, h_i\}} \right], & \text{for } 1 < i < \frac{N}{2}, \\ C [(\varepsilon_2 + h_i)h_i + \varepsilon_1^{-1}B_{\varepsilon_1}^1(x_i) + \varepsilon_2^{-1}B_{\varepsilon_2}^1(x_i)], & \text{for } i = \frac{N}{2}, \\ C [H_2^2 + H_2^2 (\varepsilon_1^{-3}B_{\varepsilon_1}^1(x_i) + \varepsilon_2^{-3}B_{\varepsilon_2}^1(x_i))], & \text{for } \frac{N}{2} < i \leq \frac{3N}{4}, \\ C [H_3^2 + H_3^2 (\varepsilon_1^{-3}B_{\varepsilon_1}^1(x_i) + \varepsilon_2^{-3}B_{\varepsilon_2}^1(x_i))], & \text{for } \frac{3N}{4} < i \leq N-1. \end{cases}$$

Proof. In this proof we consider different cases depending on the location of mesh points $x_i \in \bar{\Omega}_x^N$. Denote $\zeta_{i,\tilde{z}^{n+1}}^{l,x}$ and $\zeta_{i,\tilde{w}^{n+1}}^{l,x}$, as the local truncation errors corresponding to components $\tilde{z}_l^{n+1}(x)$ and $\tilde{w}_l^{n+1}(x)$, respectively.

Case 1 (Outer region): For $1 \leq i \leq N/2$. Here we consider two subcases, to find the appropriate estimate depending upon $\rho_i^{\varepsilon_l}$, $l = 1, 2$.

Subcase 1. When $\rho_i^{\varepsilon_l} \leq 1$, $l = 1, 2$. First we shall estimate the truncation error related to \tilde{z}_1^{n+1} . By using the derivative bounds (3.3.7) in (3.4.10), we obtain that

$$\begin{aligned} \left| \zeta_{i,\tilde{z}^{n+1}}^{1,x} \right| &= \left| \mathbb{L}_{mu,\varepsilon_1}^N \tilde{\vec{z}}_i - (\mathbb{L}_{x,\varepsilon_1} \tilde{\vec{z}})_{i-1/2} \right| \\ &\leq C(\varepsilon_1 + h_i)h_i + C (B_{\varepsilon_1}^1(x_{i+1}) + B_{\varepsilon_2}^1(x_{i+1})) + Ch_i \varepsilon_1^{-1} (B_{\varepsilon_1}^1(x_i) + B_{\varepsilon_2}^1(x_i)) \\ &\leq C(\varepsilon_1 + h_i)h_i + C (B_{\varepsilon_1}^1(x_{i+1}) + B_{\varepsilon_2}^1(x_{i+1})). \end{aligned} \quad (3.4.12)$$

In a similar way, one can deduce that

$$\left| \zeta_{i, \tilde{z}^{n+1}}^{2,x} \right| \leq C(\varepsilon_2 + h_i)h_i + C(B_{\varepsilon_1}^1(x_{i+1}) + B_{\varepsilon_2}^1(x_{i+1})). \quad (3.4.13)$$

In addition, we have

$$\left| \zeta_{i, \tilde{w}^{n+1}}^{1,x} \right| \leq C\varepsilon_1^{-1}B_{\varepsilon_1}^1(x_i), \quad \left| \zeta_{i, \tilde{w}^{n+1}}^{2,x} \right| \leq C\varepsilon_2^{-1}B_{\varepsilon_2}^1(x_i). \quad (3.4.14)$$

Hence, by utilizing the estimate of error terms $\left| \zeta_{i, \tilde{z}^{n+1}}^{l,x} \right|$, $\left| \zeta_{i, \tilde{w}^{n+1}}^{l,x} \right|$, $l = 1, 2$, we obtain

$$\left| \zeta_{i, \tilde{u}^{n+1}}^{1,x} \right| \leq C(\varepsilon_1 + h_i)h_i + C(\varepsilon_1^{-1}B_{\varepsilon_1}^1(x_{i+1}) + \varepsilon_2^{-1}B_{\varepsilon_2}^1(x_{i+1})), \quad (3.4.15)$$

$$\left| \zeta_{i, \tilde{u}^{n+1}}^{2,x} \right| \leq C(\varepsilon_2 + h_i)h_i + C(\varepsilon_1^{-1}B_{\varepsilon_1}^1(x_{i+1}) + \varepsilon_2^{-1}B_{\varepsilon_2}^1(x_{i+1})). \quad (3.4.16)$$

Subcase 2. When $\rho_i^{\varepsilon_l} \geq 1$, $l = 1, 2$. Arguing in the same way done in **Subcase 1**, we can obtain that

$$\left| \zeta_{i, \tilde{z}^{n+1}}^{1,x} \right| \leq \begin{cases} C(\varepsilon_1 + h_i)h_i + C(B_{\varepsilon_1}^1(x_{i+1}) + B_{\varepsilon_2}^1(x_{i+1})), & \text{for } 1 \leq i < N/2, \\ C(\varepsilon_1 + h_i)h_i + Ch_i\varepsilon_1^{-1}(B_{\varepsilon_1}^1(x_{i+1}) + B_{\varepsilon_2}^1(x_{i+1})), & \text{for } i = N/2, \end{cases} \quad (3.4.17)$$

using $h_i = h_{i+1} = H_1$ and $s^k \exp(-s) \leq C$, for all $s \geq 0$, k a positive integer, in the first inequality. In a similar way, we get

$$\left| \zeta_{i, \tilde{z}^{n+1}}^{2,x} \right| \leq \begin{cases} C(\varepsilon_2 + h_i)h_i + C(B_{\varepsilon_1}^1(x_{i+1}) + B_{\varepsilon_2}^1(x_{i+1})), & \text{for } 1 \leq i < N/2, \\ C(\varepsilon_2 + h_i)h_i + Ch_i\varepsilon_2^{-1}(B_{\varepsilon_1}^1(x_i) + B_{\varepsilon_2}^1(x_i)), & \text{for } i = N/2. \end{cases} \quad (3.4.18)$$

Next, we will acquire error estimate for the component, \tilde{w}

$$\begin{aligned} \zeta_{i, \tilde{w}^{n+1}}^{1,x} &= r_{mu,1,i}^-(\tilde{w}_{1,i-1} - \tilde{w}_{1,i}) + r_{mu,1,i}^+(\tilde{w}_{1,i+1} - \tilde{w}_{1,i}) + \frac{1}{2}\varepsilon_1(\tilde{w}_{1,i}'' + \tilde{w}_{1,i-1}'') \\ &\quad - \frac{1}{2}(a_{1,i}\tilde{w}_{1,i}' + a_{1,i-1}\tilde{w}_{1,i-1}') - \frac{1}{2}(b_{11,i}\tilde{w}_{1,i} - b_{11,i-1}\tilde{w}_{1,i-1}) \\ &\quad - \frac{1}{2}(b_{12,i-1}\tilde{w}_{2,i} + b_{12,i}\tilde{w}_{2,i-1}). \end{aligned} \quad (3.4.19)$$

By using (3.3.6), we obtain the following estimates:

$$\begin{aligned} \left| \frac{1}{2}\varepsilon_1(\tilde{w}_{1,i}'' + \tilde{w}_{1,i-1}'') \right| &\leq C\varepsilon_1^{-1} \exp(-a_1(1)(1-x_i)/\varepsilon_1), \\ \left| \frac{1}{2}(a_{1,i}\tilde{w}_{1,i}' + a_{1,i-1}\tilde{w}_{1,i-1}') \right| &\leq C\varepsilon_1^{-1} \exp(-a_1(1)(1-x_i)/\varepsilon_1), \\ \left| \frac{1}{2}(b_{11,i}\tilde{w}_{1,i} - b_{11,i-1}\tilde{w}_{1,i-1}) \right| &\leq C \exp(-a_1(1)(1-x_i)/\varepsilon_1), \\ \left| \frac{1}{2}(b_{12,i-1}\tilde{w}_{2,i} + b_{12,i}\tilde{w}_{2,i-1}) \right| &\leq C \exp(-a_2(1)(1-x_i)/\varepsilon_2). \end{aligned} \quad (3.4.20)$$

From (3.4.2), we get

$$|r_{mu,1,i}^-| \leq \frac{2\varepsilon_1}{\tilde{h}_i h_i} + \frac{a_{1,i-1/2}}{h_i} + \frac{b_{11,i-1/2}}{2} \leq \frac{C}{h_i}, \quad |r_{mu,1,i}^-| \leq \frac{2\varepsilon_1}{\tilde{h}_i h_{i+1}} \leq \frac{C}{h_{i+1}}. \quad (3.4.21)$$

Now, for $1 \leq i < N/2$, using (3.3.7) and (3.4.21), we obtain that

$$|r_{mu,1,i}^-(\tilde{w}_{1,i-1} - \tilde{w}_{1,i}) + r_{mu,1,i}^+(\tilde{w}_{1,i+1} - \tilde{w}_{1,i})| \leq Ch_i^{-1} \exp(-a_1(1)(1 - x_{i+1})/\varepsilon_1). \quad (3.4.22)$$

Hence, by applying the estimates (3.4.20) and (3.4.22) in (3.4.19), we have

$$\begin{aligned} \left| \zeta_{i,\vec{z}^{n+1}}^{1,x} \right| &\leq Ch_i^{-1} \exp(-a_1(1)(1 - x_{i+1})/\varepsilon_1) + \exp(-a_2(1)(1 - x_{i+1})/\varepsilon_2) \\ &\leq Ch_i^{-1} (\exp(-a_1(1)(1 - x_{i+1})/\varepsilon_1) + \exp(-a_2(1)(1 - x_{i+1})/\varepsilon_2)) \end{aligned} \quad (3.4.23)$$

In a similar way, one can deduce that

$$\left| \zeta_{i,\vec{w}}^{2,x} \right| \leq Ch_i^{-1} (\exp(-a_1(1)(1 - x_{i+1})/\varepsilon_2) + \exp(-a_2(1)(1 - x_{i+1})/\varepsilon_2)). \quad (3.4.24)$$

Next, consider for $i = N/2$. By employing (3.3.7) and (3.4.21), we have

$$\begin{aligned} &|r_{mu,1,i}^-(\tilde{w}_{1,i-1} - \tilde{w}_{1,i}) + r_{mu,1,i}^+(\tilde{w}_{1,i+1} - \tilde{w}_{1,i})| \\ &\leq |r_{mu,1,i}^-(\exp(-a_1(1)H_1/\varepsilon_1) - 1) + r_{mu,1,i}^+(\exp(a_1(1)H_2/\varepsilon_1) - 1)| \times \\ &\quad \exp(-a_1(1)(1 - x_i)/\varepsilon_1) \\ &\leq \left[\frac{C}{H_1} (1 - \exp(-a_1(1)H_1/\varepsilon_1)) + \frac{2\varepsilon_1}{H_2(H_1 + H_2)} (\exp(a_1(1)H_2/\varepsilon_1) - 1) \right] \times \\ &\quad \exp(-a_1(1)(1 - x_i)/\varepsilon_1) \\ &\leq \left(\frac{C}{H_1} + \frac{C}{H_1 + H_2} \right) \exp(-a_1(1)(1 - x_i)/\varepsilon_1) \leq CH_1^{-1} \exp(-a_1(1)(1 - x_i)/\varepsilon_1) \\ &\leq C\varepsilon_1^{-1} \exp(-a_1(1)(1 - x_{i+1})/\varepsilon_1), \end{aligned} \quad (3.4.25)$$

using $\exp(\theta) \geq 0$ and $\exp(\theta) \leq 1 + C\theta$ in closed and bounded intervals of θ , in the above inequality. By using (3.4.20) and (3.4.25) in (3.4.19), we obtain

$$\left| \zeta_{N/2,\vec{w}}^{1,x} \right| \leq C (\varepsilon_1^{-1} \exp(-a_1(1)(1 - x_{i+1})/\varepsilon_1) + \varepsilon_2^{-1} \exp(-a_2(1)(1 - x_{i+1})/\varepsilon_2)). \quad (3.4.26)$$

In a similar way, one can get

$$\left| \zeta_{N/2,\vec{w}}^{2,x} \right| \leq C (\varepsilon_1^{-1} \exp(-a_1(1)(1 - x_{i+1})/\varepsilon_1) + \varepsilon_2^{-1} \exp(-a_2(1)(1 - x_{i+1})/\varepsilon_2)) \quad (3.4.27)$$

Hence, by applying estimates (3.4.17), (3.4.18), (3.4.23), (3.4.24), (3.4.26) and (3.4.27) in (3.3.6), we obtain

$$\left| \zeta_{i,\bar{u}}^{1,x} \right| \leq \begin{cases} C(\varepsilon_1 + h_i)h_i + Ch_i^{-1} (B_{\varepsilon_1}^1(x_{i+1}) + B_{\varepsilon_2}^1(x_{i+1})), & \text{for } 1 \leq i < N/2, \\ C(\varepsilon_1 + h_i)h_i + C(\varepsilon_1^{-1}B_{\varepsilon_1}^1(x_{i+1}) + \varepsilon_2^{-1}B_{\varepsilon_2}^1(x_{i+1})), & \text{for } i = N/2, \end{cases}$$

$$\left| \zeta_{i,\bar{u}}^{2,x} \right| \leq \begin{cases} C(\varepsilon_2 + h_i)h_i + Ch_i^{-1} (B_{\varepsilon_1}^1(x_{i+1}) + B_{\varepsilon_2}^1(x_{i+1})), & \text{for } 1 \leq i < N/2, \\ C(\varepsilon_2 + h_i)h_i + C(\varepsilon_1^{-1}B_{\varepsilon_1}^1(x_{i+1}) + \varepsilon_2^{-1}B_{\varepsilon_2}^1(x_{i+1})), & \text{for } i = N/2. \end{cases}$$

Case 2 (Inner region): For $N/2 + 1 \leq i \leq N$. By using (3.3.7) and (3.4.11), we get

$$\begin{cases} \left| \zeta_{i,\bar{z}}^{l,x} \right| \leq Ch_i^2 + Ch_i\varepsilon_l^{-1} (B_{\varepsilon_l}^1(x_{i+1}) - B_{\varepsilon_l}^1(x_{i-1})), & l = 1, 2, \\ \left| \zeta_{i,\bar{w}}^{l,x} \right| \leq Ch_i\varepsilon_l^{-2} (B_{\varepsilon_l}^1(x_{i+1}) - B_{\varepsilon_l}^1(x_{i-1})), & l = 1, 2. \end{cases}$$

Finally, combining $\left| \zeta_{i,\bar{z}}^{1,x} \right|$ and $\left| \zeta_{i,\bar{w}}^{1,x} \right|$, we have

$$\begin{aligned} \left| \zeta_{i,\bar{u}}^{1,x} \right| &\leq Ch_i^2 + Ch_i\varepsilon_1^{-2} (B_{\varepsilon_1}^1(x_{i+1}) - B_{\varepsilon_1}^1(x_{i-1})) \\ &= Ch_i^2 + Ch_i\varepsilon_1^{-2} B_{\varepsilon_1}^1(x_i) \sinh(\alpha h_i/\varepsilon_1) \leq Ch_i^2 + Ch_i^2\varepsilon_1^{-3} B_{\varepsilon_1}^1(x_i) \\ &\leq Ch_i^2 + Ch_i^2 (\varepsilon_1^{-3} B_{\varepsilon_1}^1(x_i) + \varepsilon_2^{-3} B_{\varepsilon_2}^1(x_i)). \end{aligned} \quad (3.4.28)$$

Hence, the error term $\zeta_{i,\bar{u}}^{1,x}$ in $(1 - \tau_{\varepsilon_2}, 1 - \tau_{\varepsilon_1}]$ can be expressed as

$$\left| \zeta_{i,\bar{u}}^{1,x} \right| \leq CH_2^2 + CH_2^2 (\varepsilon_1^{-3} B_{\varepsilon_1}^1(x_i) + \varepsilon_2^{-3} B_{\varepsilon_2}^1(x_i)),$$

whereas in subinterval $(1 - \tau_{\varepsilon_1}, 1]$, the error term $\zeta_{i,\bar{u}}^{1,x}$ satisfies

$$\left| \zeta_{i,\bar{u}}^{1,x} \right| \leq CH_3^2 + CH_3^2 (\varepsilon_1^{-3} B_{\varepsilon_1}^1(x_i) + \varepsilon_2^{-3} B_{\varepsilon_2}^1(x_i)).$$

An analogous result holds for $\zeta_{i,\bar{u}}^{2,x}$. This completes the proof. \blacksquare

Lemma 3.4.4. *The local truncation error satisfies the following estimates:*

$$\zeta_{i,\bar{u}}^1 \leq \begin{cases} C\Delta t \left((\varepsilon_1 + h_i)h_i + \frac{B_{\varepsilon_1}^1(x_i)}{\max\{\varepsilon_1, h_i\}} + \frac{B_{\varepsilon_2}^1(x_i)}{\max\{\varepsilon_2, h_i\}} \right), & \text{for } 1 < i < \frac{N}{2}, \\ C\Delta t ((\varepsilon_1 + h_i)h_i + \varepsilon_1^{-1}B_{\varepsilon_1}^1(x_i) + \varepsilon_2^{-1}B_{\varepsilon_2}^1(x_i)), & \text{for } i = \frac{N}{2}, \\ C\Delta t (H_2^2 + H_2^2 (\varepsilon_1^{-3} B_{\varepsilon_1}^1(x_i) + \varepsilon_2^{-3} B_{\varepsilon_2}^1(x_i))), & \text{for } \frac{N}{2} < i \leq \frac{3N}{4}, \\ C\Delta t (H_3^2 + H_3^2 (\varepsilon_1^{-3} B_{\varepsilon_1}^1(x_i) + \varepsilon_2^{-3} B_{\varepsilon_2}^1(x_i))), & \text{for } \frac{3N}{4} < i \leq N - 1, \end{cases}$$

$$\zeta_{i,\vec{u}}^2 \leq \begin{cases} C\Delta t \left((\varepsilon_2 + h_i)h_i + \frac{B_{\varepsilon_1}^1(x_i)}{\max\{\varepsilon_1, h_i\}} + \frac{B_{\varepsilon_2}^1(x_i)}{\max\{\varepsilon_2, h_i\}} \right), & \text{for } 1 < i < \frac{N}{2}, \\ C\Delta t \left((\varepsilon_2 + h_i)h_i + \varepsilon_1^{-1}B_{\varepsilon_1}^1(x_i) + \varepsilon_2^{-1}B_{\varepsilon_2}^1(x_i) \right), & \text{for } i = \frac{N}{2}, \\ C\Delta t \left(H_2^2 + H_2^2 \left(\varepsilon_1^{-3}B_{\varepsilon_1}^1(x_i) + \varepsilon_2^{-3}B_{\varepsilon_2}^1(x_i) \right) \right), & \text{for } \frac{N}{2} < i \leq \frac{3N}{4}, \\ C\Delta t \left(H_3^2 + H_3^2 \left(\varepsilon_1^{-3}B_{\varepsilon_1}^1(x_i) + \varepsilon_2^{-3}B_{\varepsilon_2}^1(x_i) \right) \right), & \text{for } \frac{3N}{4} < i \leq N-1. \end{cases}$$

Proof. These estimates will directly follow from Lemma 3.4.3. \blacksquare

From Lemma 3.4.4, we have just found estimates for the local truncation error that are not uniform in $\varepsilon_1, \varepsilon_2$. Next, we define mesh function $\vec{S}_{\varepsilon_2, i} = (S_{\varepsilon_2, i}, S_{\varepsilon_2, i})^T$ as follows:

$$S_{\varepsilon_2, i}(\mu) = \prod_{j=i+1}^N \left(1 + \frac{\mu h_j}{\varepsilon_2} \right)^{-1}, \quad \text{for } i = 0, \dots, N-1,$$

and we take $S_{\varepsilon_2, N}(\mu) = 1$, where μ is a positive constant.

Lemma 3.4.5. *If $\mu < \alpha/2$, then under the hypothesis (3.4.5) and (3.4.6), for $l = 1, 2$, we have the following estimate*

$$\widehat{\mathbb{L}}_{\varepsilon_l}^N \vec{S}_{\varepsilon_2, i}(\mu) \geq \begin{cases} \frac{C\Delta t}{\max\{\varepsilon_2, h_{i+1}\}} S_{\varepsilon_2, i}(\mu), & \text{for } 1 \leq i \leq N/2 \\ \frac{C\Delta t}{\varepsilon_2} S_{\varepsilon_2, i}(\mu), & \text{for } N/2 < i \leq N-1. \end{cases}$$

Proof. First, we consider the case for $1 \leq i \leq N/2$. We have

$$\begin{aligned} \widehat{\mathbb{L}}_{\varepsilon_1}^N \vec{S}_{\varepsilon_2, i}(\mu) &= r_{1,i}^- S_{\varepsilon_2, i-1}(\mu) + r_{1,i}^c S_{\varepsilon_2, i}(\mu) + r_{1,i}^+ S_{\varepsilon_2, i+1}(\mu) \\ &\quad + q_{1,i}^- S_{\varepsilon_2, i-1}(\mu) + q_{1,i}^c S_{\varepsilon_2, i}(\mu) + q_{1,i}^+ S_{\varepsilon_2, i+1}(\mu) \\ &= \Delta t \mathbb{L}_{\mu, \varepsilon_1}^N \vec{S}_{\varepsilon_2, i}(\mu) + \frac{1}{2} S_{\varepsilon_2, i}(\mu) \left(1 + \left(1 + \frac{\mu h_i}{\varepsilon_1} \right)^{-1} \right) \geq \Delta t \mathbb{L}_{\mu, \varepsilon_1}^N \vec{S}_{\varepsilon_2, i}(\mu). \end{aligned}$$

It is easy to verify that $(S_{\varepsilon_2, i}(\mu) - S_{\varepsilon_2, i-1}(\mu)) = \frac{\mu h_i}{\varepsilon_2} S_{\varepsilon_2, i-1}(\mu)$, and if $\mu \leq \alpha/2$, we get

$$\begin{aligned} \mathbb{L}_{\mu, \varepsilon_1}^N \vec{S}_{\varepsilon_2, i}(\mu) &= -\frac{2\mu\varepsilon_1}{(h_i + h_{i+1})\varepsilon_2} (S_{\varepsilon_2, i}(\mu) - S_{\varepsilon_2, i-1}(\mu)) + a_{1, i-1/2} \frac{\mu}{\varepsilon_2} S_{\varepsilon_2, i-1}(\mu) \\ &\quad + (b_{11, i-1/2} + b_{12, i-1/2}) \frac{(S_{\varepsilon_2, i}(\mu) + S_{\varepsilon_2, i-1}(\mu))}{2} \\ &\geq C \frac{\mu}{\varepsilon_2} S_{\varepsilon_2, i-1}(\mu) \left(a_{1, i-1/2} - \frac{2\mu\varepsilon_1 h_i}{\varepsilon_2 (h_i + h_{i+1})} \right) \geq \frac{C\alpha S_{\varepsilon_2, i}(\mu)}{\varepsilon_2 + \mu h_i} \geq \frac{CS_{\varepsilon_2, i}(\mu)}{\max\{\varepsilon_2, h_i\}}. \end{aligned}$$

Hence, under the condition $\mu \leq \alpha/2$, one can obtain

$$\widehat{\mathbb{L}}_{\varepsilon_l}^N \vec{S}_{\varepsilon_2, i}(\mu) \geq \frac{C\Delta t}{\max\{\varepsilon_2, h_i\}} S_{\varepsilon_2, i}(\mu), \quad l = 1, 2.$$

Similarly, for $N/2 < i \leq N - 1$, we get

$$\widehat{\mathbb{L}}_{\varepsilon_1}^N \vec{S}_{\varepsilon_2, i}(\mu) = \Delta t \mathbb{L}_{cen, \varepsilon_1}^N \vec{S}_{\varepsilon_2, i}(\mu) + S_{\varepsilon_2, i}(\mu) \geq \Delta t \mathbb{L}_{cen, \varepsilon_1}^N \vec{S}_{\varepsilon_2, i}(\mu).$$

Next, we have

$$\begin{aligned} \mathbb{L}_{cen, \varepsilon_1}^N \vec{S}_{\varepsilon_2, i}(\mu) &= -\frac{2\mu\varepsilon_1}{(h_i + h_{i+1})\varepsilon_2} (S_{\varepsilon_2, i}(\mu) - S_{\varepsilon_2, i-1}(\mu)) + \frac{a_{1, i}}{h_i + h_{i+1}} (S_{\varepsilon_2, i+1}(\mu) - S_{\varepsilon_2, i-1}(\mu)) \\ &\quad + (b_{11, i} + b_{12, i}) (S_{\varepsilon_2, i}(\mu)) \\ &= \mathbb{L}_{mu, \varepsilon_1}^N \vec{S}_{\varepsilon_2, i}(\mu) + \left(a_{1, i} \frac{\mu^2 h_i h_{i+1}}{\varepsilon_2 (h_i + h_{i+1})} \right) S_{\varepsilon_2, i-1}(\mu) \geq \frac{CS_{\varepsilon_2, i}(\mu)}{\varepsilon_2}, \end{aligned}$$

(for $i > N/2$, the term $\mathbb{L}_{mu, \varepsilon_1}^N$ contains $a_{1, i}, b_{11, i}, b_{12, i}$ instead of $a_{1, i-1/2}, b_{11, i-1/2}, b_{12, i-1/2}$, but this is insignificant). Hence, under the condition $\mu \leq \alpha/2$, we have

$$\widehat{\mathbb{L}}_{\varepsilon_1}^N \vec{S}_{\varepsilon_2, i}(\mu) \geq \frac{C\Delta t}{\varepsilon_2} S_{\varepsilon_2, i}(\mu).$$

By using similar argument, one can deduce that

$$\widehat{\mathbb{L}}_{\varepsilon_2}^N \vec{S}_{\varepsilon_2, i}(\mu) \geq \frac{C\Delta t}{\varepsilon_2} S_{\varepsilon_2, i}(\mu).$$

This complete the proof. ■

To prove the uniform convergence of the hybrid scheme, we will use the following technical result.

Lemma 3.4.6. *If $\mu < \alpha/2$, then the following bounds hold true:*

$$1. \quad B_{\varepsilon_2}^1(x_i) \leq S_{\varepsilon_2, i}(\mu), \text{ for } i = 0, \dots, N - 1. \quad (3.4.29)$$

$$2. \quad S_{\varepsilon_2, N/2}(\mu) \leq CN^{-\mu\tau_0}. \quad (3.4.30)$$

Proof. 1. For each j , we have

$$\exp(-\alpha h_j / \varepsilon_2) \leq \exp(-\mu h_j / \varepsilon_2) \leq \left(1 + \frac{\mu h_j}{\varepsilon_2} \right)^{-1}.$$

Multiply these inequalities for $j = i + 1, \dots, N$, we obtain $B_{\varepsilon_2}^1(x_i) \leq S_{\varepsilon_2, i}(\mu)$.

2. Proof of (3.4.30) follows from [88, Lemma 3.1]. ■

Next, we discuss the convergence analysis of the hybrid scheme (3.4.4).

Theorem 3.4.7. *Let $\tilde{u}^{n+1}(x_i)$ and \tilde{U}_i^{n+1} be the exact and discrete solutions of (3.3.3) and (3.4.4) respectively, then we have the following bounds*

$$|\tilde{u}_i^{n+1} - \tilde{U}_i^{n+1}| \leq \begin{cases} \vec{C}(N^{-2} + N^{-\alpha\tau_0}), & \text{for } 1 \leq i \leq N/2, \\ \vec{C}(\tau_0^2 N^{-2} \ln^3 N + N^{-\alpha\tau_0}), & \text{for } N/2 < i \leq N - 1, \end{cases} \quad (3.4.31)$$

where $N \geq N_0$ satisfies conditions given in (3.4.5) and (3.4.6).

Proof. Define the discrete barrier function

$$\vec{\mathcal{B}}_i^{out} = \vec{C} \begin{cases} ((\varepsilon_1 + \varepsilon_2 + h_i)h_i + (\varepsilon_1^{-1} + \varepsilon_2^{-1}))(1 + x_i), & \text{for } h_i \leq \varepsilon_1 \\ (\varepsilon_1 + \varepsilon_2 + h_i)h_i(1 + x_i) + \left(1 + \frac{\mu h_{i+1}}{\varepsilon_2}\right) S_{\varepsilon_2, i}(\mu), & \text{for } h_i \geq \varepsilon_1. \end{cases}$$

Consider the following inequality

$$\varepsilon_1^{-k} B_{\varepsilon_1}^1(\xi) \leq \varepsilon_2^{-k} B_{\varepsilon_2}^1(\xi), \quad \text{for } \xi < 1 - \tau_0 \varepsilon_1, \quad k = 1, 2, \dots \quad (3.4.32)$$

Then, by using (3.4.29) and Lemmas 3.4.4 and 3.4.5 with (3.4.32), we can obtain that

$$|\widehat{\mathbb{L}}_{\varepsilon_1}^N \vec{\mathcal{B}}_i^{out}| \geq \zeta_{i, \vec{u}}^1, \quad |\widehat{\mathbb{L}}_{\varepsilon_2}^N \vec{\mathcal{B}}_i^{out}| \geq \zeta_{i, \vec{u}}^2, \quad \text{for } 1 \leq i \leq N/2.$$

Thus, by using the discrete maximum principle given in Lemma 3.4.1 for the operator $\widehat{\mathbb{L}}_{\varepsilon}^N = (\widehat{\mathbb{L}}_{\varepsilon_1}^N, \widehat{\mathbb{L}}_{\varepsilon_2}^N)^T$ on domain $[0, 1 - \tau_{\varepsilon_2}]$ with (3.4.30) and $\varepsilon_l \leq CN^{-1}$, $l = 1, 2$, we obtain that

$$|\vec{U}_i^{n+1} - \vec{U}_i^{n+1}| \leq \vec{C} (N^{-2} + N^{-\mu\tau_0}), \quad \text{for } 1 \leq i \leq N/2.$$

For $N/2 + 1 \leq i \leq N - 1$, the discrete barrier function is defined by

$$\vec{\mathcal{B}}_i^{inn} = \vec{C} \begin{cases} ((N^{-2} + N^{-\mu\tau_0})(1 + x_i) + H_2^2 \varepsilon_2^{-3}(x_i - (1 - \tau_{\varepsilon_2}))), & \text{for } \frac{N}{2} + 1 \leq i < \frac{3N}{4}, \\ ((N^{-2} + N^{-\mu\tau_0})(1 + x_i) + H_3^2(\varepsilon_1^{-3} + \varepsilon_2^{-3})(x_i - (1 - \tau_{\varepsilon_1}))), & \text{for } i > \frac{3N}{4}. \end{cases}$$

Hence, as a result, we get

$$\begin{cases} |\widehat{\mathbb{L}}_{\varepsilon_1}^N \vec{\mathcal{B}}_i^{inn}| \geq \zeta_{i, \vec{u}}^1, & |\widehat{\mathbb{L}}_{\varepsilon_2}^N \vec{\mathcal{B}}_i^{inn}| \geq \zeta_{i, \vec{u}}^2, & \text{for } N/2 < i \leq N - 1, \\ \vec{\mathcal{B}}_i^{inn} \geq |\vec{U}_{N/2}^{n+1} - \vec{U}_{N/2}^{n+1}| & \text{and } \vec{\mathcal{B}}_i^{inn} \geq |\vec{U}_N^{n+1} - \vec{U}_N^{n+1}|. \end{cases}$$

It is clear that the operator $\widehat{\mathbb{L}}_{\varepsilon}^N$ satisfies the discrete maximum principle on $[1 - \tau_{\varepsilon_2}, 1]$. Therefore, we obtain that

$$|\vec{u}_i^{n+1} - \vec{U}_i^{n+1}| \leq \vec{\mathcal{B}}_i^{inn} \leq \vec{C} (\tau_0^2 N^{-2} \ln^3 N + N^{-\mu\tau_0}), \quad \text{for } N/2 < i \leq N - 1.$$

Hence, the proof is completed. \blacksquare

An immediate consequence of the above convergence result is the following error estimate.

Corollary 3.4.8. *For a fixed $\tau_0 \geq 2/\mu$, there exists a constant C such that*

$$|\vec{u}_i^{n+1} - \vec{U}_i^{n+1}| \leq \begin{cases} \vec{C} N^{-2}, & \text{for } 1 \leq i \leq N/2 \\ \vec{C} N^{-2} \ln^3 N, & \text{for } N/2 < i \leq N - 1. \end{cases} \quad (3.4.33)$$

Therefore, the hybrid numerical method (3.4.4) is uniformly convergent of order almost two with respect to the spatial variable.

Corollary 3.4.9. *If we take $N^{-\nu} \leq C\Delta t$ with $0 < \nu < 1$, then from (3.4.33) we obtain*

$$|\tilde{u}_i^{n+1} - \tilde{U}_i^{n+1}| \leq \begin{cases} \vec{C}\Delta t N^{-2+\nu}, & \text{for } 1 \leq i \leq N/2 \\ \vec{C}\Delta t N^{-2+\nu} \ln^3 N, & \text{for } N/2 < i \leq N-1. \end{cases} \quad (3.4.34)$$

This bound is required to prove the uniform convergence of the fully discrete scheme.

3.5 The Fully Discrete Scheme

In the previous section, we have discussed the time and spatial discretization. By combining results from previous sections, this section provides the \mathcal{E} -uniform error estimate for the numerical solution of the fully discrete scheme on the mesh $\bar{Q}^{N,M} = \bar{\Omega}_x^N \times \bar{\Upsilon}^M$:

$$\left\{ \begin{array}{l} \vec{U}_i^0 = \vec{u}_0(x_i), \quad i = 0, \dots, N, \\ \left\{ \begin{array}{l} \widehat{\mathbb{L}}_{\varepsilon_1}^N \vec{U}_i^{n+1} = \frac{1}{2}(U_{1,i-1}^n + \Delta t f_{1,i-1}^{n+1}) + \frac{1}{2}(U_{1,i}^n + \Delta t f_{1,i}^{n+1}), \text{ for } 1 \leq i \leq N/2, \\ \widehat{\mathbb{L}}_{\varepsilon_2}^N \vec{U}_i^{n+1} = \frac{1}{2}(U_{2,i-1}^n + \Delta t f_{2,i-1}^{n+1}) + \frac{1}{2}(U_{2,i}^n + \Delta t f_{2,i}^{n+1}), \text{ for } 1 \leq i \leq N/2, \\ \widehat{\mathbb{L}}_{\varepsilon_1}^N \vec{U}_i^{n+1} = U_{1,i}^n + \Delta t f_{1,i}^{n+1}, \text{ for } N/2 < i \leq N-1, \\ \widehat{\mathbb{L}}_{\varepsilon_2}^N \vec{U}_i^{n+1} = U_{2,i}^n + \Delta t f_{2,i}^{n+1}, \text{ for } N/2 < i \leq N-1, \end{array} \right. \\ \vec{U}_0^{n+1} = \vec{U}_N^{n+1} = \vec{0}, \quad \text{for } n = 0, \dots, M-1, \end{array} \right. \quad (3.5.1)$$

where \vec{U}_i^n is the fully discrete approximation to the exact solution $\vec{u}(x, t)$ of (3.1.1) in the domain $\bar{Q}^{N,M}$.

Theorem 3.5.1 (Global error). *Let $\vec{u}(x_i, t_n)$ be the exact solution of (3.1.1) and $\{\vec{U}_i^n\}$ be the discrete solution of the fully discrete scheme (3.5.1). Assume that $N \geq N_0$ satisfies (3.4.5), (3.4.6) and $N^{-\nu} \leq C\Delta t$ with $0 < \nu < 1$. Then, if $\mu < \alpha/2$ and $\tau_0 \geq 2/\mu$, the error associated to the fully discrete scheme (3.5.1) satisfies*

$$\|\vec{u}(x_i, t_n) - \vec{U}_i^n\|_\infty \leq \begin{cases} \vec{C}(\Delta t + N^{-2+\nu}), & \text{for } 1 \leq i \leq N/2 \\ \vec{C}(\Delta t + N^{-2+\nu} \ln^3 N), & \text{for } N/2 < i \leq N-1. \end{cases} \quad (3.5.2)$$

Proof. By using the technique of Theorem 2.5.1, we can get the desired result. \blacksquare

3.6 Numerical Results

In this section we verify computationally the theoretical results obtained in the previous section. Error and convergence rate for the hybrid finite difference scheme are presented for the following test problem. In this test problem, we perform the numerical experiments by choosing the constant $\tau_0 = 4.2$ and the time step $\Delta t = 0.8/N$.

Example 3.6.1. Consider the following system of parabolic IBVP on $Q = (0, 1) \times (0, 1]$:

$$\begin{cases} \frac{\partial u_1}{\partial t} - \varepsilon_1 \frac{\partial^2 u_1}{\partial x^2} + (1+x) \frac{\partial u_1}{\partial x} + (2+x)u_1 - xu_2 = t(x^2 - x + 1)e^{-t}, \\ \frac{\partial u_2}{\partial t} - \varepsilon_2 \frac{\partial^2 u_2}{\partial x^2} + (1+x) \frac{\partial u_2}{\partial x} + (2+2x)u_2 - xu_1 = t^2(x^3 - x + 1)e^{-4t}, \\ u_1(x, 0) = \frac{1 - e^{-(1-x)/\varepsilon_1}}{1 - e^{-1/\varepsilon_1}} - (1-x), \quad u_2(x, 0) = \frac{1 - e^{-(1-x)/\varepsilon_2}}{1 - e^{-1/\varepsilon_2}} - (1-x), \\ u_1(0, t) = u_1(1, t) = 0, \quad u_2(0, t) = u_2(1, t) = 0, \quad t \in [0, 1]. \end{cases}$$

As the exact solution of Example 3.6.1 is not known, we have used the double mesh principle, described in the previous chapter. For our experiments, the singular perturbation parameters takes values from $S_\varepsilon = \{(\varepsilon_1, \varepsilon_2) | \varepsilon_2 = 2^{-16}, \dots, 2^{-30}, \varepsilon_1 = 2^{-10}\varepsilon_2\}$.

To visualize the appearance of the boundary layers in the numerical solutions of Example 3.6.1, we have plotted the numerical solution in Fig. 3.2 for $\varepsilon_1 = 2^{-7}, \varepsilon_2 = 2^{-5}$ and $N = 64$. From Fig. 3.2, one can notice the overlapping behavior of the two curves in the rightmost diagram.

From Table 3.1, we see the monotonically decreasing behavior of maximum errors, which confirm that the proposed numerical scheme (3.5.1) is \mathcal{E} -uniformly convergent. From Table 3.1, one can observe that the numerical order of convergence of the hybrid scheme is almost equal to two. One can see the comparison of the maximum errors and the order of convergence for upwind scheme and hybrid scheme in Table 3.1. Further, we have plotted N vs. the maximum errors in Fig. 3.3 and Fig. 3.4 in loglog scale.

To show the influence of the parameter τ_0 in the order of convergence, we have performed numerical experiment for Example 3.6.1 with different values of τ_0 . This results are given in Table 3.2. In fact, τ_0 should satisfy the condition $\tau_0 \geq 2/\mu > 4/\alpha$. Since in the Example 3.6.1, where α can be chosen as $\alpha = 1$. From Table 3.2, one can notice, when $\tau_0 < 4.2$, the order of convergence is not reflecting the theoretical results. In Table 3.3, we have given the numerical results for different Δt , which explains that the choice $\Delta t = 0.8/N$ is not necessary to produce almost second order uniform convergence.

3.7 Conclusion

In this chapter, we have proposed a finite difference numerical scheme for a class of singularly perturbed system of parabolic convection-diffusion problems. It has been shown theoretically that the proposed scheme is \mathcal{E} -uniformly convergent with first-order accurate in time and almost second-order accurate in space. Numerical results are carried out to show the accuracy of the proposed numerical method.

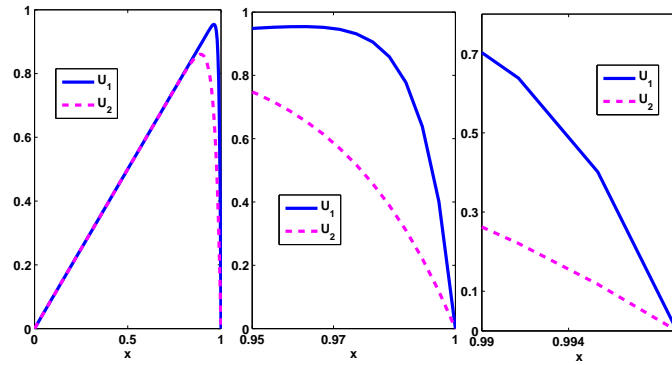


Figure 3.2: Numerical solution of Example 3.6.1 for $\varepsilon_1 = 2^{-7}$, $\varepsilon_2 = 2^{-5}$ and $N = 64$ at time $t = 1$.

Table 3.1: Comparison of uniform errors and corresponding rate of convergence between hybrid scheme and upwind scheme for Example 3.6.1.

S_ε	Scheme	Number of mesh-intervals N				
		64	128	256	512	1024
$d_1^{N,M}$	Upwind	6.6749e-02	4.4731e-02	2.4708e-02	1.3162e-02	7.4942e-03
$p_1^{N,M}$		0.5682	0.7851	0.8159	0.8492	
$d_1^{N,M}$	Hybrid	7.7391e-02	2.4202e-02	7.2436e-03	2.2541e-03	7.7006e-04
$p_1^{N,M}$		1.6098	1.7406	1.6869	1.6549	
$d_2^{N,M}$	Upwind	6.5946e-02	4.3683e-02	2.5472e-02	1.3648e-02	7.1537e-03
$p_2^{N,M}$		0.6017	0.7659	0.8862	0.9384	
$d_2^{N,M}$	Hybrid	7.4526e-02	2.4622e-02	7.2725e-03	2.2586e-03	7.7284e-04
$p_2^{N,M}$		1.5977	1.7594	1.6870	1.6472	

Table 3.2: Uniform errors and corresponding rate of convergence for Example 3.6.1 with different values of τ_0 .

$\varepsilon_1 = 2^{-14}$, $\varepsilon_2 = 2^{-10}$	τ_0	Number of mesh-intervals N				
		64	128	256	512	1024
$d_1^{N,M}$	3	1.0291e-02	4.4886e-03	2.1372e-03	1.1142e-03	5.3687e-04
$p_1^{N,M}$		1.1978	1.0715	0.9242	1.0566	
$d_2^{N,M}$		2.4556e-02	1.1687e-02	5.3928e-03	2.4589e-03	1.2033e-03
$p_2^{N,M}$		1.0712	1.1158	1.1330	1.0310	

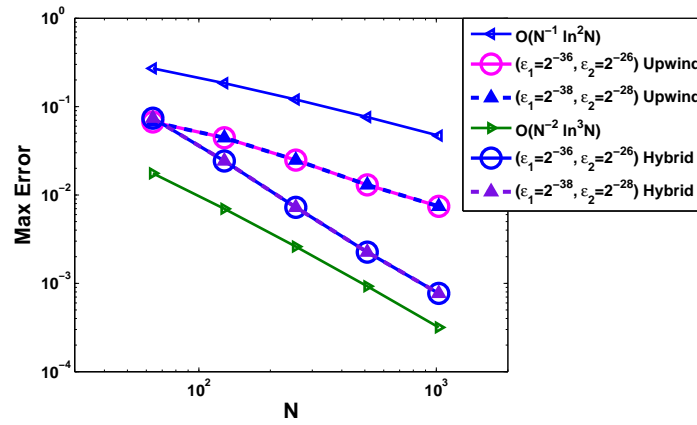


Figure 3.3: Visualization of the order of convergence through loglog plot for numerical solution U_1 of Example 3.6.1.

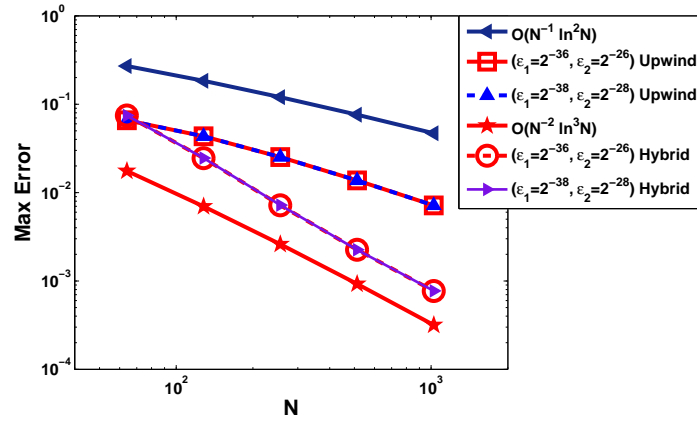


Figure 3.4: Visualization of the order of convergence through loglog plot for numerical solution U_2 of Example 3.6.1.

Table 3.3: Uniform errors and corresponding rate of convergence for Example 3.6.1.

S_ϵ	Number of mesh-intervals N /temporal mesh-size Δt				
	$64/\frac{1}{5}$	$128/\frac{1}{20}$	$256/\frac{1}{80}$	$512/\frac{1}{320}$	$1024/\frac{1}{1280}$
$d_1^{N,M}$	7.3705e-02	2.4995e-02	7.8918e-03	2.4213e-03	7.2316e-04
$p_1^{N,M}$	1.5601	1.6632	1.7046	1.7434	
$d_2^{N,M}$	6.6894e-02	2.3076e-02	7.6319e-03	2.4159e-03	7.2894e-04
$p_2^{N,M}$	1.5355	1.5963	1.6595	1.7287	

Uniformly Convergent Numerical Scheme for Singularly Perturbed System of 1D Parabolic Convection-Diffusion Problems with Interior Layers

In this chapter, we present the analysis of an upwind based finite difference scheme for singularly perturbed system of 1D parabolic convection-diffusion equations with discontinuous convection coefficient and source term. First, we discretize the domain with uniform mesh in the temporal direction and layer resolving piecewise-uniform Shishkin mesh in the spatial direction. The numerical scheme used to discretize the continuous problem, consists of the implicit-Euler scheme for the time derivative and the classical upwind scheme for the spatial derivatives. The proposed scheme is uniformly convergent of almost first-order in space and first-order in time. Numerical examples are carried out to verify the theoretical results.

4.1 Introduction

Denote the domain for describing the model problem by $Q^- = \Omega_x^- \times (0, T]$, $Q^+ = \Omega_x^+ \times (0, T]$, $Q = \Omega_x \times (0, T]$, $\Omega_x^- = (0, \xi)$, $\Omega_x^+ = (\xi, 1)$, $\Omega_x = (0, 1)$.

Consider the following class of singularly perturbed system of 1D parabolic convection-diffusion problems on the domain $Q^- \cup Q^+$:

$$\begin{cases} L_\varepsilon \vec{u} \equiv \frac{\partial \vec{u}}{\partial t} - \mathcal{E} \frac{\partial^2 \vec{u}}{\partial x^2} + A(x) \frac{\partial \vec{u}}{\partial x} + B(x) \vec{u} = \vec{f}, & (x, t) \in Q^- \cup Q^+, \\ \vec{u}(x, 0) = \vec{g}_0(x) \quad \forall x \in \bar{\Omega}_x, \\ \vec{u}(0, t) = \vec{g}_1(t), \quad \vec{u}(1, t) = \vec{g}_2(t) \quad \forall t \in [0, T], \end{cases} \quad (4.1.1)$$

with $\mathcal{E} = \text{diag}(\varepsilon_1, \varepsilon_2)$ $A = \text{diag}(a_1, a_2)$ and $B = \{b_{lm}\}_{l,m=1}^2$. The coefficients of

convection matrix A are given by

$$a_1(x) = \begin{cases} a_1^-(x), & x \in \Omega_x^- \\ a_1^+(x), & x \in \Omega_x^+, \end{cases} \quad a_2(x) = \begin{cases} a_2^-(x), & x \in \Omega_x^- \\ a_2^+(x), & x \in \Omega_x^+. \end{cases}$$

We assume that the convection coefficients and source terms satisfy

$$\begin{cases} |[a_1]| \leq C, |[a_2]| \leq C, |[f_1]| \leq C, |[f_2]| \leq C, \text{ at } x = \xi \\ \alpha_1^* \geq a_1^-(x), a_2^-(x) \geq \alpha_1 > 0, x < \xi, \\ -\alpha_2^* \leq a_1^+(x), a_2^+(x) \leq -\alpha_2 < 0, x > \xi, \end{cases} \quad (4.1.2)$$

In addition, suppose that B is an L_0 -matrix with

$$\min_{x \in \bar{\Omega}_x} \{b_{11}(x) + b_{12}(x), b_{21}(x) + b_{22}(x)\} \geq \beta > 0. \quad (4.1.3)$$

It will be assumed that the convection coefficient A is sufficiently smooth on $\Omega_x^- \cup \Omega_x^+$, whereas the source term $\vec{f}(x, t)$ is sufficiently smooth on $Q^- \cup Q^+$ and the reaction coefficient B is a sufficiently smooth function on $\bar{\Omega}_x$.

The exact solution $\vec{u} = (u_1, u_2)^T$ satisfies the following interface conditions

$$[u_l] = 0, \quad \left[\frac{\partial u_l}{\partial x} \right] = 0, \quad \text{at } x = \xi, \quad l = 1, 2. \quad (4.1.4)$$

We define the jump of the solution components u_l , denoted by $[u_l]$, across the point of discontinuity $x = \xi$ by

$$[u_l](\xi, t) = u_l(\xi^+, t) - u_l(\xi^-, t), \quad \text{where } u_l(\xi^\pm, t) = \lim_{x \rightarrow \xi^\pm 0} u_l(x, t).$$

The singular perturbation parameters satisfy $0 < \varepsilon_1 \leq \varepsilon_2 \ll 1$. Due to the presence of discontinuity in the convection coefficient $A(x)$ and the source term $\vec{f}(x, t)$, the exact solution $\vec{u}(x, t)$ of the problem (4.1.1)-(4.1.4) possesses overlapping interior layers in the neighborhood of the point $x = \xi$. In fact, the nature of the interior layer depends on the sign of the convection coefficient $A(x)$ on either side of the line of discontinuity.

We assume that the data of the model problem \vec{g}_0 , \vec{g}_1 and \vec{g}_2 are sufficiently smooth functions and also satisfy the following compatibility conditions

$$\begin{cases} \vec{g}_0(0) = \vec{g}_1(0), \quad \vec{g}_0(1) = \vec{g}_2(0), \\ \frac{\partial \vec{g}_1(0)}{\partial t} = \varepsilon \frac{\partial^2 \vec{g}_0(0)}{\partial x^2} - A(0) \frac{\partial \vec{g}_0(0)}{\partial x} - B(0) \vec{g}_0(0) + \vec{f}(0, 0), \\ \frac{\partial \vec{g}_2(0)}{\partial t} = \varepsilon \frac{\partial^2 \vec{g}_0(1)}{\partial x^2} - A(1) \frac{\partial \vec{g}_0(1)}{\partial x} - B(1) \vec{g}_0(1) + \vec{f}(1, 0). \end{cases} \quad (4.1.5)$$

The outline of this chapter is as follows: In Section 4.2, we discuss the analytical behavior of the continuous problem and introduce decomposition of the exact solution to obtain a priori bounds for the solution and its derivatives. We describe the piecewise-uniform Shishkin mesh and also introduces the implicit upwind finite difference scheme in Section 4.3. Later, we establish the error analysis. In Section 4.4, some numerical results are shown, which corroborate in practice the order of uniform convergence. Finally in Section 4.5, we summarize the main conclusions.

4.2 The Continuous Problem

This section provides the analytical behavior of the exact solution \vec{u} of the model problem (4.1.1). The differential operator of continuous problem (4.1.1) satisfies the following maximum principle.

Lemma 4.2.1. (Maximum Principle). *Suppose that a vector-valued function $\vec{\psi}$ satisfies $\vec{\psi}(x, t) \geq \vec{0}$ on ∂Q . Let $L_{\varepsilon}\vec{\psi} \geq \vec{0}$ for all $(x, t) \in Q^- \cup Q^+$ and $[\vec{\psi}_x](\xi, t) \leq \vec{0}$, $t > 0$ then $\vec{\psi}(x, t) \geq \vec{0}$, for all $(x, t) \in \bar{Q}$.*

Proof. By following the methodology from [89, Theorem 2.2], one can prove the maximum principle result. ■

An immediate consequence of the maximum principle is the following stability result, which establishes the uniqueness of the exact solution.

Lemma 4.2.2. *Let $\vec{u}(x, t)$ be the solution of (4.1.1), then*

$$\|\vec{u}\|_{\infty} \leq \|\vec{u}\|_{\infty, \partial Q} + \frac{1}{\vartheta} \|L_{\varepsilon}\vec{u}\|_{\infty},$$

where $\vartheta = \min \left\{ \frac{\alpha_1}{\xi}, \frac{\alpha_2}{1-\xi} \right\}$.

Proof. Define the barrier functions $\vec{\Phi}^{\pm}(x, t) = (\Phi_1^{\pm}, \Phi_2^{\pm})^T(x, t)$ as

$$\Phi_1^{\pm}(x, t) = \Phi_2^{\pm}(x, t) = \begin{cases} \|\vec{u}\|_{\infty, \partial Q} + \frac{x}{\vartheta\xi} \|L_{\varepsilon}\vec{u}\|_{\infty} \pm \vec{u}(x, t), & x \leq \xi, t \in [0, T] \\ \|\vec{u}\|_{\infty, \partial Q} + \frac{(1-x)}{\vartheta(1-\xi)} \|L_{\varepsilon}\vec{u}\|_{\infty} \pm \vec{u}(x, t), & x > \xi, t \in [0, T]. \end{cases}$$

By applying the maximum principle (Lemma 4.2.1) to the function $\vec{\Phi}^{\pm}(x, t)$ over the domain \bar{Q} , we can obtain the required result. ■

4.2.1 Bounds on the solution and its derivatives

In this subsection, we discuss the analytical aspect of the exact solution \bar{u} of model problem (4.1.1). Later, we study about the decomposition of exact solution and also discuss their derivative bounds.

We will obtain the bounds of the partial derivatives of the exact solution \bar{u} on the subdomains Q^- and Q^+ separately. First consider the subdomain \bar{Q}^+ and introduce a new function \bar{u}^* on the domain \bar{Q}^{+*} which is a sufficiently large neighborhood of \bar{Q}^+ beyond the point of discontinuity $x = \xi$ so that $\bar{Q}^+ \subset \bar{Q}^{+*}$. We define an extended domain Q^{+*} as $Q^{+*} = \Omega_x^{+*} \times (0, T]$, $\Omega_x^{+*} = (\xi, 1 + \kappa)$, $\kappa \ll 1$ and the extended function \bar{u}^* as solution of

$$\begin{cases} L_{\varepsilon}^* \bar{u}^* = \vec{f}^*, & \text{in } Q^{+*}, \\ \bar{u}^*(x, 0) = \vec{g}_0^*(x), & \text{on } \Gamma_b^{+*} = \{(x, 0) : x \in \Omega_x^{+*}\}, \\ \bar{u}^*(\xi, t) = \vec{g}_1^*(t), & \text{on } \Gamma_l^{+*} = \{(\xi, t) : t \in [0, T]\}, \\ \bar{u}^*(1, t) = \vec{g}_1^*(t), & \text{on } \Gamma_r^{+*} = \{(1, t) : t \in [0, T]\}, \end{cases} \quad (4.2.1)$$

with

$$L_{\varepsilon}^* \bar{u}^* \equiv (L_{\varepsilon_1}^*, L_{\varepsilon_2}^*)^T \equiv \frac{\partial \bar{u}^*}{\partial t} - \mathcal{E} \frac{\partial^2}{\partial x^2} + A^*(x) \frac{\partial}{\partial x} + B^*(x).$$

Here the coefficients A^* , B^* and source term \vec{f}^* with the initial and boundary conditions \vec{g}_0^* , \vec{g}_1^* and \vec{g}_2^* are the smooth extension of associated functions from the domain $\bar{\Omega}_x^+$ to $\bar{\Omega}_x^{+*}$ and \bar{Q}^+ to \bar{Q}^{+*} respectively. We assume that the extended initial and boundary conditions, *i.e.* \vec{g}_0^* , \vec{g}_1^* and \vec{g}_2^* with source term \vec{f}^* satisfy similar compatibility conditions as given in (4.1.5).

By following the technique from proof of Theorem 2.2.4, for $k_0 = 0, 1, 2$, we can obtain that

$$\left| \frac{\partial^{k+k_0} u_1^*}{\partial x^k \partial t^{k_0}}(x, t) \right| \leq \begin{cases} C, & \text{for } k = 0, (x, t) \in Q^{+*}, \\ C(1 + \varepsilon_1^{-1} B_{\varepsilon_1}^+(x)), & \text{for } k = 1, (x, t) \in Q^{+*}, \\ C(1 + \varepsilon_1^{1-k} (\varepsilon_1^{-1} B_{\varepsilon_1}^+(x) + \varepsilon_2^{-1} B_{\varepsilon_2}^+(x))), & \text{for } k = 2, 3, (x, t) \in Q^{+*}, \end{cases}$$

and

$$\left| \frac{\partial^{k+k_0} u_2^*}{\partial x^k \partial t^{k_0}}(x, t) \right| \leq \begin{cases} C, & \text{for } k = 0, (x, t) \in Q^{+*}, \\ C(1 + \varepsilon_2^{-1} B_{\varepsilon_2}^+(x)), & \text{for } k = 1, (x, t) \in Q^{+*}, \\ C(1 + \varepsilon_2^{1-k} (\varepsilon_1^{-1} B_{\varepsilon_1}^+(x) + \varepsilon_2^{-1} B_{\varepsilon_2}^+(x))), & \text{for } k = 2, 3, (x, t) \in Q^{+*}. \end{cases}$$

Similar methodology can be extended to obtain required derivative bounds of \bar{u}^* in Q^{-*} .

By using derivative bounds of the extended function \vec{u}^* , the exact solution \vec{u} of the model problem (4.1.1) will satisfy the following derivative bounds.

Lemma 4.2.3. *For all non-negative integers k, k_0 such that $0 \leq k \leq 3$ and $0 \leq k_0 \leq 2$, the exact solution \vec{u} satisfies estimate, for $l = 1, 2$, as follows:*

$$\left| \frac{\partial^{k+k_0} u_l}{\partial x^k \partial t^{k_0}}(x, t) \right| \leq \begin{cases} C, & \text{for } k = 0, (x, t) \in Q^-, \\ C(1 + \varepsilon_l^{-1} B_{\varepsilon_l}^-(x)), & \text{for } k = 1, (x, t) \in Q^-, \\ (1 + \varepsilon_l^{1-k} (\varepsilon_1^{-1} B_{\varepsilon_1}^-(x) + \varepsilon_2^{-1} B_{\varepsilon_2}^-(x))), & \text{for } k = 2, 3, (x, t) \in Q^-, \end{cases}$$

$$\left| \frac{\partial^{k+k_0} u_l}{\partial x^k \partial t^{k_0}}(x, t) \right| \leq \begin{cases} C, & \text{for } k = 0, (x, t) \in Q^+, \\ C(1 + \varepsilon_l^{-1} B_{\varepsilon_l}^+(x)), & \text{for } k = 1 (x, t) \in Q^+, \\ (1 + \varepsilon_l^{1-k} (\varepsilon_1^{-1} B_{\varepsilon_1}^+(x) + \varepsilon_2^{-1} B_{\varepsilon_2}^+(x))), & \text{for } k = 2, 3, (x, t) \in Q^+, \end{cases}$$

To gather some understanding of the qualitative behavior of the solution $\vec{u}(x, t)$ of (4.1.1), we consider a numerical example.

Example 4.2.4. *Consider the model problem (4.1.1) with zero initial, boundary data and values of A, B, \vec{f} are given by*

$$a_1(x) = \begin{cases} 1 + x, & x \in (0, \frac{1}{2}) \\ -(2 + x), & x \in (\frac{1}{2}, 1), \end{cases} \quad a_2(x) = \begin{cases} 1 + x^2, & x \in (0, \frac{1}{2}) \\ -(2 + x^2), & x \in (\frac{1}{2}, 1), \end{cases}$$

$$B(x) = \begin{pmatrix} 4 + x & -2 + x \\ -2 - x & 4 + 2x \end{pmatrix},$$

$$f_1(x, t) = \begin{cases} -2(1 + x^2 t^2), & \text{for } x < \frac{1}{2}, \\ 3(1 + x t^2), & \text{for } x > \frac{1}{2}, \end{cases} \quad f_2(x, t) = \begin{cases} -(1 + x^2 t^2), & \text{for } x < \frac{1}{2}, \\ (1 + x^3 t), & \text{for } x > \frac{1}{2}, \end{cases}$$

with $\varepsilon_1 = 2^{-8}$, $\varepsilon_2 = 2^{-6}$.

The interior layer behavior at $x = \xi$ can be seen in Fig. 4.1. Also, Fig. 4.1 confirms the overlapping interior layers phenomena in the solution of the model problem (4.1.1).

Next, we discuss the sharper bound of the exact solution through decomposition of exact solution into the smooth and layer component. To derive the derivative bounds of the smooth and layer component, we follow the technique from [45]. Consider $x^* = 2\varepsilon_1 \ln(1/\varepsilon_1)/\alpha$. We define the extended functions $\vec{v}^* = (v_1^*, v_2^*)^T$, $\vec{\hat{v}}^* = (\hat{v}_1^*, \hat{v}_2^*)^T$ in the

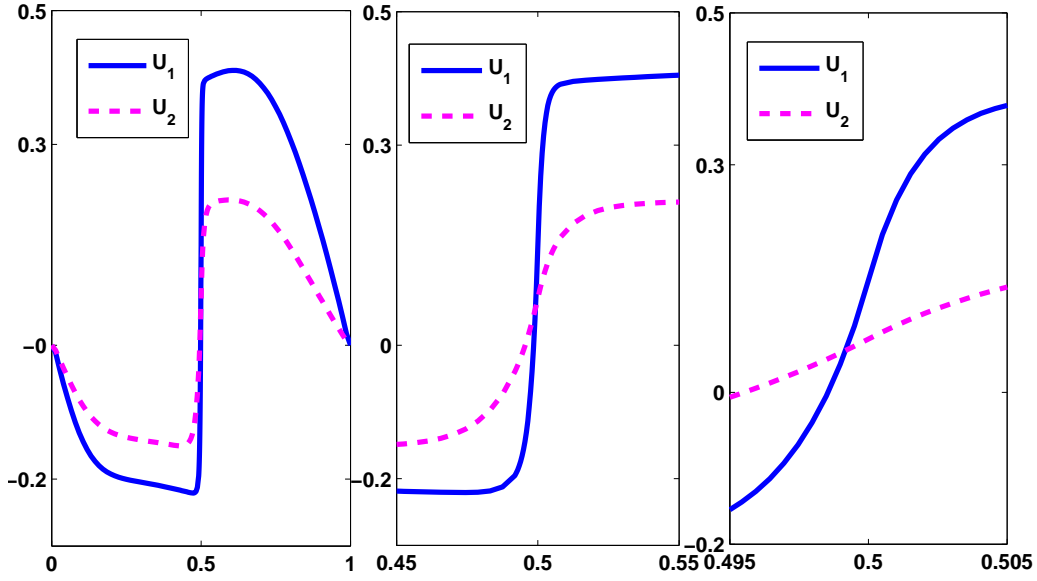


Figure 4.1: Numerical solutions for Example 4.2.4 for $N = 128$ at time $t = 1$.

domains $[\xi, 1 + \kappa] \times [0, T]$ and $[-\kappa, \xi] \times [0, T]$, respectively, for $l = 1, 2$, as follows:

$$v_l^*(x, t) = \begin{cases} \sum_{k=0}^3 \frac{(x - (\xi + x^*))^k}{k!} \frac{\partial^{k+k_0} u_l}{\partial x^k \partial t^{k_0}}(\xi + x^*, t), & \xi \leq x \leq \xi + x^*, \\ u_l^*(x, t), & \xi + x^* \leq x \leq 1 + \kappa, \end{cases} \quad (4.2.2)$$

and

$$\widehat{v}_l^*(x, t) = \begin{cases} u_l^*(x, t), & -\kappa \leq x \leq \xi - x^*, \\ \sum_{k=0}^3 \frac{(x - (\xi - x^*))^k}{k!} \frac{\partial^{k+k_0} u_l}{\partial x^k \partial t^{k_0}}(\xi - x^*, t), & \xi - x^* \leq x \leq \xi. \end{cases} \quad (4.2.3)$$

where $k_0 = 0, 1, 2$. Next, we discuss the derivative bounds for \vec{v}^* in the domain $[\xi, 1 + \kappa] \times [0, T]$. Analogously, one can obtain bounds for derivative of \vec{v}^* .

By using Lemma 4.2.3, we obtain that

$$\left| \frac{\partial^{k+k_0} u_l}{\partial x^k \partial t^{k_0}}(\xi + x^*, t) \right| \leq C (1 + \varepsilon_1^{-k} B_{\varepsilon_1}^+(\xi + x^*)) \leq C(1 + \varepsilon_1^{2-k}), \quad 0 \leq k \leq 1.$$

Assume that $x \in [\xi, \xi + x^*]$, then, by using (4.2.2), one can acquire that

$$\left| \frac{\partial^{k+k_0} v_1^*}{\partial x^k \partial t^{k_0}}(x, t) \right| \leq C (1 + \varepsilon_1^{2-k}), \quad 0 \leq k \leq 1, \quad 0 \leq k_0 \leq 2. \quad (4.2.4)$$

In a similar way, one can estimate derivative bounds for $k = 2, 3$. Next, we consider the derivative bounds for component v_2^* in the domain $[\xi, \xi + x^*]$. For $k = 0, 1$, we get

$$\left| \frac{\partial^k u_2}{\partial x^k}(x^*, t) \right| \leq C (1 + \varepsilon_2^{-k} B_{\varepsilon_2}^+(\xi + x^*)) \leq C(1 + \varepsilon_2^{2-k}).$$

By applying the previous technique, one can obtain that

$$\left| \frac{\partial^{k+k_0} v_2^*}{\partial x^k \partial t^{k_0}}(x, t) \right| \leq C(1 + \varepsilon_2^{2-k}), \quad 0 \leq k \leq 1. \quad (4.2.5)$$

A simple calculation leads to deduce the required estimate for $k = 2, 3$. Next, we consider $x \in [\xi + x^*, 1 + \kappa]$, it follows that

$$\left| \frac{\partial^{k+k_0} v_1^*}{\partial x^k \partial t^{k_0}}(x, t) \right| = \left| \frac{\partial^{k+k_0} u_1^*}{\partial x^k \partial t^{k_0}}(x, t) \right| \leq C (1 + \varepsilon_1^{-k} B_{\varepsilon_1}(\xi + x^*)) \leq C(1 + \varepsilon_1^{2-k}), \quad 0 \leq k \leq 1.$$

In a similar way, one can obtain the higher order derivative bounds for the component v_1^* . Analogously, one can obtain derivative bounds for the component v_2^* . By using the previous methodology, we can have the same derivative bound estimates for \tilde{v}^* in the domain $[-\kappa, \xi] \times [0, T]$. Therefore, for $l = 1, 2$, both functions \tilde{v}^* and \hat{v}^* satisfy the following estimates:

$$\begin{cases} \left| \frac{\partial^{k+k_0} v_l^*}{\partial x^k \partial t^{k_0}}(x, t) \right| \leq C(1 + \varepsilon_l^{2-k}), & 0 \leq k \leq 3, \quad 0 \leq k_0 \leq 2, \\ \left| \frac{\partial^{k+k_0} \hat{v}_l^*}{\partial x^k \partial t^{k_0}}(x, t) \right| \leq C(1 + \varepsilon_l^{2-k}), & 0 \leq k \leq 3, \quad 0 \leq k_0 \leq 2. \end{cases} \quad (4.2.6)$$

Now, we define the smooth component \vec{v} as follows

$$\vec{v}(x, t) = \begin{cases} \tilde{v}^*(x, t), & \text{for } (x, t) \in Q^-, \\ \hat{v}^*(x, t), & \text{for } (x, t) \in Q^+. \end{cases} \quad (4.2.7)$$

and the layer component \vec{w} is defined by

$$\vec{w}(x, t) = \vec{u}(x, t) - \vec{v}(x, t), \quad (x, t) \in Q^- \cup Q^+. \quad (4.2.8)$$

Lemma 4.2.5. *For all non-negative integers k, k_0 such that $0 \leq k \leq 3, 0 \leq k_0 \leq 2$ and $l = 1, 2$, the smooth component \vec{v} and layer component \vec{w} satisfy the following estimates*

$$\left| \frac{\partial^{k+k_0} v_l}{\partial x^k \partial t^{k_0}}(x, t) \right| \leq C(1 + \varepsilon_l^{2-k}), \quad 0 \leq k \leq 3, \quad (x, t) \in Q^- \cup Q^+,$$

$$\left| \frac{\partial^{k+k_0} w_1}{\partial x^k \partial t^{k_0}}(x, t) \right| \leq \begin{cases} C, & \text{for } k = 0, \quad (x, t) \in Q^-, \\ C (\varepsilon_1^{-k} B_{\varepsilon_1}^-(x) + \varepsilon_2^{-k} B_{\varepsilon_2}^-(x)), & \text{for } k = 1, 2, 3, \quad (x, t) \in Q^-, \end{cases}$$

$$\left| \frac{\partial^{k+k_0} w_1}{\partial x^k \partial t^{k_0}}(x, t) \right| \leq \begin{cases} C, & \text{for } k = 0, (x, t) \in Q^+, \\ C(\varepsilon_1^{-k} B_{\varepsilon_1}^+(x) + \varepsilon_2^{-k} B_{\varepsilon_2}^+(x)), & \text{for } k = 1, 2, 3, (x, t) \in Q^+, \end{cases}$$

$$\left| \frac{\partial^{k+k_0} w_2}{\partial x^k \partial t^{k_0}}(x, t) \right| \leq \begin{cases} C, & \text{for } k = 0, (x, t) \in Q^-, \\ C\varepsilon_2^{-k} B_{\varepsilon_2}^-(x), & \text{for } k = 1, 2, (x, t) \in Q^-, \\ C\varepsilon_2^{-1}(\varepsilon_1^{-2} B_{\varepsilon_1}^-(x) + \varepsilon_2^{-2} B_{\varepsilon_2}^-(x)), & \text{for } k = 3, (x, t) \in Q^-, \end{cases}$$

$$\left| \frac{\partial^{k+k_0} w_2}{\partial x^k \partial t^{k_0}}(x, t) \right| \leq \begin{cases} C, & \text{for } k = 0, (x, t) \in Q^+, \\ C\varepsilon_2^{-k} B_{\varepsilon_2}^+(x), & \text{for } k = 1, 2, (x, t) \in Q^+, \\ C\varepsilon_2^{-1}(\varepsilon_1^{-2} B_{\varepsilon_1}^+(x) + \varepsilon_2^{-2} B_{\varepsilon_2}^+(x)), & \text{for } k = 3, (x, t) \in Q^+. \end{cases}$$

Proof. By using (4.2.6) and definition of the smooth component (4.2.7), we get

$$\left| \frac{\partial^{k+k_0} v_l}{\partial x^k \partial t^{k_0}}(x, t) \right| \leq C(1 + \varepsilon_l^{2-k}), \quad 0 \leq k \leq 3, \quad 0 \leq k_0 \leq 2 \text{ and } l = 1, 2,$$

where $(x, t) \in Q^- \cup Q^+$. By employing decomposition (4.2.8) and using the technique from [10, Lemma 4], one can obtain the desired results for the layer component \vec{w} . This completes the proof. \blacksquare

4.3 Domain Discretization

Consider the domain $\bar{Q} = \bar{\Omega}_x \times [0, T]$ and let $N \geq 16$ be an even positive integer. Here, we construct a rectangular mesh $\bar{Q}^{N,M} = \bar{\Omega}_x^N \times \bar{\Upsilon}^M$, which is a combination of the piecewise-uniform Shishkin mesh condensed around the overlapping interior layers for the spatial variable and a uniform mesh for the temporal variable. On the time domain $[0, T]$, we introduce uniform mesh such that

$$\bar{\Upsilon}^M = \{t_n = n\Delta t, n = 0, \dots, M, \Delta t = T/M\}.$$

Then, we define the transition parameters $\tau_{\varepsilon_1}^-, \tau_{\varepsilon_2}^-, \tau_{\varepsilon_1}^+$ and $\tau_{\varepsilon_2}^+$ as follows

$$\tau_{\varepsilon_2}^- = \min \left\{ \frac{\xi}{2}, \frac{2\varepsilon_2}{\alpha} \ln N \right\}, \quad \tau_{\varepsilon_1}^- = \min \left\{ \frac{\xi}{4}, \frac{\tau_{\varepsilon_2}^-}{2}, \frac{2\varepsilon_1}{\alpha} \ln N \right\},$$

$$\tau_{\varepsilon_2}^+ = \min \left\{ \frac{1-\xi}{2}, \frac{2\varepsilon_2}{\alpha} \ln N \right\}, \quad \tau_{\varepsilon_1}^+ = \min \left\{ \frac{1-\xi}{4}, \frac{\tau_{\varepsilon_2}^+}{2}, \frac{2\varepsilon_1}{\alpha} \ln N \right\}.$$

A piecewise-uniform mesh $\bar{\Omega}_x^N$ is constructed by dividing the spatial domain $[0, 1]$ into six subintervals as

$$[0, 1] = [0, \xi - \tau_{\varepsilon_2}^-] \cup [\xi - \tau_{\varepsilon_2}^-, \xi - \tau_{\varepsilon_1}^-] \cup [\xi - \tau_{\varepsilon_1}^-, \xi] \cup [\xi, \xi + \tau_{\varepsilon_1}^+] \cup [\xi + \tau_{\varepsilon_1}^+, \xi + \tau_{\varepsilon_2}^+] \cup [\xi + \tau_{\varepsilon_2}^+, 1].$$

Then subdivide $[0, \xi - \tau_{\varepsilon_2}^-]$ and $[\xi + \tau_{\varepsilon_2}^+, 1]$ into $N/4$ mesh-intervals, and subdivide each of the other four subintervals into $N/8$ mesh-intervals. The proposed Shishkin mesh can be seen in the figure 4.2.

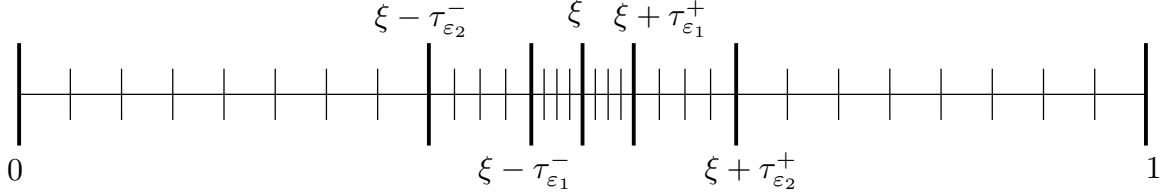


Figure 4.2: Piecewise-uniform Shishkin mesh $\bar{\Omega}_x^N$ for $N = 32$.

Assume that $\tau_{\varepsilon_1}^- = \tau_{\varepsilon_1}^+ = 2\varepsilon_1 \ln N/\alpha$ and $\tau_{\varepsilon_2}^- = \tau_{\varepsilon_2}^+ = 2\varepsilon_2 \ln N/\alpha$, as otherwise N^{-1} is exponentially small relatively to ε_l , $l = 1, 2$ (and in this case the method can be analyzed in the classical way). Also, when $\tau_{\varepsilon_1}^- = \tau_{\varepsilon_2}^-/2$, $\tau_{\varepsilon_1}^+ = \tau_{\varepsilon_2}^+/2$, therefore $\varepsilon_2 = O(\varepsilon_1)$, and the result can be easily obtained.

4.3.1 Numerical scheme

For the discretization of the continuous problem (4.1.1), the following implicit upwind finite difference scheme is used on the mesh $\bar{Q}^{N,M}$:

$$\left\{ \begin{array}{l} \vec{U}_i^0 = \vec{g}_0(x_i), \quad \text{for } i = 0, \dots, N \\ \left\{ \begin{array}{l} L_{\varepsilon}^{N,M} \vec{U}_i^{n+1} \equiv (D_t^- - \mathcal{E} \delta_x^2 + A_i \hat{D}_x^* + B_i) \vec{U}_i^{n+1} \\ \quad = \vec{f}_i^{n+1}, \quad \text{for } i = 1, \dots, N/2 - 1, N/2 + 1, \dots, N - 1, \\ D_x^+ \vec{U}_i^{n+1} - D_x^- \vec{U}_i^{n+1} = 0, \quad \text{for } i = N/2, \\ \vec{U}_0^{n+1} = \vec{g}_1(t_{n+1}), \quad \vec{U}_N^{n+1} = \vec{g}_2(t_{n+1}), \end{array} \right. \\ \text{for } n = 0, \dots, M - 1, \end{array} \right. \quad (4.3.1)$$

where difference operator \hat{D}_x^* is defined as

$$\hat{D}_x^* \vec{U}_i^n = \begin{cases} D_x^- \vec{U}_i^n, & i < N/2, \\ D_x^+ \vec{U}_i^n, & i > N/2. \end{cases}$$

The finite difference operator given in (4.3.1), satisfies the following discrete maximum principle result.

Lemma 4.3.1. (Discrete maximum principle) *Suppose that a mesh function \vec{Z}_i^{n+1} satisfies $\vec{Z} \geq \vec{0}$ on $\partial Q^{N,M}$. Then, $L_{\varepsilon}^{N,M} \vec{Z}_i^{n+1} \geq \vec{0}$, for all $(x_i, t_n) \in Q^{N,M}$ and $D_x^+ \vec{Z}_{N/2}^{n+1} - D_x^- \vec{Z}_{N/2}^{n+1} \leq \vec{0}$, for $n = 0, \dots, M - 1$, implies that $\vec{Z}_i^{n+1} \geq \vec{0}$ for each point of $Q^{N,M}$.*

Proof. By following the approach as discussed in Lemma 2.4.1, one can prove the maximum principle. ■

An immediate consequence of this discrete maximum principle and Lemma 4.2.2, the following stability result holds.

Corollary 4.3.2. *If \vec{U}_i^{n+1} is the solution of discrete problem (4.3.1), then*

$$\|\vec{U}\|_\infty \leq \|\vec{U}\|_{\infty, \partial Q^{N,M}} + \frac{1}{\vartheta} \|L_\varepsilon^{N,M} \vec{U}\|_\infty,$$

where $\vartheta = \min \left\{ \frac{\alpha_1}{\xi}, \frac{\alpha_2}{1-\xi} \right\}$.

This concludes that the discrete scheme (4.3.1) is stable.

4.3.2 Error analysis

This subsection deals with the error analysis of the proposed numerical scheme (4.3.1).

We split the error term as follows:

$$\begin{aligned} L_\varepsilon^{N,M}(\vec{U}_i^{n+1} - \vec{u}(x_i, t_{n+1})) &= (L_\varepsilon - L_\varepsilon^{N,M})\vec{u}(x_i, t_{n+1}) \\ &= (L_\varepsilon - L_\varepsilon^{N,M})\vec{v}(x_i, t_{n+1}) + (L_\varepsilon - L_\varepsilon^{N,M})\vec{w}(x_i, t_{n+1}). \end{aligned} \quad (4.3.2)$$

The following results will be used in the proof of truncation error estimate.

Lemma 4.3.3. *Let $\vec{g}(x) = (g_1(x), g_2(x))^T$ be a smooth function defined on $[0, 1]$. Then, for $l = 1, 2$, the following estimates for the truncation error hold true*

$$\begin{aligned} |(L_{\varepsilon_l} - L_{\varepsilon_l}^{N,M})\vec{g}_i| &\leq C\varepsilon_l \int_{x_{i-1}}^{x_{i+1}} |g_l'''(s)| ds + C \int_{x_{i-1}}^{x_i} |g_l''(s)| ds, \quad \text{for } 0 < i < N/2, \\ |(L_{\varepsilon_l} - L_{\varepsilon_l}^{N,M})\vec{g}_i| &\leq C\varepsilon_l \int_{x_{i-1}}^{x_{i+1}} |g_l'''(s)| ds + C \int_{x_i}^{x_{i+1}} |g_l''(s)| ds, \quad \text{for } N/2 < i < N, \end{aligned}$$

where $\vec{g}_i = \vec{g}(x_i)$.

Proof. By following the methodology of [40, Lemma 3.3], one can prove the above estimates. ■

Now, we will discuss the error estimate for the smooth and layer components, separately.

Lemma 4.3.4. *At each mesh point $(x_i, t_n) \in Q^{N,M}$, the error associated to the smooth components satisfy the following estimates*

$$\left| (L_\varepsilon - L_\varepsilon^{N,M})\vec{v}(x_i, t_{n+1}) \right| \leq C(N^{-1} + \Delta t), \quad (x_i, t_{n+1}) \in (Q^{N,M} \cap Q^-) \cup (Q^{N,M} \cap Q^+).$$

Proof. Note that

$$\begin{aligned} & |(L_{\varepsilon_1} - L_{\varepsilon_1}^{N,M})\vec{v}(x_i, t_{n+1})| \\ & \leq \begin{cases} C \left(\frac{\varepsilon_1}{3}(h_i + h_{i+1}) \left\| \frac{\partial^3 v_1}{\partial x^3} \right\|_{\infty} + \frac{h_i}{2} \left\| \frac{\partial^2 v_1}{\partial x^2} \right\|_{\infty} + \frac{\Delta t}{2} \left\| \frac{\partial^2 v_1}{\partial t^2} \right\|_{\infty} \right), \\ \hspace{15em} \text{for } 1 \leq i \leq \frac{N}{2} - 1, \\ C \left(\frac{\varepsilon_1}{3}(h_i + h_{i+1}) \left\| \frac{\partial^3 v_1}{\partial x^3} \right\|_{\infty} + \frac{h_{i+1}}{2} \left\| \frac{\partial^2 v_1}{\partial x^2} \right\|_{\infty} + \frac{\Delta t}{2} \left\| \frac{\partial^2 v_1}{\partial t^2} \right\|_{\infty} \right), \\ \hspace{15em} \text{for } \frac{N}{2} + 1 \leq i \leq N - 1. \end{cases} \end{aligned}$$

Then, by using $h_i \leq CN^{-1}$ and the derivative bounds of \vec{v} given in Lemma 4.2.5, we get

$$|(L_{\varepsilon_1} - L_{\varepsilon_1}^{N,M})\vec{v}(x_i, t_{n+1})| \leq C(N^{-1} + \Delta t), \text{ for } \left\{ 1 \leq i \leq \frac{N}{2} - 1 \right\} \cup \left\{ \frac{N}{2} + 1 \leq i \leq N - 1 \right\}. \quad (4.3.3)$$

In a similar manner, one can obtain that

$$|(L_{\varepsilon_2} - L_{\varepsilon_2}^{N,M})\vec{v}(x_i, t_{n+1})| \leq C(N^{-1} + \Delta t), \text{ for } \left\{ 1 \leq i \leq \frac{N}{2} - 1 \right\} \cup \left\{ \frac{N}{2} + 1 \leq i \leq N - 1 \right\}, \quad (4.3.4)$$

which leads to the desired result. \blacksquare

Lemma 4.3.5. *The error associated to the layer components satisfy the following estimate:*

$$\left| (L_{\bar{\varepsilon}} - L_{\bar{\varepsilon}}^{N,M})\vec{w}(x_i, t_{n+1}) \right| \leq \begin{cases} \bar{C}(N^{-1} + \Delta t), & \text{for } x_i \in [0, \xi - \tau_{\varepsilon_2}^-] \cup [\xi - \tau_{\varepsilon_2}^+, 1] \\ \bar{C}(\varepsilon_2^{-1}N^{-1} \ln N + \Delta t), \\ \hspace{10em} \text{for } x_i \in (\xi - \tau_{\varepsilon_2}^-, \xi - \tau_{\varepsilon_1}^-] \cup [\xi + \tau_{\varepsilon_1}^+, \xi + \tau_{\varepsilon_2}^+), \\ \bar{C}((\varepsilon_1^{-1} + \varepsilon_2^{-1})N^{-1} \ln N + \Delta t), \\ \hspace{10em} \text{for } x_i \in [\xi - \tau_{\varepsilon_1}^-, \xi) \cup (\xi, \xi - \tau_{\varepsilon_1}^+]. \end{cases}$$

Proof. We split the proof of the error estimate into two different cases depending on the location of mesh points.

Case 1: (Interior layer region) First consider the subinterval $(\xi - \tau_{\varepsilon_2}^-, \xi - \tau_{\varepsilon_1}^-]$. By using the inequality

$$\varepsilon_1^{-k} \exp\left(-\frac{(\xi - \tau)\alpha}{\varepsilon_1}\right) \leq C\varepsilon_2^{-k} \exp\left(-\frac{(\xi - \tau)\alpha}{\varepsilon_2}\right), \quad \text{for } \tau < \xi - \tau_{\varepsilon_1}^-, \quad k = 1, 2, \dots,$$

and Lemma 4.2.5 with Lemma 4.3.3, we obtain

$$\begin{aligned}
|(L_{\varepsilon_1} - L_{\varepsilon_1}^{N,M})\vec{w}(x_i, t_{n+1})| &\leq C\Delta t + C \left(\varepsilon_1 \int_{x_{i-1}}^{x_{i+1}} \left| \frac{\partial^3 w_1}{\partial x^3}(x, t_{n+1}) \right| dx \right. \\
&\quad \left. + \int_{x_{i-1}}^{x_i} \left| \frac{\partial^2 w_1}{\partial x^2}(x, t_{n+1}) \right| dx \right) \\
&\leq C\Delta t + C (N^{-1} \ln N (\varepsilon_1^{-1} B_{\varepsilon_1}^-(x_i) + \varepsilon_2^{-1} B_{\varepsilon_2}^-(x_i))) \\
&\leq C (\Delta t + \varepsilon_2^{-1} N^{-1} \ln N B_{\varepsilon_2}^-(x_i)). \tag{4.3.5}
\end{aligned}$$

In a similar manner, one can obtain that

$$\begin{aligned}
|(L_{\varepsilon_2} - L_{\varepsilon_2}^{N,M})\vec{w}(x_i, t_{n+1})| &\leq C\Delta t + C \left(\varepsilon_2 \int_{x_{i-1}}^{x_{i+1}} \left| \frac{\partial^3 w_2}{\partial x^3}(x, t_{n+1}) \right| dx \right. \\
&\quad \left. + \int_{x_{i-1}}^{x_i} \left| \frac{\partial^2 w_2}{\partial x^2}(x, t_{n+1}) \right| dx \right) \\
&\leq C (\Delta t + \varepsilon_2^{-1} N^{-1} \ln N B_{\varepsilon_2}^-(x_i)). \tag{4.3.6}
\end{aligned}$$

Next, we consider the subinterval $[\xi - \tau_{\varepsilon_1}^-, \xi)$. By applying the previous argument, for $l = 1, 2$, we get

$$\begin{aligned}
|(L_{\varepsilon_l} - L_{\varepsilon_l}^{N,M})\vec{w}(x_i, t_{n+1})| &\leq C\Delta t + C (N^{-1} \ln N (\varepsilon_1^{-1} B_{\varepsilon_1}^-(x_i) + \varepsilon_2^{-1} B_{\varepsilon_2}^-(x_i))) \\
&\leq C (\Delta t + N^{-1} \ln N (\varepsilon_1^{-1} B_{\varepsilon_1}^-(x_i) + \varepsilon_2^{-1} B_{\varepsilon_2}^-(x_i))). \tag{4.3.7}
\end{aligned}$$

In a similar way, for subinterval $(\xi, \xi + \tau_{\varepsilon_1}^+]$, one can obtain the following bound

$$|(L_{\varepsilon} - L_{\varepsilon}^{N,M})\vec{w}(x_i, t_{n+1})| \leq \vec{C} (\Delta t + N^{-1} \ln N (\varepsilon_1^{-1} B_{\varepsilon_1}^+(x_i) + \varepsilon_2^{-1} B_{\varepsilon_2}^+(x_i))). \tag{4.3.8}$$

Finally, we take the subinterval $[\xi + \tau_{\varepsilon_1}^+, \xi + \tau_{\varepsilon_2}^+)$. By applying the inequality

$$\varepsilon_1^{-k} \exp\left(-\frac{(\tau - \xi)\alpha}{\varepsilon_1}\right) \leq C\varepsilon_2^{-k} \exp\left(-\frac{(\tau - \xi)\alpha}{\varepsilon_2}\right), \quad \text{for } \tau > \xi + \tau_{\varepsilon_1}^+, \quad k = 1, 2, \dots,$$

and Lemma 4.2.5 with Lemma 4.3.3, we acquire

$$\begin{aligned}
|(L_{\varepsilon_l} - L_{\varepsilon_l}^{N,M})\vec{w}(x_i, t_{n+1})| &\leq C\Delta t + C (N^{-1} \ln N (\varepsilon_1^{-1} B_{\varepsilon_1}^+(x_i) + \varepsilon_2^{-1} B_{\varepsilon_2}^+(x_i))) \\
&\leq C (\Delta t + \varepsilon_2^{-1} N^{-1} \ln N B_{\varepsilon_2}^+(x_i)). \tag{4.3.9}
\end{aligned}$$

Case 2: (Outer layer region) For $1 \leq i \leq N/4$ and $3N/4 \leq i \leq N - 1$. From (4.2.8) and using the technique from **Case 1**, one can deduce that

$$|(L_{\varepsilon} - L_{\varepsilon}^{N,M})\vec{w}(x_i, t_{n+1})| \leq \vec{C}(N^{-1} + \Delta t), \quad \text{for } 1 \leq i \leq N/4 \text{ and } 3N/4 \leq i \leq N - 1. \tag{4.3.10}$$

By combining results (4.3.5)-(4.3.10), the desired estimates follow. \blacksquare

The main result of this chapter is discussed in the following theorem.

Theorem 4.3.6. Let $\vec{u}(x, t)$, \vec{U}_i^n be the solutions of the (4.1.1) and (4.3.1), respectively. Then, the error satisfy the following bound:

$$|\vec{U}_i^n - \vec{u}(x_i, t_n)| \leq \vec{C}(N^{-1}(\ln N)^2 + \Delta t),$$

where C is independent of $N, \Delta t$ and $\varepsilon_1, \varepsilon_2$.

Proof. Firstly, we consider the error estimate at the point of discontinuity $x_i = \xi$:

$$\begin{aligned} & \left| (D_x^+ - D_x^-) \left(\vec{U}_{N/2}^{n+1} - \vec{u}(\xi, t_{n+1}) \right) \right| \\ &= \left| (D_x^- - D_x^+) \vec{u}(x_{N/2}, t_{n+1}) + \left(\frac{\partial \vec{u}}{\partial x} \right) (\xi, t_{n+1}) \right| \quad (4.3.11) \\ &\leq \left| D_x^- \vec{u}(x_{N/2}, t_{n+1}) - \frac{\partial \vec{u}}{\partial x}(x_{N/2}, t_{n+1}) \right| + \left| D_x^+ \vec{u}(x_{N/2}, t_{n+1}) - \frac{\partial \vec{u}}{\partial x}(x_{N/2}, t_{n+1}) \right| \\ &\leq \begin{pmatrix} CN^{-1} + CN^{-1} (\tau_{\varepsilon_1}^+ \varepsilon_1^{-1} (\varepsilon_1^{-1} B_{\varepsilon_1}^+(x_i) + \varepsilon_2^{-1} B_{\varepsilon_2}^+(x_i))) \\ CN^{-1} + CN^{-1} (\tau_{\varepsilon_1}^+ \varepsilon_2^{-1} (\varepsilon_1^{-1} B_{\varepsilon_1}^+(x_i) + \varepsilon_2^{-1} B_{\varepsilon_2}^+(x_i))) \end{pmatrix} \\ &\quad + \begin{pmatrix} CN^{-1} (\tau_{\varepsilon_1}^- \varepsilon_1^{-1} (\varepsilon_1^{-1} B_{\varepsilon_1}^-(x_i) + \varepsilon_2^{-1} B_{\varepsilon_2}^-(x_i))) \\ CN^{-1} (\tau_{\varepsilon_1}^- \varepsilon_2^{-1} (\varepsilon_1^{-1} B_{\varepsilon_1}^-(x_i) + \varepsilon_2^{-1} B_{\varepsilon_2}^-(x_i))) \end{pmatrix}. \end{aligned}$$

Define the discrete barrier function $\vec{\chi}_B^\pm(x_i, t_{n+1}) = \vec{\Theta}(x_i, t_{n+1}) \pm (\vec{U}_i^{n+1} - \vec{u}(x_i, t_{n+1}))$, $\vec{\Theta} = (\Theta_1, \Theta_2)^T$, for $l = 1, 2$, as follows

$$\Theta_l(x_i, t_{n+1}) = C(N^{-1} + \Delta t) + C N^{-1} \ln N \begin{cases} \varepsilon_2^{-1}(x_i - (\xi - \tau_{\varepsilon_2}^-)), & x_i \in (\xi - \tau_{\varepsilon_2}^-, \xi - \tau_{\varepsilon_1}^-] \\ (\varepsilon_1^{-1} + \varepsilon_2^{-1})(x_i - (\xi - \tau_{\varepsilon_1}^-)), & x_i \in (\xi - \tau_{\varepsilon_1}^-, \xi] \\ (\varepsilon_1^{-1} + \varepsilon_2^{-1})(\xi + \tau_{\varepsilon_1}^+ - x_i), & x_i \in [\xi, \xi + \tau_{\varepsilon_1}^+) \\ \varepsilon_2^{-1}(\xi + \tau_{\varepsilon_2}^+ - x_i), & x_i \in [\xi + \tau_{\varepsilon_1}^+, \xi + \tau_{\varepsilon_2}^+) \\ 0, & \text{otherwise.} \end{cases}$$

Using the error estimate of the smooth and layer components given in Lemma 4.3.4 and Lemma 4.3.5 with (4.3.11), we can show that

$$\begin{cases} L_{\vec{\varepsilon}}^{N,M} \vec{\chi}_B^\pm(x_i, t_{n+1}) \geq \vec{0}, & \text{for } (x, t) \in (Q^{N,M} \cap Q^-) \cup (Q^{N,M} \cap Q^+), \\ (D_x^+ - D_x^-) \vec{\chi}_B^\pm(x_i, t_{n+1}) > \vec{0}, & \text{for } (x, t) \in \{\xi\} \times [0, T]. \end{cases} \quad (4.3.12)$$

Applying the discrete maximum principle (Lemma 4.3.1) to $\vec{\chi}_B^\pm(x_i, t_{n+1})$ on the domain $\overline{Q}^{N,M}$ and by using (4.3.12), we conclude that

$$|\vec{U}_i^{n+1} - \vec{u}(x_i, t_{n+1})| \leq \vec{C}(N^{-1}(\ln N)^2 + \Delta t),$$

This completes the proof. ■

4.4 Numerical Results

In this section, we present some numerical results to illustrate the accuracy of the proposed method and the theoretical analysis, we consider two numerical examples on the piecewise-uniform rectangular mesh $\bar{Q}^{N,M}$. For both the test problems, the errors and the corresponding order of convergence are presented in the form of tables and figures.

Example 4.4.1. Consider the following system of parabolic IBVP on $Q = (0, 1) \times (0, 1]$:

$$\begin{cases} \frac{\partial u_1}{\partial t} - \varepsilon_1 \frac{\partial^2 u_1}{\partial x^2} + a_1(x) \frac{\partial u_1}{\partial x} + 4u_1 - 2u_2 = f_1(x, t), \\ \frac{\partial u_2}{\partial t} - \varepsilon_2 \frac{\partial^2 u_2}{\partial x^2} + a_2(x) \frac{\partial u_2}{\partial x} - 2u_1 + 4u_2 = f_2(x, t), \\ u_1(x, 0) = 0, \quad u_2(x, 0) = 0, \\ u_1(0, t) = u_1(1, t) = 0, \quad u_2(0, t) = u_2(1, t) = 0, \quad t \in [0, 1], \end{cases}$$

where the convection coefficients are

$$a_1(x) = \begin{cases} 1, & 0 < x < \frac{1}{2}, \\ -2, & \frac{1}{2} < x < 1, \end{cases} \quad a_2(x) = \begin{cases} 2, & 0 < x < \frac{1}{2}, \\ -1, & \frac{1}{2} < x < 1, \end{cases}$$

and the source terms are given by

$$f_1(x, t) = \begin{cases} -2, & 0 < x < \frac{1}{2}, \\ 3, & \frac{1}{2} < x < 1, \end{cases} \quad f_2(x, t) = \begin{cases} -2, & 0 < x < \frac{1}{2}, \\ 2, & \frac{1}{2} < x < 1. \end{cases}$$

Example 4.4.2. Consider the following system of parabolic IBVP on $Q = (0, 1) \times (0, 1]$:

$$\begin{cases} \frac{\partial u_1}{\partial t} - \varepsilon_1 \frac{\partial^2 u_1}{\partial x^2} + a_1(x) \frac{\partial u_1}{\partial x} + (4+x)u_1 - (2-x)u_2 = f_1(x, t), \\ \frac{\partial u_2}{\partial t} - \varepsilon_2 \frac{\partial^2 u_2}{\partial x^2} + a_2(x) \frac{\partial u_2}{\partial x} - (2+x)u_1 + (4+2x)u_2 = f_2(x, t), \\ u_1(x, 0) = x(1-x), \quad u_2(x, 0) = x(1-x^2), \\ u_1(0, t) = u_1(1, t) = 0, \quad u_2(0, t) = u_2(1, t) = 0, \quad t \in [0, 1], \end{cases}$$

where the convection coefficients are given by

$$a_1(x) = \begin{cases} 1+x, & 0 < x < \frac{1}{2}, \\ -(2+x), & \frac{1}{2} < x < 1, \end{cases} \quad a_2(x) = \begin{cases} 1+x^2, & 0 < x < \frac{1}{2}, \\ -(2+x^2), & \frac{1}{2} < x < 1, \end{cases}$$

and the source terms are

$$f_1(x, t) = \begin{cases} -2(1+x^2t^2), & 0 < x < \frac{1}{2}, \\ (3+xt^2), & \frac{1}{2} < x < 1, \end{cases} \quad f_2(x, t) = \begin{cases} -(1+x^2t^2), & 0 < x < \frac{1}{2}, \\ (1+x^3t), & \frac{1}{2} < x < 1. \end{cases}$$

For the numerical experiments, the singular perturbation parameters take values from the set $S_\varepsilon = \{(\varepsilon_1, \varepsilon_2) | \varepsilon_2 = 2^{-5}, \dots, 2^{-9}, \varepsilon_1 = 2^{-2}\varepsilon_2\}$, which is sufficiently a small choice to bring out the singularly perturbed nature of the problem. To visualize the appearance of the interior layers near the point of discontinuity at $x = 1/2$ in the numerical solution of Example 4.4.1, we have plotted the numerical solution in Fig. 4.3, Fig. 4.4 whereas Fig. 4.5 and Fig. 4.6 show the interior layers phenomena of Example 4.4.2.

From Tables 4.1 and 4.2, we see the monotonically decreasing behavior of ε -uniform errors, which ensures the ε -uniform convergence of the proposed scheme (4.3.1). Also from Tables 4.1 and 4.2, we observe that the numerical order of convergence of the proposed scheme is almost equal to one. In order to reveal the numerical order of convergence, we have plotted the maximum point-wise errors in loglog plot for Example 4.4.1 in Fig. 4.8 and 4.8, which again shows the accuracy of the numerical scheme. For Example 4.4.2, we have presented the loglog plot for the maximum errors in Fig. 4.9 and Fig. 4.10.

4.5 Conclusions

In this chapter, an upwind difference scheme is proposed for solving singularly perturbed system of 1D parabolic convection-diffusion equations of the form (4.1.1) with discontinuous convection coefficients and source terms. To obtain the uniformly convergent solution by the proposed numerical scheme, we have used the piecewise-uniform Shishkin mesh fitted to the overlapping interior layers for the spatial domain and a uniform mesh for the temporal domain. Error analysis is provided which shows that the numerical method is approximately first-order accurate. Numerical experiments validate the theoretical findings.

Table 4.1: Uniform errors and the corresponding order of convergence for Example 4.4.1.

$\varepsilon_1, \varepsilon_2 \in S_\varepsilon$	Number of mesh-intervals N					
	32	64	128	256	512	1024
$d_1^{N,M}$	8.4982e-02	5.9682e-02	3.9308e-02	2.4560e-02	1.4929e-02	8.9017e-03
$p_1^{N,M}$	0.5098	0.6024	0.6785	0.7181	0.74607	
$d_2^{N,M}$	9.5801e-02	6.8158e-02	4.5651e-02	2.9271e-02	1.8191e-02	1.0960e-02
$p_2^{N,M}$	0.4911	0.5782	0.6411	0.6862	0.7310	

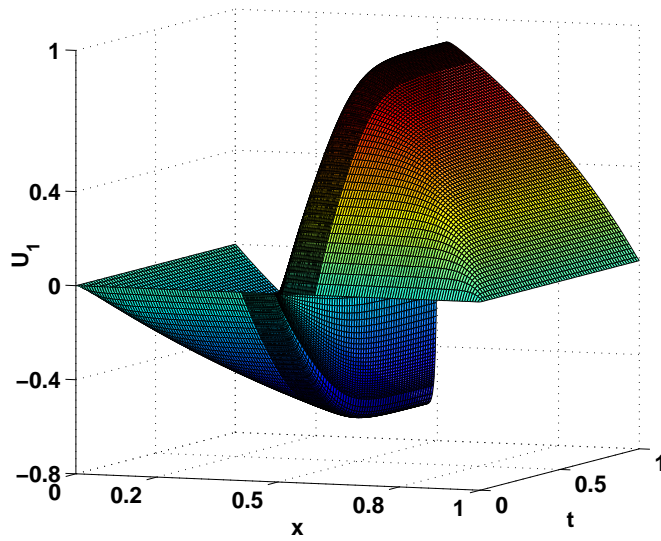


Figure 4.3: Surface plot of the numerical solution U_1 for $\varepsilon_1 = 2^{-8}, \varepsilon_2 = 2^{-6}$ and $N = 128, M = 32$ of Example 4.4.1.

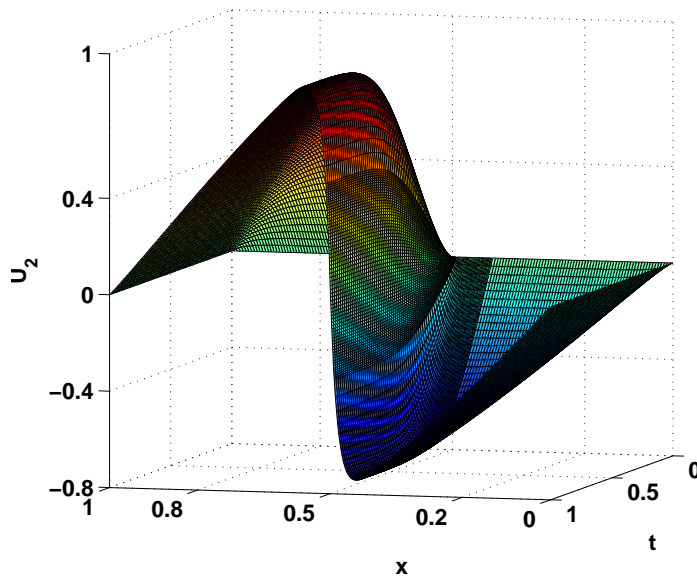


Figure 4.4: Surface plot of the numerical solution U_2 for $\varepsilon_1 = 2^{-8}, \varepsilon_2 = 2^{-6}$ and $N = 128, M = 32$ of Example 4.4.1.

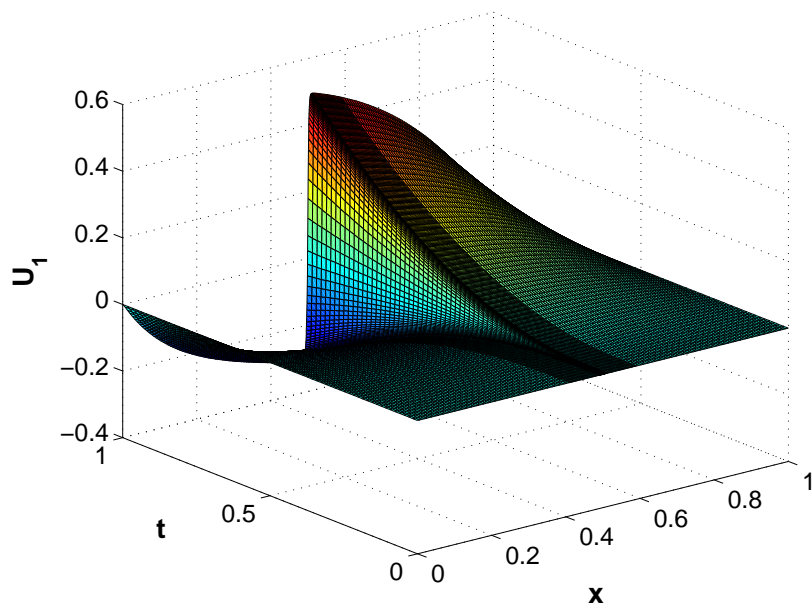


Figure 4.5: Surface plot of the numerical solution U_1 for $\varepsilon_1 = 2^{-8}, \varepsilon_2 = 2^{-6}$ and $N = 128, M = 32$ of Example 4.4.2.

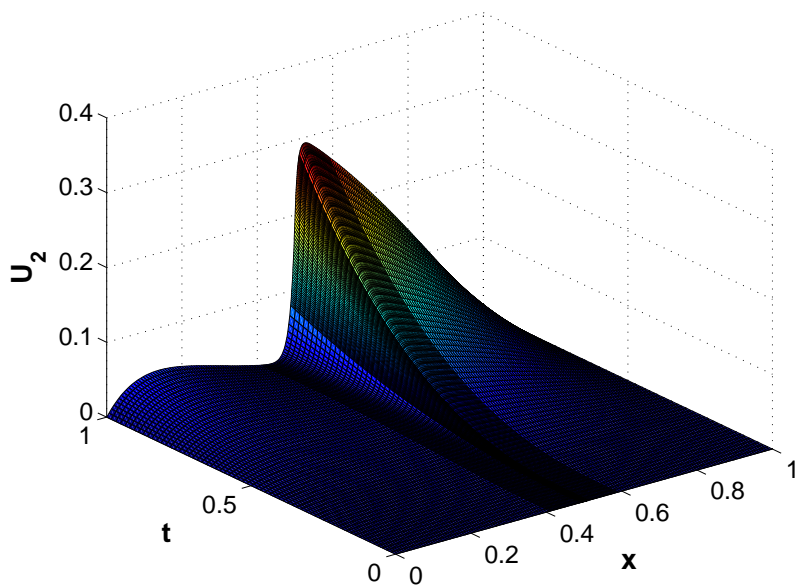


Figure 4.6: Surface plot of the numerical solution U_2 for $\varepsilon_1 = 2^{-8}, \varepsilon_2 = 2^{-6}$ and $N = 128, M = 32$ of Example 4.4.2.

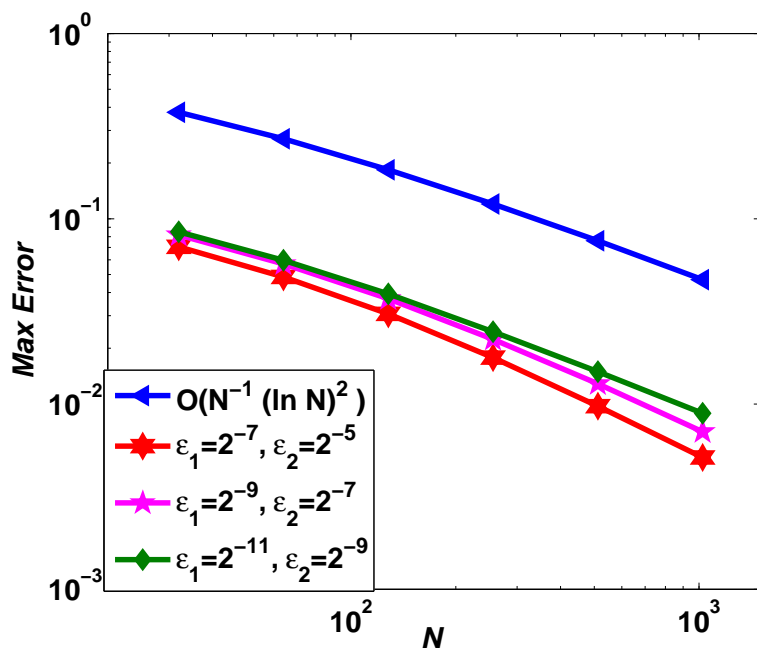


Figure 4.7: *Loglog plot associated with numerical solution U_1 for Example 4.4.1.*

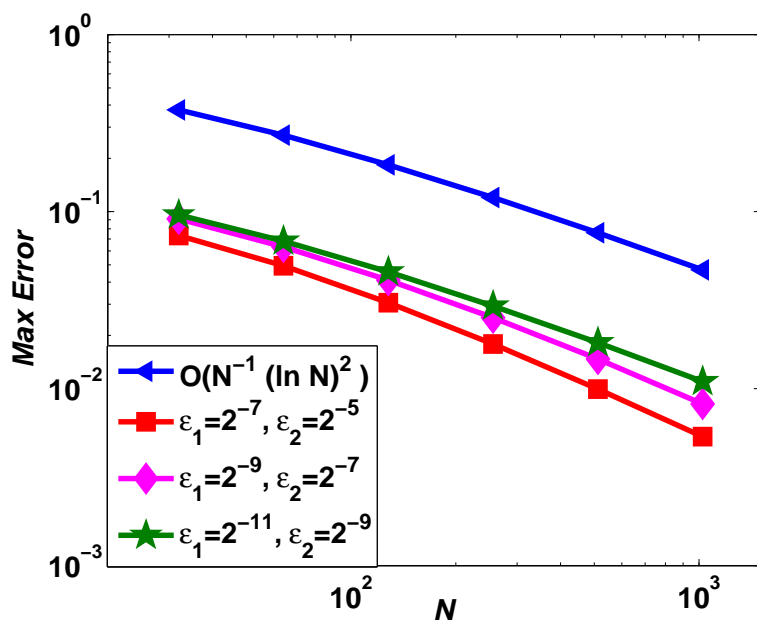


Figure 4.8: *Loglog plot associated with numerical solution U_2 for Example 4.4.1.*

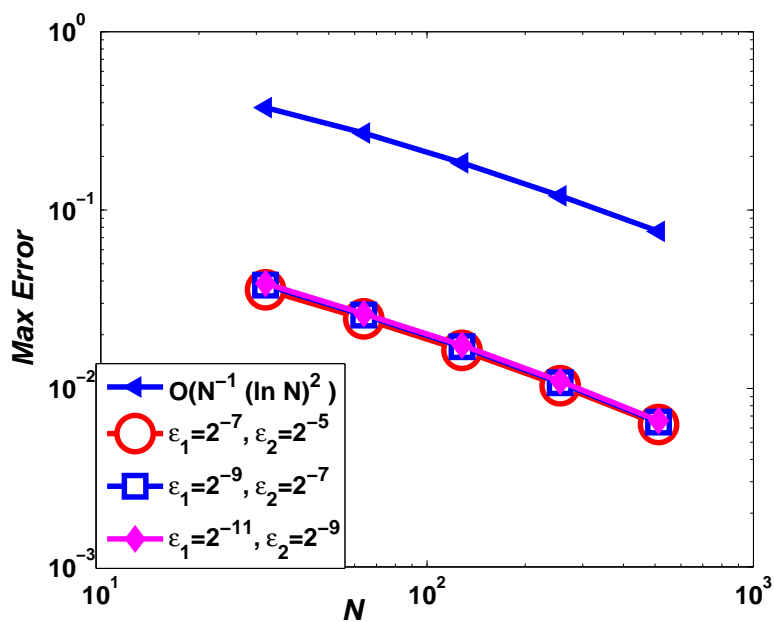
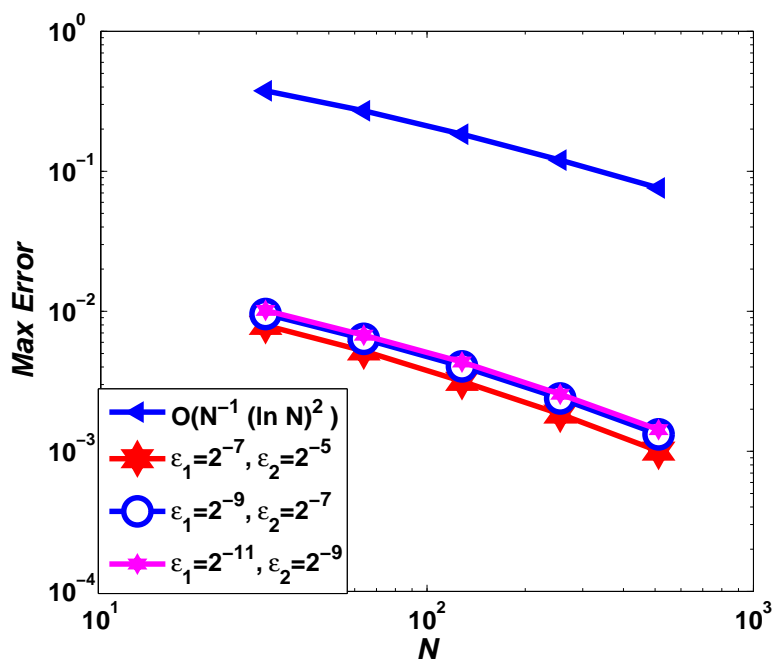
Figure 4.9: *Loglog plot associated with numerical solution U_1 for Example 4.4.2.*Figure 4.10: *Loglog plot associated with numerical solution U_2 for Example 4.4.2.*

Table 4.2: Uniform errors and the corresponding order of convergence for Example 4.4.2.

$\varepsilon_1, \varepsilon_2 \in \mathcal{S}_\varepsilon$	Number of mesh-intervals N				
	32	64	128	256	512
$d_1^{N,M}$	3.8799e-02	2.6244e-02	1.7482e-02	1.0981e-02	6.5893e-03
$p_1^{N,M}$	0.5640	0.5861	0.6709	0.7367	
$d_2^{N,M}$	1.0162e-02	6.7527e-03	4.3469e-03	2.5592e-03	1.4281e-03
$p_2^{N,M}$	0.5897	0.6355	0.7643	0.8416	

A Robust Fractional-Step Method for Singularly Perturbed System of 2D Parabolic Convection-Diffusion Problems

This chapter presents a numerical method to solve singularly perturbed system of 2D parabolic convection-diffusion problems. The numerical scheme comprises of a fractional-step method on uniform mesh for time discretization and the classical upwind scheme on a piecewise-uniform Shishkin mesh for spatial discretization. For the proposed scheme, the stability analysis is presented, and parameter-uniform error estimates are derived. It is shown that the numerical scheme is uniformly convergent with respect to the singular perturbation parameter. The proposed numerical method is applied to a test problem to verify the theoretical results numerically.

5.1 Introduction

We consider the following class of singularly perturbed 2D system of parabolic convection-diffusion IBVP on the domain $\mathcal{G} := \mathcal{D} \times (0, T]$, $\mathcal{D} = \Omega_x \times \Omega_y = (0, 1) \times (0, 1)$:

$$\begin{cases} \frac{\partial \vec{u}}{\partial t} + \mathcal{L}_{\varepsilon} \vec{u} = \vec{f}, & (x, y, t) \in \mathcal{G}, \\ \vec{u}(x, y, 0) = \vec{u}_0(x, y), & (x, y) \in \bar{\mathcal{D}}, \\ \vec{u}(0, y, t) = \vec{u}(1, y, t) = \vec{0}, & (y, t) \in [0, 1] \times [0, T], \\ \vec{u}(x, 0, t) = \vec{u}(x, 1, t) = \vec{0}, & (x, t) \in [0, 1] \times [0, T], \end{cases} \quad (5.1.1)$$

where the spatial differential operator $\mathcal{L}_{\varepsilon}$ is given by

$$\mathcal{L}_{\varepsilon} \equiv -\mathcal{E} \left(\frac{\partial^2}{\partial x^2} + \frac{\partial^2}{\partial y^2} \right) + A_1(x, y) \frac{\partial}{\partial x} + A_2(x, y) \frac{\partial}{\partial y} + B(x, y).$$

The coefficient matrices of the model problem (5.1.1) are given as $\mathcal{E} = \text{diag}(\varepsilon, \varepsilon)$, $0 < \varepsilon \ll 1$ with $A_1 = \text{diag}(a_{11}, a_{12})$, $A_2 = \text{diag}(a_{21}, a_{22})$ and $B = \{b_{lm}\}_{l,m=1}^2$.

In this chapter, we have proposed an upwind based numerical scheme on piecewise-uniform Shishkin mesh for discretization in the spatial derivatives and the fractional-step method for discretization in the time derivative for solving the singularly perturbed system of 2D parabolic convection-diffusion problem (5.1.1). The proposed scheme is shown to be ε -uniformly convergent in the discrete maximum norm and also almost first-order accurate with respect to the spatial variable and first-order accurate with respect to the temporal variable. Apart from this, the proposed numerical scheme carries the advantage of a fractional-step method, in which, one solves 1D stationary problem with respect to spatial variables x and y alternately.

We organize the rest of the chapter as follows: In Section 5.2, we discuss the existence of the exact solution to the model problem (5.1.1). Also, we describe the analytical behavior of the exact solution. Section 5.3 introduces the time semidiscretization, which uses the fractional-step method. Later in this section we discuss the asymptotic behavior of the solutions of the resulting semidiscrete problems and their spatial derivatives. In Section 5.4, we define the spatial discretization by using an upwind finite difference scheme on a piecewise-uniform Shishkin mesh. The fully finite difference scheme is given in Section 5.5 and also the main theoretical result, namely, the ε -uniform convergence theorem is established. In Section 5.6, we present the numerical results for a test problem to validate the theoretical findings.

5.2 Continuous Problem and Solution Bounds

Throughout this chapter, we assume that the coefficients of the convection matrices $A_l(x, y)$, $l = 1, 2$, satisfy the following positivity conditions

$$a_{11}(x, y), a_{12}(x, y) > \alpha_1 > 0, \quad a_{21}(x, y), a_{22}(x, y) > \alpha_2 > 0, \quad \alpha = \min\{\alpha_1, \alpha_2\}, \quad (5.2.1)$$

and the matrix $B(x, y)$ satisfies

$$\begin{cases} b_{ll}(x, y) > \gamma_\beta > 0, & b_{lm}(x, y) \leq 0, \text{ for } l \neq m, \\ \min_{(x,y) \in \overline{\mathcal{D}}} \{b_{11}(x, y) + b_{12}(x, y), b_{21}(x, y) + b_{22}(x, y)\} \geq \beta > 0. \end{cases} \quad (5.2.2)$$

Also $\gamma_1 = \max_{\overline{\mathcal{D}}} \{|b_{12}(x, y)| / b_{11}(x, y)\}$, $\gamma_2 = \max_{\overline{\mathcal{D}}} \{|b_{21}(x, y)| / b_{22}(x, y)\}$,

$$0 \leq \gamma := \max\{\gamma_1, \gamma_2\} < 1. \quad (5.2.3)$$

We assume that the data of the 2D parabolic IBVP (5.1.1) satisfy following smoothness and compatibility conditions

$$\vec{f} \in (\mathcal{C}_\lambda^2(\overline{\mathcal{G}}))^2 \quad \text{and} \quad \vec{u}_0 \in (\mathcal{C}_0^4(\overline{\mathcal{D}}))^2. \quad (5.2.4)$$

and

$$\begin{cases} \vec{u}_0(x, y) = \vec{0}, & \text{on } \partial\mathcal{D}, \\ \vec{f}(x, y, 0) - \mathcal{L}_\varepsilon \vec{u}_0(x, y) = \vec{0}, & \text{on } \partial\mathcal{D}, \\ \vec{f}_t(x, y, 0) + (\mathcal{L}_\varepsilon)^2 \vec{u}_0(x, y) - \mathcal{L}_\varepsilon \vec{f}(x, y, 0) = \vec{0}, & \text{on } \partial\mathcal{D}, \\ \vec{f}(x, y, t) = \vec{0}, & \text{on } \{0, 1\} \times \{0, 1\} \times (0, T], \end{cases} \quad (5.2.5)$$

Under these smoothness and compatibility conditions imposed on the functions \vec{u}_0 and \vec{f} , the exact solution \vec{u} of model problem (5.1.1) exhibits a regular boundary layer of width $O(\varepsilon)$ in the neighborhood of the sides along $x = 1$ and $y = 1$ of \mathcal{D} and corner layer at point $(1, 1)$.

Lemma 5.2.1. (Maximum Principle). *Let $(\frac{\partial}{\partial t} + \mathcal{L}_\varepsilon)$ be the differential operator defined in (5.1.1) and assume that the matrices A_1 , A_2 and B satisfy the conditions given in (5.2.1) and (5.2.2), respectively. Then for $\vec{z} \geq \vec{0}$ on $\partial\mathcal{G}$ and $(\frac{\partial}{\partial t} + \mathcal{L}_\varepsilon) \vec{z} \geq \vec{0}$ in \mathcal{G} , we have $\vec{z} \geq \vec{0}$ for all $(x, y, t) \in \bar{\mathcal{G}}$.*

Proof. We prove this lemma by contradiction. Assume that there exists a point $(x_0, y_0, t_0) \in \mathcal{G}$ such that

$$\min\{z_1(x_0, y_0, t_0), z_2(x_0, y_0, t_0)\} = \min\left\{\min_{(x,y,t) \in \bar{\mathcal{G}}} z_1(x, y, t), \min_{(x,y,t) \in \bar{\mathcal{G}}} z_2(x, y, t)\right\} < 0.$$

Without loss of generality we assume that $z_1(x_0, y_0, t_0) \leq z_2(x_0, y_0, t_0)$. It follows that

$$\left(\frac{\partial z_1}{\partial t} + (\mathcal{L}_\varepsilon)_1 \vec{z}\right)(x_0, y_0, t_0) \leq b_{11}(x_0, y_0)z_1(x_0, y_0, t_0) + b_{12}(x_0, y_0)z_2(x_0, y_0, t_0) < 0,$$

which contradicts the hypothesis of this lemma, therefore $\vec{z} \geq \vec{0}$ for all $(x, y, t) \in \bar{\mathcal{G}}$. ■

Define the decoupled differential operators by

$$\mathcal{L}_l v = \frac{\partial v}{\partial t} - \varepsilon \left(\frac{\partial^2}{\partial x^2} + \frac{\partial^2}{\partial y^2} \right) v + a_{1l}(x, y) \frac{\partial v}{\partial x} + a_{2l}(x, y) \frac{\partial v}{\partial y} + b_l(x, y)v, \quad l = 1, 2.$$

It can be easily verified that the differential operator \mathcal{L}_l satisfies the maximum principle.

Lemma 5.2.2. *If $v \in \mathcal{C}(\bar{\mathcal{G}}) \cap \mathcal{C}^2(\mathcal{G})$, with $\mathcal{L}_l v = \phi$ on \mathcal{G} and $v = \psi$ on $\bar{\mathcal{G}}$. Then v satisfies*

$$\|v\|_\infty \leq \|\phi/b_l\|_\infty + \|\psi\|_\infty.$$

Proof. Consider the barrier function

$$\varphi = \|\phi/b_l\|_\infty + \|\psi\|_\infty.$$

Clearly, we have $\varphi \geq v$ on $\partial\mathcal{G}$. And for all $(x, y, t) \in \mathcal{G}$, we obtain

$$\begin{aligned}\mathcal{L}_l\varphi(x, y, t) &= b_u(x, y, t) (\|\phi/b_u\|_\infty + \|\psi\|_\infty) \\ &\geq b_u(x, y, t) |(\phi/b_u)(x, y, t)| = |\phi(x, y, t)| = |\mathcal{L}_l v(x, y, t)|.\end{aligned}$$

By applying the maximum principle for \mathcal{L}_l , the required result follows. \blacksquare

Next, we construct a sequence of uncoupled problems whose solutions converge to the exact solution of the continuous problem (5.1.1).

Lemma 5.2.3. *Let \vec{u} be the solution of (5.1.1). For $j = 0, 1, \dots$, define the sequence of vector-valued functions $\vec{u}^{[j]} = (u_1^{[j]}, u_2^{[j]})^T$ as follows: let $\vec{u}^{[0]}$ be any function in $(C(\bar{\mathcal{G}}))^2$ and for $j = 0, 1, \dots$, the function $\vec{u}^{[j]}$ satisfy*

$$\begin{cases} \mathcal{L}_1 u_1^{[j]} = f_1 - b_{12} u_2^{[j-1]}, & \mathcal{L}_2 u_2^{[j]} = f_2 - b_{21} u_1^{[j-1]} \\ \vec{u}^{[j]}(x, y, 0) = \vec{u}_0(x, y), & (x, y) \in \mathcal{D}, \\ \vec{u}^{[j]}(x, y, t) = \vec{0}, & \text{on } \partial\mathcal{D} \times [0, T]. \end{cases} \quad (5.2.6)$$

Then $\lim_{j \rightarrow \infty} \vec{u}^{[j]} = \vec{u}$. Furthermore, we have

$$\|\vec{u}\|_\infty \leq \frac{1}{1-\gamma} \left(\frac{1}{\gamma_\beta} \|\vec{f}\|_\infty + \|\vec{u}_0\|_\infty \right). \quad (5.2.7)$$

Proof. For $j = 0, 1, \dots$, set $\vec{e}_u = \vec{u} - \vec{u}^{[j]}$. Then, for $j \geq 1$, \vec{e}_u is the solution of the following problem:

$$\begin{cases} \mathcal{L}_1 e_{u_1}^{[j]} = -b_{12} e_{u_2}^{[j-1]}, & e_{u_1}^{[j]}(x, y, t) = 0 \text{ on } \partial\mathcal{G}, \\ \mathcal{L}_2 e_{u_2}^{[j]} = -b_{21} e_{u_1}^{[j-1]}, & e_{u_2}^{[j]}(x, y, t) = 0 \text{ on } \partial\mathcal{G}. \end{cases}$$

From Lemma 5.2.2, we obtain

$$\begin{cases} \|e_{u_1}^{[j]}\|_\infty = \|b_{12} e_{u_2}^{[j-1]}/b_{11}\|_\infty \leq \gamma_1 \|e_u^{[j-1]}\|_\infty, \\ \|e_{u_2}^{[j]}\|_\infty = \|b_{21} e_{u_1}^{[j-1]}/b_{22}\|_\infty \leq \gamma_2 \|e_u^{[j-1]}\|_\infty. \end{cases}$$

Hence, one can deduce that

$$\|e_u^{[j]}\|_\infty \leq \gamma \|e_u^{[j-1]}\|_\infty \leq \gamma^j \|e_u^{[0]}\|_\infty.$$

It implies that $\|e_u^{[j]}\|_\infty \rightarrow 0$, i.e., $\lim_{j \rightarrow \infty} \vec{u}^{[j]} = \vec{u}$.

Next, consider $\vec{u}^{[0]} = \vec{0}$. And set $\hat{e}_u^{[j]} = \vec{u}^{[j]} - \vec{u}^{[j-1]}$ for $j = 0, 1, \dots$. From (5.2.6), it is easy to verify that

$$\mathcal{L}_1 \hat{e}_{u_1}^{[j]} = -b_{12} \hat{e}_{u_2}^{[j-1]}, \quad \mathcal{L}_2 \hat{e}_{u_2}^{[j]} = -b_{21} \hat{e}_{u_1}^{[j-1]}.$$

Again, by using Lemma 5.2.2, we get

$$\|\widehat{e}_{u_1}^{[j]}\|_\infty = \|b_{12}\widehat{e}_{u_2}^{[j-1]}/b_{11}\|_\infty, \quad \|\widehat{e}_{u_2}^{[j]}\|_\infty = \|b_{21}\widehat{e}_{u_1}^{[j-1]}/b_{22}\|_\infty, \quad j = 2, 3, \dots$$

Which implies that $\|\widetilde{e}_u^{[j]}\|_\infty \leq \gamma\|\widetilde{e}_u^{[j-1]}\|_\infty$ for $j = 2, 3, \dots$. Consequently, we have

$$\|\widetilde{e}_u^{[j]}\|_\infty \leq \gamma^{j-1}\|\widetilde{e}_u^{[1]}\|_\infty, \quad \text{for } j = 1, 2, \dots$$

Therefore,

$$\|\widetilde{e}_u^{[1]}\|_\infty = \|\vec{u}^{[1]}\|_\infty \leq \frac{1}{\gamma_\beta}\|\vec{f}\|_\infty + \|\vec{u}_0\|_\infty.$$

Hence, for all $j = 1, 2, \dots$, one can obtain that

$$\|\widetilde{e}_u^{[j]}\|_\infty \leq \gamma^{j-1} \left(\frac{1}{\gamma_\beta}\|\vec{f}\|_\infty + \|\vec{u}_0\|_\infty \right).$$

Finally, we get

$$\|\vec{u}\|_\infty = \lim_{j_1 \rightarrow \infty} \left\| \sum_{j=1}^{j_1} \widetilde{e}_u^{[j]} \right\|_\infty \leq \lim_{j_1 \rightarrow \infty} \sum_{j=1}^{j_1} \|\widetilde{e}_u^{[j]}\|_\infty \leq \frac{1}{1-\gamma} \left(\frac{1}{\gamma_\beta}\|\vec{f}\|_\infty + \|\vec{u}_0\|_\infty \right). \quad \blacksquare$$

An immediate consequence of Lemma 5.2.3 is the following corollary, which discusses the existence and uniqueness of the exact solution of the model problem (5.1.1).

Corollary 5.2.4. *The continuous problem (5.1.1) admits a unique solution.*

Proof. If $\vec{f} = \vec{u}_0 = \vec{0}$, then one can easily see from (5.2.7) that $\vec{u} = \vec{0}$ is the only solution of (5.1.1). By using the standard theory for solutions of system of partial differential equations from [42, Section 7.5], one can show that the system of PDE (5.1.1) has a unique solution. \blacksquare

Lemma 5.2.5. *For all non-negative integer k_0 satisfying $0 \leq k_0 \leq 2$, the time derivatives of the exact solution \vec{u} of the IBVP (5.1.1) satisfy the following estimate*

$$\left| \frac{\partial^{k_0} \vec{u}}{\partial t^{k_0}}(x, y, t) \right| \leq \vec{C}, \quad \text{for all } (x, y, t) \in \mathcal{G}.$$

Proof. By following the argument of Theorem 2.2.4, the desired result follows. \blacksquare

In remaining part of this section, the decomposition of the exact solution is discussed. Also, we establish sharper bounds on the derivatives of the exact solution \vec{u} of the model problem (5.1.1). To find these bounds, the solution \vec{u} is decomposed as follows:

$$\vec{u}(x, y, t) = \vec{v}(x, y, t) + \vec{w}(x, y, t), \quad (x, y, t) \in \overline{\mathcal{G}}.$$

The regular component \vec{v} can be obtained from

$$\begin{cases} \mathcal{L}_{\varepsilon}^* \vec{v}^* = \vec{f}^*, & \text{in } \mathcal{G}^* = \mathcal{D}^* \times (0, T], \\ \vec{v}^*(x, y, 0) = \vec{u}_0^*(x, y), & \text{in } \mathcal{D}^*, \\ \vec{v}^*(x, y, t) = \vec{0}, & \text{in } \partial\mathcal{D}^* \times [0, T], \end{cases} \quad (5.2.8)$$

as a restriction to \mathcal{G} , where \mathcal{D}^* is the smooth extension of \mathcal{D} and $A_1^*, A_2^*, B^*, \vec{f}^*$ are the smooth extensions of A_1, A_2, B, \vec{f} to \mathcal{G}^* , also \vec{u}_0^* is a smooth extension of \vec{u}_0 to \mathcal{D} .

Next, \vec{w} will be decomposed in terms of layer components as follows

$$\vec{w} = \vec{w}_1 + \vec{w}_2 + \vec{w}_{12},$$

where the boundary layer component \vec{w}_1 can be obtained as a restriction to \mathcal{G} of the exact solution of the following problem

$$\begin{cases} \mathcal{L}_{\varepsilon}^{**} \vec{w}_1^{**} = \vec{0}, & \text{in } \mathcal{G}^{**} = \mathcal{D}^{**} \times (0, T], \\ \vec{w}_1^{**}(x, y, 0) = \vec{0}, & \text{in } \mathcal{D}^{**}, \\ \vec{w}_1^{**}(x, y, t) = -\vec{v}^{**}, & \text{in } \partial\mathcal{D}_1^{**} \times [0, T], \\ \vec{w}_1^{**}(x, y, t) = \vec{0}, & \text{in } \partial\mathcal{D}_2^{**} \times [0, T], \end{cases} \quad (5.2.9)$$

where \mathcal{D}^{**} is the smooth extension of \mathcal{D} near the vertex $(1, 1)$, $\partial\mathcal{D}_1^{**}$ is an extension of side $x = 1$ beyond the vertex $(1, 1)$ and $\partial\mathcal{D}_2^{**} = \partial\mathcal{D}^{**} \setminus \partial\mathcal{D}_1^{**}$ and also \vec{v}^{**} is a smooth and compatible extension of $\vec{v}(1, y, t)$ to $\partial\mathcal{D}_1^{**}$, as well as $A_1^{**}, A_2^{**}, B^{**}$ are the smooth extensions of A_1, A_2, B to \mathcal{G}^{**} .

The function \vec{w}_2^{**} is the smooth extension of the boundary layer function \vec{w}_2 to \mathcal{G} and it satisfies the following IBVP:

$$\begin{cases} \mathcal{L}_{\varepsilon}^{**} \vec{w}_2^{**} = \vec{0}, & \text{in } \mathcal{G}^{**} = \mathcal{D}^{**} \times (0, T], \\ \vec{w}_2^{**}(x, y, 0) = \vec{0}, & \text{in } \mathcal{D}^{**}, \\ \vec{w}_2^{**}(x, y, t) = \vec{0}, & \text{in } \partial\tilde{\mathcal{D}}_1^{**} \times [0, T], \\ \vec{w}_2^{**}(x, y, t) = -\vec{v}^{**}, & \text{in } \partial\tilde{\mathcal{D}}_2^{**} \times [0, T], \end{cases} \quad (5.2.10)$$

where $\tilde{\mathcal{D}}_2^{**}$ is an extension of side $y = 1$ beyond the vertex $(1, 1)$ and $\tilde{\mathcal{D}}_2^{**} = \mathcal{D}^{**} \setminus \tilde{\mathcal{D}}_1^{**}$. \vec{v}^{**} is a smooth and compatible extension of $\vec{v}(x, 1, t)$ to $\partial\tilde{\mathcal{D}}_2^{**}$.

Finally, the corner layer component \vec{w}_{12} is the solution of

$$\begin{cases} \mathcal{L}_{\varepsilon} \vec{w}_{12} = \vec{0}, & \text{in } \mathcal{G} = \mathcal{D} \times (0, T], \\ \vec{w}_{12}(x, y, 0) = \vec{0}, & \text{in } \mathcal{D}, \\ \vec{w}_{12}(x, y, t) = -(\vec{v} + \vec{w}_1 + \vec{w}_2), & \text{in } \partial\mathcal{D} \times [0, T]. \end{cases} \quad (5.2.11)$$

By following the technique of [38, Lemma 2.3] and [39, Theorem 4.1] with Lemma 5.2.5 (bounds of time derivative of exact solution), one can conclude that the smooth and layer components, \vec{v} , \vec{w}_1 , \vec{w}_2 , \vec{w}_{12} satisfy the following estimates:

$$\begin{aligned} & \left| \frac{\partial^{k_s+k_t} \vec{v}}{\partial x^{k_x} \partial y^{k_y} \partial t^{k_t}}(x, y, t) \right| \vec{C}, \\ & \left| \frac{\partial^{k_s+k_t} \vec{w}_1}{\partial x^{k_x} \partial y^{k_y} \partial t^{k_t}}(x, y, t) \right| \leq \vec{C} \varepsilon^{-k_x} B_\varepsilon^1(x) \\ & \left| \frac{\partial^{k_s+k_t} \vec{w}_2}{\partial x^{k_x} \partial y^{k_y} \partial t^{k_t}}(x, y, t) \right| \leq \vec{C} \varepsilon^{-k_y} B_\varepsilon^1(y), \\ & \left| \frac{\partial^{k_s+k_t} \vec{w}_{12}}{\partial x^{k_x} \partial y^{k_y} \partial t^{k_t}}(x, y, t) \right| \leq \vec{C} \varepsilon^{-k_s} \min\{B_\varepsilon^1(x), B_\varepsilon^1(y)\} \end{aligned} \quad (5.2.12)$$

where $k_s = k_x + k_y$, and $k_s + 2k_t \leq 4$, for all $(x, y, t) \in \mathcal{D} \times [0, T]$.

5.3 Time Semidiscretization

In this section, we propose the numerical scheme which discretizes the continuous problem (5.1.1) in the time direction. Before getting into the details of the time semidiscretization process, we split the spatial differential operator \mathcal{L}_ε as $\mathcal{L}_\varepsilon = \mathcal{L}_{\vec{1},\varepsilon} + \mathcal{L}_{\vec{2},\varepsilon}$, where $\mathcal{L}_{\vec{1},\varepsilon}$ and $\mathcal{L}_{\vec{2},\varepsilon}$ are given by

$$\begin{cases} \mathcal{L}_{\vec{1},\varepsilon} \equiv (\mathcal{L}_{11,\varepsilon}, \mathcal{L}_{12,\varepsilon})^T = -\mathcal{E} \frac{\partial^2}{\partial x^2} + A_1(x, y) \frac{\partial}{\partial x} + B_1(x, y), \\ \mathcal{L}_{\vec{2},\varepsilon} \equiv (\mathcal{L}_{21,\varepsilon}, \mathcal{L}_{22,\varepsilon})^T = -\mathcal{E} \frac{\partial^2}{\partial y^2} + A_2(x, y) \frac{\partial}{\partial y} + B_2(x, y), \end{cases}$$

where the coefficients of matrices $B_\ell(x, y) = \{b_{lm}^\ell(x, y)\}_{l,m=1}^2$, $\ell = 1, 2$ are given by

$$b_{lm} = b_{lm}^1(x, y) + b_{lm}^2(x, y), \quad l, m = 1, 2.$$

In addition, we assume that the reaction coefficient matrices $B_\ell(x, y)$, $\ell = 1, 2$, satisfy the following conditions:

$$\begin{cases} b_{ll}^\ell(x, y) > \gamma_\beta^\ell, \quad b_{lm}^\ell(x, y) \leq 0, \quad \text{for } l \neq m, \quad l, m = 1, 2, \quad \ell = 1, 2, \\ \min_{(x,y) \in \mathcal{D}} \{b_{11}^\ell + b_{12}^\ell, b_{21}^\ell + b_{22}^\ell\} \geq \beta^\ell > 0 > 0, \quad \ell = 1, 2. \end{cases} \quad (5.3.1)$$

Let us consider the decomposition of the source term as $\vec{f} = \vec{f}_1 + \vec{f}_2$, where $\vec{f}_1 = (f_{11}, f_{12})^T$ and $\vec{f}_2 = (f_{21}, f_{22})^T$ satisfy the following conditions:

$$f_{lm}(x, 0, t) = f_{lm}(x, 1, t) = 0, \quad f_{lm}(0, y, t) = f_{lm}(1, y, t) = 0, \quad \text{for } l, m = 1, 2. \quad (5.3.2)$$

The fractional implicit-Euler method for the time semidiscretization on the uniform mesh $\bar{\Upsilon}^M = \{t_n = n\Delta t, n = 0, 1, \dots, M, \Delta t = T/M\}$ is described as follows:

$$\bar{u}^0 = \bar{u}_0(x, y), \quad (x, y) \in \bar{\mathcal{D}}, \quad (5.3.3)$$

$$\begin{cases} (I + \Delta t \mathcal{L}_{\bar{1}, \varepsilon}) \bar{u}^{n+1/2}(x, y) = \bar{u}^n(x, y) + \Delta t \bar{f}_1^{n+1}(x, y), & (x, y) \in \mathcal{D}, \\ \bar{u}^{n+1/2}(0, y) = \vec{0}, \quad \bar{u}^{n+1/2}(1, y) = \vec{0}, & y \in [0, 1], \end{cases} \quad (5.3.4)$$

and

$$\begin{cases} (I + \Delta t \mathcal{L}_{\bar{2}, \varepsilon}) \bar{u}^{n+1}(x, y) = \bar{u}^{n+1/2}(x, y) + \Delta t \bar{f}_2^{n+1}(x, y), & (x, y) \in \mathcal{D}, \\ \bar{u}^{n+1}(x, 0) = \vec{0}, \quad \bar{u}^{n+1}(x, 1) = \vec{0}, & x \in [0, 1]. \end{cases} \quad (5.3.5)$$

In such a way, one can obtain the numerical approximation $\bar{u}^n(x, y)$ to the exact solution $\bar{u}(x, y, t)$ of the model problem (5.1.1).

Lemma 5.3.1. (Maximum Principle). *Let $(I + \Delta t \mathcal{L}_{\bar{l}, \varepsilon}), l = 1, 2$, be the differential operators defined in (5.3.4)-(5.3.5) and assume that the entries of the matrices A_ℓ and B_ℓ satisfy the conditions given in (5.2.1) and (5.3.1). Then for $\bar{z}^{n+1} \geq \vec{0}$ on $\partial \mathcal{D}$ and $(I + \Delta t \mathcal{L}_{\bar{l}, \varepsilon}) \bar{z}^{n+1} \geq \vec{0}$ in \mathcal{D} , we have $\bar{z}^{n+1} \geq \vec{0}$ for all $(x, y) \in \bar{\mathcal{D}}$.*

Proof. We prove this lemma by contradiction. We prove the maximum principle related to the operator $(I + \Delta t \mathcal{L}_{\bar{1}, \varepsilon})$. One can prove for second operator in an analogous way. Assume that there exists a point $(x_0, y_0) \in \mathcal{D}$ such that

$$\min\{z_1^{n+1}(x_0, y_0), z_2^{n+1}(x_0, y_0)\} = \min\left\{\min_{(x,y) \in \bar{\mathcal{D}}} z_1^{n+1}, \min_{(x,y) \in \bar{\mathcal{D}}} z_2^{n+1}\right\} < 0.$$

Without loss of generality we assume that $z_1^{n+1}(x_0, y_0) \leq z_2^{n+1}(x_0, y_0)$. Then the first component of $(I + \Delta t \mathcal{L}_{\bar{1}, \varepsilon}) \bar{z}^{n+1}$ satisfies

$$(I + \Delta t \mathcal{L}_{11, \varepsilon}) \bar{z}^{n+1}(x_0, y_0) \leq (1 + \Delta t b_{11}^1) z_1^{n+1}(x_0, y_0) + \Delta t b_{12}^1 z_2^{n+1}(x_0, y_0) < 0,$$

which contradicts the hypothesis of this lemma, therefore $\bar{z}^{n+1} \geq \vec{0}$ for all $(x, y) \in \bar{\mathcal{D}}$. ■

Stability

Next, we will discuss the stability of the semidiscrete scheme (5.3.3)-(5.3.5). By using the stability and consistency, one can easily prove the convergence analysis of the numerical scheme by following the classical arguments.

Since the operators $(I + \Delta t \mathcal{L}_{\bar{l}, \varepsilon}), l = 1, 2$, satisfy the maximum principle (given in Lemma 5.3.1), it follows that

$$\|(I + \Delta t \mathcal{L}_{\bar{1}, \varepsilon})^{-1}\|_\infty \leq \frac{1}{1 + \beta^1 \Delta t}, \quad \|(I + \Delta t \mathcal{L}_{\bar{2}, \varepsilon})^{-1}\|_\infty \leq \frac{1}{1 + \beta^2 \Delta t}. \quad (5.3.6)$$

These estimates ensure stability of the time semidiscrete scheme (5.3.3)-(5.3.5).

Consistency

The local truncation error \bar{e}^{n+1} of the semidiscrete scheme (5.3.3)-(5.3.5) at the time level t_{n+1} is defined by

$$\bar{e}^{n+1} = \bar{u}(t_{n+1}) - \bar{u}^{n+1},$$

where \bar{u}^{n+1} is the solution of

$$\begin{cases} (I + \Delta t \mathcal{L}_{\bar{1}, \bar{\varepsilon}}) \bar{u}^{n+1/2}(x, y) = \bar{u}(t_n) + \Delta t \bar{f}_1^{n+1}(x, y), & (x, y) \in \mathcal{D}, \\ \bar{u}^{n+1/2}(0, y) = \bar{0}, \quad \bar{u}^{n+1/2}(1, y) = \bar{0}, & y \in [0, 1], \end{cases} \quad (5.3.7)$$

and

$$\begin{cases} (I + \Delta t \mathcal{L}_{\bar{2}, \bar{\varepsilon}}) \bar{u}^{n+1}(x, y) = \bar{u}^{n+1/2}(x, y) + \Delta t \bar{f}_2^{n+1}(x, y), & (x, y) \in \mathcal{D}, \\ \bar{u}^{n+1}(x, 0) = \bar{0}, \quad \bar{u}^{n+1}(x, 1) = \bar{0}, & x \in [0, 1]. \end{cases} \quad (5.3.8)$$

The next lemma shows the consistency result of the time semidiscrete scheme.

Lemma 5.3.2. *The local truncation error corresponding to the time semidiscrete scheme (5.3.7)-(5.3.8) satisfies the following estimate*

$$\|\bar{e}^{n+1}\|_{\infty} \leq C(\Delta t)^2.$$

Proof. By using the Taylor's expansion and the maximum principle (Lemma 5.3.1), one can obtain the required result. ■

Uniform convergence

The global error of the time semidiscrete scheme (5.3.3)-(5.3.5) at the time level t_n is given by

$$\vec{E}^n = \sup_{n \leq T/\Delta t} \|\bar{u}(t_n) - \bar{u}^n\|_{\infty}.$$

By applying the stability (5.3.6) and consistency (Lemma 5.3.2), we obtain the following result.

Lemma 5.3.3. *If we assume the hypothesis of Lemma 5.3.2, then we have*

$$\sup_{n \leq T/\Delta t} \|\bar{u}(t_n) - \bar{u}^n\|_{\infty} \leq C\Delta t.$$

Hence, we conclude that the time semidiscretization process is uniformly convergent of order one.

5.3.1 Asymptotic behavior of the semidiscrete solution

In this subsection, we study the analytical behavior of the exact solution \tilde{u}^{n+1} of the time semidiscrete scheme (5.3.7)-(5.3.8). First, we discuss the analytical behavior of the exact solution of (5.3.7) and their derivatives.

Lemma 5.3.4. *The differential operators $\mathcal{L}_{1m,\varepsilon}$, $m = 1, 2$, satisfy the following estimates*

$$\|\mathcal{L}_{1m,\varepsilon}\vec{u}\|_\infty \leq C, \quad \|\mathcal{L}_{1m,\varepsilon}^2\vec{u}\|_\infty \leq C, \quad m = 1, 2.$$

Proof. We use the bound of the smooth component \vec{v} and the layer components \vec{w}_1 , \vec{w}_2 and \vec{w}_{12} given in (5.2.12) to prove the required estimate. By using the derivative bounds of \vec{v} given in (5.2.12), for $m = 1, 2$, it is clear that $\mathcal{L}_{1m,\varepsilon}\vec{v}$, $\mathcal{L}_{2m,\varepsilon}\vec{v}$, $\mathcal{L}_{1m,\varepsilon}^2\vec{v}$ and $\mathcal{L}_{2m,\varepsilon}^2\vec{v}$ are uniformly bounded.

Next, we will prove similar bounds for the layer components. First we decompose \vec{w}_1 as $\vec{w}_1 = \vec{w}_1^1 + \varepsilon\vec{w}_1^2 + \vec{w}_1^3$, where \vec{w}_1^1 , \vec{w}_1^2 and \vec{w}_1^3 satisfy the following IBVPs:

$$\left\{ \begin{array}{ll} \frac{\partial \vec{w}_1^1}{\partial t} + A_1(x, y) \frac{\partial \vec{w}_1^1}{\partial x} + A_2(x, y) \frac{\partial \vec{w}_1^1}{\partial y} + B(x, y) \vec{w}_1^1 = \vec{0}, & \text{in } \mathcal{G}, \\ \vec{w}_1^1(x, y, 0) = \vec{0}, & \text{in } \mathcal{D}, \\ \vec{w}_1^1(0, y, t) = \vec{0}, \quad \vec{w}_1^1(1, y, t) = -\vec{v}(1, y, t), & \text{in } [0, 1] \times [0, T], \\ \vec{w}_1^1(x, 0, t) = \vec{0}, \quad \vec{w}_1^1(x, 1, t) = \vec{0}, & \text{in } \partial\mathcal{D}_2 \times [0, T], \end{array} \right. \quad (5.3.9)$$

$$\left\{ \begin{array}{l} \frac{\partial \vec{w}_1^2}{\partial t} + A_1(x, y) \frac{\partial \vec{w}_1^2}{\partial x} + A_2(x, y) \frac{\partial \vec{w}_1^2}{\partial y} + B(x, y) \vec{w}_1^2 = \left(\frac{\partial^2 \vec{w}_1^1}{\partial x^2} + \frac{\partial^2 \vec{w}_1^1}{\partial y^2} \right), \text{ in } \mathcal{G}, \\ \vec{w}_1^2(x, y, t) = \vec{0}, \text{ in } \partial\mathcal{G}, \end{array} \right. \quad (5.3.10)$$

and

$$\left\{ \begin{array}{l} \frac{\partial \vec{w}_1^3}{\partial t}(x, y, t) + \mathcal{L}_\varepsilon \vec{w}_1^3 = \varepsilon^2 \left(\frac{\partial^2 \vec{w}_1^2}{\partial x^2} + \frac{\partial^2 \vec{w}_1^2}{\partial y^2} \right), \text{ in } \mathcal{G}, \\ \vec{w}_1^3(x, y, t) = \vec{0}, \text{ in } \partial\mathcal{G}. \end{array} \right. \quad (5.3.11)$$

From (5.3.9), (5.3.10) and (5.3.11), we can get

$$\left| \frac{\partial^{k_s+k_t} \vec{w}_1^l(x, y, t)}{\partial x^{k_x} \partial y^{k_y} \partial t^{k_t}} \right| \leq \vec{C}, \quad l = 1, 2, \quad \text{for } k_s + 2k_t \leq 2, \quad (5.3.12)$$

and

$$\left| \frac{\partial^{k_s+k_t} \vec{w}_1^3(x, y, t)}{\partial x^{k_x} \partial y^{k_y} \partial t^{k_t}} \right| \leq \vec{C} \varepsilon^{2-k_s}, \quad \text{for } k_s + 2k_t \leq 2. \quad (5.3.13)$$

By employing (5.3.12), we obtain $|\mathcal{L}_{\bar{1},\varepsilon}\bar{w}_1^l| \leq \bar{C}$, for $l = 1, 2$. Now, applying the operator $\mathcal{L}_{\bar{1},\varepsilon}$ in (5.3.11) on the domain \mathcal{G} , we have

$$\begin{cases} \frac{\partial(\mathcal{L}_{\bar{1},\varepsilon}\bar{w}_1^3)}{\partial t}(x, y, t) + \mathcal{L}_{\bar{1},\varepsilon}(\mathcal{L}_{\bar{1},\varepsilon}\bar{w}_1^3)(x, y, t) = \bar{\Xi}_w, & \text{in } \mathcal{G}, \\ \mathcal{L}_{\bar{1},\varepsilon}\bar{w}_1^3(x, y, t) = \bar{0}, & \text{in } \partial\mathcal{G}, \end{cases} \quad (5.3.14)$$

where

$$\begin{aligned} \bar{\Xi}_w = & \varepsilon \left(\frac{\partial^2 A_2}{\partial x^2} \frac{\partial \bar{w}_1^3}{\partial y} + 2 \frac{\partial A_2}{\partial x} \frac{\partial^2 \bar{w}_1^3}{\partial x \partial y} + 2 \frac{\partial B_2}{\partial x} \frac{\partial \bar{w}_1^3}{\partial x} + \frac{\partial^2 B_2}{\partial x^2} \bar{w}_1^3 - \frac{\partial^2 A_1}{\partial y^2} \frac{\partial \bar{w}_1^3}{\partial x} \right. \\ & \left. - 2 \frac{\partial A_1}{\partial y} \frac{\partial^2 \bar{w}_1^3}{\partial x \partial y} - 2 \frac{\partial B_1}{\partial y} \frac{\partial \bar{w}_1^3}{\partial y} - \frac{\partial^2 B_1}{\partial y^2} \bar{w}_1^3 \right) + A_2 \frac{\partial A_1}{\partial y} \frac{\partial \bar{w}_1^3}{\partial x} - A_1 \frac{\partial A_2}{\partial x} \frac{\partial \bar{w}_1^3}{\partial y} \\ & + A_2 \frac{\partial B_1}{\partial y} \bar{w}_1^3 - A_1 \frac{\partial B_2}{\partial x} \bar{w}_1^3 + \frac{\partial B_1}{\partial t} \bar{w}_1^3. \end{aligned}$$

By using the bound of \bar{w}_1^3 given in (5.3.13), it is easy to show that $|\bar{\Xi}_w| \leq \bar{C}$. Use, the maximum principle to obtain that $|\mathcal{L}_{\bar{1},\varepsilon}\bar{w}_1^3| \leq \bar{C}$, which implies that $|\mathcal{L}_{\bar{1},\varepsilon}\bar{w}_1| \leq \bar{C}$. In a similar way, we can obtain that $|\mathcal{L}_{\bar{1},\varepsilon}\bar{w}_2| \leq \bar{C}$ and $|\mathcal{L}_{\bar{1},\varepsilon}\bar{w}_{12}| \leq \bar{C}$, by using appropriate decomposition of layer components \bar{w}_2 and \bar{w}_{12} .

By combining the bounds of $|\mathcal{L}_{11,\varepsilon}\bar{v}|$, $|\mathcal{L}_{11,\varepsilon}\bar{w}_1|$, $|\mathcal{L}_{11,\varepsilon}\bar{w}_2|$ and $|\mathcal{L}_{11,\varepsilon}\bar{w}_{12}|$, one can get that $|\mathcal{L}_{11,\varepsilon}\bar{u}| \leq C$. In a similar way, we can prove the estimates for remaining terms of Lemma 5.3.4. \blacksquare

The exact solution $\bar{u}^{n+1/2}(x, y)$ of (5.3.7) can be decomposed in the following way:

$$\bar{u}^{n+1/2}(x, y) = \bar{c}_y \bar{v}^{n+1/2}(x, y) + \bar{z}^{n+1/2}(x, y). \quad (5.3.15)$$

Lemma 5.3.5. *The components $\bar{v}^{n+1/2}(x, y)$ and $\bar{z}^{n+1/2}(x, y)$ satisfy the following estimates:*

$$\hat{v}_l^{n+1/2}(x, y) = \exp\left(\frac{-a_{1l}(1, y)(1-x)}{\varepsilon}\right), \quad c_y^l = \frac{\varepsilon}{a_{1l}(1, y)} \frac{\partial \hat{u}_l^{n+1/2}}{\partial x}(1, y), \quad (5.3.16)$$

$$\left| \frac{\partial^k \hat{z}_l^{n+1/2}}{\partial x^k}(x, y) \right| \leq C (1 + \varepsilon^{-k+1} B_\varepsilon^1(x)), \quad 0 \leq k \leq 4, \quad l = 1, 2. \quad (5.3.17)$$

Proof. By following the approach from proof of Lemma 3.3.1 and using Lemma 5.3.4, one can obtain the required estimate. \blacksquare

Next, we consider the derivative bounds for the exact solution $\bar{u}^{n+1}(x, y)$ of (5.3.8). In the right hand side of (5.3.8), we have $\bar{u}^{n+1/2}(x, y)$. Therefore, to acquire bounds for the derivative of $\bar{u}^{n+1}(x, y)$ with respect to y , one needs to obtain derivative bound

of $\tilde{u}^{\overline{n+1/2}}(x, y)$ with respect to y . By differentiating (5.3.7) w.r.t y and using estimates from Lemma 5.3.5, we obtain

$$\left| \frac{\partial^k \tilde{u}^{\overline{n+1/2}}}{\partial y^k}(x, y) \right| \leq \vec{C} (1 + \varepsilon^{-k} B_\varepsilon^1(y)), \quad 0 \leq k \leq 4. \quad (5.3.18)$$

Therefore, it follows that

$$\|\mathcal{L}_{2m, \varepsilon} \tilde{u}^{\overline{n+1/2}}\|_\infty \leq C, \quad \|\mathcal{L}_{2m, \varepsilon}^2 \tilde{u}^{\overline{n+1/2}}\|_\infty \leq C, \quad m = 1, 2. \quad (5.3.19)$$

Next, the exact solution $\tilde{u}^{\overline{n+1}}(x, y)$ of (5.3.8) can be decomposed in the following way:

$$\tilde{u}^{\overline{n+1}}(x, y) = \vec{c}_x \tilde{v}^{\overline{n+1}}(x, y) + \tilde{z}^{\overline{n+1}}(x, y). \quad (5.3.20)$$

Lemma 5.3.6. *The components $\tilde{v}^{\overline{n+1}}(x, y)$ and $\tilde{z}^{\overline{n+1}}(x, y)$ satisfy the following estimates:*

$$\hat{v}_l^{\overline{n+1}}(x, y) = \exp\left(\frac{-a_{1l}(x, 1)(1 - y)}{\varepsilon}\right), \quad c_x^l = \frac{\varepsilon}{a_{1l}(x, 1)} \frac{\partial \hat{u}_l^{\overline{n+1}}}{\partial y}(x, 1), \quad (5.3.21)$$

$$\left| \frac{\partial^k \tilde{z}_l^{\overline{n+1}}}{\partial y^k}(x, y) \right| \leq C (1 + \varepsilon^{-k+1} B_\varepsilon^1(y)), \quad 0 \leq k \leq 4, \quad l = 1, 2. \quad (5.3.22)$$

Proof. By using bounds (5.3.19) and following the argument of Lemma 3.3.1, we can obtain the required derivative bounds. \blacksquare

5.4 Analysis of the Spatial Discretization

We discretize problem (5.3.7)-(5.3.8) on a rectangular mesh $\overline{\mathcal{D}}_\varepsilon^N = \overline{\Omega}_x^N \times \overline{\Omega}_y^N \subset \overline{\mathcal{D}}$ (for simplicity, we assume that the number of mesh points is same for both the spatial variables), where $\overline{\Omega}_x^N, \overline{\Omega}_y^N$ are constructed as follows:

Define the transition parameters τ_x, τ_y which are used to separate the coarse and fine parts of the meshes in both the spatial directions, by

$$\tau_x = \min \left\{ \frac{1}{2}, \sigma_x \varepsilon \ln N \right\}, \quad \tau_y = \min \left\{ \frac{1}{2}, \sigma_y \varepsilon \ln N \right\},$$

where σ_x, σ_y are positive constants to be chosen later. Now, we define the mesh $\overline{\Omega}_x^N$ by dividing the interval $[0, 1]$ into two subintervals such as $[0, 1 - \tau_x], [1 - \tau_x, 1]$, then divide each subinterval into $N/2$ mesh-intervals and analogously we proceed in the y -direction. Hence, the step sizes in both the spatial directions will be described as

$$\begin{cases} h_{x,i} = x_i - x_{i-1}, \quad i = 1, \dots, N, & \tilde{h}_{x,i} = h_{x,i} + h_{x,i+1}, \quad i = 1, \dots, N-1, \\ h_{y,j} = y_j - y_{j-1}, \quad j = 1, \dots, N, & \tilde{h}_{y,j} = h_{y,j} + h_{y,j+1}, \quad j = 1, \dots, N-1. \end{cases}$$

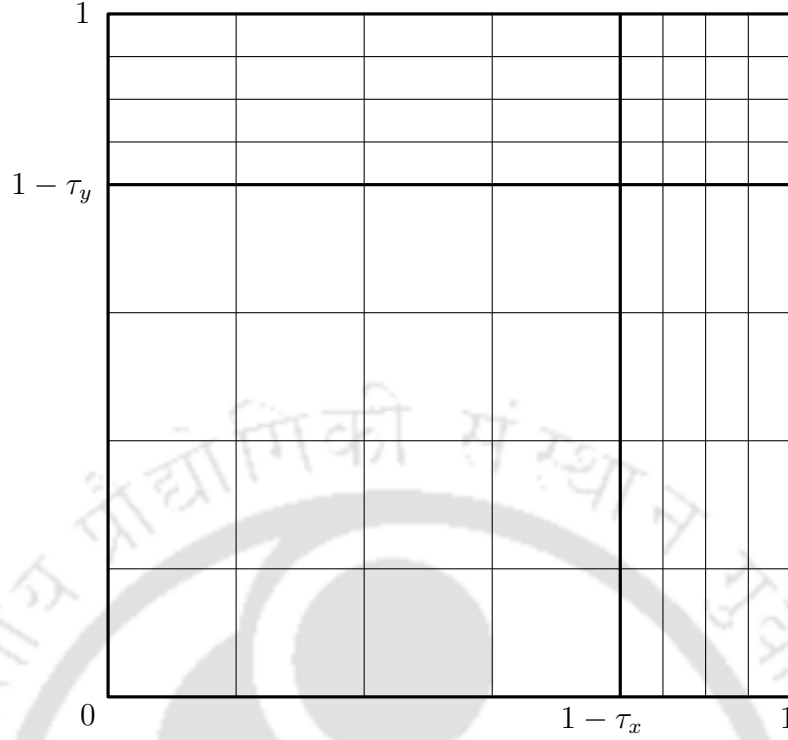


Figure 5.1: A typical example of piecewise-uniform Shishkin mesh $\overline{\mathcal{D}}_\varepsilon^N$ for $N = 8$.

Note that when $\tau_x = \tau_y = 1/2$, the mesh will become uniform and N^{-1} is exponentially small relative to ε (and in this case the method can be analyzed in the classical way).

Also, assume that $H_x = 2(1 - \tau_x)/N$, $H_y = 2(1 - \tau_y)/N$ and $h_x = 2\tau_x/N$, $h_y = 2\tau_y/N$ are the mesh widths in $[0, 1 - \tau_x]$, $[0, 1 - \tau_y]$ and $[1 - \tau_x, 1]$, $[1 - \tau_y, 1]$, respectively. Then, one can easily see that

$$N^{-1} \leq H_x, H_y \leq 2N^{-1}, \quad h_x = 2\sigma_x \varepsilon N^{-1} \ln N, \quad h_y = 2\sigma_y \varepsilon N^{-1} \ln N.$$

5.4.1 The finite difference scheme

Let us denote that $\Omega_{x,\varepsilon}^N = \overline{\Omega}_x^N \cap (0, 1)$, $\Omega_{y,\varepsilon}^N = \overline{\Omega}_y^N \cap (0, 1)$. For simplicity, denote that $a_{1l,i} = a_{1l}(x_i, y)$, $a_{2l,j} = a_{2l}(x, y_j)$, $l = 1, 2$ and also $b_{l1,i}^m = b_{l1}^m(x_i)$, $b_{l2,j}^m = b_{l2}^m(x, y_j)$, $l, m = 1, 2$.

For spatial discretization of (5.3.7)-(5.3.8), we propose the following finite difference scheme:

$$\tilde{U}_{x_i, y_j}^0 = \vec{u}_0(x_i, y_j), \quad (x_i, y_j) \in \overline{\mathcal{D}}_\varepsilon^N, \quad (5.4.1)$$

$$\begin{cases} \left(I + \Delta t \mathcal{L}_{1,\varepsilon}^N \right) \tilde{U}_{x_i, y}^{n+1/2} = \vec{u}(x_i, y, t_n) + \Delta t \vec{f}_1^{n+1}(x_i, y), & (x_i, y) \in \overline{\mathcal{D}}_\varepsilon^N, \\ \tilde{U}_{0, y}^{n+1/2} = \vec{0}, \quad \tilde{U}_{1, y}^{n+1/2} = \vec{0}, & y \in \overline{\Omega}_y^N, \end{cases} \quad (5.4.2)$$

$$\begin{cases} \left(I + \Delta t \mathcal{L}_{2,\varepsilon}^N \right) \vec{U}_{x,y_j}^{n+1} = \vec{U}_{x,y_j}^{n+1/2} + \Delta t f_2^{n+1}(x, y_j), & (x, y_j) \in \overline{\mathcal{D}}_\varepsilon^N, \\ \vec{U}_{x,0}^{n+1} = \vec{0}, \quad \vec{U}_{x,1}^{n+1} = 0, & x \in \overline{\Omega}_x^N, \end{cases} \quad (5.4.3)$$

where $\mathcal{L}_{1,\varepsilon}^N = (\mathcal{L}_{11,\varepsilon}^N, \mathcal{L}_{12,\varepsilon}^N)^T$ and $\mathcal{L}_{2,\varepsilon}^N = (\mathcal{L}_{21,\varepsilon}^N, \mathcal{L}_{22,\varepsilon}^N)^T$ are given by

$$\begin{cases} \mathcal{L}_{1,\varepsilon}^N \equiv -\mathcal{E}\delta_x^2 + A_1(x_i, y)D_x^- + B_1(x_i, y), \\ \mathcal{L}_{2,\varepsilon}^N \equiv -\mathcal{E}\delta_y^2 + A_2(x, y_j)D_y^- + B_2(x, y_j). \end{cases}$$

To simplify the notation, we rewrite the above difference operators as follows:

$$\begin{aligned} \left(I + \Delta t \mathcal{L}_{1,\varepsilon}^N \right) \vec{U}_{x_i,y}^{n+1/2} &= \widehat{\mathcal{L}}_{1,\varepsilon}^N \vec{U}_{x_i,y}^{n+1/2}, \\ \left(I + \Delta t \mathcal{L}_{2,\varepsilon}^N \right) \vec{U}_{x,y_j}^{n+1} &= \widehat{\mathcal{L}}_{2,\varepsilon}^N \vec{U}_{x,y_j}^{n+1}. \end{aligned}$$

After rearranging the terms in (5.4.1)-(5.4.3), the numerical scheme takes the following form:

$$\begin{cases} \widehat{\mathcal{L}}_{11,\varepsilon}^N \vec{U}_{x_i,y}^{n+1/2} \equiv r_{1,i}^{1,-} \widehat{U}_{1,x_{i-1},y}^{n+1/2} + r_{1,i}^{1,c} \widehat{U}_{1,x_i,y}^{n+1/2} + r_{1,i}^{1,+} \widehat{U}_{1,x_{i+1},y}^{n+1/2} + q_{1,i}^{1,c} \widehat{U}_{2,x_i,y}^{n+1/2} \\ \quad = u_1(x_i, y, t_n) + \Delta t f_{11}^{n+1}(x_i, y), & (x_i, y) \in \overline{\mathcal{D}}_\varepsilon^N, \\ \widehat{\mathcal{L}}_{12,\varepsilon}^N \vec{U}_{x_i,y}^{n+1/2} \equiv r_{2,i}^{1,-} \widehat{U}_{2,x_{i-1},y}^{n+1/2} + r_{2,i}^{1,c} \widehat{U}_{2,x_i,y}^{n+1/2} + r_{2,i}^{1,+} \widehat{U}_{2,x_{i+1},y}^{n+1/2} + q_{2,i}^{1,c} \widehat{U}_{1,x_i,y}^{n+1/2} \\ \quad = u_2(x_i, y, t_n) + \Delta t f_{12}^{n+1}(x_i, y), & (x_i, y) \in \overline{\mathcal{D}}_\varepsilon^N, \\ \vec{U}_{0,y}^{n+1/2} = \vec{0}, \quad \vec{U}_{1,y}^{n+1/2} = \vec{0}, & y \in \overline{\Omega}_y^N, \end{cases} \quad (5.4.4)$$

$$\begin{cases} \widehat{\mathcal{L}}_{21,\varepsilon}^N \vec{U}_{x,y_j}^{n+1} \equiv r_{1,j}^{2,-} \widehat{U}_{1,x,y_{j-1}}^{n+1} + r_{1,j}^{2,c} \widehat{U}_{1,x,y_j}^{n+1} + r_{1,j}^{2,+} \widehat{U}_{1,x,y_{j+1}}^{n+1} + q_{1,j}^{2,c} \widehat{U}_{2,x,y_j}^{n+1} \\ \quad = \widehat{U}_{1,x,y_j}^{n+1/2} + \Delta t f_{21}^{n+1}(x, y_j), & (x, y_j) \in \overline{\mathcal{D}}_\varepsilon^N, \\ \widehat{\mathcal{L}}_{22,\varepsilon}^N \vec{U}_{x,y_j}^{n+1} \equiv r_{2,j}^{2,-} \widehat{U}_{2,x,y_{j-1}}^{n+1} + r_{2,j}^{2,c} \widehat{U}_{2,x,y_j}^{n+1} + r_{2,j}^{2,+} \widehat{U}_{2,x,y_{j+1}}^{n+1} + q_{2,j}^{2,c} \widehat{U}_{1,x,y_j}^{n+1} \\ \quad = \widehat{U}_{2,x,y_j}^{n+1/2} + \Delta t f_{22}^{n+1}(x, y_j), & (x, y_j) \in \overline{\mathcal{D}}_\varepsilon^N, \\ \vec{U}_{x,0}^{n+1} = \vec{0}, \quad \vec{U}_{x,1}^{n+1} = \vec{0}, & x \in \overline{\Omega}_x^N, \end{cases} \quad (5.4.5)$$

where the coefficients $r_{l,k}^{m,\bullet}$, $q_{l,k}^{m,\bullet}$, $l, m = 1, 2$, $1 \leq k \leq N-1$, are given by

$$\begin{cases} r_{l,i}^{1,-} = \Delta t r_{l,x,i}^{1,-}, & r_{l,i}^{1,c} = \Delta t r_{l,x,i}^{1,c} + 1, & r_{l,i}^{1,+} = \Delta t r_{l,x,i}^{1,+}, & q_{l,i}^{1,c} = \Delta t q_{l,x,i}^{1,c} \\ r_{l,j}^{2,-} = \Delta t r_{l,y,j}^{2,-}, & r_{l,j}^{2,c} = \Delta t r_{l,y,j}^{2,c} + 1, & r_{l,j}^{2,+} = \Delta t r_{l,y,j}^{2,+}, & q_{l,j}^{2,c} = \Delta t q_{l,y,j}^{2,c}. \end{cases}$$

with

$$\left\{ \begin{array}{l} r_{l,x,i}^{1,-} = \frac{-2\varepsilon}{\tilde{h}_{x,i}h_{x,i}} - \frac{a_{1l,i}}{h_{x,i}}, \\ r_{l,x,i}^{1,c} = \frac{2\varepsilon}{h_{x,i+1}h_{x,i}} + \frac{a_{1l,i}}{h_{x,i}} + b_{ll,i}^1, \\ r_{l,x,i}^{1,+} = \frac{-2\varepsilon}{\tilde{h}_{x,i}h_{x,i+1}}, \\ q_{1,x,i}^{1,c} = b_{12,i}^1, \quad q_{2,x,i}^{1,c} = b_{21,i}^1, \end{array} \right. \left\{ \begin{array}{l} r_{l,y,j}^{2,-} = \frac{-2\varepsilon}{\tilde{h}_{y,j}h_{y,j}} - \frac{a_{2l,j}}{h_{y,j}}, \\ r_{l,y,j}^{2,c} = \frac{2\varepsilon}{h_{y,j+1}h_{y,j}} + \frac{a_{2l,j}}{h_{y,j}} + b_{ll,j}^2, \\ r_{l,y,j}^{2,+} = \frac{-2\varepsilon}{\tilde{h}_{y,j}h_{y,j+1}}, \\ q_{1,y,j}^{2,c} = b_{12,j}^2, \quad q_{2,y,j}^{2,c} = b_{21,j}^2. \end{array} \right.$$

5.4.2 Error analysis

Here, we study the stability of the proposed numerical scheme (5.4.4)-(5.4.5). Finally, we will analyze the ε -uniform convergence.

The difference operator satisfies the following discrete maximum principle.

Lemma 5.4.1. (Discrete maximum principle) *Let $\widehat{\mathcal{L}}_{lm,\varepsilon}^N$, $l, m = 1, 2$, be the difference operators given in (5.4.4)-(5.4.5). Then for any mesh function \vec{Z} , if $\vec{Z} \geq \vec{0}$ on $\partial\mathcal{D}_\varepsilon^N$ and $\widehat{\mathcal{L}}_{lm,\varepsilon}^N \vec{Z} \geq \vec{0}$ in $\mathcal{D}_\varepsilon^N$, then we have $\vec{Z} \geq \vec{0}$ for all $(x_i, y_j) \in \overline{\mathcal{D}_\varepsilon^N}$.*

Proof. By following the approach discussed in Lemma 2.4.1, one can prove maximum principle. \blacksquare

The discrete operator $(I + \Delta t \mathcal{L}_{lm,\varepsilon}^N)$, $l, m = 1, 2$, satisfy the maximum principle, one can easily obtain the following stability bound:

$$\left\| (I + \Delta t \mathcal{L}_{lm,\varepsilon}^N)^{-1} \right\|_\infty \leq \frac{1}{1 + \beta^\ell \Delta t}, \quad \text{for } l, m = 1, 2, \ell = 1, 2. \quad (5.4.6)$$

Hence, the proposed numerical scheme (5.4.2)-(5.4.3) is uniformly stable in the supremum norm. Next, we discuss some technical results which will be used to prove the uniform convergence of the difference scheme (5.4.4)-(5.4.5).

Define the mesh function

$$S_i(\lambda) = \prod_{k=i+1}^N \left(1 + \frac{\lambda h_{x,k}}{\varepsilon} \right)^{-1},$$

where λ is a constant to be fixed later.

Lemma 5.4.2. *If we assume that $\lambda \leq \alpha_1/2$, then the following estimates hold:*

$$\widehat{\mathcal{L}}_{1l,\varepsilon}^N \vec{S}_i(\lambda) \geq \frac{C(\lambda)\Delta t}{\max\{\varepsilon, h_{x,i}\}} S_i(\lambda), \quad l = 1, 2,$$

for $1 \leq i \leq N - 1$, $\vec{S}_i(\lambda) = (S_i(\lambda), S_i(\lambda))^T$.

Proof. We consider

$$\begin{aligned}
\widehat{\mathcal{L}}_{11,\varepsilon}^N \vec{S}_i(\lambda) &= r_{1,i}^{1,-} S_{i-1}(\lambda) + r_{1,i}^{1,c} S_i(\lambda) + r_{1,i}^{1,+} S_{i+1}(\lambda) + q_{1,i}^{1,c} S_i(\lambda) \\
&\geq S_i(\lambda) \left[r_{1,i}^{1,-} \left(\left(1 + \frac{\lambda h_{x,i}}{\varepsilon} \right)^{-1} - 1 \right) + r_{1,i}^{1,+} \left(\left(1 + \frac{\lambda h_{x,i+1}}{\varepsilon} \right) - 1 \right) \right] \\
&= S_i(\lambda) \left[\frac{a_{11,i} \Delta t}{h_{x,i}} \left(\frac{\lambda h_{x,i}}{\varepsilon + \lambda h_{x,i}} \right) + \frac{2\varepsilon \Delta t}{\tilde{h}_{x,i} h_{x,i}} \left(\frac{\lambda h_{x,i}}{\varepsilon + \lambda h_{x,i}} \right) - \frac{2\lambda \Delta t}{\tilde{h}_{x,i}} \right] \\
&\geq S_i(\lambda) \frac{\lambda \Delta t}{\tilde{h}_{x,i}} \frac{(a_{11,i} - 2\lambda) h_{x,i}}{(\varepsilon + \lambda h_{x,i})} \geq \frac{C(\lambda) \Delta t}{\max\{\varepsilon, h_{x,i}\}} S_i(\lambda).
\end{aligned}$$

In a similar manner, one can easily obtain the estimates for the operator $\widehat{\mathcal{L}}_{12,\varepsilon}^N$. ■

Lemma 5.4.3. For $\lambda > 0$, the following bounds hold true:

1. $S_i(\lambda) \geq \exp(-\lambda(1 - x_i)/\varepsilon)$.
2. If $h_{x,i} \leq \varepsilon$ for $k \geq i + 1$, then

$$\prod_{k=i+1}^N \left(1 + \frac{\lambda h_{x,k}}{\varepsilon} \right)^{-1} \leq C \prod_{k=i+1}^N \exp\left(\frac{-2\lambda h_{x,i}}{\varepsilon} \right).$$

Proof.

1. For each k , we have $\exp\left(\frac{-\lambda h_{x,k}}{\varepsilon} \right) \leq \left(1 + \frac{\lambda h_{x,k}}{\varepsilon} \right)^{-1}$.

Multiply these inequalities for $k = i + 1, \dots, N$, we obtain $\exp(-\lambda(1 - x_i)/\varepsilon) \leq S_i(\lambda)$.

2. Since, $h_{x,i} \leq \varepsilon$ for $k \geq i + 1$. Therefore $\exp(2\lambda h_{x,i}/\varepsilon) \leq \exp(2\lambda)$. One can easily obtain that $\exp(2\lambda) \leq C$, for sufficiently large positive constant C . Hence, we have

$$\exp\left(\frac{2\lambda h_{x,i}}{\varepsilon} \right) \leq C \left(1 + \frac{\lambda h_{x,k}}{\varepsilon} \right).$$

Multiply these inequalities for $k = i + 1, \dots, N$, we obtain the desired result. ■

Truncation error

In the remaining part of this section, we study the error analysis of the spatially discretized scheme (5.4.4)-(5.4.5). We will show the convergence of the discrete solution of problem (5.4.4) to the exact solution of (5.3.7), analogously one can obtain the error analysis for (5.3.8).

Now, for the numerical scheme (5.4.4), we define the local truncation error as follows

$$\left\{ \begin{array}{l} \zeta_{i,u}^{1,n+1/2} = (I + \Delta t \mathcal{L}_{11,\varepsilon}^N) \tilde{u}^{n+1/2}(x_i) - (I + \Delta t \mathcal{L}_{11,\varepsilon}) \tilde{u}^{n+1/2}(x_i) \\ \quad = \Delta t \zeta_{x,u}^{1,n+1/2}, \quad 1 \leq i \leq N-1, \\ \zeta_{i,u}^{2,n+1/2} = (I + \Delta t \mathcal{L}_{12,\varepsilon}^N) \tilde{u}^{n+1/2}(x_i) - (I + \Delta t \mathcal{L}_{12,\varepsilon}) \tilde{u}^{n+1/2}(x_i) \\ \quad = \Delta t \zeta_{x,u}^{2,n+1/2}, \quad 1 \leq i \leq N-1, \end{array} \right. \quad (5.4.7)$$

therefore

$$\left\{ \begin{array}{l} \zeta_{x,u}^{1,n+1/2} = (\mathcal{L}_{11,\varepsilon}^N - \mathcal{L}_{11,\varepsilon}) \tilde{u}^{n+1/2}(x_i), \\ \zeta_{x,u}^{2,n+1/2} = (\mathcal{L}_{12,\varepsilon}^N - \mathcal{L}_{12,\varepsilon}) \tilde{u}^{n+1/2}(x_i). \end{array} \right. \quad (5.4.8)$$

For $l = 1, 2$, the truncation error $\zeta_{i,u}^{l,n+1/2}$ is used for 1D convection-diffusion problem (5.3.7), where the dependence on the parameter y is omitted.

Lemma 5.4.4. *The local truncation error given in (5.4.7) satisfies the following estimate:*

$$\left| \zeta_{i,u}^{l,n+1/2} \right| \leq \left\{ \begin{array}{l} C \left[\Delta t h_{x,i} + \frac{\Delta t}{\max\{\varepsilon, h_{x,i}\}} B_\varepsilon^1(x_{i+1}) \right], \quad \text{for } 0 < x_i \leq 1 - \tau_x, \\ C [\Delta t h_{x,i} + \Delta t h_{x,i} \varepsilon^{-2} B_\varepsilon^1(x_i)], \quad \text{for } 1 - \tau_x < x_i < 1, \end{array} \right.$$

where $l = 1, 2$, also C is independent of both $h_{x,i}$ and perturbation parameter ε .

Proof. We consider different cases depending on the location of the mesh point $x_i \in \Omega_{x,\varepsilon}^N$.

Case 1. (Outer region): For $0 < x_i \leq 1 - \tau_x$. To find the appropriate estimate, we consider two subcases depending upon the mesh width $h_{x,i}$ and parameter ε .

Subcase (i). If $h_{x,i} \leq \varepsilon$. By applying (5.3.17) and (4.3.3), we obtain

$$\left| \zeta_{x,z}^{l,n+1/2} \right| \leq C \varepsilon [h_{x,i} + \varepsilon^{-1} B_\varepsilon^1(x_{i+1})] \leq C [h_{x,i} + B_\varepsilon^1(x_{i+1})], \quad l = 1, 2.$$

In addition, one can get

$$\left| \zeta_{x,v}^{l,n+1/2} \right| \leq C \varepsilon^{-1} B_\varepsilon^1(x_{i+1}), \quad \text{for } l = 1, 2.$$

Therefore, combining $\left| \zeta_{x,z}^{l,n+1/2} \right|$, $\left| \zeta_{x,v}^{l,n+1/2} \right|$, $l = 1, 2$, with the spatial decomposition (5.3.15), we deduce that

$$\left| \zeta_{x,u}^{l,n+1/2} \right| \leq C [h_{x,i} + \varepsilon^{-1} B_\varepsilon^1(x_{i+1})], \quad \text{for } l = 1, 2. \quad (5.4.9)$$

Subcase (ii). Assume that $h_{x,i} \geq \varepsilon$. By following the similar argument as in **Case 1**, we obtain

$$|\zeta_{x,z}^{l,n+1/2}| \leq C [h_{x,i} + B_\varepsilon^1(x_{i+1})], \quad \text{for } l = 1, 2. \quad (5.4.10)$$

For $1 \leq i < N/2$, we have

$$\begin{aligned} |\zeta_{x,v}^{1,n+1/2}| &= \left| r_{1,x,i}^{1,-} \widehat{v}_1^{n+1/2}(x_{i-1}) + r_{1,x,i}^{1,c} \widehat{v}_1^{n+1/2}(x_i) + r_{1,x,i}^{1,+} \widehat{v}_1^{n+1/2}(x_{i+1}) \right. \\ &\quad \left. + q_{1,x,i}^{1,c} \widehat{v}_2^{n+1/2}(x_i) - \left(-\varepsilon \frac{\partial^2 \widehat{v}_1^{n+1/2}(x_i)}{\partial x^2} + a_{11}(x_i) \frac{\partial \widehat{v}_1^{n+1/2}(x_i)}{\partial x} \right) \right. \\ &\quad \left. + (b_{11}^1(x_i)) \widehat{v}_1^{n+1/2}(x_i) + b_{12}^1(x_i) \widehat{v}_2^{n+1/2}(x_i) \right| \\ &= \widehat{v}_1^{n+1/2}(x_i) \left[r_{1,x,i}^{1,-} (e^{-a_{11}(1) h_{x,i}/\varepsilon} - 1) + r_{1,x,i}^{1,+} (e^{a_{11}(1) h_{x,i+1}/\varepsilon} - 1) \right. \\ &\quad \left. + a_{11}(1) \frac{(a_{11}(1) - a_{11}(x_i))}{\varepsilon} \right] \\ &\leq Ch_{x,i}^{-1} B_\varepsilon^1(x_{i+1}) + C\varepsilon^{-1} B_\varepsilon^1(x_i). \end{aligned} \quad (5.4.11)$$

In a similar manner, one can easily obtain the estimate for $\zeta_{x,v}^{2,n+1/2}$. By combining results (5.4.10), (5.4.11), for $l = 1, 2$, we get

$$\begin{aligned} |\zeta_{x,u}^{1,n+1/2}| &\leq |\zeta_{x,z}^{1,n+1/2}| + |\zeta_{x,v}^{1,n+1/2}| \leq Ch_{x,i} + C\varepsilon^{-1} B_\varepsilon^1(x_i) + Ch_{x,i}^{-1} B_\varepsilon^1(x_{i+1}) \\ &\leq Ch_{x,i} + Ch_{x,i}^{-1} B_\varepsilon^1(x_{i+1}), \end{aligned}$$

using $\exp(-\theta) \leq 1 + C\theta$, where $\theta = \varepsilon/h_{x,i+1}$ in the above inequality. Same estimate will hold for $|\tau_{x,u}^{2,n+1/2}|$, using analogous technique.

For $i = N/2$, by following the similar technique used in (5.4.11), one can obtain that

$$|\zeta_{x,v}^{l,n+1/2}| \leq Ch_{x,i}^{-1} B_\varepsilon^1(x_i), \quad l = 1, 2. \quad (5.4.12)$$

Hence combining estimates (5.4.10) and (5.4.12), for $l = 1, 2$, we get

$$|\zeta_{x,u}^{l,n+1/2}| \leq Ch_{x,i} + Ch_{x,i}^{-1} B_\varepsilon^1(x_{i+1}).$$

Case 2. (Inner region): For $1 - \tau_x < x_i < 1$. By applying the derivative bound estimates (5.3.17) and (4.3.3), we have

$$|\zeta_{x,z}^{l,n+1/2}| \leq Ch_{x,i} + (B_\varepsilon^1(x_{i+1}) - B_\varepsilon^1(x_{i-1})) \leq Ch_{x,i} (1 + \varepsilon^{-1} B_\varepsilon^1(x_{i+1})), \quad l = 1, 2.$$

and

$$|\zeta_{x,v}^{l,n+1/2}| \leq Ch_{x,i} \varepsilon^{-2} B_\varepsilon^1(x_{i+1}), \quad l = 1, 2. \quad (5.4.13)$$

For $l = 1, 2$, adding both the above estimates, one can get

$$|\zeta_{x,u}^{l,n+1/2}| \leq C h_{x,i} + C h_{x,i} \varepsilon^{-2} B_\varepsilon^1(x_{i+1}).$$

By combining these estimates, we can obtain the desired result. \blacksquare

Next, we discuss the convergence theorem for the numerical scheme (5.4.2) which will be used to prove the convergence analysis of the fully discrete difference scheme in the next section.

Lemma 5.4.5. *Let $\vec{u}^{n+1/2}(x, y)$ and $\vec{U}_{x,y}^{n+1/2}$ be the continuous and the discrete solutions of (5.3.7) and (5.4.2), respectively. If we assume that $\sigma_x \geq 1/\alpha_1$ and $\lambda = \alpha_1/2$, then we have the following error bound*

$$\left| \vec{u}^{n+1/2}(x_i, y) - \vec{U}_{x_i,y}^{n+1/2} \right| \leq \vec{C} N^{-1} \ln N, \quad y \in \bar{\Omega}_{y,\varepsilon}^N, \quad (5.4.14)$$

where C is a positive constant independent of y , ε and N .

Proof. To estimate the error term $\left| \vec{u}^{n+1/2}(x_i, y) - \vec{U}_{x_i,y}^{n+1/2} \right|$, we consider the following discrete barrier function

$$\mathfrak{B}_{cd}^\pm(x_i) = \vec{\mathbb{B}}_u \pm \left(\vec{u}^{n+1/2}(x_i, y) - \vec{U}_{x_i,y}^{n+1/2} \right), \quad \text{for } 0 \leq i \leq N,$$

where $\vec{\mathbb{B}}_u = (\mathbb{B}_u, \mathbb{B}_u)^T$ is defined as

$$\mathbb{B}_u(x_i) = \begin{cases} Ch_{x,i}(1+x_i) + C \frac{h_{x,i}}{\varepsilon} S_i(\lambda), & \text{for } h_{x,i} \leq \varepsilon, \\ Ch_{x,i}(1+x_i) + CS_{i+1}(\lambda), & \text{for } h_{x,i} \geq \varepsilon. \end{cases}$$

If $h_{x,i} \leq \varepsilon$, by employing Lemma 5.4.2 and Lemma 5.4.3, we obtain that

$$\widehat{\mathcal{L}}_{11,\varepsilon}^N \vec{\mathbb{B}}_u \geq C \Delta t h_{x,i} + C \frac{h_{x,i}}{\varepsilon} \frac{\Delta t}{\max\{\varepsilon, h_{x,i}\}} S_i(\lambda) \geq \left| \zeta_{i,u}^{1,n+1/2} \right|,$$

In a similar way, one can show that $\widehat{\mathcal{L}}_{12,\varepsilon}^N \vec{\mathbb{B}}_u \geq \left| \zeta_{i,u}^{2,n+1/2} \right|$.

Consider the case $h_{x,i} \geq \varepsilon$, from Lemma 5.4.2 and Lemma 5.4.3, we obtain that

$$\widehat{\mathcal{L}}_{11,\varepsilon}^N \vec{\mathbb{B}}_u \geq C \Delta t h_{x,i} + C \frac{\Delta t}{h_{x,i}} S_{i+1}(\lambda) \geq \left| \zeta_{i,u}^{1,n+1/2} \right|.$$

An analogous estimate holds for the error component $\zeta_{i,u}^{2,n+1/2}$. Therefore, by applying the discrete maximum principle (Lemma 5.4.1) to $\mathfrak{B}_{cd}^\pm(x_i)$, we deduce that

$$\left| \vec{u}^{n+1/2}(x_i, y) - \vec{U}_{x_i,y}^{n+1/2} \right| \leq \vec{C} N^{-1} \ln N. \quad \blacksquare$$

Lemma 5.4.6. Let $\tilde{u}^n(x, y)$ be the exact solution of (5.3.7)-(5.3.8) and \tilde{U}_{x_i, y_j}^n be the spatial semidiscrete solution of (5.4.2)-(5.4.3). Then, the following error estimate holds:

$$\left| \tilde{u}^{n+1}(x_i, y_j) - \tilde{U}_{x_i, y_j}^{n+1} \right| \leq \vec{C} N^{-1} \ln N, \text{ for all } (x_i, y_j) \in \overline{\mathcal{D}}_\varepsilon^N, \quad (5.4.15)$$

where \vec{C} is a positive constant independent of ε and N .

Proof. Let $\tilde{u}^{n+1/2}(x, y)$ be the exact solution of (5.3.7) and its numerical approximation be $\tilde{U}_{x_i, y_j}^{n+1/2}$. Then from Lemma 5.4.5, we have

$$\left| \tilde{u}^{n+1/2}(x_i, y) - \tilde{U}_{x_i, y}^{n+1/2} \right| \leq \vec{C} N^{-1} \ln N, \quad y \in \overline{\Omega}_y^N.$$

Next, we introduce the auxiliary equation

$$\begin{cases} \left(I + \Delta t \mathcal{L}_{\frac{\bar{x}, \bar{y}}{2}, \varepsilon}^N \right) \tilde{U}_{x, y_j}^{n+1} = \tilde{u}^{n+1/2}(x, y_j) + \Delta t \vec{f}_2^{n+1}(x, y_j), & (x, y_j) \in \overline{\mathcal{D}}_\varepsilon^N, \\ \tilde{U}_{x, 0}^{n+1} = \vec{0}, \quad \tilde{U}_{x, 1}^{n+1} = \vec{0}, & x \in \overline{\Omega}_x^N, \end{cases} \quad (5.4.16)$$

By following the argument used in Lemma 5.4.5, one can obtain that

$$\left| \tilde{u}^{n+1}(x, y_j) - \tilde{U}_{x, y_j}^{n+1} \right| \leq \vec{C} N^{-1} \ln N, \quad x \in \overline{\Omega}_x^N.$$

The error term can be expressed as

$$\tilde{u}^{n+1}(x_i, y_j) - \tilde{U}_{x_i, y_j}^{n+1} = \tilde{u}^{n+1}(x_i, y_j) - \tilde{U}_{x_i, y_j}^{n+1} + \tilde{U}_{x_i, y_j}^{n+1} - \tilde{U}_{x_i, y_j}^{n+1}.$$

Also, we have

$$\tilde{U}_{x_i, y_j}^{n+1} - \tilde{U}_{x_i, y_j}^{n+1} = \left(I + \Delta t \mathcal{L}_{\frac{\bar{x}, \bar{y}}{2}, \varepsilon}^N \right)^{-1} \left(\tilde{u}^{n+1/2}(x_i, y_j) - \tilde{U}_{x_i, y_j}^{n+1/2} \right).$$

Then, by using the stability condition (5.4.6), the required result (5.4.15) follows. \blacksquare

The spatial semidiscretization defined on the piecewise-uniform Shishkin mesh is uniformly convergent of almost first-order (up to a logarithmic factor). An immediate consequence of the above theorem is the following result.

Lemma 5.4.7. If $N^{-\nu} \leq C \Delta t$ with $0 < \nu < 1$, then from (5.4.15), one can have the following estimate:

$$\left| \tilde{u}^{n+1}(x_i, y_j) - \tilde{U}_{x_i, y_j}^{n+1} \right| \leq \vec{C} \Delta t N^{-1+\nu} \ln N, \quad (x_i, y_j) \in \overline{\mathcal{D}}_\varepsilon^N. \quad (5.4.17)$$

This error estimate helps us to obtain the uniform convergence of the numerical solution of the fully discrete scheme in the following section.

5.5 The Fully Discrete Scheme

Combining the time semidiscretization scheme (5.3.7)-(5.3.8) and the spatial discretization (5.4.4)-(5.4.5), the following fully discrete scheme is deduced on the mesh $\bar{\mathcal{G}}^{N,M} = \bar{\mathcal{D}}_\varepsilon^N \times \bar{\Upsilon}^M$:

$$\left\{ \begin{array}{l} \vec{U}_{x_i, y_j}^0 = \vec{u}_0(x_i, y_j), \quad (x_i, y_j) \in \bar{\mathcal{D}}_\varepsilon^N, \\ \left\{ \begin{array}{l} \widehat{\mathcal{L}}_{11, \varepsilon}^N \vec{U}_{x_i, y}^{n+1/2} \equiv r_{1,i}^{1,-} U_{1,x_{i-1}, y}^{n+1/2} + r_{1,i}^{1,c} U_{1,x_i, y}^{n+1/2} + r_{1,i}^{1,+} U_{1,x_{i+1}, y}^{n+1/2} + q_{1,i}^{1,c} U_{2,x_i, y}^{n+1/2} \\ = U_{1,x_i, y}^n + \Delta t f_{11}^{n+1}(x_i, y), \quad (x_i, y) \in \bar{\mathcal{D}}_\varepsilon^N, \\ \widehat{\mathcal{L}}_{12, \varepsilon}^N \vec{U}_{x_i, y}^{n+1/2} \equiv r_{2,i}^{1,-} U_{2,x_{i-1}, y}^{n+1/2} + r_{2,i}^{1,c} U_{2,x_i, y}^{n+1/2} + r_{2,i}^{1,+} U_{2,x_{i+1}, y}^{n+1/2} + q_{2,i}^{1,c} U_{1,x_i, y}^{n+1/2} \\ = U_{2,x_i, y}^n + \Delta t f_{12}^{n+1}(x_i, y), \quad (x_i, y) \in \bar{\mathcal{D}}_\varepsilon^N \end{array} \right. \\ \vec{U}_{0,y}^{n+1/2} = \vec{0}, \quad \vec{U}_{1,y}^{n+1/2} = \vec{0}, \quad y \in \bar{\Omega}_y^N, \end{array} \right. \quad (5.5.1)$$

$$\left\{ \begin{array}{l} \left\{ \begin{array}{l} \widehat{\mathcal{L}}_{21, \varepsilon}^N \vec{U}_{x, y_j}^{n+1} \equiv r_{1,j}^{2,-} U_{1,x, y_{j-1}}^{n+1} + r_{1,j}^{2,c} U_{1,x, y_j}^{n+1} + r_{1,j}^{2,+} U_{1,x, y_{j+1}}^{n+1} + q_{1,j}^{2,c} U_{2,x, y_j}^{n+1} \\ = U_{1,x, y_j}^{n+1/2} + \Delta t f_{21}^{n+1}(x, y_j), \quad (x, y_j) \in \bar{\mathcal{D}}_\varepsilon^N, \\ \widehat{\mathcal{L}}_{22, \varepsilon}^N \vec{U}_{x, y_j}^{n+1} \equiv r_{2,j}^{2,-} U_{2,x, y_{j-1}}^{n+1} + r_{2,j}^{2,c} U_{2,x, y_j}^{n+1} + r_{2,j}^{2,+} U_{2,x, y_{j+1}}^{n+1} + q_{2,j}^{2,c} U_{1,x, y_j}^{n+1} \\ = U_{2,x, y_j}^{n+1/2} + \Delta t f_{22}^{n+1}(x, y_j), \quad (x, y_j) \in \bar{\mathcal{D}}_\varepsilon^N, \end{array} \right. \\ \vec{U}_{x,0}^{n+1} = \vec{0}, \quad \vec{U}_{x,1}^{n+1} = \vec{0}, \quad x \in \bar{\Omega}_x^N, \end{array} \right. \quad (5.5.2)$$

where the coefficients $r_{l,k}^{m,\bullet}$, $q_{l,k}^{m,\bullet}$, $l, m = 1, 2$, $1 \leq k \leq N-1$, are described in (5.4.1) and $\vec{U}_{x_i, y_j}^n = \vec{U}(x_i, y_j, t_n)$ is the discrete approximation to the exact solution $\vec{u}(x, y, t)$ of the model problem (5.1.1).

Theorem 5.5.1. (Global error) *Let $\vec{u}(x, y, t_n)$ be the exact solution of (5.1.1) and \vec{U}_{x_i, y_j}^n be the numerical solution of the fully discrete scheme (5.5.1)-(5.5.2) at time level $t_n = \Delta t$. If $N^{-\nu} \leq C\Delta t$ with $0 < \nu < 1$, then the global error associated with the numerical method (5.5.1)-(5.5.2) satisfies*

$$\left\| \vec{u}(x_i, y_j, t_n) - \vec{U}_{x_i, y_j}^n \right\|_\infty \leq C(\Delta t + N^{-1+\nu} \ln N), \quad (x_i, y_j, t_n) \in \bar{\mathcal{G}}_\varepsilon^{N,M}. \quad (5.5.3)$$

where C is a positive constant independent of ε and N .

Proof. By using the methodology from the proof of Theorem 2.5.1, the desired result (5.5.3) follows. \blacksquare

5.6 Numerical Results

In this section, we present numerical results obtained by applying the numerical method described in Section 5.5 to a test problem. For the sake of simplicity, we have chosen the decomposition for the reaction term as: $b_{lm}^1(x, y, t) = b_{lm}^2(x, y, t) = b_{lm}(x, y, t)/2$, $l, m = 1, 2$, in the test problem.

Example 5.6.1. Consider the following system of parabolic IBVP on $\mathcal{G} = (0, 1)^2 \times (0, 1]$:

$$\left\{ \begin{array}{l} \frac{\partial u_1}{\partial t} - \varepsilon \Delta u_1 + \left(1 + \frac{xy}{2}\right) \frac{\partial u_1}{\partial x} + (1 + x^2 y) \frac{\partial u_1}{\partial y} + (4 + 2(x^2 + y^2))u_1 - (x^2 + y^2)u_2 \\ \qquad \qquad \qquad = xy(1-x)(1-y)t^2 + x^2 y^2(1-x)(1-y)e^{-t}, \\ \frac{\partial u_2}{\partial t} - \varepsilon \Delta u_2 + (1 + x^2 y) \frac{\partial u_2}{\partial x} + \left(1 + \frac{x^2 y}{2}\right) \frac{\partial u_2}{\partial y} - (2x^2 + y^2)u_1 + (2 + (2x^2 + y^2))u_2 \\ \qquad \qquad \qquad = xy(1-x^2)(1-y^2)t + xy(1-x)(1-y)e^{-t}, \\ \vec{u}(x, y, 0) = \vec{0}, \quad (x, y) \in (0, 1)^2, \\ \vec{u}(0, y, t) = \vec{u}(1, y, t) = \vec{0}, \quad (y, t) \in [0, 1] \times [0, 1], \\ \vec{u}(x, 0, t) = \vec{u}(x, 1, t) = \vec{0}, \quad (x, t) \in [0, 1] \times [0, 1]. \end{array} \right.$$

The exact solution of Example 5.6.1 is not known, in order to compute maximum error and order of convergence of the proposed scheme, we use the double mesh principle which is described as follows:

Let $\vec{U}_{x_{2i}, y_{2j}}^{2n}$ denotes the numerical solution obtained on the fine mesh $\mathcal{G}_\varepsilon^{2N, 2M} = \mathcal{D}_\varepsilon^{2N} \times \Upsilon^{2M}$ with $2N$ mesh-intervals in both x - and y -directions and $2M$ mesh-intervals in the t -direction, which contains the mesh points of the original mesh and their midpoints. Then for each ε , the maximum pointwise error and the uniform error are calculated by

$$E_{l,\varepsilon}^{N,M} = \max_{(x_i, y_j, t_n) \in \bar{\mathcal{G}}_\varepsilon^{N,M}} \left| U_{l, x_{2i}, y_{2j}}^{2n} - U_{l, x_i, y_j}^n \right|, \quad E_l^{N,M} = \max_{S_\varepsilon} E_{l,\varepsilon}^{N,M}, \quad l = 1, 2.$$

The corresponding order of convergence is given by

$$P_{l,\varepsilon}^{N,M} = \log_2 \left(\frac{E_{l,\varepsilon}^{N,M}}{E_{l,\varepsilon}^{2N, 2M}} \right), \quad P_l^{N,M} = \log_2 \left(\frac{E_l^{N,M}}{E_l^{2N, 2M}} \right), \quad l = 1, 2.$$

For the numerical computation, we have taken the number of intervals in the spatial and temporal directions as $N = 8, 16, 32, 64, 128$, and $M = N/4$, respectively. For evaluating the uniform error and the order of convergence, we consider the singular perturbation parameters from the set $S_\varepsilon = \{\varepsilon | \varepsilon = 2^{-2}, \dots, 2^{-10}\}$.

In order to visualize the numerical solution for Example 5.6.1, we displayed the surface plots of the numerical solution components U_1 and U_2 in Fig. 5.2 and Fig. 5.3 at $t = 1$.

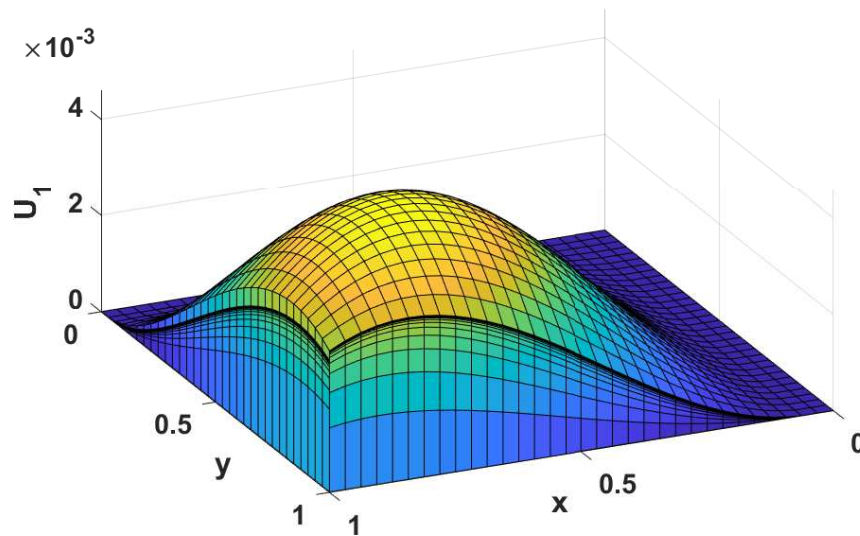


Figure 5.2: Numerical solution U_1 of Example 5.6.1 for $\varepsilon = 2^{-14}$ with $N = 32$, $M = 8$.

For various values of N and M , the maximum errors $E_l^{N,M}$ and the corresponding order of convergence $P_l^{N,M}$ for Example 5.6.1 are presented in Table 5.1. The numerical results given in this table reveal the convergence of almost first-order in space and first-order in time, independent of ε .

In order to reveal the numerical order of convergence, we have plotted N vs. the maximum pointwise errors in loglog plot in Fig. 5.4 and Fig. 5.5 which again confirms the almost first-order convergence of the numerical solution.

5.7 Conclusion

In this chapter, a computational method has been proposed for solving singularly perturbed system of 2D parabolic convection-diffusion IBVP. To accomplish this purpose, the scheme is constructed on a special rectangular mesh involving the tensor-product of 1D piecewise-uniform Shishkin meshes for the spatial discretization and uniform mesh for the temporal discretization. In the proposed numerical scheme we have combined the fractional-step method for the time discretization and the classical upwind difference scheme for the spatial discretization. It has been proved that the numerical scheme converges ε -uniformly with almost first-order (up to a logarithmic factor) accurate in space and first-order accurate in time. Numerical results are presented to validate the efficiency of the proposed scheme.

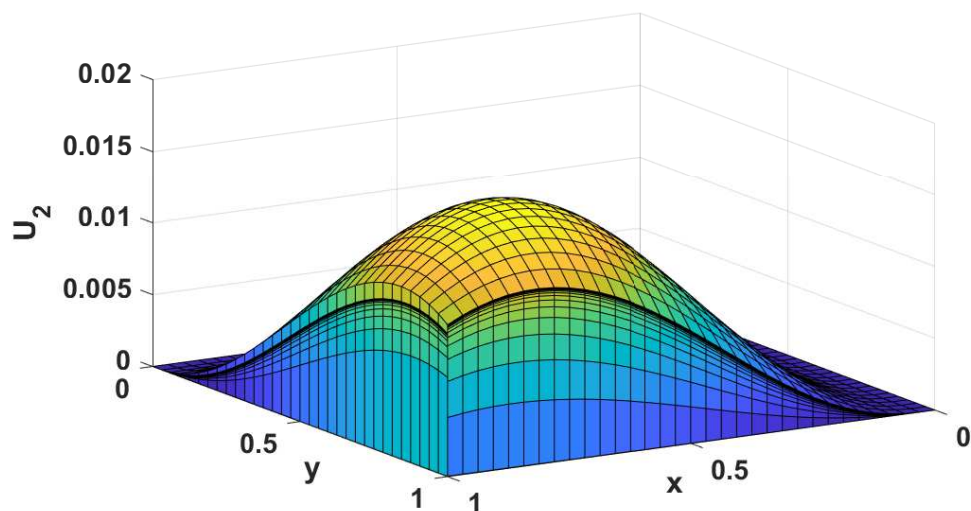


Figure 5.3: Numerical solution U_2 of Example 5.6.1 for $\varepsilon = 2^{-14}$ with $N = 32$, $M = 8$.

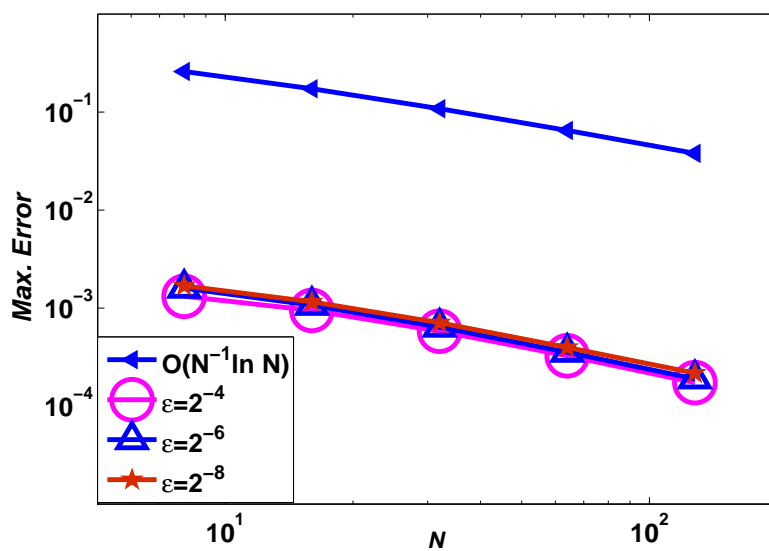
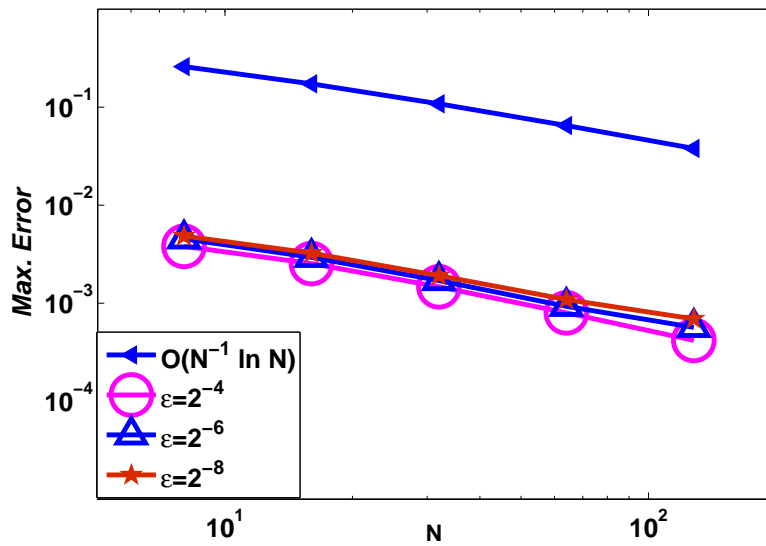


Figure 5.4: Loglog plot for the spatial order of convergence associated with numerical solution U_1 of Example 5.6.1.

Table 5.1: Uniform errors and the corresponding orders of convergence for Example 5.6.1.

$\varepsilon \in S_\varepsilon$	Number of mesh-intervals N				
	8	16	32	64	128
$E_1^{N,M}$	1.6937e-03	1.1800e-03	7.2475e-04	4.0656e-04	2.2103e-04
$P_1^{N,M}$	0.5214	0.7031	0.8340	0.8792	
$E_2^{N,M}$	4.8767e-03	3.3157e-03	1.9569e-03	1.1518e-03	6.9843e-04
$P_2^{N,M}$	0.5566	0.7607	0.7646	0.8217	

Figure 5.5: Loglog plot for the spatial order of convergence associated with numerical solution U_2 of Example 5.6.1.

Uniformly Convergent Fractional-Step Method for Singularly Perturbed System of 2D Parabolic Reaction-Diffusion Problems

This chapter discusses the numerical solution of singularly perturbed system of 2D parabolic reaction-diffusion problems. The proposed numerical scheme consists of a fractional-step method on uniform mesh for time discretization and the classical central difference scheme on a piecewise-uniform Shishkin mesh for spatial discretization. Parameter-uniform error estimates are derived and it has been proved that the proposed numerical scheme is of first-order convergence in time and second-order convergence up to a logarithmic factor in space. To support the theoretical results, numerical experiments are carried out.

6.1 Introduction

In this chapter, we consider the following singularly perturbed system of 2D parabolic reaction-diffusion IBVP on the domain $\mathcal{G} := \mathcal{D} \times (0, T]$, $\mathcal{D} = \Omega_x \times \Omega_y = (0, 1) \times (0, 1)$:

$$\begin{cases} \frac{\partial \vec{u}}{\partial t} + \mathcal{L}_\varepsilon \vec{u} = \vec{f}, & (x, y, t) \in \mathcal{G}, \\ \vec{u}(x, y, 0) = \vec{u}_0(x, y), & (x, y) \in \mathcal{D}, \\ \vec{u}(0, y, t) = \vec{u}(1, y, t) = \vec{0}, & (y, t) \in [0, 1] \times [0, T], \\ \vec{u}(x, 0, t) = \vec{u}(x, 1, t) = \vec{0}, & (x, t) \in [0, 1] \times [0, T], \end{cases} \quad (6.1.1)$$

where the spatial differential operator \mathcal{L}_ε is given by

$$\mathcal{L}_\varepsilon \equiv -\varepsilon^2 \Delta + B(x, y, t).$$

The diffusion and reaction coefficients of the model problem (6.1.1) are given by $\mathcal{E} = \text{diag}(\varepsilon, \varepsilon)$, $0 < \varepsilon \ll 1$ and $B = \{b_{lm}\}_{l,m=1}^2$, respectively. Throughout this chapter, the

reaction coefficient matrix $B(x, y, t)$ satisfies the following conditions:

$$\begin{cases} b_{ll}(x, y, t) > \gamma_\beta > 0, & b_{lm}(x, y, t) \leq 0, \text{ for } l \neq m, \\ \min_{(x,y,t) \in \bar{\mathcal{G}}} \{b_{11}(x, y, t) + b_{12}(x, y, t), b_{21}(x, y, t) + b_{22}(x, y, t)\} \geq \beta^2 > 0. \end{cases} \quad (6.1.2)$$

Also we assume that $\gamma_1 = \max_{\bar{\mathcal{G}}} \{|b_{12}|/b_{11}\}$, $\gamma_2 = \max_{\bar{\mathcal{G}}} \{|b_{21}|/b_{22}\}$,

$$0 \leq \gamma := \max\{\gamma_1, \gamma_2\} < 1. \quad (6.1.3)$$

We consider the following smoothness assumptions for the source term and the initial condition:

$$\vec{f} \in (\mathcal{C}_\lambda^2(\bar{\mathcal{G}}))^2 \quad \text{and} \quad \vec{u}_0 \in (\mathcal{C}_0^4(\bar{\mathcal{D}}))^2, \quad (6.1.4)$$

with the compatibility conditions at the corner points

$$\begin{cases} \vec{u}_0(x, y) = \vec{0}, & \text{on } \partial\mathcal{D}, \\ \vec{f}(x, y, 0) - \mathcal{L}_\varepsilon \vec{u}_0(x, y) = \vec{0}, & \text{on } \partial\mathcal{D}, \\ \vec{f}_t(x, y, 0) + (\mathcal{L}_\varepsilon)^2 \vec{u}_0(x, y) - \mathcal{L}_\varepsilon \vec{f}(x, y, 0) = \vec{0}, & \text{on } \partial\mathcal{D}, \\ \vec{f}(x, y, t) = \vec{0}, & \text{on } \{0, 1\} \times \{0, 1\} \times (0, T]. \end{cases} \quad (6.1.5)$$

Under the above assumptions, the model problem (6.1.1) admits a unique solution, which exhibits the boundary layer along sides $x = 0, 1$ and $y = 0, 1$ with corner layers at $(0, 0), (1, 0), (0, 1)$ and $(1, 1)$.

The rest of this chapter is organized as follows: In Section 6.2, we discuss some results concerning to the analytic behavior of the exact solution. In Section 6.3, the time semidiscretization has been introduced and this section ends with discussion of the asymptotic behaviour of the exact solution of the semidiscrete problems resulting after the time discretization. The spatial discretization process has been introduced by using a finite differences scheme on a piecewise-uniform Shishkin mesh in Section 6.4. Later, we deduce the main convergence result of this chapter. Numerical results are presented in Section 6.5 and the chapter ends with Section 6.6 that summarize the main conclusions.

6.2 The Continuous Problem

In this section, we concentrate on analytical aspect of the exact solution $\vec{u}(x, t)$ of the continuous problem (6.1.1).

Lemma 6.2.1. (Maximum Principle). Let $(\frac{\partial}{\partial t} + \mathcal{L}_{\vec{z}})$ be the differential operator defined in (6.1.1) and assume that the coefficients of the matrix B satisfies (6.1.2). Then for $\vec{z} \geq \vec{0}$ on $\partial\mathcal{G}$ and $(\frac{\partial}{\partial t} + \mathcal{L}_{\vec{z}})\vec{z} \geq \vec{0}$ in \mathcal{G} , we have $\vec{z} \geq \vec{0}$, for all $(x, y, t) \in \bar{\mathcal{G}}$.

Proof. We prove this lemma by contradiction. Assume that there exists a point $(x_0, y_0, t_0) \in \mathcal{G}$ such that

$$\min\{z_1(x_0, y_0, t_0), z_2(x_0, y_0, t_0)\} = \min\left\{\min_{(x,y,t) \in \bar{\mathcal{G}}} z_1(x, y, t), \min_{(x,y,t) \in \bar{\mathcal{G}}} z_2(x, y, t)\right\} < 0.$$

Without loss of generality we assume that $z_1(x_0, y_0, t_0) \leq z_2(x_0, y_0, t_0)$. Then, we have

$$\left(\frac{\partial z_1}{\partial t} + (\mathcal{L}_{\vec{z}})_1 z_1\right)(x_0, y_0, t_0) \leq b_{11}(x_0, y_0, t_0)z_1(x_0, y_0, t_0) + b_{12}(x_0, y_0, t_0)z_2(x_0, y_0, t_0) < 0,$$

which contradicts the hypothesis of the lemma, hence $\vec{z} \geq \vec{0}$, for all $(x, y, t) \in \bar{\mathcal{G}}$. ■

Next, define the decoupled differential operators by

$$\mathcal{L}_l v = \frac{\partial v}{\partial t} - \varepsilon \left(\frac{\partial^2 v}{\partial x^2} + \frac{\partial^2 v}{\partial y^2} \right) + b_{ll} v, \quad l = 1, 2.$$

Lemma 6.2.2. Let \vec{u} be the solution of the model problem (6.1.1). For $j = 0, 1, \dots$, define the sequence of vector-valued functions $\vec{u}^{[j]} = (u_1^{[j]}, u_2^{[j]})^T$ as follows: let $\vec{u}^{[0]}$ be any function in $C(\bar{\mathcal{G}})^2$ and for $j = 0, 1, \dots$, the function $\vec{u}^{[k]}$ satisfy

$$\begin{cases} \mathcal{L}_1 u_1^{[j]} = f_1 - b_{12} u_2^{[j-1]}, & \mathcal{L}_2 u_2^{[j]} = f_2 - b_{21} u_1^{[j-1]} \\ u_l^{[j]}(x, y, 0) = u_{0l}(x, y), & (x, y) \in \mathcal{D}, \quad l = 1, 2, \\ u_l^{[j]}(x, y, t) = 0, & \text{on } \partial\mathcal{D} \times [0, T], \quad l = 1, 2. \end{cases} \quad (6.2.1)$$

Then $\lim_{j \rightarrow \infty} \vec{u}^{[j]} = \vec{u}$. Furthermore, we have

$$\|\vec{u}\|_{\infty} \leq \frac{1}{1 - \gamma} \left(\frac{1}{\gamma_{\beta}} \|f\|_{\infty} + \|\vec{u}_0\|_{\infty} \right). \quad (6.2.2)$$

Proof. By following the methodology of Lemma 5.2.3, one can obtain the required estimate. ■

From Lemma 6.2.2, one can also conclude that the continuous problem (6.1.1) has a unique solution.

Lemma 6.2.3. For all non-negative integer k_0 satisfying $0 \leq k_0 \leq 2$, the time derivatives of the exact solution \vec{u} of the IBVP (6.1.1) satisfy the following estimate

$$\left| \frac{\partial^{k_0} \vec{u}}{\partial t^{k_0}}(x, y, t) \right| \leq \vec{C}, \quad \text{for all } (x, y, t) \in \mathcal{G}.$$

Proof. To prove the bounds of the time derivative of exact solution \vec{u} of (6.1.1), we consider various cases.

Case 1. Firstly, we consider the case for $k_0 = 0$. From Lemma 6.2.2, we have

$$\|\vec{u}\|_\infty \leq \frac{1}{1-\gamma} \left(\frac{1}{\gamma\beta} \|\vec{f}\|_\infty + \|\vec{u}_0\|_\infty \right).$$

By using the regularity of the source term \vec{f} and the initial condition \vec{u}_0 as given in (6.1.4), we can obtain that $|\vec{u}(x, y, t)| \leq \vec{C}$ for all $(x, y, t) \in \mathcal{G}$.

Case 2. Next, consider $k_0 = 1$. On $\partial\mathcal{D} \times [0, T]$, we have $\vec{u} = \vec{0}$ therefore $\vec{u}_t = \vec{0}$. By using the regularity condition (6.1.4), we get $|\vec{u}_t(x, y, 0)| \leq \vec{C}$ for all $(x, y) \in \mathcal{D}$.

Differentiating (6.1.1) with respect to t , we get

$$\left(\frac{\partial}{\partial t} + \mathcal{L}_\varepsilon \right) \vec{u}_t(x, t) = \vec{u}_{tt} + \mathcal{L}_\varepsilon \vec{u}_t = \vec{f}_t - B_t \vec{u}. \quad (6.2.3)$$

Therefore, we have $\left| \left(\frac{\partial}{\partial t} + \mathcal{L}_\varepsilon \right) \vec{u}_t(x, t) \right| \leq \vec{C}$, as \vec{f}_t, B_t are sufficiently smooth functions.

By using the maximum principle, Lemma 6.2.1, one can obtain that $|\vec{u}_t| \leq \vec{C}$.

Case 3. Finally, we consider the case for $k_0 = 2$. On $\partial\mathcal{D} \times [0, T]$, we have $\vec{u} = \vec{0}$, therefore $\vec{u}_t = \vec{0}$ and $\vec{u}_{tt} = \vec{0}$. Again, by using the regularity condition (6.1.4), we get $|\vec{u}_{tt}(x, y, 0)| \leq \vec{C}$, for all $(x, y) \in \mathcal{D}$.

Differentiating (6.2.3) with respect to t , we get

$$\left(\frac{\partial}{\partial t} + \mathcal{L}_\varepsilon \right) \vec{u}_{tt}(x, t) = \vec{u}_{ttt} + \mathcal{L}_\varepsilon \vec{u}_{tt} = \vec{f}_{tt} - 2B_t \vec{u}_t - B_{tt} \vec{u}. \quad (6.2.4)$$

Since, \vec{f}_{tt}, B_t and B_{tt} are sufficiently smooth, by using the maximum principle given in Lemma 6.2.1, we can show that $|\vec{u}_{tt}| \leq \vec{C}$. This completes the proof. ■

Lemma 6.2.4. For all non-negative integer k satisfying $0 \leq k \leq 4$, the exact solution \vec{u} of the IBVP (6.1.1) satisfy the following estimate

$$\left| \frac{\partial^k u_l}{\partial x^k}(x, y, t) \right| \leq C (1 + \varepsilon^{-i} \mathcal{B}_\varepsilon(x)), \quad \left| \frac{\partial^k u_l}{\partial y^k}(x, y, t) \right| \leq C (1 + \varepsilon^{-i} \mathcal{B}_\varepsilon(y)),$$

where $l = 1, 2$ and $(x, y, t) \in \mathcal{G}$.

Proof. By using the technique of [38, Lemma 2.3] and Lemma 6.2.3, one can obtain the required estimate. ■

6.3 The Time Semidiscretization

In this section, we discuss about the time semidiscretization process of the IBVP (6.1.1) and later, we establish the asymptotic behavior of the exact solution of the resulting semidiscrete problem.

Firstly, we split the spatial differential operator $\mathcal{L}_{\varepsilon}$ as $\mathcal{L}_{\varepsilon} = \mathcal{L}_{1,\varepsilon} + \mathcal{L}_{2,\varepsilon}$ where $\mathcal{L}_{1,\varepsilon}$ and $\mathcal{L}_{2,\varepsilon}$ are given by

$$\begin{cases} \mathcal{L}_{1,\varepsilon} \equiv (\mathcal{L}_{11,\varepsilon}, \mathcal{L}_{12,\varepsilon})^T = -\varepsilon^2 \frac{\partial^2}{\partial x^2} + B_1(x, y, t), \\ \mathcal{L}_{2,\varepsilon} \equiv (\mathcal{L}_{21,\varepsilon}, \mathcal{L}_{22,\varepsilon})^T = -\varepsilon^2 \frac{\partial^2}{\partial y^2} + B_2(x, y, t), \end{cases}$$

where the coefficients of matrices $B_{\ell}(x, y, t) = \{b_{lm}^{\ell}(x, y, t)\}_{l,m=1}^2$, $\ell = 1, 2$ are defined by

$$b_{lm}(x, y, t) = b_{lm}^1(x, y, t) + b_{lm}^2(x, y, t), \quad l, m = 1, 2.$$

We decompose the source term as $\vec{f} = \vec{f}_1 + \vec{f}_2$, where $\vec{f}_1 = (f_{11}, f_{12})^T$ and $\vec{f}_2 = (f_{21}, f_{22})^T$ satisfy the compatibility conditions:

$$\begin{cases} f_{lm}(x, 0, t) = f_{lm}(x, 1, t) = 0, \\ f_{lm}(0, y, t) = f_{lm}(1, y, t) = 0, \quad \text{for } l, m = 1, 2. \end{cases} \quad (6.3.1)$$

In addition, assume that the reaction coefficient matrices $B_{\ell}(x, y, t)$, satisfy the following conditions:

$$\begin{cases} b_{ll}^{\ell}(x, y, t) > \gamma_{\beta}^{\ell} > 0, \quad b_{lm}^{\ell}(x, y, t) \leq 0, \quad \text{for } l \neq m, \quad l, m = 1, 2, \quad \ell = 1, 2, \\ \min_{(x,y,t) \in \bar{\mathcal{D}}} \{b_{11}^{\ell} + b_{12}^{\ell}, b_{21}^{\ell} + b_{22}^{\ell}\} \geq \beta_{\ell}^2 > 0, \quad \text{with } \beta = \min\{\beta_1, \beta_2\}. \end{cases} \quad (6.3.2)$$

First, consider the uniform mesh $\bar{\Upsilon}^M = \{t_n = n\Delta t, n = 0, 1, \dots, M\}$ for the time discretization. Then, we discretize time derivative by the fractional-step method. Let $\bar{u}^n(x, y)$ be the semidiscrete solution of the following problem:

$$\bar{u}^0 = \bar{u}_0(x, y), \quad (x, y) \in \bar{\mathcal{D}}, \quad (6.3.3)$$

$$\begin{cases} \left(I + \Delta t \mathcal{L}_{1,\varepsilon}^{n+1}\right) \bar{u}^{n+1/2}(x, y) = \bar{u}^n(x, y) + \Delta t \vec{f}_1^{n+1}(x, y), \\ \bar{u}^{n+1/2}(0, y) = \vec{0}, \quad \bar{u}_2^{n+1/2}(1, y) = \vec{0}, \quad y \in [0, 1], \end{cases} \quad (6.3.4)$$

and

$$\begin{cases} \left(I + \Delta t \mathcal{L}_{2,\varepsilon}^{n+1}\right) \bar{u}^{n+1}(x, y) = \bar{u}^{n+1/2}(x, y) + \Delta t \vec{f}_2^{n+1}(x, y), \\ \bar{u}^{n+1}(x, 0) = \vec{0}, \quad \bar{u}^{n+1}(x, 1) = \vec{0}, \quad x \in [0, 1]. \end{cases} \quad (6.3.5)$$

Lemma 6.3.1. *Let $\left(I + \Delta t \mathcal{L}_{1,\varepsilon}^{n+1}\right)$ be the differential operator defined in (6.3.4) and assume that the coefficients of the matrix B_1 satisfy (6.3.2). Then $\bar{z}^{n+1/2}(0, y) \geq \vec{0}$ and $\bar{z}^{n+1/2}(1, y) \geq \vec{0}$ on $[0, 1]$ with $\left(I + \Delta t \mathcal{L}_{1,\varepsilon}^{n+1}\right) \bar{z}^{n+1/2} \geq \vec{0}$ in \mathcal{D} , we have $\bar{z}^{n+1/2} \geq \vec{0}$, for all $(x, y) \in \bar{\mathcal{D}}$.*

Proof. By following argument of Lemma 5.3.1, one can prove the maximum principle.

■

By using the methodology from (2.3.2), we can get

$$\|(I + \Delta t \mathcal{L}_{\vec{1}, \vec{\varepsilon}}^{n+1})^{-1}\|_{\infty} \leq \frac{1}{1 + \beta_1^2 \Delta t}, \quad \|(I + \Delta t \mathcal{L}_{\vec{2}, \vec{\varepsilon}}^{n+1})^{-1}\|_{\infty} \leq \frac{1}{1 + \beta_2^2 \Delta t}. \quad (6.3.6)$$

Next, we define the local truncation error \vec{e}^{n+1} of the semidiscrete scheme (6.3.3)-(6.3.5) as follows:

$$\vec{e}^{n+1} = \vec{u}(t_{n+1}) - \vec{u}^{n+1},$$

where \vec{u}^{n+1} is solution of the following system:

$$\begin{cases} \left(I + \Delta t \mathcal{L}_{\vec{1}, \vec{\varepsilon}}^{n+1} \right) \vec{u}^{n+1/2}(x, y) = \vec{u}(t_n) + \Delta t \vec{f}_1^{n+1}(x, y), \\ \vec{u}^{n+1/2}(0, y) = \vec{0}, \quad \vec{u}^{n+1/2}(1, y) = \vec{0}, \quad y \in [0, 1], \end{cases} \quad (6.3.7)$$

and

$$\begin{cases} \left(I + \Delta t \mathcal{L}_{\vec{2}, \vec{\varepsilon}}^{n+1} \right) \vec{u}^{n+1}(x, y) = \vec{u}^{n+1/2}(x, y) + \Delta t \vec{f}_2^{n+1}(x, y), \\ \vec{u}^{n+1}(x, 0) = \vec{0}, \quad \vec{u}^{n+1}(x, 1) = \vec{0}, \quad x \in [0, 1]. \end{cases} \quad (6.3.8)$$

Lemma 6.3.2. *The local truncation error satisfies*

$$\|\vec{e}^{n+1}\|_{\infty} \leq C(\Delta t)^2.$$

Lemma 6.3.3. *The global error of the time semidiscrete scheme (6.3.3)-(6.3.5) satisfies the following estimate*

$$\sup_{n \leq T/\Delta t} \|\vec{u}(t_n) - \vec{u}^n\|_{\infty} \leq C\Delta t.$$

Hence, we conclude that the semidiscrete scheme (6.3.3)-(6.3.5) is of first-order uniformly convergent.

Now, we discuss the asymptotic behavior of the exact solutions of the semidiscrete BVP (6.3.7)-(6.3.8) in order to estimate the local truncation error associated with the spatial discretization of the semidiscrete problems.

Lemma 6.3.4. *For all non-negative integer k satisfying $0 \leq k \leq 4$, the exact solution $\vec{u}^{n+1/2}$ of the semidiscrete problem (6.3.7)-(6.3.8) satisfies the following estimate*

$$\left| \frac{\partial^k \widehat{u}_l^{n+1/2}}{\partial x^k} \right| \leq C(1 + \varepsilon^{-k} \mathcal{B}_{\varepsilon}(x)), \quad (6.3.9)$$

$$\left| \frac{\partial^k \widehat{u}_l^{n+1}}{\partial y^k} \right| \leq C(1 + \varepsilon^{-k} \mathcal{B}_{\varepsilon}(y)), \quad l = 1, 2. \quad (6.3.10)$$

Proof. By using the maximum principle (Lemma 6.3.1) and the uniform boundedness of $\vec{u}(t_n)$ and $\vec{f}_1^{n+1}(x, y)$, we obtain that $\|\vec{u}^{\vec{n}+1/2}\|_\infty \leq C$. Next, define $\vec{\Theta} = \mathcal{L}_{1,\varepsilon}^{n+1} \vec{u}^{\vec{n}+1/2}$ is the solution of the following problem:

$$\begin{cases} \left(I + \Delta t \mathcal{L}_{1,\varepsilon}^{n+1} \right) \vec{\Theta} = \mathcal{L}_{1,\varepsilon}^{n+1} \vec{u}(t_n) + \Delta t \mathcal{L}_{1,\varepsilon}^{n+1} \vec{f}_1^{n+1}(x, y), \\ \vec{\Theta}(0, y) = \vec{0}, \quad \vec{\Theta}(1, y) = \vec{0}, \quad y \in [0, 1]. \end{cases} \quad (6.3.11)$$

By applying the derivative bounds of $\vec{u}(t_n)$ (Lemma 6.2.4), one can obtain that $|\mathcal{L}_{1,\varepsilon}^{n+1} \vec{u}(x, y, t_n)| \leq \vec{C}$. Also, by using the smoothness of source function \vec{f}_1^{n+1} , we have $|\mathcal{L}_{1,\varepsilon}^{n+1} \vec{f}_1^{n+1}(x, y)| \leq \vec{C}$. Therefore, by employing the maximum principle, we get that $\|\vec{\Theta}\|_\infty \leq C$. Next, $\vec{u}^{\vec{n}+1/2}$ can be written as the solution of the following problem

$$\begin{cases} \mathcal{L}_{1,\varepsilon}^{n+1} \vec{u}^{\vec{n}+1/2} = \vec{\Theta}, \\ \vec{u}^{\vec{n}+1/2}(0, y) = \vec{0}, \quad \vec{u}^{\vec{n}+1/2}(1, y) = \vec{0}, \quad y \in [0, 1]. \end{cases} \quad (6.3.12)$$

For $l = 1, 2$, by using a similar approach carried out in Lemma 3.3.1, we can deduce that

$$\left| \frac{\partial^k \widehat{u}_l^{\vec{n}+1/2}}{\partial x^k}(x, y) \right| \leq C (1 + \varepsilon^{-k} \mathcal{B}_\varepsilon(x)), \quad 0 \leq k \leq 4.$$

Next, we differentiate (6.3.7) with respect to y and apply the previous technique and bounds from Lemma 6.2.4 to obtain

$$\left| \frac{\partial^k \widehat{u}_l^{\vec{n}+1/2}}{\partial y^k}(x, y) \right| \leq C (1 + \varepsilon^{-k} \mathcal{B}_\varepsilon(y)), \quad l = 1, 2, \quad 0 \leq k \leq 4.$$

Now, it can be easily verified that

$$\|\mathcal{L}_{2m,\varepsilon}^{n+1} \vec{u}^{\vec{n}+1/2}\|_\infty \leq C, \quad \|(\mathcal{L}_{2m,\varepsilon}^{n+1})^2 \vec{u}^{\vec{n}+1/2}\|_\infty \leq C, \quad m = 1, 2. \quad (6.3.13)$$

By using the previous technique, for $1 \leq k \leq 4$, we can obtain that

$$\left| \frac{\partial^k \widehat{u}_l^{n+1}}{\partial y^k} \right| \leq C (1 + \varepsilon^{-k} \mathcal{B}_\varepsilon(y)), \quad l = 1, 2.$$

This completes the proof. \blacksquare

Next, by following the technique of [38], we consider the decomposition of the exact solution $\vec{u}^{\vec{n}+1/2}(x, y)$ of (6.3.7) as follows

$$\vec{u}^{\vec{n}+1/2}(x, y) = \vec{v}^{\vec{n}+1/2}(x, y) + \vec{w}^{\vec{n}+1/2}(x, y)$$

where the smooth component $\vec{v}^{\vec{n}+1/2}$ and layer component $\vec{w}^{\vec{n}+1/2}$ satisfy following estimates:

$$\left| \frac{\partial^k \widehat{v}_l^{\vec{n}+1/2}}{\partial x^k} \right| \leq C(1 + \varepsilon^{2-k}), \quad \left| \frac{\partial^k \widehat{w}_l^{\vec{n}+1/2}}{\partial x^k} \right| \leq C\varepsilon^{-k} \mathcal{B}_\varepsilon(x), \quad 0 \leq k \leq 4. \quad (6.3.14)$$

In a similar manner, one can decompose the exact solution of $\bar{u}^{n+1}(x, y)$ of (6.3.8) as $\bar{u}^{n+1} = \bar{v}^{n+1} + \bar{w}^{n+1}$ and show that

$$\left| \frac{\partial^k \widehat{v}_l^{n+1}}{\partial y^k} \right| \leq C(1 + \varepsilon^{2-k}), \quad \left| \frac{\partial^k \widehat{w}_l^{n+1}}{\partial y^k} \right| \leq C\varepsilon^{-k} \mathcal{B}_\varepsilon(y), \quad 0 \leq k \leq 4. \quad (6.3.15)$$

These bounds will be used in the truncation error analysis of the fully discrete scheme in the next section.

6.4 The Spatial Discretization

In this section, we describe the layer-adapted Shishkin meshes for the spatial directions, then we discretize the spatial derivatives in the semidiscrete scheme (6.3.7)-(6.3.8).

The piecewise-uniform Shishkin mesh

Let the rectangular mesh $\bar{\mathcal{D}}_\varepsilon^N$ be defined by the tensor product of the 1D Shishkin meshes, *i.e.*, $\bar{\mathcal{D}}_\varepsilon^N = \bar{\Omega}_x^N \times \bar{\Omega}_y^N \subset \bar{\mathcal{D}}$, which is constructed as follows:

First, we define the transition parameters τ_x, τ_y by

$$\tau_x = \min \left\{ \frac{1}{4}, \frac{2}{\beta} \varepsilon \ln N \right\} \quad \text{and} \quad \tau_y = \min \left\{ \frac{1}{4}, \frac{2}{\beta} \varepsilon \ln N \right\}.$$

In the analysis, we shall assume that $\tau_x = \tau_y = (2/\beta)\varepsilon \ln N$. Note that when $\tau_x = \tau_y = 1/4$, the mesh will become uniform, therefore, in this case the classical approach can be applied for derivation of the truncation error estimates.

To obtain the piecewise-uniform Shishkin mesh, we divide the domain $\bar{\Omega}_x^N$ into three subintervals such as $[0, \tau_x]$, $[\tau_x, 1 - \tau_x]$ and $[1 - \tau_x, 1]$. Then divide $[\tau_x, 1 - \tau_x]$ into $N/2$ mesh-intervals and divide subintervals $[0, \tau_x]$, $[1 - \tau_x, 1]$ into $N/4$ mesh-intervals. Analogously, we proceed for $\bar{\Omega}_y^N$. Fig. 6.1 exhibits piecewise-uniform Shishkin mesh $\bar{\mathcal{D}}_\varepsilon^N$.

The step sizes in both the spatial directions are given by

$$\begin{cases} h_{x,i} = x_i - x_{i-1}, \quad i = 1, \dots, N, & \tilde{h}_{x,i} = h_{x,i} + h_{x,i+1}, \quad i = 1, \dots, N-1, \\ h_{y,i} = y_i - y_{i-1}, \quad i = 1, \dots, N, & \tilde{h}_{y,i} = h_{y,i} + h_{y,i+1}, \quad i = 1, \dots, N-1. \end{cases}$$

The finite difference scheme

For simplicity, denote that $b_{l1,i}^{m,n+1} = b_{l1}^m(x_i, y, t_{n+1})$, $b_{l2,j}^{m,n+1} = b_{l2}^m(x, y_j, t_{n+1})$, $l, m = 1, 2$.

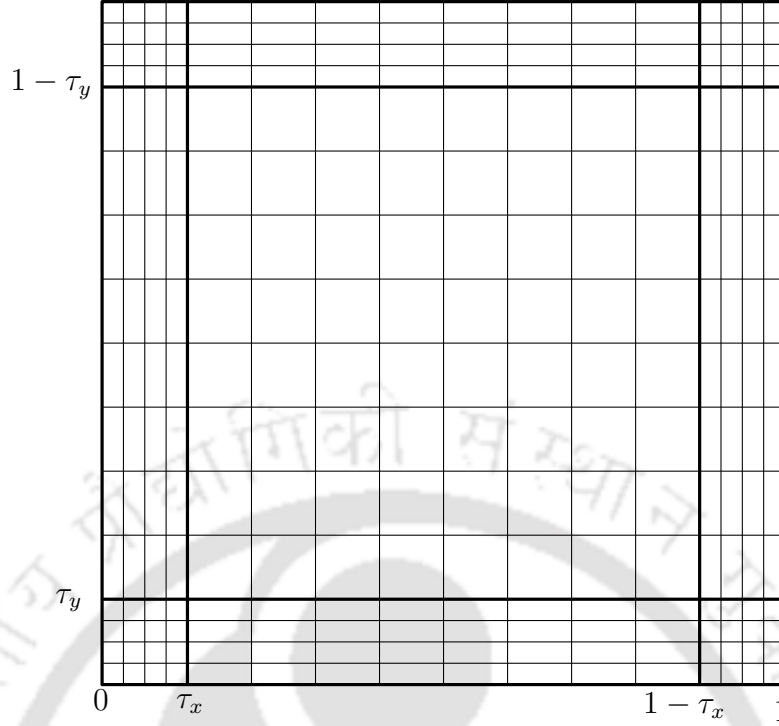


Figure 6.1: A typical example of piecewise-uniform Shishkin mesh $\bar{\mathcal{D}}_\varepsilon^N$ for $N = 16$.

For spatial discretization of (6.3.7)-(6.3.8), we propose the following finite difference scheme:

$$\begin{cases} \vec{U}_{x_i, y_j}^0 = \vec{u}_0(x_i, y_j), & (x_i, y_j) \in \bar{\mathcal{D}}_\varepsilon^N, \\ \left(I + \Delta t \mathcal{L}_{1, \varepsilon}^{n+1, N} \right) \vec{U}_{x_i, y}^{n+1/2} = \vec{u}(x_i, y, t_n) + \Delta t \vec{f}_1^{n+1}(x_i, y), \\ \vec{U}_{0, y}^{n+1/2} = \vec{0}, \quad \vec{U}_{1, y}^{n+1/2} = \vec{0}, \quad y \in \bar{\Omega}_y^N, \end{cases} \quad (6.4.1)$$

$$\begin{cases} \left(I + \Delta t \mathcal{L}_{2, \varepsilon}^{n+1, N} \right) \vec{U}_{x, y_j}^{n+1} = \vec{U}_{x, y_j}^{n+1/2} + \Delta t \vec{f}_2^{n+1}(x, y_j), \\ \vec{U}_{x, 0}^{n+1} = \vec{0}, \quad \vec{U}_{x, 1}^{n+1} = \vec{0}, \quad x \in \bar{\Omega}_x^N, \end{cases} \quad (6.4.2)$$

where $\mathcal{L}_{1, \varepsilon}^{n+1, N} = (\mathcal{L}_{11, \varepsilon}^{n+1, N}, \mathcal{L}_{12, \varepsilon}^{n+1, N})^T$ and $\mathcal{L}_{2, \varepsilon}^{n+1, N} = (\mathcal{L}_{21, \varepsilon}^{n+1, N}, \mathcal{L}_{22, \varepsilon}^{n+1, N})^T$ are given by

$$\begin{cases} \mathcal{L}_{1, \varepsilon}^{n+1, N} \equiv -\mathcal{E}^2 \delta_x^2 + B_1(x_i, y, t_{n+1}), \\ \mathcal{L}_{2, \varepsilon}^{n+1, N} \equiv -\mathcal{E}^2 \delta_y^2 + B_2(x, y_j, t_{n+1}), \end{cases}$$

where δ_x^2, δ_y^2 are central difference operators associated with x, y variables, respectively.

Lemma 6.4.1. (Discrete maximum principle) Let $(I + \Delta t \mathcal{L}_{l, \varepsilon}^{n+1, N})$, $l = 1, 2$, be the difference operators given in (6.4.1)-(6.4.2). Then for any mesh function \vec{Z} , if $\vec{Z} \geq \vec{0}$ on $\partial \mathcal{D}_\varepsilon^N$ and $(I + \Delta t \mathcal{L}_{l, \varepsilon}^{n+1, N}) \vec{Z} \geq \vec{0}$ in $\mathcal{D}_\varepsilon^N$, then we have $\vec{Z} \geq \vec{0}$ for all $(x_i, y_j) \in \bar{\mathcal{D}}_\varepsilon^N$.

Proof. By following the approach discussed in Lemma 2.4.1, one can prove maximum principle. \blacksquare

Hence, the discrete operator $\left(I + \Delta t \mathcal{L}_{lm,\varepsilon}^{n+1,N}\right)$ satisfy stability condition (6.3.6).

Next, we define the fully discrete scheme as follows:

$$\begin{cases} \vec{U}_{x_i,y_j}^0 = \vec{u}_0(x_i, y_j), & (x_i, y_j) \in \overline{\mathcal{D}}_\varepsilon^N, \\ \left(I + \Delta t \mathcal{L}_{1,\varepsilon}^{n+1,N}\right) \vec{U}_{x_i,y}^{n+1/2} = \vec{U}_{x_i,y}^n + \Delta t \vec{f}_1^{n+1}(x_i, y), \\ \vec{U}_{0,y}^{n+1/2} = \vec{0}, \quad \vec{U}_{1,y}^{n+1/2} = \vec{0}, \quad y \in \overline{\Omega}_y^N, \end{cases} \quad (6.4.3)$$

and

$$\begin{cases} \left(I + \Delta t \mathcal{L}_{2,\varepsilon}^{n+1,N}\right) \vec{U}_{x,y_j}^{n+1} = \vec{U}_{x,y_j}^{n+1/2} + \Delta t \vec{f}_2^{n+1}(x, y_j), \\ \vec{U}_{x,0}^{n+1} = \vec{0}, \quad \vec{U}_{x,1}^{n+1} = \vec{0}, \quad x \in \overline{\Omega}_x^N. \end{cases} \quad (6.4.4)$$

In the following subsection, we discuss the convergence analysis of the proposed numerical scheme.

6.4.1 Error analysis

For the discrete problem (6.4.1), we define the local truncation error as follows

$$\begin{cases} \zeta_{i,u}^{1,n+1/2} = \left(I + \Delta t \mathcal{L}_{11,\varepsilon}^{n+1,N}\right) \vec{u}^{n+1/2}(x_i) - \left(I + \Delta t \mathcal{L}_{11,\varepsilon}^{n+1}\right) \vec{u}^{n+1/2}(x_i) \\ = \Delta t \zeta_{x,u}^{1,n+1/2}, \quad 1 \leq i \leq N-1, \\ \zeta_{i,u}^{2,n+1/2} = \left(I + \Delta t \mathcal{L}_{12,\varepsilon}^{n+1,N}\right) \vec{u}^{n+1/2}(x_i) - \left(I + \Delta t \mathcal{L}_{12,\varepsilon}^{n+1}\right) \vec{u}^{n+1/2}(x_i), \\ = \Delta t \zeta_{x,u}^{2,n+1/2}, \quad 1 \leq i \leq N-1. \end{cases} \quad (6.4.5)$$

therefore

$$\begin{cases} \zeta_{x,u}^{1,n+1/2} = \left(\mathcal{L}_{11,\varepsilon}^{n+1,N} - \mathcal{L}_{11,\varepsilon}^{n+1}\right) \vec{u}^{n+1/2}(x_i), \\ \zeta_{x,u}^{2,n+1/2} = \left(\mathcal{L}_{12,\varepsilon}^{n+1,N} - \mathcal{L}_{12,\varepsilon}^{n+1}\right) \vec{u}^{n+1/2}(x_i). \end{cases} \quad (6.4.6)$$

Let $g \in C^4(0, 1)$ be a smooth function defined on $[0, 1]$. Then the Taylor's expansion shows that

$$\left|(g_{xx} - \delta_x^2 g)_i\right| \leq \begin{cases} 2|(g_{xx})_i|_{[x_{i-1}, x_{i+1}]}, & \text{if } h_i \neq h_{i+1} \\ \frac{1}{2}(h_i + h_{i+1})|(g_{xxx})_i|_{[x_{i-1}, x_{i+1}]}, & \text{if } h_i \neq h_{i+1} \\ \frac{1}{12}(h_i)^2|(g_{xxx})_i|_{[x_{i-1}, x_{i+1}]}, & \text{if } h_i = h_{i+1}. \end{cases} \quad (6.4.7)$$

Next, we discuss the error analysis for the numerical scheme (6.4.1).

Lemma 6.4.2. Let $\vec{u}^{n+1/2}(x, y)$ and $\vec{U}_{x_i, y}^{n+1/2}$ be the exact and the discrete solutions of (6.3.7) and (6.4.1), respectively, satisfy the following error bound:

$$\left| \vec{u}^{n+1/2}(x_i, y) - \vec{U}_{x_i, y}^{n+1/2} \right| \leq \vec{C} N^{-2} \ln^2 N, \quad y \in \bar{\Omega}_y^N, \quad (6.4.8)$$

where C is a positive constant independent of y , ε and N .

Proof. From (6.4.6), we have

$$\zeta_{x,u}^{l,n+1/2} = \varepsilon^2 \left(\frac{\partial^2 \hat{v}_l^{n+1/2}}{\partial x^2} - \delta_x^2 \hat{v}_l^{n+1/2} \right) + \varepsilon^2 \left(\frac{\partial^2 \hat{w}_l^{n+1/2}}{\partial x^2} - \delta_x^2 \hat{w}_l^{n+1/2} \right), \quad l = 1, 2.$$

First, consider the error term corresponding to the smooth component. If $x_i \in \{\tau_x, 1 - \tau_x\}$, then we use the second bound of (6.4.7) otherwise use the third bound of (6.4.7) with (6.3.14) to get

$$\varepsilon^2 \left| \frac{\partial^2 \hat{v}_l^{n+1/2}}{\partial x^2} - \delta_x^2 \hat{v}_l^{n+1/2} \right| \leq \begin{cases} C\varepsilon N^{-1}, & x_i \in \{\tau_x, 1 - \tau_x\} \\ CN^{-2}, & \text{otherwise} \end{cases} \quad (6.4.9)$$

Next, we deduce the error estimate for the layer component. Here, we consider the cases for outer region and inner region separately. First, we assume the case for the outer region, *i.e.*, $x_i \in [\tau_x, 1 - \tau_x]$. By using the first estimate of (6.4.7) and derivative bound (6.3.14), we obtain

$$\begin{aligned} \varepsilon^2 \left| \frac{\partial^2 \hat{w}_l^{n+1/2}}{\partial x^2} - \delta_x^2 \hat{w}_l^{n+1/2} \right| &\leq C \left[\exp\left(\frac{-\beta x_{N/4-1}}{\varepsilon}\right) + \exp\left(\frac{-\beta(1-x_{3N/4+1})}{\varepsilon}\right) \right] \\ &= 2C \exp\left(\frac{-\beta\tau_x}{\varepsilon}\right) \exp\left(\frac{\beta h_{N/4}}{\varepsilon}\right) \leq CN^{-2}. \end{aligned} \quad (6.4.10)$$

Next, we consider the case for the inner region, *i.e.*, $x_i \in (0, \tau_x) \cup (1 - \tau_x, 1)$. Again, by applying the third estimate of (6.4.7) and derivative bound (6.3.14) to deduce

$$\varepsilon^2 \left| \frac{\partial^2 \hat{w}_l^{n+1/2}}{\partial x^2} - \delta_x^2 \hat{w}_l^{n+1/2} \right| \leq CN^{-2} \ln^2 N. \quad (6.4.11)$$

Define the piecewise linear function φ_ε as follows

$$\varphi_\varepsilon(x) = \begin{cases} x\tau_x^{-1}, & \text{for } x \in [0, \tau_x], \\ 1, & \text{for } x \in [\tau_x, 1 - \tau_x], \\ (1-x)\tau_x^{-1}, & \text{for } x \in [1 - \tau_x, 1], \end{cases}$$

Now, we define the discrete barrier function as follows

$$\vec{\mathfrak{B}}_{rd}^\pm(x_i) = \vec{C} N^{-2} \ln^2 N (1 + \varphi_\varepsilon(x_i)) \pm \left(\hat{u}^{n+1/2}(x_i, y) - \hat{U}_{x_i, y}^{n+1/2} \right), \quad \text{for } 0 \leq i \leq N.$$

Hence, as a result, we get

$$\left| \left(I + \Delta t \mathcal{L}_{11,\varepsilon}^{n+1,N} \right) \vec{\mathfrak{B}}_{rd}^{\pm}(x_i) \right| \geq 0, \quad \left| \left(I + \Delta t \mathcal{L}_{12,\varepsilon}^{n+1,N} \right) \vec{\mathfrak{B}}_{rd}^{\pm}(x_i) \right| \geq 0, \quad \text{for } 0 \leq i \leq N.$$

Thus, by using the discrete maximum principle (Lemma 6.4.1), we can get (6.4.8). ■

Lemma 6.4.3. *Let $\vec{u}^n(x, y)$ be the exact solution of (6.3.7)-(6.3.8) and \vec{U}_{x_i, y_j}^n be solution of the semidiscrete scheme (6.4.1)-(6.4.2). Then, the following error estimate holds:*

$$\left| \vec{u}^{n+1}(x_i, y_j) - \vec{U}_{x_i, y_j}^{n+1} \right| \leq \vec{C} N^{-2} \ln^2 N, \quad \text{for all } (x_i, y_j) \in \overline{\mathcal{D}}_{\varepsilon}^N, \quad (6.4.12)$$

where \vec{C} is a positive constant independent of ε and N .

Proof. By following the proof of Lemma 5.4.6, we can obtain the required estimate. ■

Now, by following the similar technique as presented in Chapter 5, one can deduce

$$\left| \widehat{u}^{n+1}(x_i, y_j) - \widehat{U}_{x_i, y_j}^{n+1} \right| \leq \vec{C} \Delta t N^{-2+\nu} \ln^2 N, \quad (x_i, y_j) \in \overline{\mathcal{D}}_{\varepsilon}^N, \quad (6.4.13)$$

where $N^{-\nu} \leq C \Delta t$ with $0 < \nu < 1$.

By combing results from Lemma 6.3.3 and Lemma 6.4.3 and stability condition (6.3.6) with (6.4.13), we can obtain the main convergence result as follows:

Theorem 6.4.4. *Let $\vec{u}(x, y, t_n)$ be the exact solution of (6.1.1) and \vec{U}_{x_i, y_j}^n be the solution of the discrete problem (6.4.3)-(6.4.4). If $N^{-\nu} \leq C \Delta t$ with $0 < \nu < 1$, then there exists a constant C , independent of ε and N , such that*

$$\left\| \vec{u}(x_i, y_j, t_n) - \vec{U}_{x_i, y_j}^n \right\|_{\infty} \leq C(\Delta t + N^{-2+\nu} \ln^2 N), \quad (x_i, y_j, t_n) \in \overline{\mathcal{G}}_{\varepsilon}^{N,M}. \quad (6.4.14)$$

Proof. By using the methodology from the proof of Theorem 2.5.1, the desired result follows. ■

6.5 Numerical Results

In this section, we shall present the numerical results obtained by the discrete scheme (6.4.3)-(6.4.4). We have chosen the decomposition for reaction term as: $b_{lm}^1(x, y, t) = b_{lm}^2(x, y, t) = b_{lm}(x, y, t)/2$, $l, m = 1, 2$, in the following test problem.

Example 6.5.1. Consider the system of 2D parabolic reaction-diffusion IBVP on $\mathcal{G} := (0, 1)^2 \times (0, 1]$:

$$\begin{cases} \frac{\partial u_1}{\partial t} - \varepsilon^2 \Delta u_1 + (4 + 2(x^2 + y^2)t)u_1 - (x^2 + y^2)t u_2 = f_1(x, y, t), \\ \frac{\partial u_2}{\partial t} - \varepsilon^2 \Delta u_2 + (4x^2 + y^2)t u_1 + (2 + (2x^2t + y^2t^2))u_2 = f_2(x, y, t), \\ \vec{u}(x, y, 0) = \vec{0}, \quad (x, y) \in (0, 1)^2, \\ \vec{u}(0, y, t) = \vec{u}(1, y, t) = \vec{0}, \quad (y, t) \in [0, 1] \times [0, 1], \\ \vec{u}(x, 0, t) = \vec{u}(x, 1, t) = \vec{0}, \quad (x, t) \in [0, 1] \times [0, 1], \end{cases}$$

where the source term $\vec{f} = (f_1, f_2)^T$ is given by

$$\begin{cases} f_1 = xy(1-x)(1-y)t^2 + x^2y^2(1-x)(1-y)e^{-t}, \\ f_2 = xy(1-x^2)(1-y^2)t + xy(1-x)(1-y)e^{-t}. \end{cases}$$

Since the exact solution of Example 6.5.1 is not known, the accuracy of the numerical solution will be determined by using the double mesh principle, *i.e.*, the mesh obtained for $\mathcal{G}_\varepsilon^{N,M} = \mathcal{D}_\varepsilon^N \times \Upsilon^M$ will be exactly taken to produce another set of mesh $\mathcal{G}_\varepsilon^{2N,2M} = \mathcal{D}_\varepsilon^{2N} \times \Upsilon^{2M}$ with $2N$ mesh-intervals in both the x - and y -directions and $2M$ mesh-intervals in the t -direction, by bisecting the original mesh $\mathcal{G}_\varepsilon^{N,M}$.

For each ε , the maximum point-wise error is calculated by

$$E_{l,\varepsilon}^{N,M} = \max_{(x_i, y_j, t_n) \in \mathcal{G}_\varepsilon^{N,M}} \left| U_{l,x_i, y_j}^{2n} - U_{l,x_i, y_j}^n \right|, \quad E_l^{N,M} = \max_{S_\varepsilon} E_{l,\varepsilon}^{N,M}, \quad l = 1, 2,$$

where U_{l,x_i, y_j}^n is the computed solution with N mesh-intervals in both the x - and y -directions and M mesh-intervals in the t -direction and $U_{l,x_{2i}, y_{2j}}^{2n}$ is the numerical solution at $2N$ mesh-intervals in both the x - and y -directions and $2M$ mesh-intervals in the t -direction. And the orders of convergence are calculated by

$$P_{l,\varepsilon}^{N,M} = \log_2 \left(\frac{E_{l,\varepsilon}^{N,M}}{E_{l,\varepsilon}^{2N,2M}} \right), \quad P_l^{N,M} = \log_2 \left(\frac{E_l^{N,M}}{E_l^{2N,2M}} \right), \quad l = 1, 2.$$

From Table 6.1, we see that the order of convergence is one. Therefore, we can conclude that the global errors are dominated by the errors corresponding to the time discretization. In order to reveal the numerical order of convergence, we have plotted the maximum pointwise errors in log-log scale for Example 6.5.1 in the Fig. 6.4 and Fig. 6.5, which again shows the accuracy of the numerical scheme.

In order to visualize the numerical solution of Example 6.5.1, we display the surface plots of the numerical solutions U_1 and U_2 in Fig. 6.2 and Fig. 6.3. From the surface plots, one can observe the layer behavior of the numerical solution.

To show the contribution to global error of both spatial and time discretizations, we calculate the following orders of convergence

$$\mathcal{P}_{l,\varepsilon}^{N,M} = \log_2 \left(\frac{E_{l,\varepsilon}^{N,M}}{E_{l,\varepsilon}^{2N,4M}} \right), \quad \mathcal{P}_l^{N,M} = \log_2 \left(\frac{E_l^{N,M}}{E_l^{2N,4M}} \right), \quad l = 1, 2.$$

To calculate the second-order uniform convergence of the numerical solution, we have taken the number of intervals in the spatial and temporal directions as $N = 8, 16, 32, 64, 128$, and $M = 2, 8, 32, 128, 512$, respectively. For evaluating the maximum error and order of convergence, we consider the singular perturbation parameters from the set $S_\varepsilon = \{\varepsilon | \varepsilon = 2^{-10}, 2^{-12}, \dots, 2^{-20}\}$ which is a sufficiently small choice to bring out the singularly perturbed nature of the problem.

Note that, we have divided the time step by four, whereas the mesh points in space is doubled at each spatial direction. The reason for choosing such divisions is that, the order of convergence in time is one, but the order of convergence in space is almost two. Therefore, the contributions of order of convergence associated with the spatial discretization and the time discretization can be adjusted. One can verify from Table 6.2, the almost second-order of convergence and thus we conclude that the global errors are dominated by the errors corresponding to the space discretization. As a complement of this observation, we have displayed the maximum pointwise errors over the full domain for Example 6.5.1 in Fig. 6.6 and Fig. 6.7.

6.6 Conclusions

In this chapter, we have analyzed a numerical scheme for a class of singularly perturbed system of 2D parabolic reaction-diffusion problems. For discretizing the time derivative, a fraction-step method on the uniform mesh has been used and then the central difference scheme on the piecewise-uniform Shishkin mesh has been used for the resulting 1D stationary problems. Truncation error estimate and the stability analysis are obtained. Error estimate are derived for the proposed numerical scheme which shows that the the numerical scheme is ε -uniformly convergent of almost second-order in space and first-order in time. Numerical experiments confirm the theoretical findings for system of parabolic reaction-diffusion problems.

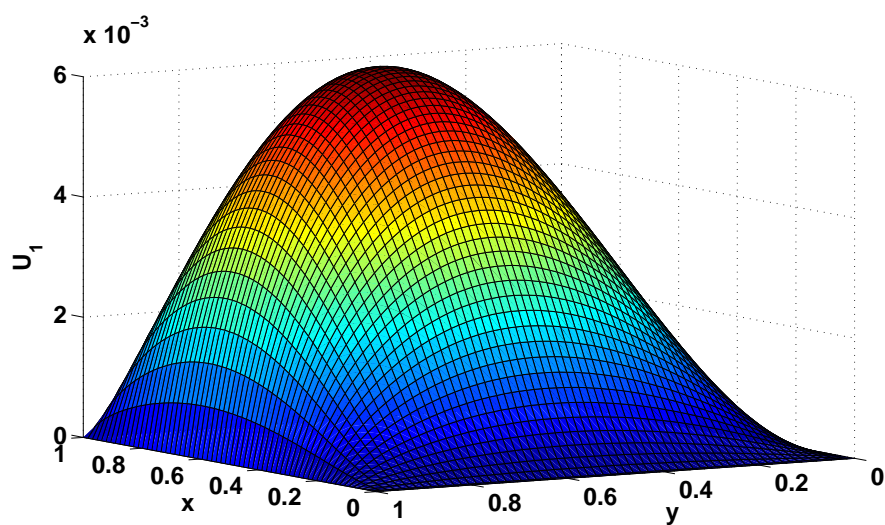


Figure 6.2: Surface plot of the numerical solution U_1 for $\varepsilon = 2^{-10}$, $N = 64$, $M = 4$.

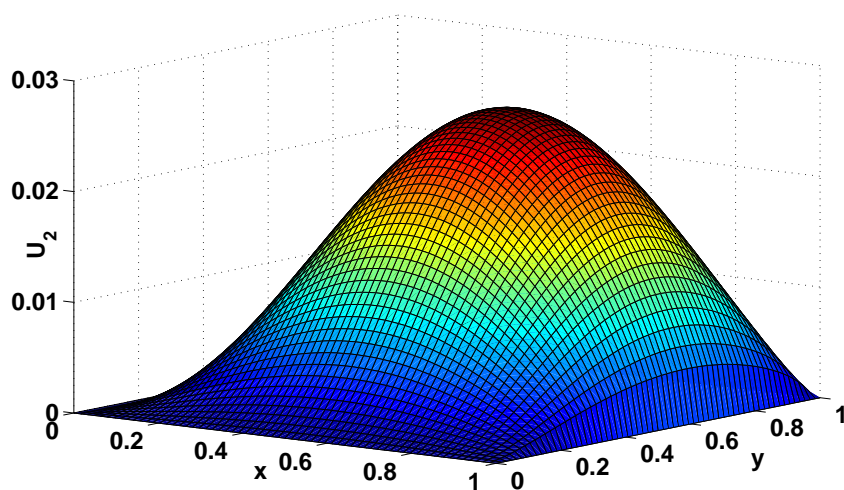


Figure 6.3: Surface plot of the numerical solution U_2 for $\varepsilon = 2^{-10}$, $N = 64$, $M = 4$.

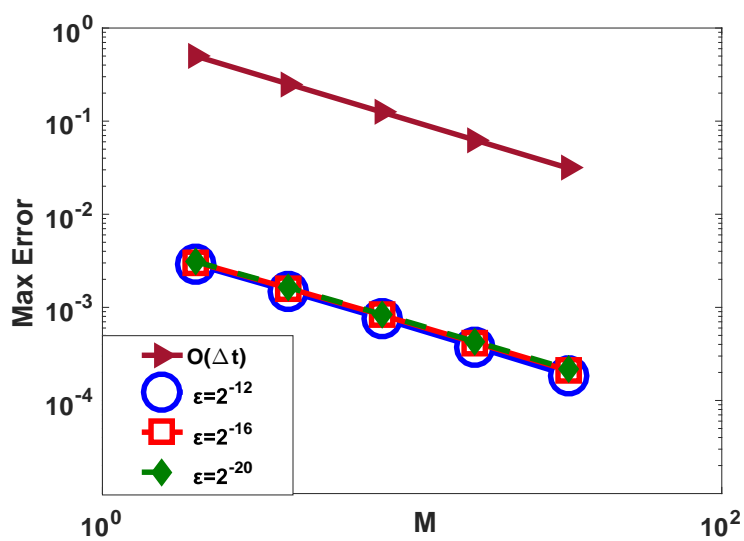


Figure 6.4: *Loglog plot (for the temporal order of convergence) associated with numerical solution U_1 of Example 6.5.1.*

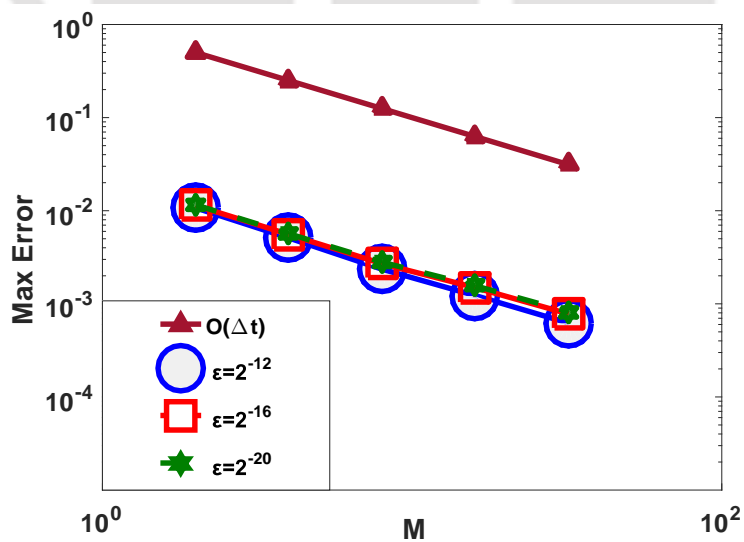


Figure 6.5: *Loglog plot (for the temporal order of convergence) associated with numerical solution U_2 of Example 6.5.1.*

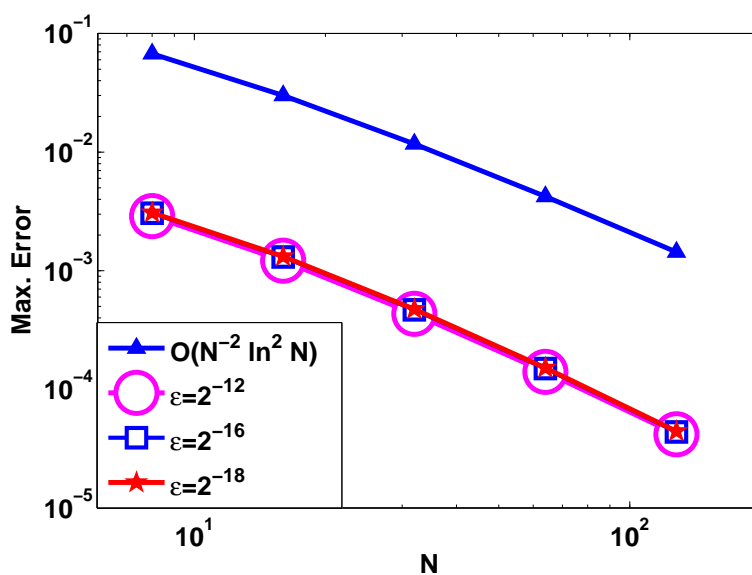


Figure 6.6: Visualization of the order of convergence (with respect to spatial variable) through loglog plot associated with numerical solution U_1 of Example 6.5.1.

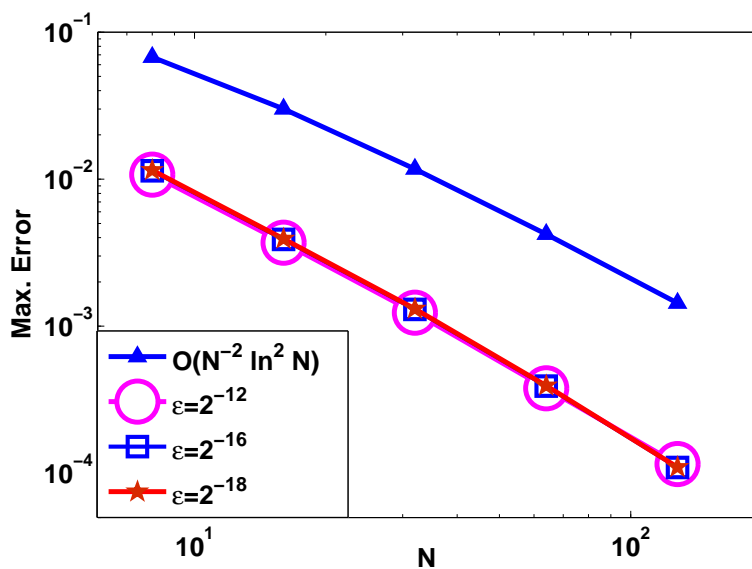


Figure 6.7: Visualization of the order of convergence (with respect to spatial variable) through loglog plot associated with numerical solution U_2 of Example 6.5.1.

Table 6.1: Uniform errors and the corresponding orders of convergence for Example 6.5.1.

$\varepsilon \in S_\varepsilon$	Number of mesh-intervals N /temporal mesh-size Δt				
	$8/\frac{1}{2}$	$16/\frac{1}{4}$	$32/\frac{1}{8}$	$64/\frac{1}{16}$	$128/\frac{1}{32}$
$E_1^{N,M}$	3.0990e-03	1.6282e-03	8.4090e-04	4.2792e-04	2.1700e-04
$P_1^{N,M}$	0.9485	0.9532	0.9746	0.9796	
$E_2^{N,M}$	1.1557e-02	5.6603e-03	2.4997e-03	1.5610e-03	8.2221e-04
$P_2^{N,M}$	1.0298	1.0156	0.9728	0.9948	

Table 6.2: Uniform errors and the corresponding orders of convergence for Example 6.5.1.

$\varepsilon \in S_\varepsilon$	Number of mesh-intervals N /temporal mesh-size Δt				
	$8/\frac{1}{2}$	$16/\frac{1}{8}$	$32/\frac{1}{32}$	$64/\frac{1}{128}$	$128/\frac{1}{512}$
$E_1^{N,M}$	3.0990e-3	1.3277e-3	4.7668e-4	1.5254e-4	4.4517e-5
$\mathcal{P}_1^{N,M}$	1.2229	1.4778	1.6439	1.7767	
$E_2^{N,M}$	1.1557e-2	3.9458e-3	1.3179e-3	3.9545e-4	1.1019e-4
$\mathcal{P}_2^{N,M}$	1.5504	1.5821	1.7366	1.8435	

Analysis of Uniformly Convergent Numerical Scheme for Singularly Perturbed System of 2D Parabolic Reaction-Diffusion Problems

In this chapter, we devise a uniformly convergent numerical scheme to solve singularly perturbed system of 2D parabolic reaction-diffusion problems. The proposed numerical scheme consists of the central difference scheme on piecewise-uniform Shishkin mesh for spatial semidiscretization processes and the implicit-Euler scheme on uniform mesh for time discretization. We derive error estimate for the proposed numerical scheme, which shows that the scheme is \mathcal{E} -uniformly convergent of almost second-order (up to a logarithmic factor) in space and first-order in time. Numerical results are presented to validate the theoretical results.

7.1 Introduction

In this chapter, we consider the following singularly perturbed system of 2D parabolic reaction-diffusion IBVP on the domain $\mathcal{G} := \mathcal{D} \times (0, T]$, $\mathcal{D} = \Omega_x \times \Omega_y = (0, 1) \times (0, 1)$:

$$\begin{cases} \frac{\partial \vec{u}}{\partial t} + \mathfrak{L}_{\varepsilon} \vec{u} = \vec{f}, & (x, y, t) \in \mathcal{G}, \\ \vec{u}(x, y, 0) = \vec{u}_0(x, y), & (x, y) \in \mathcal{D}, \\ \vec{u}(0, y, t) = \vec{u}(1, y, t) = \vec{0}, & (y, t) \in [0, 1] \times [0, T], \\ \vec{u}(x, 0, t) = \vec{u}(x, 1, t) = \vec{0}, & (x, t) \in [0, 1] \times [0, T], \end{cases} \quad (7.1.1)$$

where the spatial differential operator $\mathfrak{L}_{\varepsilon}$ is given by

$$\mathfrak{L}_{\varepsilon} \equiv -\mathcal{E}^2 \Delta + B(x, y, t).$$

The diffusion and reaction coefficients of the model problem (7.1.1) are given as $\mathcal{E} = \text{diag}(\varepsilon_1, \varepsilon_2)$, $0 < \varepsilon_1 \leq \varepsilon_2 \ll 1$ and $B = (b_{lm})_{2 \times 2}$, respectively.

We assume that the coefficients of reaction matrix B satisfy

$$\begin{cases} b_{lm} > \gamma_\beta > 0, & b_{lm} \leq 0, \text{ for } l \neq m, \text{ with } b_{21} > b_{12}, \\ \min_{(x,y,t) \in \bar{\mathcal{G}}} \{b_{11} + b_{12}, b_{21} + b_{22}\} \geq \beta^2 > 0. \end{cases} \quad (7.1.2)$$

Also assume that B satisfies the coercivity condition, *i.e.*, there exist $\kappa > 0$ such that

$$\vec{\xi}^T B \vec{\xi} \geq \kappa^2 \vec{\xi}^T \vec{\xi}, \quad \text{for all } \vec{\xi} \in \mathbb{R}^2, \quad \text{in } \mathcal{G}. \quad (7.1.3)$$

Under sufficient smoothness with compatibility conditions imposed on the source term and the initial data (discussed in Chapter 6), the model problem (7.1.1) admits a unique solution, which follows from [42].

The main objective of this chapter is to propose a uniformly convergent numerical scheme for the singularly perturbed system of 2D parabolic reaction-diffusion problems (7.1.1) on layer-adapted Shishkin mesh. Initially, we discretize the IBVP (7.1.1) in space by employing the central difference scheme on layer-resolving Shishkin mesh. Later on, we integrate the resulting stiff initial-value problems by the implicit-Euler scheme on uniform mesh. We prove that the proposed method is \mathcal{E} -uniformly convergent of almost second-order in space and first-order in time.

The rest of the chapter is organized as follows: In Section 7.2, we have discussed derivative bounds of the exact solution and solution decomposition has been established. In Section 7.3, the spatial semidiscretization has been introduced and we have provided its error analysis. For the time discretization, we have used implicit-Euler scheme on uniform mesh in Section 7.4. Later, the uniform convergence of the fully discrete scheme has been established. Numerical results are presented in Section 7.5. Finally in Section 7.6, we summarize the main conclusions.

7.2 Derivative Bounds and the Solution Decomposition

In this section, we discuss the partial derivative bounds of the exact solution \vec{u} of the model problem (7.1.1) with respect to spatial variables.

For sake of simplicity, set $\vec{\mathcal{B}}_k(x) = (\mathcal{B}_k^1(x), \mathcal{B}_k^2(x))^T$, where $\mathcal{B}_k^1(x)$, $\mathcal{B}_k^2(x)$ are given by

$$\mathcal{B}_k^1(x) = (1 + \varepsilon_1^{-k} \mathcal{B}_{\varepsilon_1}(x) + \varepsilon_2^{-k} \mathcal{B}_{\varepsilon_2}(x)), \quad k = 1, 2, 3, 4,$$

$$\mathcal{B}_k^2(x) = (1 + \varepsilon_2^{-k} \mathcal{B}_{\varepsilon_2}(x)), \quad k = 1, 2,$$

$$\mathcal{B}_k^2(x) = (1 + \varepsilon_2^{2-k} (\varepsilon_1^{-2} \mathcal{B}_{\varepsilon_1}(x) + \varepsilon_2^{-2} \mathcal{B}_{\varepsilon_2}(x))), \quad k = 3, 4,$$

where $\beta \in (0, \kappa)$.

Define matrix $B^*(x, y, t)$ as

$$B^* = \{b_{lm}^*\}_{l,m=1}^2, \text{ with } b_{ll}^* = b_{ll}, \quad b_{lm}^* = b_{lm} \frac{\mathcal{B}_k^m}{\mathcal{B}_k^l}, \quad l \neq m.$$

By using assumptions (7.1.2) and (7.1.3), we obtain that

$$\vec{\xi}^T B^* \vec{\xi} \geq \kappa^2 \vec{\xi}^T \vec{\xi}, \text{ in } \mathcal{G}, \quad \text{for all } \vec{\xi} \in \mathbb{R}^2. \quad (7.2.1)$$

For the derivation of the spatial partial derivative bounds of the exact solution \vec{u} of the model problem (7.1.1), without loss of generality we assume that the initial condition is identically zero. To establish the spatial derivative bounds of the exact solution \vec{u} , we follow the methodology of Kellogg et al. [38, Lemma 2.3].

Lemma 7.2.1. *The spatial derivatives of the exact solution \vec{u} of the model problem (7.1.1) satisfy the following estimates:*

$$\begin{aligned} \left| \frac{\partial^k u_1}{\partial x^k} \right| &\leq C [1 + \varepsilon_1^{-k} \mathcal{B}_{\varepsilon_1}(x) + \varepsilon_2^{-k} \mathcal{B}_{\varepsilon_2}(x)], \quad k = 1, 2, 3, 4, \\ \left| \frac{\partial^k u_2}{\partial x^k} \right| &\leq C [1 + \varepsilon_2^{-k} \mathcal{B}_{\varepsilon_2}(x)], \quad k = 1, 2, \\ \left| \frac{\partial^k u_2}{\partial x^k} \right| &\leq C [1 + \varepsilon_2^{2-k} (\varepsilon_1^{-2} \mathcal{B}_{\varepsilon_1}(x) + \varepsilon_2^{-2} \mathcal{B}_{\varepsilon_2}(x))], \quad k = 3, 4, \end{aligned}$$

for all $(x, y, t) \in \mathcal{G}$.

Proof. First, we derive bounds for the partial derivatives of exact solution \vec{u} on the initial and boundary points. Since $\vec{u}(x, y, 0) = \vec{0}$ for $(x, y) \in \overline{\mathcal{D}}$, it implies that $\partial^k \vec{u} / \partial x^k = \partial^k \vec{u} / \partial y^k = \vec{0}$ for $(x, y) \in \overline{\mathcal{D}}$. Next, we consider $\vec{u}(x, 0, t) = \vec{u}(x, 1, t) = \vec{0}$ in $x \in [0, 1], t \in [0, T]$ which implies that $\partial^k \vec{u} / \partial x^k = \vec{0}$. Next, take $\vec{u}(0, y, t) = \vec{u}(1, y, t) = \vec{0}$ for $y \in [0, 1], t \in [0, T]$, which implies that $\partial^k \vec{u} / \partial y^k = \vec{0}$. For a fixed $t \in [0, T]$, by using the technique of [52, Lemma 4] and Lemma 6.2.3, we can deduce that, for $(0, y, t), (1, y, t), y \in [0, 1]$ and $t \in [0, T]$:

$$\left| \frac{\partial^k u_1}{\partial x^k} \right| \leq C(\varepsilon_1^{-k} + \varepsilon_2^{-k}), \quad k = 1, 2, 3, 4$$

and

$$\begin{aligned} \left| \frac{\partial^k u_2}{\partial x^k} \right| &\leq C \varepsilon_2^{-k}, \quad k = 1, 2, \\ \left| \frac{\partial^k u_2}{\partial x^k} \right| &\leq C \varepsilon_2^{-2} (\varepsilon_1^{2-k} + \varepsilon_2^{2-k}), \quad k = 3, 4. \end{aligned}$$

To establish the derivative bounds of the exact solution \vec{u} in \mathcal{G} , we use the induction principle. Differentiating (6.1.1) with respect to x , k times, we get

$$\frac{\partial^{k+1}\vec{u}}{\partial x^k \partial t} - \varepsilon^2 \Delta \left(\frac{\partial^k \vec{u}}{\partial x^k} \right) + B \frac{\partial^k \vec{u}}{\partial x^k} = \sum_{k_2=0}^{k-1} \binom{k}{k_1} \frac{\partial^{k-k_1} B}{\partial x^{k-k_1}} \frac{\partial^{k_1} \vec{u}}{\partial x^{k_1}} =: \vec{\Phi}_k, \quad (7.2.2)$$

where $\vec{\Phi}_k$ satisfies $|\vec{\Phi}_k| \leq C\mathcal{B}_{k-1}(x)$, as consequence of inductive hypothesis. Next, define $\partial^k \vec{u} / \partial x^k = (\mathcal{B}_k^1 \tilde{u}_1, \mathcal{B}_k^2 \tilde{u}_2)^T$. Then, we have

$$\begin{cases} \frac{\partial \mathcal{B}_k^1 \tilde{u}_1}{\partial t} - \varepsilon_1^2 \Delta (\mathcal{B}_k^1 \tilde{u}_1) + b_{11} (\mathcal{B}_k^1 \tilde{u}_1) + b_{12} (\mathcal{B}_k^2 \tilde{u}_2) = \Phi_{k,1}, \\ \frac{\partial \mathcal{B}_k^2 \tilde{u}_2}{\partial t} - \varepsilon_2^2 \Delta (\mathcal{B}_k^2 \tilde{u}_2) + b_{21} (\mathcal{B}_k^1 \tilde{u}_1) + b_{22} (\mathcal{B}_k^2 \tilde{u}_2) = \Phi_{k,2}. \end{cases}$$

After simplification it is easy to express the above equations as

$$\begin{cases} \frac{\partial \tilde{u}_1}{\partial t} - \varepsilon_1^2 \Delta \tilde{u}_1 - 2\varepsilon_1^2 \frac{1}{\mathcal{B}_k^1} \frac{\partial \mathcal{B}_k^1}{\partial x} \frac{\partial \tilde{u}_1}{\partial x} + \left(b_{11} - \varepsilon_1^2 \frac{1}{\mathcal{B}_k^1} \frac{\partial^2 \mathcal{B}_k^1}{\partial x^2} \right) \tilde{u}_1 + b_{12} \frac{\mathcal{B}_k^2}{\mathcal{B}_k^1} \tilde{u}_2 = \frac{\Phi_{k,1}}{\mathcal{B}_k^1}, \\ \frac{\partial \tilde{u}_2}{\partial t} - \varepsilon_2^2 \Delta \tilde{u}_2 - 2\varepsilon_2^2 \frac{1}{\mathcal{B}_k^2} \frac{\partial \mathcal{B}_k^2}{\partial x} \frac{\partial \tilde{u}_2}{\partial x} + b_{21} \frac{\mathcal{B}_k^1}{\mathcal{B}_k^2} \tilde{u}_1 + \left(b_{22} - \varepsilon_2^2 \frac{1}{\mathcal{B}_k^2} \frac{\partial^2 \mathcal{B}_k^2}{\partial x^2} \right) \tilde{u}_2 = \frac{\Phi_{k,2}}{\mathcal{B}_k^2}. \end{cases}$$

From definition of matrix B^* and barrier function $\vec{\mathcal{B}}_k(x)$, it is easy to verify that

$$\frac{\partial \vec{u}}{\partial t} - \varepsilon_2^2 \Delta \vec{u} - 2\varepsilon_2 \beta \frac{\partial \vec{u}}{\partial x} + (B^* - \beta^2 I) \vec{u} \leq \frac{\vec{\Phi}_k}{\vec{\mathcal{B}}_k}. \quad (7.2.3)$$

Taking inner product by \vec{u} in (7.2.3) and using assumption (7.2.1), one can deduce that

$$\frac{\partial \hat{u}_k}{\partial t} - \varepsilon_2^2 \Delta \hat{u}_k - 2\varepsilon_2 \beta \frac{\partial \hat{u}_k}{\partial x} + 2(\kappa^2 - \beta^2) \hat{u}_k \leq C \|\vec{u}\|_\infty, \quad (7.2.4)$$

where $\hat{u}_k = \frac{1}{2} |\vec{u}|^2$. Using the estimate of boundary condition of \vec{u} , it follows that $\|\vec{u}\|_{\infty, \partial \mathcal{G}} \leq C$. Therefore, employing the maximum principle on scalar parabolic problem (7.2.4), we get $\|\vec{u}\|_\infty \leq C$. Hence, by definition of \vec{u} , we obtain that

$$\left| \frac{\partial^k u_l}{\partial x^k}(x, y, t) \right| \leq C \mathcal{B}_k^l(x), \quad \text{for } k = 1, 2, 3, 4 \quad \text{and } l = 1, 2,$$

where $(x, y, t) \in \bar{\mathcal{G}}$. This completes the proof. \blacksquare

Next, we discuss the derivative bounds of the exact solution \vec{u} of the continuous problem (7.1.1) with respect to spatial variable y .

Lemma 7.2.2. *Let \vec{u} be solution of (7.1.1), then the partial derivatives of \vec{u} with respect to y satisfy following bounds*

$$\begin{aligned} \left| \frac{\partial^k u_1}{\partial y^k} \right| &\leq C [1 + \varepsilon_1^{-k} \mathcal{B}_{\varepsilon_1}(y) + \varepsilon_2^{-k} \mathcal{B}_{\varepsilon_2}(y)], \quad k = 1, 2, 3, 4, \\ \left| \frac{\partial^k u_2}{\partial y^k} \right| &\leq C [1 + \varepsilon_2^{-k} \mathcal{B}_{\varepsilon_2}(y)], \quad k = 1, 2, \\ \left| \frac{\partial^k u_2}{\partial y^k} \right| &\leq C [1 + \varepsilon_2^{2-k} (\varepsilon_1^{-2} \mathcal{B}_{\varepsilon_1}(y) + \varepsilon_2^{-2} \mathcal{B}_{\varepsilon_2}(y))], \quad k = 3, 4. \end{aligned}$$

Proof. By following the technique of proof of Lemma 7.2.1, one can derive the required estimates. \blacksquare

Here, we consider a numerical example to show boundary layer behavior of exact solution \vec{u} .

Example 7.2.3. *Consider the model problem (7.1.1) on $\mathcal{G} := (0, 1)^2 \times (0, 1]$:*

Assume that the reaction matrix B as

$$B = \begin{pmatrix} 5 & -3 \\ -1 & 4 \end{pmatrix}$$

and the source term $\vec{f} = (f_1, f_2)^T$ is given by

$$f_1 = 1 + xy, \quad f_2 = 1 + x^2 y^2,$$

with zero initial and boundary data.

For fixed $t = 1$, the computed solution is shown in Fig. 7.1 along $x = y$ line. One can see from Fig. 7.1(b) and Fig. 7.1(c), the differences in layer behavior of both the numerical solution components U_1 and U_2 .

Next, we derive sharper bounds on the derivatives of the exact solution \vec{u} of the problem (7.1.1), which will be used later in the error estimate. Here, we consider $x^* = 2\varepsilon_1/\alpha \ln(1/\varepsilon_1) \leq 1/4$. For $l = 1, 2$ and $(x, y, t) \in \bar{\mathcal{G}}$, set

$$v_l(x, y, t) = \begin{cases} \sum_{k=0}^4 \frac{(x - x^*)^k}{k!} \frac{\partial^k u_l}{\partial x^k}(x^*, y, t), & 0 \leq x < x^*, \\ u_l(x, y, t), & x^* \leq x \leq 1 - x^*, \\ \sum_{k=0}^4 \frac{(x - 1 + x^*)^k}{k!} \frac{\partial^k u_l}{\partial x^k}(1 - x^*, y, t), & 1 - x^* < x \leq 1. \end{cases} \quad (7.2.5)$$

and

$$\vec{w}(x, y, t) = \vec{u}(x, y, t) - \vec{v}(x, y, t), \quad (x, y, t) \in \bar{\mathcal{G}}, \quad (7.2.6)$$

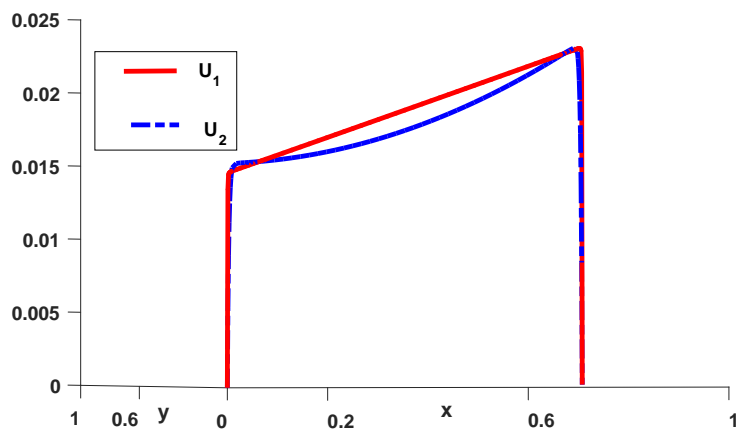
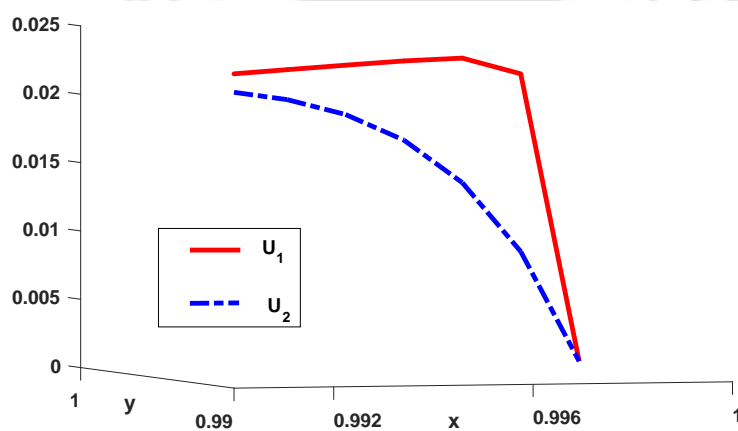
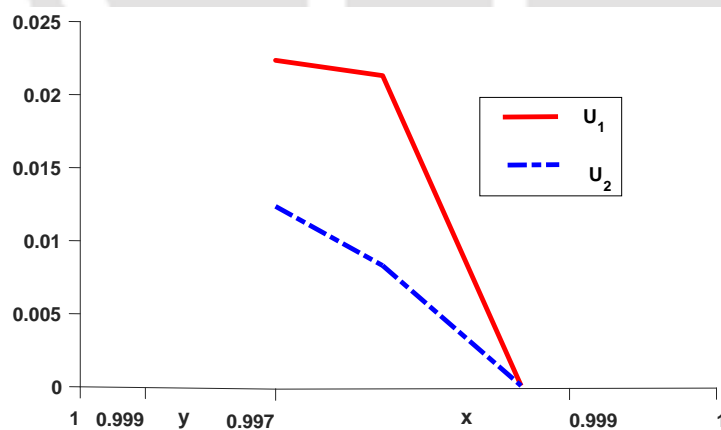
(a) Original plot along $x = y$ line(b) Layer behavior along $x = y$ line(c) Overlapping layer behavior along $x = y$ line

Figure 7.1: Plots of the numerical solution along the line $x = y$, for $\varepsilon_1 = 2^{-16}$, $\varepsilon_2 = 2^{-10}$ with discretization parameter $N = 64$ at time $t = 1$.

where \vec{v} is smooth component and \vec{w} is layer component.

Now, we discuss the derivative bounds for both the components \vec{v}, \vec{w} with respect to the spatial variable x only. Analogously, one can deduce derivative bounds of both components \vec{v}, \vec{w} for spatial variable y .

Lemma 7.2.4. *For all non-negative integer k satisfying $0 \leq k \leq 4$, the smooth component \vec{v} and layer component \vec{w} satisfy the following estimates:*

$$\left| \frac{\partial^k v_l}{\partial x^k} \right| \leq C (1 + \varepsilon_l^{2-k}), \quad 0 \leq k \leq 4, \quad l = 1, 2$$

and

$$\left| \frac{\partial^k w_1}{\partial x^k} \right| \leq C (\varepsilon_1^{-k} \mathcal{B}_{\varepsilon_1}(x) + \varepsilon_2^{-k} \mathcal{B}_{\varepsilon_2}(x)), \quad 0 \leq k \leq 4,$$

$$\left| \frac{\partial^k w_2}{\partial x^k} \right| \leq C \varepsilon_2^{-k} \mathcal{B}_{\varepsilon_2}(x), \quad 0 \leq k \leq 2,$$

$$\left| \frac{\partial^k w_2}{\partial x^k} \right| \leq C (\varepsilon_2^{2-k} (\varepsilon_1^{-2} \mathcal{B}_{\varepsilon_1}(x) + \varepsilon_2^{-2} \mathcal{B}_{\varepsilon_2}(x))), \quad k = 3, 4,$$

for all $(x, y, t) \in \mathcal{G}$.

Proof. By using Lemma 7.2.1, we obtain that

$$\begin{aligned} \left| \frac{\partial^k u_1}{\partial x^k}(x^*, y, t) \right| &\leq C (1 + \varepsilon_1^{-k} \mathcal{B}_{\varepsilon_1}(x^*) + \varepsilon_2^{-k} \mathcal{B}_{\varepsilon_2}(x^*)) \\ &\leq (1 + C_1 \varepsilon_1^{-k} \varepsilon_1^2 + C_2 \varepsilon_2^{-k} \varepsilon_1^2) \leq C(1 + \varepsilon_1^{2-k}), \quad 0 \leq k \leq 4. \end{aligned}$$

Assume that $x \in [0, x^*]$, then use definition of the smooth component from (7.2.5) to deduce that

$$\left| \frac{\partial^k v_1}{\partial x^k}(x, y, t) \right| \leq C (1 + \varepsilon_1^{2-k}), \quad 0 \leq k \leq 4. \quad (7.2.7)$$

Next, we consider the second component in $x \in [0, x^*]$, for $k = 0, 1, 2$, we have

$$\left| \frac{\partial^k u_2}{\partial x^k}(x^*, y, t) \right| \leq C (1 + \varepsilon_2^{-k} \mathcal{B}_{\varepsilon_2}(x^*)) \leq C(1 + \varepsilon_2^{2-k}).$$

Therefore, by using the previous technique, one can easily deduce that

$$\left| \frac{\partial^k v_2}{\partial x^k}(x, y, t) \right| \leq C (1 + \varepsilon_2^{2-k}), \quad 0 \leq k \leq 2. \quad (7.2.8)$$

A simple calculation leads to obtain the required estimate for $k = 3, 4$ for the smooth component v_2 .

In a similar manner, we can obtain the required estimate in $[1 - x^*, 1]$. For $x \in [x^*, 1 - x^*]$, it is easy to verify that

$$\begin{aligned} \left| \frac{\partial^k v_1}{\partial x^k}(x, y, t) \right| &= \left| \frac{\partial^k u_1}{\partial x^k}(x, y, t) \right| \leq C (1 + \varepsilon_1^{-k} \mathcal{B}_{\varepsilon_1}(x^*) + \varepsilon_2^{-k} \mathcal{B}_{\varepsilon_2}(x^*)) \\ &\leq C (1 + \varepsilon_1^{2-k}), \quad 0 \leq k \leq 4. \end{aligned}$$

An analogous result holds for the smooth component v_2 . By using the decomposition (7.2.6), we can obtain the desired results for the layer component \vec{w} . ■

Lemma 7.2.5. *Suppose that $\varepsilon_1 < \varepsilon_2$. Then, the layer component $\vec{w} = (w_1, w_2)^T$ can be decomposed as*

$$w_1 = w_{1,\varepsilon_1} + w_{1,\varepsilon_2}, \quad w_2 = w_{2,\varepsilon_1} + w_{2,\varepsilon_2},$$

where the layer components w_{l,ε_l} , $l = 1, 2$ satisfy following estimates

$$\begin{aligned} \left| \frac{\partial^2 w_{1,\varepsilon_1}}{\partial x^2} \right| &\leq C \varepsilon_1^{-2} \mathcal{B}_{\varepsilon_1}(x), & \left| \frac{\partial^2 w_{2,\varepsilon_1}}{\partial x^2} \right| &\leq C \varepsilon_2^{-2} \mathcal{B}_{\varepsilon_1}(x) \\ \left| \frac{\partial^3 w_{1,\varepsilon_2}}{\partial x^3} \right| &\leq C \varepsilon_1^{-3} \mathcal{B}_{\varepsilon_2}(x), & \left| \frac{\partial^3 w_{2,\varepsilon_2}}{\partial x^3} \right| &\leq C \varepsilon_2^{-3} \mathcal{B}_{\varepsilon_2}(x). \end{aligned}$$

Further, the layer component $\vec{w} = (w_1, w_2)^T$ can be decomposed as

$$w_1 = \bar{w}_{1,\varepsilon_1} + \bar{w}_{1,\varepsilon_2}, \quad w_2 = \bar{w}_{2,\varepsilon_1} + \bar{w}_{2,\varepsilon_2},$$

and these layer components satisfy

$$\begin{aligned} \left| \frac{\partial^2 \bar{w}_{1,\varepsilon_1}}{\partial x^2} \right| &\leq C \varepsilon_1^{-2} \mathcal{B}_{\varepsilon_1}(x), & \left| \frac{\partial^2 \bar{w}_{2,\varepsilon_1}}{\partial x^2} \right| &\leq C \varepsilon_2^{-2} \mathcal{B}_{\varepsilon_1}(x) \\ \left| \frac{\partial^4 \bar{w}_{1,\varepsilon_2}}{\partial x^4} \right| &\leq C \varepsilon_1^{-2} \varepsilon_2^{-2} \mathcal{B}_{\varepsilon_2}(x), & \left| \frac{\partial^4 \bar{w}_{2,\varepsilon_2}}{\partial x^4} \right| &\leq C \varepsilon_2^{-4} \mathcal{B}_{\varepsilon_2}(x). \end{aligned}$$

Proof. By using the methodology of [52, Lemma 5] and [49, Lemma 2], one can derive required estimates. ■

7.3 The Spatial Semidiscretization

In this section, we describe the layer-adapted Shishkin meshes for the spatial directions, then we discretize the spatial derivatives of the model problem (7.1.1) by using the central difference scheme. Before closing this section, we will discuss the truncation error estimate for the spatial discretization process.

7.3.1 Discretization of the domain

We discretize the problem (7.1.1) on a rectangular mesh $\overline{\mathcal{D}}_\varepsilon^N = \overline{\Omega}_x^N \times \overline{\Omega}_y^N$. The mesh transition parameters τ_{x,ε_1} , τ_{x,ε_2} , τ_{y,ε_1} and τ_{y,ε_2} are defined by

$$\tau_{x,\varepsilon_2} = \tau_{y,\varepsilon_2} = \min \left\{ \frac{1}{4}, \frac{2\varepsilon_2}{\beta} \ln N \right\}, \quad \text{and} \quad \tau_{x,\varepsilon_1} = \tau_{y,\varepsilon_1} = \min \left\{ \frac{1}{8}, \frac{\tau_{x,\varepsilon_2}}{2}, \frac{2\varepsilon_1}{\beta} \ln N \right\}.$$

We construct the mesh $\overline{\Omega}_x^N$ by dividing the interval $[0, 1]$ into five subintervals such as $[0, \tau_{x,\varepsilon_1}]$, $[\tau_{x,\varepsilon_1}, \tau_{x,\varepsilon_2}]$, $[\tau_{x,\varepsilon_2}, 1 - \tau_{x,\varepsilon_2}]$, $[1 - \tau_{x,\varepsilon_2}, 1 - \tau_{x,\varepsilon_1}]$ and $[1 - \tau_{x,\varepsilon_1}, 1]$. Then divide $[\tau_{x,\varepsilon_2}, 1 - \tau_{x,\varepsilon_2}]$ into $N/2$ mesh-intervals and divide other subintervals into $N/8$ mesh-intervals. Analogously, we proceed for $\overline{\Omega}_y^N$. The step sizes in both the spatial directions will be expressed as

$$\begin{cases} h_{x,i} = x_i - x_{i-1}, & i = 1, \dots, N, & \tilde{h}_{x,i} = h_{x,i} + h_{x,i+1}, & i = 1, \dots, N-1, \\ h_{y,j} = y_j - y_{j-1}, & j = 1, \dots, N, & \tilde{h}_{y,j} = h_{y,j} + h_{y,j+1}, & j = 1, \dots, N-1. \end{cases}$$

Figure 7.2 shows a typical discretized domain with the Shishkin meshes.

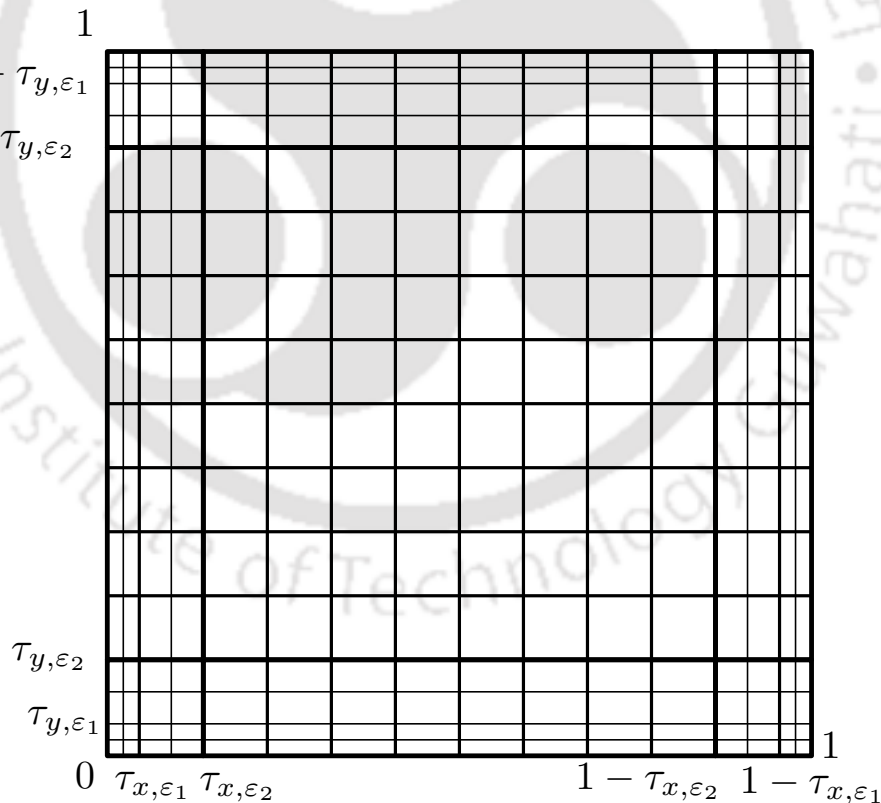


Figure 7.2: Example of Shishkin mesh $\overline{\mathcal{D}}_\varepsilon^N$ for $N = 16$

Note that when $\tau_{x,\varepsilon_2} = \tau_{y,\varepsilon_2} = 1/4$, the meshes will become uniform and N^{-1} is exponentially small relative to ε_2 , therefore, in this case the classical approach can be

applied for derivation of the truncation error. If $\tau_{x,\varepsilon_1} = \tau_{x,\varepsilon_2}/2$, $\tau_{y,\varepsilon_1} = \tau_{y,\varepsilon_2}/2$ then $\varepsilon_2 = O(\varepsilon_1)$ and the result can be easily obtained. Therefore, we only consider the case $\tau_{x,\varepsilon_1} < \tau_{x,\varepsilon_2}/2$, and $\tau_{y,\varepsilon_1} < \tau_{y,\varepsilon_2}/2$.

7.3.2 The semidiscrete scheme

Here, we present the numerical scheme (finite difference spatial semidiscretization) for the model problem (7.1.1) to obtain the approximation of the exact solution $\vec{u}(x_i, y_j, t)$, where (x_i, y_j) are the mesh points of the rectangular mesh $\overline{\mathcal{D}}_\varepsilon^N$. Let us denote $[\cdot]_N$ the restriction of a function defined on $\overline{\Omega}_x$ to $\overline{\Omega}_x^N$. The central difference scheme is used to approximate the differential operator \mathfrak{L}_ε . Thus, $\vec{u}_N(t)$ is defined as the solution of following IVP of the form

$$\begin{cases} \vec{u}'_N(t) + \mathfrak{L}_\varepsilon^N \vec{u}_N(t) = [\vec{f}]_N(t), & \text{in } \overline{\mathcal{D}}_\varepsilon^N, \\ \vec{u}_N(0) = [\vec{u}_0]_N, \end{cases} \quad (7.3.1)$$

where $\mathfrak{L}_\varepsilon^N$ is spatial discretization of the system of the elliptic reaction-diffusion operator \mathfrak{L}_ε and the source term \vec{f} is given by

$$[\vec{f}]_N(t) = \begin{cases} \vec{f}(x_i, y_j, t), & (x_i, y_j) \in \mathcal{D}_\varepsilon^N, \\ \vec{0}, & (x_i, y_j) \in \partial\mathcal{D}_\varepsilon^N = \overline{\mathcal{D}}_\varepsilon^N \setminus \mathcal{D}_\varepsilon^N. \end{cases}$$

Hence, the difference scheme can be expressed as follows:

$$\left\{ \begin{array}{l} \mathfrak{L}_{\varepsilon_1}^N \vec{u}_N(t)(x_i, y_j) \equiv r_{i,j-}^1 u_{1N}(t)(x_i, y_{j-1}) + r_{i,j-}^1 u_{1N}(t)(x_{i-1}, y_j) \\ \quad + r_{i,j}^1 u_{1N}(t)(x_i, y_j) + r_{i,j+}^1 u_{1N}(t)(x_i, y_{j+1}) \\ \quad + r_{i+,j}^1 u_{1N}(t)(x_{i+1}, y_j) + q_{i,j}^1 u_{2N}(t)(x_i, y_j), \\ \quad \text{for } i, j = 1, \dots, N-1, \\ \mathfrak{L}_{\varepsilon_1}^N \vec{u}_N(t)(x_i, y_j) \equiv u_{1N}(x_i, y_j, t) = 0, \quad \text{for } i, j = 0, N, \\ \mathfrak{L}_{\varepsilon_2}^N \vec{u}_N(t)(x_i, y_j) \equiv r_{i,j-}^2 u_{2N}(t)(x_i, y_{j-1}) + r_{i,j-}^2 u_{2N}(t)(x_{i-1}, y_j) \\ \quad + r_{i,j}^2 u_{2N}(t)(x_i, y_j) + r_{i,j+}^2 u_{2N}(t)(x_i, y_{j+1}) \\ \quad + r_{i+,j}^2 u_{2N}(t)(x_{i+1}, y_j) + q_{i,j}^2 u_{1N}(t)(x_i, y_j), \\ \quad \text{for } i, j = 1, \dots, N-1, \\ \mathfrak{L}_{\varepsilon_2}^N \vec{u}_N(t)(x_i, y_j) \equiv u_{2N}(x_i, y_j, t) = 0, \quad \text{for } i, j = 0, N, \end{array} \right. \quad (7.3.2)$$

where the coefficients are given by

$$\begin{cases} r_{i,j-}^l(t) = \frac{-2\varepsilon_l}{\tilde{h}_{y,j}h_{y,j}}, & r_{i-,j}^l(t) = \frac{-2\varepsilon_l}{\tilde{h}_{x,i}h_{x,i}}, \quad l = 1, 2, \\ r_{i,j+}^l(t) = \frac{-2\varepsilon_l}{\tilde{h}_{y,j}h_{y,j+1}}, & r_{i+,j}^l(t) = \frac{-2\varepsilon_l}{\tilde{h}_{x,i+1}h_{x,i}}, \\ r_{i,j}^l(t) = b_{ll}(x_i, y_j, t) - r_{i,j-}^l(t) - r_{i-,j}^l(t) - r_{i,j+}^l(t) - r_{i+,j}^l(t), \\ q_{ij}^1(t) = b_{12}(x_i, y_j, t), \quad q_{ij}^2(t) = b_{21}(x_i, y_j, t). \end{cases} \quad (7.3.3)$$

Lemma 7.3.1. (Discrete maximum principle) Let $\mathfrak{L}_{\varepsilon}^N$, be the difference operators given in (7.3.2)-(7.3.3). If $[\vec{f}]_N \geq \vec{0}$ and $[\vec{u}_0]_N \geq \vec{0}$, for any $(x_i, y_j) \in \overline{\mathcal{D}}_{\varepsilon}^N$, then we have $\vec{u}_N(t) \geq \vec{0}$ for all $(x_i, y_j, t) \in \overline{\mathcal{D}}_{\varepsilon}^N \times [0, T]$.

Proof. We prove this lemma by contradiction. Assume that there exists a point $(x_{i^*}, y_{j^*}) \in \mathcal{D}_{\varepsilon}^N$, $t > 0$ such that

$$\begin{aligned} & \min \{u_{1N}(t)(x_{i^*}, y_{j^*}), u_{2N}(t)(x_{i^*}, y_{j^*})\} \\ &= \min \left\{ \min_{(x_i, y_j) \in \mathcal{D}_{\varepsilon}^N} u_{1N}(t)(x_i, y_j), \min_{(x_i, y_j) \in \mathcal{D}_{\varepsilon}^N} u_{2N}(t)(x_i, y_j) \right\} < 0, \end{aligned}$$

without loss of generality we assume that $u_{1N}(t)(x_{i^*}, y_{j^*}) \leq u_{2N}(t)(x_{i^*}, y_{j^*})$. Therefore, it follows that $u'_{1N}(t)(x_{i^*}, y_{j^*}) \leq 0$ for $t \in (0, T]$.

Next, consider the first component of the source term as

$$\begin{aligned} f_1(x_{i^*}, y_{j^*}, t) &= u'_{1N}(t)(x_{i^*}, y_{j^*}) + \mathfrak{L}_{\varepsilon_1}^N \vec{u}_N(t)(x_{i^*}, y_{j^*}) \\ &\leq r_{i,j-}^1 u_{1N}(t)(x_{i^*}, y_{j^*-1}) + r_{i-,j}^1 u_{1N}(t)(x_{i^*-1}, y_{j^*}) \\ &\quad + r_{i,j}^1 u_{1N}(t)(x_{i^*}, y_{j^*}) + r_{i,j+}^1 u_{1N}(t)(x_{i^*}, y_{j^*+1}) \\ &\quad + r_{i+,j}^1 u_{1N}(t)(x_{i^*+1}, y_{j^*}) + q_{i,j}^1 u_{2N}(t)(x_{i^*}, y_{j^*}) < 0, \end{aligned}$$

which contradicts the hypothesis of the lemma, therefore, we have $\vec{u}_N(t) \geq \vec{0}$, for all $(x_i, y_j, t) \in \overline{\mathcal{D}}_{\varepsilon}^N \times [0, T]$. \blacksquare

An immediate consequence of Lemma 7.3.1 is the following result.

Corollary 7.3.2. If a vector function $\vec{\phi}$ defined on $\mathcal{D}_{\varepsilon}^N \times [0, T]$, $\vec{\phi}(x_i, y_j, 0) \geq \vec{0}$ and it satisfies that

$$\vec{\phi}'(t)(x, y) + \left(\mathfrak{L}_{\varepsilon}^N \vec{\phi}(t) \right) (x, y) \geq \vec{0}, \quad \forall (x, y, t) \in \mathcal{D}_{\varepsilon}^N \times [0, T],$$

then, $\vec{\phi}(t)(x, y) \geq \vec{0}$ for all $(x, y, t) \in \overline{\mathcal{D}}_{\varepsilon}^N \times [0, T]$.

7.3.3 Truncation error

Next, we define the global error $\vec{e}_N(t)$ and the local truncation error $\vec{e}_N^L(t)$ for spatial discrete scheme (7.3.1) at any time $t \in [0, T]$, as follows

$$\vec{e}_N(t) = [\vec{u}(t)]_N - \vec{u}_N(t), \quad \vec{e}_N^L(t) = \left(\frac{d}{dt} + \mathfrak{L}_\varepsilon^N \right) [\vec{u}(t)]_N - \left[\left(\frac{\partial}{\partial t} + \mathfrak{L}_\varepsilon \right) \vec{u}(t) \right]_N.$$

By using the smoothness properties of \vec{u} , the local truncation error $\vec{e}_N^L(t)$ can be written as

$$\vec{e}_N^L(t) = \mathfrak{L}_\varepsilon^N [\vec{u}(t)]_N - [\mathfrak{L}_\varepsilon \vec{u}(t)]_N. \quad (7.3.4)$$

From the definition of the global error $\vec{e}_N(t)$ and the local truncation error $\vec{e}_N^L(t)$, we deduce the following relation

$$\left(\frac{d}{dt} + \mathfrak{L}_\varepsilon^N \right) \vec{e}_N(t) = \vec{e}_N^L(t). \quad (7.3.5)$$

The local truncation error $\vec{e}_N^L(t)$ can be written as

$$\vec{e}_N^L(t) = \vec{e}_{x,N}^L(t) + \vec{e}_{y,N}^L(t),$$

where

$$\vec{e}_{x,N}^L(t) = \mathcal{E}^2 ([\vec{u}_{xx}(t)]_N - \delta_x^2 \vec{u}_N(t)), \quad \vec{e}_{y,N}^L(t) = \mathcal{E}^2 ([\vec{u}_{yy}(t)]_N - \delta_y^2 \vec{u}_N(t)).$$

Also, express the global error as $\vec{e}_N(t) = \vec{e}_{x,N}(t) + \vec{e}_{y,N}(t)$. Hence, we split (7.3.5) as follows:

$$\left(\frac{d}{dt} + \mathfrak{L}_\varepsilon^N \right) \vec{e}_{x,N}(t) = \vec{e}_{x,N}^L(t), \quad (7.3.6)$$

$$\left(\frac{d}{dt} + \mathfrak{L}_\varepsilon^N \right) \vec{e}_{y,N}(t) = \vec{e}_{y,N}^L(t). \quad (7.3.7)$$

Here, we analyze the error related to (7.3.6), analogously one can proceed for (7.3.7).

By using the solution decomposition (7.2.6), the local truncation error can be expressed as

$$\begin{cases} \vec{e}_{x,N}^L(t) = \mathcal{E}^2 ([\vec{v}_{xx}(t)]_N - \delta_x^2 \vec{v}_N(t)) + \mathcal{E}^2 ([\vec{w}_{xx}(t)]_N - \delta_x^2 \vec{w}_N(t)), \\ \vec{e}_{y,N}^L(t) = \mathcal{E}^2 ([\vec{v}_{yy}(t)]_N - \delta_y^2 \vec{v}_N(t)) + \mathcal{E}^2 ([\vec{w}_{yy}(t)]_N - \delta_y^2 \vec{w}_N(t)). \end{cases}$$

By following the approach of [49] and using the derivative bound of smooth and layer component (given in Lemma 7.2.4 and Lemma 7.2.5) with appropriate estimate from

(6.4.7), the local truncation error $\vec{e}_{x,N}^L(t) = ((\vec{e}_{x,N}^L)_1, (\vec{e}_{x,N}^L)_2)(t)$ satisfies

$$(\vec{e}_{x,N}^L)_l(t) = \begin{cases} CN^{-2} \ln^2 N, & \text{for } x_i \notin \{\tau_{x,\varepsilon_1}, \tau_{x,\varepsilon_2}, 1 - \tau_{x,\varepsilon_2}, 1 - \tau_{x,\varepsilon_1}\}, l = 1, 2, \\ C(\varepsilon_1 \varepsilon_2^{-1} N^{-1} + N^{-2}), & \text{for } x_i \in \{\tau_{x,\varepsilon_1}, 1 - \tau_{x,\varepsilon_1}\}, l = 1, \\ C(\varepsilon_1^{-1} \varepsilon_2 N^{-1} + N^{-2}), & \text{for } x_i \in \{\tau_{x,\varepsilon_1}, 1 - \tau_{x,\varepsilon_1}\}, l = 2, \\ C(\varepsilon_1^2 \varepsilon_2^{-1} N^{-1} + N^{-2}), & \text{for } x_i \in \{\tau_{x,\varepsilon_2}, 1 - \tau_{x,\varepsilon_2}\}, l = 1, \\ C(\varepsilon_2 N^{-1} + N^{-2}), & \text{for } x_i \in \{\tau_{x,\varepsilon_2}, 1 - \tau_{x,\varepsilon_2}\}, l = 2. \end{cases}$$

Next, we construct barrier functions for the truncation error. Define the piecewise linear functions φ_{ε_1} and φ_{ε_2} as follows

$$\varphi_{\varepsilon_l}(x) = \begin{cases} x\tau_{x,\varepsilon_l}^{-1}, & \text{for } x \in [0, \tau_{x,\varepsilon_l}], \\ 1, & \text{for } x \in [\tau_{x,\varepsilon_l}, 1 - \tau_{x,\varepsilon_l}], \\ (1-x)\tau_{x,\varepsilon_l}^{-1}, & \text{for } x \in [1 - \tau_{x,\varepsilon_l}, 1], \end{cases}$$

for $l = 1, 2$. The discrete barrier function $\vec{\Psi}(x_i, y_j, t)$ is given by

$$\vec{\Psi}(x_i, y_j, t) = \vec{C}N^{-2} \ln^2 N (1 + \varphi_{\varepsilon_1}(x_i) + \varphi_{\varepsilon_2}(x_i)) c \pm \vec{e}_{x,N}(t)(x_i, y_j).$$

It is easy to verify that

$$\begin{cases} \vec{\Psi}'(t)(x_i, y_j) + \left(\mathcal{L}_{\varepsilon}^N \vec{\Psi}(t)\right)(x_i, y_j) \geq \vec{0}, & \forall (x_i, y_j, t) \in \mathcal{D}_{\varepsilon}^N \times [0, T], \\ \vec{\Psi}(t)(x_i, y_j, 0) > \vec{0}, & \forall (x_i, y_j) \in \overline{\mathcal{D}}_{\varepsilon}^N. \end{cases}$$

Therefore, by using the maximum principle given in Lemma 7.3.1 on $\overline{\mathcal{D}}_{\varepsilon}^N \times [0, T]$, we obtain that

$$|\vec{e}_{x,N}(t)| \leq \vec{C}N^{-2} \ln^2 N.$$

By following the similar technique, one can show that $|\vec{e}_{y,N}(t)| \leq \vec{C}N^{-2} \ln^2 N$. \blacksquare

We have the following truncation error estimate for the spatial discretization process (7.3.1).

Theorem 7.3.3. *Let $\vec{u}_N(t)$ be the numerical approximation of the exact solution \vec{u} of model problem (7.1.1). Then, the global error $\vec{e}_N(t)$ satisfies*

$$\|\vec{e}_N(t)\|_{\infty} \leq CN^{-2} \ln^2 N, \quad \text{for all } t \in [0, T]. \quad (7.3.8)$$

Hence, we conclude that the spatial discretization is an almost second-order uniformly convergent scheme.

7.4 The Discrete Problem

In this section, we introduce the numerical scheme (consists of the implicit-Euler method) to discretize the semidiscrete problem (7.3.1). Later, the convergence analysis of the fully discrete scheme has been established.

7.4.1 The fully discrete scheme

We consider the implicit-Euler method for the time discretization. Consider the uniform mesh $\bar{\Upsilon}^M = \{t_n = n\Delta t, \Delta t = T/M, n = 0, 1, \dots, M\}$. Assume that \vec{u}_N^n is the numerical approximation of $\vec{u}_N(t_n)$, be the solution of the following fully discrete scheme:

$$\begin{cases} \frac{\vec{u}_N^n - \vec{u}_N^{n-1}}{\Delta t} + \mathfrak{L}_{\bar{\varepsilon}}^{N,M} \vec{u}_N^n = [\tilde{f}]_N(t_n), & n = 1, \dots, M, \\ \vec{u}_N^0 = [\vec{u}_0]_N. \end{cases} \quad (7.4.1)$$

The fully discrete scheme (7.4.1) can be expressed as

$$\begin{cases} \left(I + \Delta t \mathfrak{L}_{\bar{\varepsilon}}^{N,M} \right) \vec{u}_N^n = \vec{u}_N^{n-1} + \Delta t [\tilde{f}]_N(t_n), \\ \vec{u}_N^0 = [\vec{u}_0]_N. \end{cases} \quad (7.4.2)$$

By following the technique described in Lemma 6.2.3, one can obtain the following time derivative estimate

$$\|\vec{u}_N''(t)\|_{\infty} \leq C, \quad t \in [0, T]. \quad (7.4.3)$$

Stability

Lemma 7.4.1. *The difference operator $\left(I_N + \Delta t \mathfrak{L}_{\bar{\varepsilon}}^{N,M} \right)$ defined in (7.4.2) satisfies stability condition as follows:*

$$\left\| \left(I + \Delta t \mathfrak{L}_{\bar{\varepsilon}}^{N,M} \right)^{-1} \right\|_{\infty} \leq 1.$$

Proof. By following the methodology of [14], it can be easily deduced. ■

Consistency

The local truncation error \bar{e}_N^n of the numerical scheme (7.4.1) at the time level t_m is defined by

$$\bar{e}_N^n = \vec{u}_N(t_n) - \left(I + \Delta t \mathfrak{L}_{\bar{\varepsilon}}^{N,M} \right)^{-1} \left(\vec{u}_N(t_{n-1}) + \Delta t [\tilde{f}]_N(t_n) \right).$$

Lemma 7.4.2. *The local truncation error corresponding to the discrete scheme (7.4.1) satisfies the following estimate*

$$\|\vec{e}_N^n\|_\infty \leq C(\Delta t)^2.$$

Proof. By applying the Taylor expansion on $\vec{u}_N(t_{n-1})$ and using the derivative bound (7.4.3) with stability condition (Lemma 7.4.1), one can obtain the desired estimate. ■

Convergence

Define the global error in time for numerical scheme (7.4.1) as follows

$$\vec{E}_N^n = \vec{u}_N(t_n) - \vec{u}_N^n.$$

By combining the consistency and stability results, we obtain the convergence results:

Lemma 7.4.3. *The global truncation error of the discrete scheme (7.4.1) satisfies*

$$\|\vec{E}_N^n\|_\infty \leq C\Delta t.$$

Proof. By combining the stability result (Lemma 7.4.1) and the consistency result given in Lemma 7.4.2, we get the required result. ■

7.4.2 Uniform convergence

We define the global error at each spatial mesh point (x_i, y_j) and at each time level t_m as usual, *i.e.*,

$$\vec{E}_{i,j}^n = \vec{u}(x_i, y_j, t_n) - \vec{u}_N^n(x_i, y_j).$$

The main result of this chapter is discussed in the following theorem.

Theorem 7.4.4. *The global truncation error satisfies*

$$\|\vec{E}_{i,j}^n\|_\infty \leq C(N^{-2} \ln^2 N + \Delta t),$$

where constant C is independent of $\varepsilon_1, \varepsilon_2, N$ and M .

Proof. Split the error contribution of the time and the spatial discretization process as follows:

$$\|\vec{E}_{i,j}^n\|_\infty \leq C\|\vec{u}(x_i, y_j, t_n) - \vec{u}_N(t_n)\|_\infty + \|\vec{E}_N^n\|_\infty.$$

By combining the uniform convergence results of the spatial and the time discretization process (7.3.8) and Lemma 7.4.3 respectively, we obtain the required estimate. ■

7.5 Numerical Results

To illustrate the accuracy of the numerical method and the theoretical results of the error analysis, we present some numerical results. The numerical experiments are performed by choosing the time discretization parameter $\Delta t = 1/M$.

Example 7.5.1. Consider the following system of 2D parabolic reaction-diffusion IBVP on $\mathcal{G} := (0, 1)^2 \times (0, 1]$:

$$\begin{cases} \frac{\partial u_1}{\partial t} - \varepsilon_1^2 \Delta u_1 + (2 + x^2 y^2 t^2) u_1 - (1 + x^2 y^2 t) u_2 = e^{-t} x y (1-x)(1-y), \\ \frac{\partial u_2}{\partial t} - \varepsilon_2^2 \Delta u_2 - (x^2 y^2 t) u_1 + (4 + x^2 y^2 t^2) u_2 = e^{-t} x^2 y^2 (1-x)(1-y), \\ \vec{u}(x, y, 0) = (x + y + 1, x^2 y^2 + 1)^T, \quad (x, y) \in (0, 1)^2, \\ \vec{u}(0, y, t) = \vec{u}(1, y, t) = \vec{0}, \quad (y, t) \in [0, 1] \times [0, 1], \\ \vec{u}(x, 0, t) = \vec{u}(x, 1, t) = \vec{0}, \quad (x, t) \in [0, 1] \times [0, 1]. \end{cases}$$

For our experiments, the singular perturbation parameters takes value on the set $S_\varepsilon = \{(\varepsilon_1, \varepsilon_2) | (2^{-12}, 2^{-10}), (2^{-16}, 2^{-12}), (2^{-20}, 2^{-14})\}$, which is a sufficiently small choice to bring out the singularly perturbed nature of the problem.

From Table 7.1, we can see that the order of convergence is one. Therefore, we can conclude that the global errors are dominated by the errors corresponding to the time discretization. In order to visualize the numerical order of convergence, we have plotted the maximum pointwise errors in loglog plot for Example 7.5.1 in Fig. 7.3 and Fig. 7.4, which again shows the accuracy of the numerical scheme.

From Table 7.2, one can verify the almost second-order convergence and therefore, we conclude that the global errors are dominated by the errors corresponding to the space discretization. To visualize the order of convergence of the numerical solutions, we have also plotted the maximum point-wise errors for Example 7.5.1 and in Fig. 7.5 and Fig. 7.6.

7.6 Conclusions

In this chapter, we have numerically solved the singularly perturbed system of 2D parabolic reaction-diffusion problem of the form (7.1.1), using the uniform mesh for the temporal domain and the piecewise-uniform Shishkin mesh for the spatial domains. For discretizing the spatial derivatives, central difference scheme has been used and then the implicit-Euler scheme has been used in the resulting semidiscrete scheme. For the proposed scheme, the stability and error analysis have been carried out, which shows

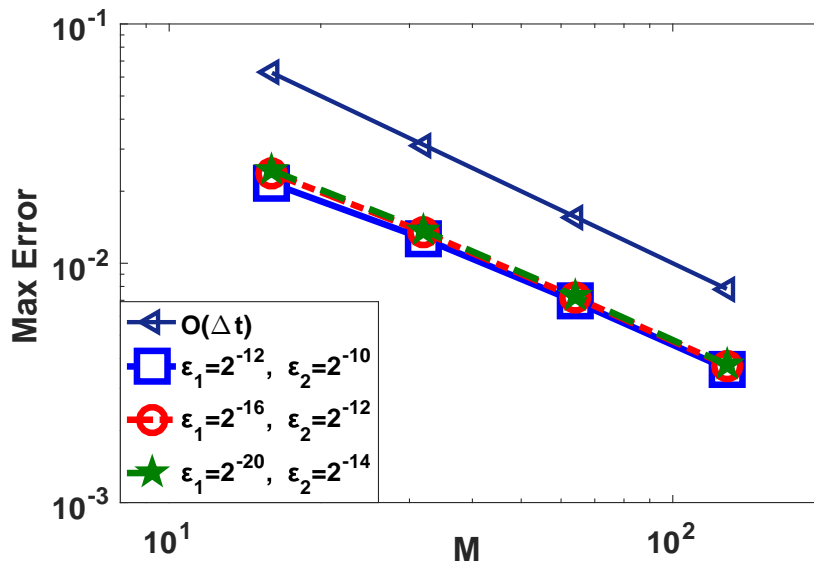


Figure 7.3: Loglog plot (for the temporal order of convergence) associated with numerical solution U_1 of Example 7.5.1.

that the method converges uniformly with second-order (up to a logarithmic factor) in space and first-order in time. Along with the analysis, we have presented numerical example to verify the theoretical findings.

Table 7.1: Uniform errors and the corresponding orders of convergence for Example 7.5.1.

S_ε	Number of mesh-intervals N /temporal mesh-size Δt			
	$16/\frac{1}{8}$	$32/\frac{1}{16}$	$64/\frac{1}{32}$	$128/\frac{1}{64}$
$E_1^{N,M}$	2.4424e-02	1.3726e-02	7.3077e-03	3.7730e-03
$P_1^{N,M}$	0.8313	0.9094	0.9537	
$E_2^{N,M}$	2.3839e-02	1.2967e-02	6.9265e-03	3.6540e-03
$P_2^{N,M}$	0.8784	0.9046	0.9226	

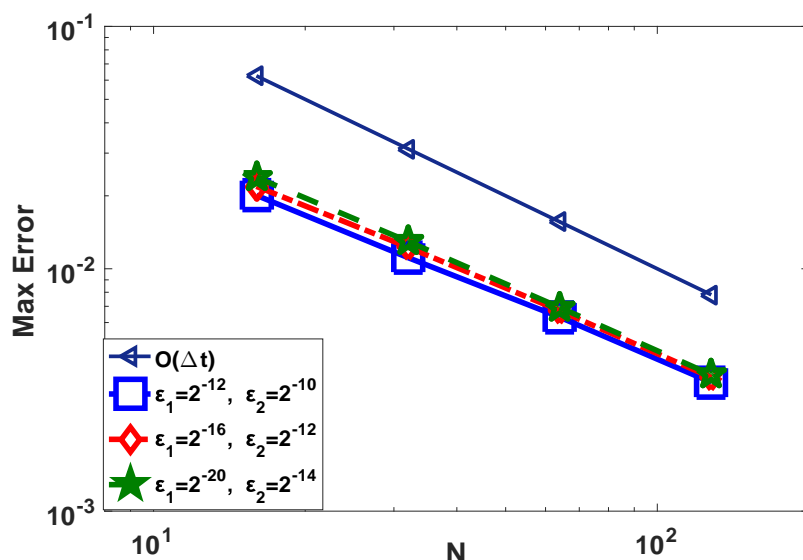


Figure 7.4: *Loglog plot (for the temporal order of convergence) associated with numerical solution U_2 of Example 7.5.1.*

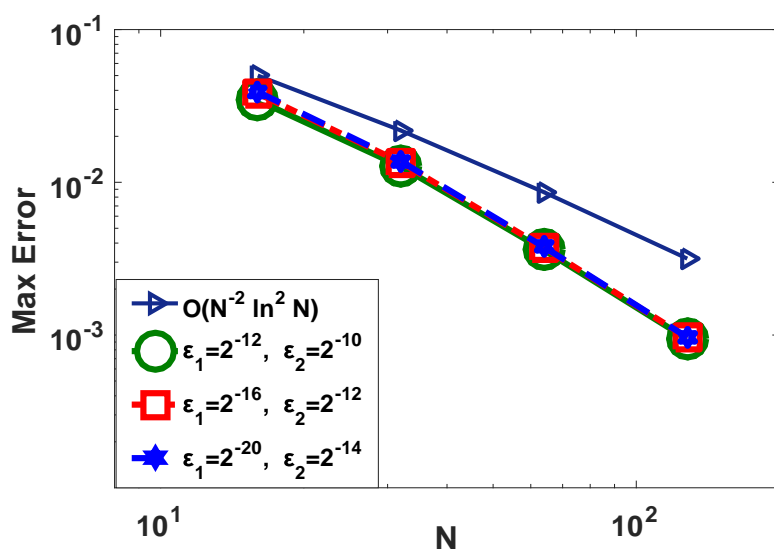
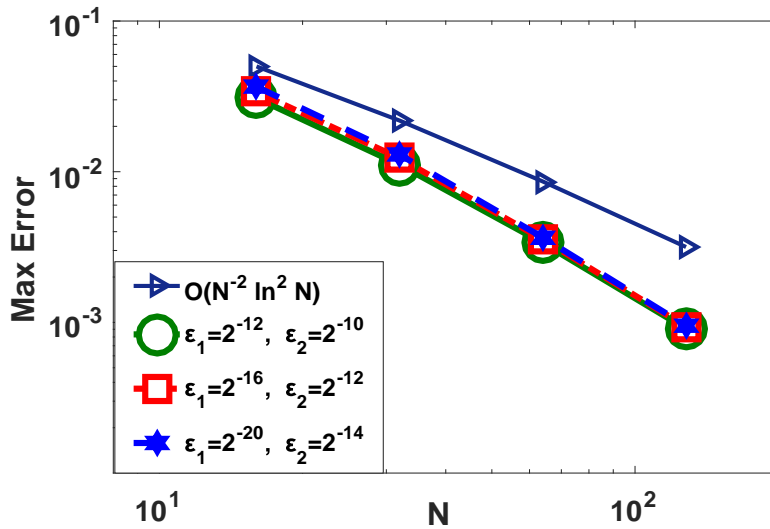


Figure 7.5: *Loglog plot associated with numerical solution U_1 of Example 7.5.1.*

Table 7.2: Uniform errors and the corresponding orders of convergence for Example 7.5.1.

S_ε	Number of mesh-intervals N /temporal mesh-size Δt			
	$16/\frac{1}{8}$	$32/\frac{1}{32}$	$64/\frac{1}{128}$	$128/\frac{1}{512}$
$E_1^{N,M}$	3.9144e-02	1.3726e-02	3.7693e-03	9.6636e-04
$\mathcal{P}_1^{N,M}$	1.5118	1.8646	1.9637	
$E_2^{N,M}$	3.6640e-02	1.2967e-02	3.6592e-03	9.5164e-04
$\mathcal{P}_2^{N,M}$	1.4986	1.8252	1.9430	

Figure 7.6: Loglog plot associated with numerical solution U_2 of Example 7.5.1.

Summary and Future Scopes

This chapter is devoted to a brief overview of main results achieved in this thesis. It also highlights the scope for possible extension and future investigations.

8.1 Summary of the Results

The main core of this thesis is to develop \mathcal{E} -uniform fitted mesh methods for solving singularly perturbed system of parabolic PDEs in one- and two-dimensions. The results of this thesis with some important observations are briefly described below:

- A uniformly convergent upwind finite scheme is proposed and analyzed for singularly perturbed system of 1D parabolic convection-diffusion problems. First, the time derivative is discretized by the implicit-Euler scheme on uniform mesh. Then, the spatial derivatives are substituted by the classical upwind scheme on piecewise-uniform Shishkin mesh in the resulting time semidiscrete problem. It is shown that the numerical method is almost first-order accurate in the discrete supremum norm. This computational technique is extended for singularly perturbed system of linear and semilinear parabolic convection-diffusion problems. Later, a post-processing technique is discussed, which improves the accuracy of the proposed numerical scheme on the piecewise-uniform Shishkin mesh. Numerical experiments are conducted to validate the theoretical findings.
- Next, a parameter-uniform hybrid numerical is considered for solving singularly perturbed system of 1D parabolic convection-diffusion IBVP on Shishkin mesh. The scheme consists of the implicit-Euler scheme for the time derivative and the hybrid numerical scheme for the spatial derivatives. Hybrid numerical scheme is a proper combination of midpoint scheme and central difference scheme. It is shown that the discrete solution obtained by this technique is almost second-order spatial

accurate in the discrete supremum norm, provided the perturbation parameters ε_1 and ε_2 satisfy $\varepsilon_1, \varepsilon_2 \leq N^{-1}$ (the most important case from practical point of view). Numerical results are presented to verify the theoretical error estimates.

- Then, singularly perturbed system of 1D parabolic convection-diffusion with discontinuous convection coefficient and source term is analyzed using implicit-Euler for the time derivative and upwind difference for the spatial derivative on piecewise-uniform spatial mesh and uniform time mesh. The parameter-uniform error estimates are derived for the numerical solution. To support the theoretical results, numerical experiments are carried out. Moreover, maximum errors are plotted in the loglog scale to show the convergence rate.
- In the literature, so far there exist no result where a singularly perturbed system of 2D parabolic convection-diffusion problem is solved numerically. To discretize the time derivative, the fractional-step method is used. Then the classical upwind scheme is used on the piecewise-uniform Shishkin meshes in the spatial directions, for the 1D stationary problems resulting of the previous step. Error estimates are derived for the numerical scheme, which are independent of the singular perturbation parameter ε . Numerical results reveal the theoretical error estimate.
- We proposed a parameter-uniform fractional-step method to solve singularly perturbed system of 2D parabolic reaction-diffusion IBVP with one perturbation parameter. The theoretical and numerical results explains that the error converges at the rate of first-order in temporal variable and almost second-order in the spatial variables.
- Finally, we have solved numerically the singularly perturbed system of 2D parabolic reaction-diffusion problems with different perturbation parameters. First, spatial derivatives are discretized by the central difference scheme on piecewise-uniform Shishkin mesh. Then, the time derivative is discretized, in resulting IVP, by the implicit-Euler scheme on uniform mesh. It is shown that the error estimate obtained for the proposed numerical scheme is almost second-order accurate in space and first-order in time. Numerical results are produced to validate the theoretical error estimates.

8.2 Scope for Future Work

A brief outline, describing the possible extensions of the current work to be carried out in the future with suitable model problems, are presented below:

In Chapter 2 we presented the numerical analysis for singularly perturbed weakly coupled system of parabolic convection-diffusion IBVP exhibiting boundary layers. The problem is analyzed using implicit-Euler difference scheme for the time derivative and upwind difference scheme for the spatial derivative on a layer-adapted mesh.

The numerical scheme applied developed in Chapter 2 can be applied to strongly coupled system of parabolic convection-diffusion problem of the form

$$\begin{cases} \frac{\partial \vec{u}}{\partial t} - \mathcal{E} \frac{\partial^2 \vec{u}}{\partial x^2} - \mathcal{A}(x) \frac{\partial \vec{u}}{\partial x} + \mathcal{B}(x) \vec{u} = \vec{f}, & (x, t) \in Q, \\ \vec{u}(x, 0) = \vec{u}_0(x), & x \in \bar{\Omega}_x, \\ \vec{u}(0, t) = \vec{0}, \quad \vec{u}(1, t) = \vec{0}, & t \in (0, T], \end{cases} \quad (8.2.1)$$

where $\mathcal{E} = \text{diag}(\varepsilon_1, \varepsilon_2)$ and $\mathcal{A}(x) = (a_{lm}(x))_{2 \times 2}$, $\mathcal{B}(x) = (b_{lm}(x))_{2 \times 2}$. The coefficients matrices A, B satisfy the following positivity conditions:

$$\begin{cases} a_{11}(x) \geq \alpha > 0, & a_{22}(x) \geq \alpha > 0, \\ \min_{x \in \bar{\Omega}_x} \{b_{11}(x) + b_{12}(x), b_{21}(x) + b_{22}(x)\} \geq \beta > 0. \end{cases}$$

In addition assume that \mathcal{B} is an L_0 -matrix. The coefficients of matrices \mathcal{A}, \mathcal{B} , source term \vec{f} are sufficiently smooth.

The hybrid difference scheme discussed in Chapter 3 can be applied to the above model problem (8.2.1) and also one can use this numerical scheme to obtain higher order numerical approximate solution of the model problem discussed in Chapter 4.

In Chapter 4, we analyzed upwind based difference scheme for singularly perturbed system of parabolic convection-diffusion with discontinuous convection coefficient and source term. One can use this method to solve system of convection-diffusion problem with degenerate convective term and a discontinuous source term of the form

$$\begin{cases} \frac{\partial \vec{u}}{\partial t} - \mathcal{E}^2 \frac{\partial^2 \vec{u}}{\partial x^2} - \mu x^{2p+1} A(x) \frac{\partial \vec{u}}{\partial x} + B(x) \vec{u} = \vec{f}, & (x, t) \in \tilde{Q}^- \cup \tilde{Q}^+, \\ \vec{u}(x, 0) = \vec{u}_0(x), & x \in [-d, d], \\ \vec{u}(0, t) = \vec{0}, \quad \vec{u}(1, t) = \vec{0}, & t \in (0, T], \end{cases} \quad (8.2.2)$$

where $0 \leq \mu \ll 1$, $\mathcal{E} = \text{diag}(\varepsilon_1, \varepsilon_2)$, $\mu \leq \varepsilon_1, \varepsilon_2$, $\tilde{Q}^- = (-d, 0) \times (0, T]$ and $\tilde{Q}^+ = (0, d) \times (0, T]$. The coefficients of convection matrix $A(x) = \text{diag}(a_1, a_2)$ and reaction matrix $B(x) = (b_{lm}(x))_{2 \times 2}$ are sufficiently smooth and satisfy the following conditions

$$\begin{cases} a_1(x), a_2(x) \geq \alpha > 0, & x \in [-d, d] \\ \min_{x \in [-d, d]} \{b_{11}(x) + b_{12}(x), b_{21}(x) + b_{22}(x)\} \geq \beta > 0. \end{cases}$$

The source term $\vec{f}(x, t)$ is sufficiently smooth on $\tilde{Q}^- \cup \tilde{Q}^+$.

In Chapter 5, we considered singularly perturbed system of 2D parabolic convection-diffusion problem with one parameter. It will be interesting to develop fractional-step method for system of 2D parabolic IBVP of the form

$$\begin{cases} \frac{\partial \vec{u}}{\partial t} - \mathcal{E} \left(\frac{\partial^2 \vec{u}}{\partial x^2} + \frac{\partial^2 \vec{u}}{\partial y^2} \right) + A(x, y) \frac{\partial \vec{u}}{\partial x} + B(x, y) \vec{u} = \vec{f}, & (x, y, t) \in \mathcal{G}, \\ \vec{u}(x, y, 0) = \vec{u}_0(x, y), & (x, y) \in \bar{\mathcal{D}}, \\ \vec{u}(0, y, t) = \vec{u}(1, y, t) = \vec{0}, & (y, t) \in [0, 1] \times [0, T], \\ \vec{u}(x, 0, t) = \vec{u}(x, 1, t) = \vec{0}, & (x, t) \in [0, 1] \times [0, T], \end{cases} \quad (8.2.3)$$

where $\mathcal{E} = \text{diag}(\varepsilon_1, \varepsilon_2)$ with $A = \text{diag}(a_1, a_2)$ and $B = \{b_{lm}\}_{l,m=1}^2$. We assume that the matrices A, B are sufficiently smooth and satisfy the following conditions

$$\begin{cases} a_1(x, y), a_2(x, y) > \alpha > 0, \\ b_{ll}(x, y) > \gamma_\beta > 0, \quad b_{lm}(x, y) \leq 0, \text{ for } l \neq m, \\ \min_{(x,y) \in \bar{\mathcal{D}}} \{b_{11}(x, y) + b_{12}(x, y), b_{21}(x, y) + b_{22}(x, y)\} \geq \beta > 0, \\ \gamma_1 = \max_{\bar{\mathcal{D}}} \{|b_{12}(x, y)| / b_{11}(x, y)\}, \quad \gamma_2 = \max_{\bar{\mathcal{D}}} \{|b_{21}(x, y)| / b_{22}(x, y)\}. \end{cases}$$

We assume that the source term and initial data of the model problem (8.2.3) are satisfy certain smoothness conditions.

Finally, in Chapter 7, we presented uniformly convergent numerical scheme to solve singularly perturbed system of 2D parabolic reaction-diffusion problem. It will be interesting to develop parameter uniform computation technique to solve system of 2D parabolic reaction-diffusion type problem with discontinuous source term.

- [1] L. R. Abrahamsson, H. B. Keller, and H. O. Kreiss. Difference approximations for singular perturbations of systems of ordinary differential equations. *Numer. Math.*, 22:367–391, 1974.
- [2] N. S. Bakhvalov. The optimization of methods of solving boundary value problems with a boundary layer. *Comput. Math. Math. Phys.*, 9(4):139–166, 1969.
- [3] G. Barenblatt, I. Zheltov, and I. Kochina. Basic concepts in the theory of seepage of homogeneous liquids in fissured rocks. *J. Appl. Math. Mech.*, 24(5):1286–1303, 1960.
- [4] R. K. Bawa and S. Natesan. A computational method for self-adjoint singular perturbation problems using quintic spline. *Comput. Math. Appl.*, 50(8-9):1371–1382, 2005.
- [5] S. Bellew and E. O’Riordan. A parameter robust numerical method for a system of two singularly perturbed convection-diffusion equations. *Appl. Numer. Math.*, 51(2-3):171–186, 2004.
- [6] A. E. Berger, J. M. Solomon, and M. Ciment. An analysis of a uniformly accurate difference method for a singular perturbation problem. *Mathematics of computation*, 37(155):79–94, 1981.
- [7] A. E. Berger, J. M. Solomon, M. Ciment, S. H. Leventhal, and B. C. Weinberg. Generalized operator compact implicit schemes for boundary layer problems. *Mathematics of Computation*, 35(151):695–731, 1980.
- [8] A. W. Bush. *Perturbation Methods for Engineers and Scientists*. CRC Press, London, 1992.
- [9] X. Cai and F. Liu. A Reynolds uniform scheme for singularly perturbed parabolic differential equation. *ANZIAM J.*, 47((C)):C633–C648, 2005.
- [10] Z. Cen. Parameter-uniform finite difference scheme for a system of coupled singularly perturbed convection-diffusion equations. *Int. J. Comput. Math.*, 82(2):177–192, 2005.
- [11] Z. Cen, A. Xu, and A. Le. A second-order hybrid finite difference scheme for a system of singularly perturbed initial value problems. *J. Comput. Appl. Math.*, 234(12):3445–3457, 2010.
- [12] C. Clavero, J. L. Gracia, and M. Stynes. A simpler analysis of a hybrid numerical method for time-dependent convection-diffusion problems. *J. Comput. Appl. Math.*, 235(17):5240–5248, 2011.
- [13] C. Clavero and J. C. Jorge. Another uniform convergence analysis technique of some numerical methods for parabolic singularly perturbed problems. *Comput. Math. Appl.*, 70(3):222–235, 2015.
- [14] C. Clavero and J. C. Jorge. Uniform convergence and order reduction of the fractional implicit Euler method to solve singularly perturbed 2D reaction-diffusion problems. *Appl. Math. Comput.*, 287/288:12–27, 2016.

- [15] C. Clavero, J. C. Jorge, F. Lisbona, and G. I. Shishkin. A fractional step method on a special mesh for the resolution of multidimensional evolutionary convection-diffusion problems. *Appl. Numer. Math.*, 27(3):211–231, 1998.
- [16] C. Clavero, J. C. Jorge, F. Lisbona, and G. I. Shishkin. An alternating direction scheme on a nonuniform mesh for reaction-diffusion parabolic problems. *IMA J. Numer. Anal.*, 20(2):263–280, 2000.
- [17] A. Das and S. Natesan. Uniformly convergent hybrid numerical scheme for singularly perturbed delay parabolic convection-diffusion problems on Shishkin mesh. *Appl. Math. Comput.*, 271:168–186, 2015.
- [18] A. Das and S. Natesan. Higher-order convergence with fractional-step method for singularly perturbed 2D parabolic convection-diffusion problems on Shishkin mesh. *Comput. Math. Appl.*, 75(7):2387–2403, 2018.
- [19] A. Das and S. Natesan. Parameter-uniform numerical method for singularly perturbed 2d delay parabolic convection-diffusion problems on Shishkin mesh. *J. Appl. Math. Comput.*, doi: 10.1007/s12190-018-1175-y, 2018.
- [20] P. Das and S. Natesan. Numerical solution of a system of singularly perturbed convection-diffusion boundary-value problems using mesh equidistribution technique. *Aust. J. Math. Anal. Appl.*, 10(1):Art. 14, 17, 2013.
- [21] P. Das and S. Natesan. A uniformly convergent hybrid scheme for singularly perturbed system of reaction-diffusion Robin type boundary-value problems. *J. Appl. Math. Comput.*, 41(1-2):447–471, 2013.
- [22] P. Das and S. Natesan. Optimal error estimate using mesh equidistribution technique for singularly perturbed system of reaction-diffusion boundary-value problems. *Appl. Math. Comput.*, 249:265–277, 2014.
- [23] D. N. de G. Allen and R. V. Southwell. Relaxation methods applied to determine the motion, in two dimensions, of a viscous fluid past a fixed cylinder. *The Quarterly Journal of Mechanics and Applied Mathematics*, 8(2):129–145, 1955.
- [24] B. S. Deb and S. Natesan. Richardson extrapolation method for singularly perturbed coupled system of convection-diffusion boundary-value problems. *CMES Comput. Model. Eng. Sci.*, 38(2):179–200, 2008.
- [25] E. P. Doolan, J. J. H. Miller, and W. H. A. Schilders. *Uniform Numerical Methods for Problems with Initial and Boundary Layers*. Boole Press, Dublin, 1980.
- [26] P. A. Farrell. Sufficient conditions for uniform convergence of a class of difference schemes for a singularly perturbed problem. *IMA J. Numer. Anal.*, 7(4):459–472, 1987.
- [27] P. A. Farrell, A. F. Hegarty, J. J. H. Miller, E. O’Riordan, and G. I. Shishkin. *Robust Computational Techniques for Boundary Layers*. Chapman & Hall/CRC, Boca Raton, FL, 2000.

- [28] V. Franklin, M. Paramasivam, J. J. H. Miller, and S. Valarmathi. Second order parameter-uniform convergence for a finite difference method for a singularly perturbed linear parabolic system. *Int. J. Numer. Anal. Model.*, 10(1):178–202, 2013.
- [29] K. O. Friedrichs and W. R. Wasow. Singular perturbations of nonlinear oscillations. *Duke Math. J.*, 13:367–381, 1946.
- [30] S. Gowrisankar and S. Natesan. A robust numerical scheme for singularly perturbed delay parabolic initial-boundary-value problems on equidistributed grids. *Electron. Trans. Numer. Anal.*, 41:376–395, 2014.
- [31] S. Gowrisankar and S. Natesan. ε -Uniformly convergent numerical scheme for singularly perturbed delay parabolic partial differential equations. *Int. J. Comput. Math.*, 94(5):902–921, 2017.
- [32] J. L. Gracia and F. J. Lisbona. A uniformly convergent scheme for a system of reaction-diffusion equations. *J. Comput. Appl. Math.*, 206(1):1–16, 2007.
- [33] J. L. Gracia, F. J. Lisbona, and E. O’Riordan. A coupled system of singularly perturbed parabolic reaction-diffusion equations. *Adv. Comput. Math.*, 32(1):43–61, 2010.
- [34] M. K. Kadalbajoo and K. C. Patidar. A survey of numerical techniques for solving singularly perturbed ordinary differential equations. *Appl. Math. Comput.*, 130(2-3):457–510, 2002.
- [35] M. K. Kadalbajoo and K. C. Patidar. Singularly perturbed problems in partial differential equations: a survey. *Appl. Math. Comput.*, 134(2-3):371–429, 2003.
- [36] M. K. Kadalbajoo and Y. N. Reddy. Asymptotic and numerical analysis of singular perturbation problems: a survey. *Appl. Math. Comput.*, 30(3):223–259, 1989.
- [37] H. B. Keller. *Numerical Methods for Two-Point Boundary Value Problems*. Dover, New York, 1992.
- [38] R. B. Kellogg, T. Linß, and M. Stynes. A finite difference method on layer-adapted meshes for an elliptic reaction-diffusion system in two dimensions. *Math. Comp.*, 77(264):2085–2096, 2008.
- [39] R. B. Kellogg, N. Madden, and M. Stynes. A parameter-robust numerical method for a system of reaction-diffusion equations in two dimensions. *Numer. Methods Partial Differential Equations*, 24(1):312–334, 2008.
- [40] R. B. Kellogg and A. Tsan. Analysis of some difference approximations for a singular perturbation problem without turning points. *Math. Comp.*, 32(144):1025–1039, 1978.
- [41] J. Kevorkian and J. D. Cole. *Multiple Scale and Singular Perturbation Methods*. Springer-Verlag, New York, 1996.
- [42] O. A. Ladyzenskaja, V. A. Solonnikov, and N. N. Ural’ceva. *Linear and Quasi-Linear Equations of Parabolic Type*. American Mathematical Society, Rhode Island, 1988.

- [43] P. A. Lagerstrom. *Matched Asymptotic Expansions*. Springer-Verlag, New York, 1988.
- [44] P. A. Lagerstrom and R. G. Casten. Basic concepts underlying singular perturbation techniques. *SIAM Rev.*, 14:63–120, 1972.
- [45] T. Linß. The necessity of Shishkin decompositions. *Appl. Math. Lett.*, 14(7):891–896, 2001.
- [46] T. Linß. Analysis of an upwind finite-difference scheme for a system of coupled singularly perturbed convection-diffusion equations. *Computing*, 79(1):23–32, 2007.
- [47] T. Linß. *Layer-Adapted Meshes for Reaction-Convection-Diffusion Problems*, volume 1985 of *Lecture Notes in Mathematics*. Springer-Verlag, Berlin, 2010.
- [48] T. Linß and N. Madden. An improved error estimate for a numerical method for a system of coupled singularly perturbed reaction-diffusion equations. *Comput. Methods Appl. Math.*, 3(3):417–423, 2003. Dedicated to John J. H. Miller on the occasion of his 65th birthday.
- [49] T. Linß and N. Madden. Accurate solution of a system of coupled singularly perturbed reaction-diffusion equations. *Computing*, 73(2):121–133, 2004.
- [50] T. Linß and M. Stynes. Numerical solution of systems of singularly perturbed differential equations. *Comput. Methods Appl. Math.*, 9(2):165–191, 2009.
- [51] L.-B. Liu and Y. Chen. A robust adaptive grid method for a system of two singularly perturbed convection-diffusion equations with weak coupling. *J. Sci. Comput.*, 61(1):1–16, 2014.
- [52] N. Madden and M. Stynes. A uniformly convergent numerical method for a coupled system of two singularly perturbed linear reaction-diffusion problems. *IMA J. Numer. Anal.*, 23(4):627–644, 2003.
- [53] A. Majumdar and S. Natesan. Alternating direction numerical scheme for singularly perturbed 2D degenerate parabolic convection-diffusion problems. *Appl. Math. Comput.*, 313:453–473, 2017.
- [54] A. Majumdar and S. Natesan. Second-order uniformly convergent Richardson extrapolation method for singularly perturbed degenerate parabolic PDEs. *Int. J. Appl. Comput. Math.*, 3(suppl. 1):S31–S53, 2017.
- [55] G. I. Marchuk. Splitting and alternating direction methods. *Handbook of numerical analysis*, 1:197–462, 1990.
- [56] S. Matthews, E. O’Riordan, and G. I. Shishkin. A numerical method for a system of singularly perturbed reaction-diffusion equations. *J. Comput. Appl. Math.*, 145(1):151–166, 2002.
- [57] J. J. H. Miller, E. O’Riordan, and G. I. Shishkin. *Fitted Numerical Methods for Singular Perturbation Problems*. World Scientific, Singapore, revised edition, 2012.

- [58] P. D. Miller. *Applied Asymptotic Analysis*. Graduate Studies in Mathematics. American Mathematical Society, Providence, RI, 2006.
- [59] J. Mohapatra and S. Natesan. Uniformly convergent second-order numerical method for singularly perturbed delay differential equations. *Neural Parallel Sci. Comput.*, 16(3):353–370, 2008.
- [60] J. Mohapatra and S. Natesan. Uniform convergence analysis of finite difference scheme for singularly perturbed delay differential equation on an adaptively generated grid. *Numer. Math. Theory Methods Appl.*, 3(1):1–22, 2010.
- [61] J. Mohapatra and S. Natesan. Uniformly convergent numerical method for singularly perturbed differential-difference equation using grid equidistribution. *Int. J. Numer. Methods Biomed. Eng.*, 27(9):1427–1445, 2011.
- [62] K. W. Morton. *Numerical Solution of Convection-Diffusion Problems*. Chapman & Hall, London, 1996.
- [63] K. Mukherjee and S. Natesan. Parameter-uniform hybrid numerical scheme for time-dependent convection-dominated initial-boundary-value problems. *Computing*, 84(3-4):209–230, 2009.
- [64] K. Mukherjee and S. Natesan. Richardson extrapolation technique for singularly perturbed parabolic convection-diffusion problems. *Computing*, 92(1):1–32, 2011.
- [65] K. Mukherjee and S. Natesan. ε -uniform error estimate of hybrid numerical scheme for singularly perturbed parabolic problems with interior layers. *Numer. Algorithms*, 58(1):103–141, 2011.
- [66] J. B. Munyakazi. A uniformly convergent nonstandard finite difference scheme for a system of convection–diffusion equations. *Computational and Applied Mathematics*, 34(3):1153–1165, 2015.
- [67] J. D. Murray. *Mathematical Biology*. Springer-Verlag, Berlin, 1989.
- [68] S. Natesan and N. Ramanujam. Booster method for singularly-perturbed one-dimensional convection-diffusion Neumann problems. *J. Optim. Theory Appl.*, 99(1):53–72, 1998.
- [69] S. Natesan and N. Ramanujam. “Shooting method” for singular perturbation problems arising in chemical reactor theory. *Int. J. Comput. Math.*, 70(2):251–262, 1998.
- [70] S. Natesan and N. Ramanujam. A “booster method” for singular perturbation problems arising in chemical reactor theory. *Appl. Math. Comput.*, 100(1):27–48, 1999.
- [71] S. Natesan and N. Ramanujam. Improvement of numerical solution of self-adjoint singular perturbation problems by incorporation of asymptotic approximations. *Appl. Math. Comput.*, 98(2-3):119–137, 1999.
- [72] A. H. Nayfeh. *Perturbation Methods*. John Wiley & Sons, New York, 1973.

- [73] R. E. O'Malley, Jr. *Introduction to Singular Perturbations*. Academic Press, New York, 1974.
- [74] R. E. O'Malley, Jr. *Singular Perturbation Methods for Ordinary Differential Equations*. Applied Mathematical Sciences. Springer-Verlag, New York, 1991.
- [75] E. O'Riordan and M. Stynes. Numerical analysis of a strongly coupled system of two singularly perturbed convection-diffusion problems. *Adv. Comput. Math.*, 30(2):101–121, 2009.
- [76] C. V. Pao. *Nonlinear Parabolic and Elliptic Equations*. Plenum Press, New York, 1992.
- [77] L. Prandtl. Uber flussigkeits-bewegung bei kleiner reibung. In *Verhandlungen, III Inter. Math. Kongresses, Tuebner, Leipzig*, pages 484–491, 1905.
- [78] R. M. Priyadharshini, N. Ramanujam, and A. Tamilselvan. Hybrid difference schemes for a system of singularly perturbed convection-diffusion equations. *J. Appl. Math. & Informatics.*, 27(5-6):1001–1015, 2009.
- [79] J. I. Ramos. An exponentially-fitted method for singularly-perturbed ordinary differential equations with turning points and parabolic problems. *Appl. Math. Comput.*, 165(3):549–564, 2005.
- [80] J. I. Ramos. Exponential methods for singularly perturbed ordinary differential-difference equations. *Appl. Math. Comput.*, 182(2):1528–1541, 2006.
- [81] S. C. S. Rao and V. Srivastava. Parameter-robust numerical method for time-dependent weakly coupled linear system of singularly perturbed convection-diffusion equations. *Differ. Equ. Dyn. Syst.*, 25(2):301–325, 2017.
- [82] H.-G. Roos, M. Stynes, and L. Tobiska. *Robust Numerical Methods for Singularly Perturbed Differential Equations*. Springer Series in Computational Mathematics. Springer-Verlag, Berlin, second edition, 2008.
- [83] G. I. Shishkin. A difference scheme on a non-uniform mesh for a differential equation with a small parameter in the highest derivative. *USSR Computational Mathematics and Mathematical Physics*, 23(3):59–66, 1983.
- [84] G. I. Shishkin and L. P. Shishkina. *Difference Methods for Singular Perturbation Problems*, volume 140. CRC Press, Boca Raton, FL, 2009.
- [85] D. R. Smith. The multivariable method in singular perturbation analysis. *SIAM Review*, 17(2):221–273, 1975.
- [86] M. Stynes. Steady-state convection-diffusion problems. *Acta Numer.*, 14:445–508, 2005.
- [87] M. Stynes and H.-G. Roos. The midpoint upwind scheme. *Appl. Numer. Math.*, 23(3):361–374, 1997.
- [88] M. Stynes and L. Tobiska. A finite difference analysis of a streamline diffusion method on a Shishkin mesh. *Numer. Algorithms*, 18(3-4):337–360, 1998.

- [89] A. Tamilselvan and N. Ramanujam. A parameter uniform numerical method for a system of singularly perturbed convection-diffusion equations with discontinuous convection coefficients. *Int. J. Comput. Math.*, 87(6):1374–1388, 2010.
- [90] A. Tamilselvan, N. Ramanujam, and V. Shanthi. A numerical method for singularly perturbed weakly coupled system of two second order ordinary differential equations with discontinuous source term. *J. Comput. Appl. Math.*, 202(2):203–216, 2007.
- [91] M. Van Dyke. *Perturbation methods in fluid mechanics*. Applied Mathematics and Mechanics, Vol. 8. Academic Press, New York-London, 1964.
- [92] J. Vigo-Aguiar and S. Natesan. A parallel boundary value technique for singularly perturbed two-point boundary value problems. *J. Supercomput.*, 27(2):195–206, 2004.
- [93] J. Vigo-Aguiar and S. Natesan. An efficient numerical method for singular perturbation problems. *J. Comput. Appl. Math.*, 192(1):132–141, 2006.
- [94] C. Xenophontos, S. Franz, and L. Ludwig. Finite element approximation of convection-diffusion problems using an exponentially graded mesh. *Comput. Math. Appl.*, 72(6):1532–1540, 2016.
- [95] C. Xenophontos and L. Oberbroeckling. On the finite element approximation of systems of reaction-diffusion equations by p/hp methods. *J. Comput. Math.*, 28(3):386–400, 2010.
- [96] N. N. Yanenko. The method of fractional steps for solving multidimensional problems of mathematical physics. *Novosibirsk Science*, 196, 1967.

List of published and communicated papers

Based on the work in this thesis, the following research articles are published or communicated.

1. M. K. Singh and S. Natesan. Richardson extrapolation technique for singularly perturbed system of parabolic partial differential equations with exponential boundary layers. *Appl. Math. Comput.*, 333:254–275, 2018.
2. M. K. Singh and S. Natesan. A robust computational method for singularly perturbed system of 2D parabolic convection-diffusion problems. *International Journal of Mathematical Modelling and Numerical Optimisation*, to appear.
3. M. K. Singh and S. Natesan. Numerical analysis of singularly perturbed system of parabolic convection-diffusion problem with regular boundary layers (communicated).
4. M. K. Singh and S. Natesan. A parameter-uniform hybrid finite difference scheme for singularly perturbed system of parabolic convection-diffusion problems (communicated).
5. M. K. Singh and S. Natesan. Uniformly convergent computational method for singularly perturbed system of parabolic convection-diffusion problems with interior layers (communicated).
6. M. K. Singh and S. Natesan. A fractional step method for singularly perturbed system of 2D parabolic reaction-diffusion problems (communicated).
7. M. K. Singh and Natesan, S. Analysis of uniformly convergent numerical scheme for singularly perturbed system of 2D parabolic reaction-diffusion problems (communicated).